ISSN 0021-9673

VOL. 605 NO. 1 JULY 10, 1992

JOURNAL OF CHROMATOGRAPHY

INCLUDING ELECTROPHORESIS AND OTHER SEPARATION METHODS

ELSEVIER

JOURNAL OF CHROMATOGRAPHY

INCLUDING ELECTROPHORESIS AND OTHER SEPARATION METHODS

Scope. The *Journal of Chromatography* publishes papers on all aspects of chromatography, electrophoresis and related methods. Contributions consist mainly of research papers dealing with chromatographic theory, instrumental development and their applications. The section *Biomedical Applications*, which is under separate editorship, deals with the following aspects: developments in and applications of chromatographic and electrophoretic techniques related to clinical diagnosis or alterations during medical treatment; screening and profiling of body fluids or tissues with special reference to metabolic disorders; results from basic medical research with direct consequences in clinical practice; drug level monitoring and pharmacokinetic studies; clinical toxicology; analytical studies in occupational medicine.

Submission of Papers. Manuscripts (in English; *four* copies are required) should be submitted to: Editorial Office of *Journal of Chromatography*, P.O. Box 681, 1000 AR Amsterdam, Netherlands, Telefax (+31-20) 5862 304, or to: The Editor of *Journal of Chromatography, Biomedical Applications*, P.O. Box 681, 1000 AR Amsterdam, Netherlands. Review articles are invited or proposed by letter to the Editors. An outline of the proposed review should first be forwarded to the Editors for preliminary discussion prior to preparation. Submission of an article is understood to imply that the article is original and unpublished and is not being considered for publication elsewhere. For copyright regulations, see below.

Publication. The *Journal of Chromatography* (incl. *Biomedical Applications*) has 39 volumes in 1992. The subscription prices for 1992 are:

J. Chromatogr. (incl. *Cum. Indexes, Vols. 551–600*) + *Biomed. Appl.* (Vols. 573–611):
Dfl. 7722.00 plus Dfl. 1209.00 (p.p.h.) (total *ca.* US$ 4880.25)

J. Chromatogr. (incl. *Cum. Indexes, Vols. 551–600*) only (Vols. 585–611):
Dfl. 6210.00 plus Dfl. 837.00 (p.p.h.) (total *ca.* US$ 3850.75)

Biomed. Appl. only (Vols. 573–584):
Dfl. 2760.00 plus Dfl. 372.00 (p.p.h.) (total *ca.* US$ 1711.50).

Subscription Orders. The Dutch guilder price is definitive. The US$ price is subject to exchange-rate fluctuations and is given as a guide. Subscriptions are accepted on a prepaid basis only, unless different terms have been previously agreed upon. Subscriptions orders can be entered only by calender year (Jan.–Dec.) and should be sent to Elsevier Science Publishers, Journal Department, P.O. Box 211, 1000 AE Amsterdam, Netherlands, Tel. (+31-20) 5803 642, Telefax (+31-20) 5803 598, or to your usual subscription agent. Postage and handling charges include surface delivery except to the following countries where air delivery via SAL (Surface Air Lift) mail is ensured: Argentina, Australia, Brazil, Canada, China, Hong Kong, India, Israel, Japan*, Malaysia, Mexico, New Zealand, Pakistan, Singapore, South Africa, South Korea, Taiwan, Thailand, USA. *For Japan air delivery (SAL) requires 25% additional charge of the normal postage and handling charge. For all other countries airmail rates are available upon request. Claims for missing issues must be made within three months of our publication (mailing) date, otherwise such claims cannot be honoured free of charge. Back volumes of the *Journal of Chromatography* (Vols. 1–572) are available at Dfl. 217.00 (plus postage). Customers in the USA and Canada wishing information on this and other Elsevier journals, please contact Journal Information Center, Elsevier Science Publishing Co. Inc., 655 Avenue of the Americas, New York, NY 10010, USA, Tel. (+1-212) 633 3750, Telefax (+1-212) 633 3990.

Abstracts/Contents Lists published in Analytical Abstracts, Biochemical Abstracts, Biological Abstracts, Chemical Abstracts, Chemical Titles, Chromatography Abstracts, Clinical Chemistry Lookout, Current Contents/Life Sciences, Current Contents/Physical, Chemical & Earth Sciences, Deep-Sea Research/Part B: Oceanographic Literature Review, Excerpta Medica, Index Medicus, Mass Spectrometry Bulletin, PASCAL-CNRS, Pharmaceutical Abstracts, Referativnyi Zhurnal, Research Alert, Science Citation Index and Trends in Biotechnology.

US Mailing Notice. *Journal of Chromatography* (main section ISSN 0021-9673, *Biomedical Applications* section ISSN 0378-4347) is published (78 issues/year) by Elsevier Science Publishers (Sara Burgerhartstraat 25, P.O. Box 211, 1000 AE Amsterdam, Netherlands). Annual subscription price in the USA US$ 4880.25 (subject to change), including air speed delivery. Application to mail at second class postage rate is pending at Jamaica, NY 11431. **USA POSTMASTERS:** Send address changes to *Journal of Chromatography*, Publications Expediting, Inc., 200 Meacham Avenue, Elmont, NY 11003. Airfreight and mailing in the USA by Publication Expediting.

See inside back cover for Publication Schedule, Information for Authors and information on Advertisements.

0021-9673/92/$05.00

This issue is printed on acid-free paper.

Printed in the Netherlands

CONTENTS

(Abstracts/Contents Lists published in Analytical Abstracts, Biochemical Abstracts, Biological Abstracts, Chemical Abstracts, Chemical titles, Chromatography Abstracts, Current Contents/Life Sciences, Current Contents/Physical, Chemical & Earth Sciences, Deep-Sea Research/Part B: Oceanographic Literature Review, Excerpta Medica, Index Medicus, Mass Spectrometry Bulletin, PASCAL-CNRS, Referativnyi Zhurnal, Research Alert and Science Citation Index)

REGULAR PAPERS

Column Liquid Chromatography

Gas Chromatography

Supercritical Fluid Chromatography

Electrophoresis

(Continued overleaf)

Contents (continued)

SHORT COMMUNICATIONS

Column Liquid Chromatography

Gas Chromatography

Electrophoresis

LETTER TO THE EDITOR

BOOK REVIEW

In articles with more than one author, the name of the author to whom correspondence should be addressed is indicated in the article heading by a 6-pointed asterisk (*).

JOURNAL OF CHROMATOGRAPHY

VOL. 605 (1992)

JOURNAL of CHROMATOGRAPHY

INCLUDING ELECTROPHORESIS AND OTHER SEPARATION METHODS

ELSEVIER

AMSTERDAM — LONDON — NEW YORK — TOKYO

0021-9673/92/$05.00

Printed in the Netherlands

Journal of Chromatography, 605 (1992) 1–17
Elsevier Science Publishers B.V., Amsterdam

CHROM. 24 189

Adsorption isotherms of cholesterol and related compounds in non-aqueous reversed-phase chromatographic systems

Pavel Jandera* and Georges Guiochon

Department of Chemistry, University of Tennessee, Knoxville, TN 37996-1501 and Division of Analytical Chemistry, Oak Ridge National Laboratory, Oak Ridge, TN 37831-6120 (USA)

(First received January 14th, 1992; revised manuscript received March 17th, 1992)

ABSTRACT

The adsorption isotherms of cholesterol, cholesteryl acetate, cholesteryl formate and cholestanone were measured on two different chemically bonded C_{18} silica columns, using acetonitrile–dichloromethane or acetonitrile–*n*-hexane as mobile phases. In all instances the experimental isotherms are nearly but not extactly linear, exhibit significant deviations from Langmuir isotherm behavior and are fairly well described by a three-parameter quadratic equation. However, the best representation of the experimental data is obtained with a four-parameter quadratic isotherm. A model was worked out to account for these isotherms and to attempt an explanation of the physical meaning of the isotherm parameters on the basis of the limited solubility of the compounds studied in the bulk liquid phase, of two-layer adsorption and of an association between the sorbed molecules. A detailed study of the dependence of the isotherm coefficients on various experimental parameters (*e.g.*, type and specific surface area of the C_{18} phase, type and concentration of the solvents in the mobile phase) gave results in qualitative agreement with the model.

INTRODUCTION

The experimental determination of the equilibrium isotherms of the components of a mixture in chromatographic systems, the modeling of these isotherms and the study of their relationships to band profiles are important problems in preparative chromatography. Accurate predictive calculations of the individual band profiles by computer simulations require the exact description of these equilibrium isotherms [1]. From such profiles, precise optimum values of the experimental conditions for maximum production rate can be derived.

Because high solute concentrations are required to achieve high throughputs in preparative chromatography, the adsorption isotherms are rarely linear in the concentration range of interest. The simple Langmuir isotherm [2] describes properly the sorption equilibrium behavior in a few cases only, or in a low concentration range [3]. It usually fails because it assumes an ideal behavior of both the solution and the adsorbed layer [2], and it does not take into account the secondary effects which are important at high concentrations, such as the interactions between adsorbed molecules, the solvation effects or solubility limitations.

To account for these deviations from Langmuir adsorption behavior, a number of more sophisticated models have been suggested. The best known isotherm equations are the bilangmuir [4], the Fowler [5], the Volmer [6], the quadratic [7,8], the Toth [9] and the Unilan isotherms [10]. The formalism of the more rigorous models, based on

Correspondence to: Professor G. Guiochon, Department of Chemistry, University of Tennessee, Knoxville, TN 37996-1501, USA.

* On leave from the Institute of Chemical Technology, Pardubice, Czechoslovakia.

0021-9673/92/$05.00

statistical thermodynamics [6–11], takes into account several phenomena ignored by the Langmuir model. In so doing, however, these models include more parameters, which explains, at least in part, their greater success in describing experimental data: they are more flexible. Conversely, it is often difficult to correlate these coefficients to the physical nature of the phenomena taking place in a given liquid–solid system and to give them a physical meaning.

Models of isotherms can be considered from two entirely different viewpoints. On the empirical front, they are fitting models, or equations used to fit to the experimental data for the purpose of representing simply these data in further calculations. From a theoretical point of view, they are the translation in mathematical language of our ideas of what is or should be the behavior of molecules in phase equilibria. A confusion arises easily because poor theoretical models can be good fitting models (*e.g.*, the Langmuir model). A good fit alone is never a proof of the theoretical value of a model.

Most studies on liquid–solid adsorption have been carried out using relatively simple compounds. Because of the development of the applications of preparative chromatography, there is a need for experimental data and for modeling of these data in the case of compounds more representative of those to which the method is routinely applied. The availability of series of results on similar compounds could help separation chemists in finding the most suitable equations to fit to their data.

In a recent study dealing with the simulation of the elution bands of a poorly soluble compound [12], we observed significant deviations from the Langmuir adsorption behavior for cholesterol in non-aqueous reversed-phase (NARP) systems. An empirical combination of a linear and a Langmuir isotherm was successfully fitted to the experimental data sets. This behavior appeared to be related to the limited solubility of cholesterol in most solvents commonly used in NARP and to a likely association of the flat hydrophobic molecules of steroid in the adsorbed layer.

The aim of this work was a deeper investigation of this adsorption behavior, a broadening of the earlier study to closely related steroids and a comparison of the results obtained when fitting the adsorption data to several isotherm equations.

THEORETICAL

Langmuir model

Although the Langmuir adsorption isotherm can easily be derived from statistical thermodynamics [6–11], its original derivation is based on a kinetic argument [2]. The equation is obtained by equating the adsorption and desorption rates:

$$\frac{dq}{dt} = k_1 C(q_s - q) \tag{1a}$$

$$-\frac{dq}{dt} = k_2 q \tag{1b}$$

where C and q are concentrations of the compound in the mobile and stationary phase, respectively, k_1 and k_2 are adsorption and desorption rate constants, respectively, and q_s is the adsorbent specific saturation capacity (*i.e.*, saturation capacity per unit mass). The Langmuir isotherm is

$$q = \frac{\frac{k_1}{k_2} \cdot q_s C}{1 + \frac{k_1}{k_2} \cdot C} = \frac{bq_s C}{1 + bC} = \frac{aC}{1 + bC} \tag{2}$$

where a ($= bq_s$) and b ($= k_1/k_2$) are auxiliary constants. The model assumes localized adsorption in a monolayer, no molecular interactions in either phase, an ideal solution and an ideal adsorbed layer.

Bilayer adsorption isotherm

The original Langmuir isotherm can be improved by introducing additional phenomena in the adsorption model in an attempt to make it more realistic. For example, we can consider that adsorption proceeds in two adsorption layers instead of a monolayer, with some competition between the first and the second layers. Then, the adsorption isotherm in the first layer is given by eqn. 1 (with $q = q_1$), and the following equations give the rates of adsorption and desorption from the second layer:

$$\frac{dq_2}{dt} = k_1^* C(q_1 - q_2) \tag{3a}$$

$$-\frac{dq_2}{dt} = k_2^* q_2 \tag{3b}$$

where q_1 and q_2 are the adsorbate concentrations in the first and the second layers, respectively, and k_1^*

and k_2^* are the adsorption and desorption rate constants for the competitive adsorption in the second layer, respectively. Combining eqns. 1 and 3 gives the following isotherm equation for the total concentration q in the stationary phase, assuming two-layer adsorption (bilayer model):

$$q = q_1 + q_2 = \frac{A_1C + A_2C^2}{1 + B_1C + B_2C^2} \quad (4)$$

Eqn. 4 is a special case of a quadratic isotherm with the coefficients A_1, A_2, B_1 and B_2 given as

$$A_1 = \frac{k_1}{k_2} \cdot q_s \quad (5a)$$

$$A_2 = 2 \cdot \frac{k_1}{k_2} \cdot \frac{k_1^*}{k_2^*} \cdot q_s \quad (5b)$$

$$B_1 = \frac{k_1}{k_2} + \frac{k_1^*}{k_2^*} \quad (5c)$$

$$B_2 = \frac{k_1}{k_2} \cdot \frac{k_1^*}{k_2^*} \quad (5d)$$

Clearly, the isotherm given in eqn. 5 depends only on three parameters, the two rate constant ratios (k_1/k_2, k_1^*/k_2^*) and the total specific saturation capacity of the adsorbent (q_s). In spite of this, the isotherm in eqn. 4 is different from the general quadratic isotherm derived by statistical thermodynamics, also a three-parameter equation. Statistical thermodynamics gives as general equation for the isotherm the ratio $C\,P'(C)/P(C)$, where $P(C)$ is a polynomial of degree n an $P'(C)$ its first differential [5–7]. The quadratic isotherm is written as

$$q = \frac{q_sC(b_1 + 2\,b_2C)}{1 + b_1C + b_2C^2} \quad (6)$$

Although the correct relationship (eqn. 5) holds between the coefficients A_2 and B_2, it does not hold between A_1 and B_1, and eqns. 4 and 6 are not equivalent.

Previous workers have used the three-parameter eqn. 6 in the calculation of chromatographic band profiles [13]. An isotherm equation similar to eqn. 4 was derived by Svoboda [8], following an approach similar to ours. However, the rationale for introducing a "blocking coefficient" in the denominator of eqn. 4 and not in the numerator (which makes the isotherm a four-parameter equation) is unclear.

If the approach followed for the derivation of eqn. 4 is applied to model the adsorption isotherm on a surface covered with two different types of independent adsorption sites, we obtain the bilangmuir isotherm. This isotherm is formally a special case of the quadratic isotherm where the parameters B_1 and B_2 are those given in the eqn. 4, but where the parameters A_1 and A_2 are different from the case of a bilayer adsorption and are

$$A_1 = q_{s1} \cdot \frac{k_1}{k_2} + q_{s2} \cdot \frac{k_1^*}{k_2^*} \quad (7a)$$

$$A_2 = (q_{s1} + q_{s2}) \frac{k_1}{k_2} \cdot \frac{k_1^*}{k_2^*} \quad (7b)$$

where q_{s1} and q_{s2} are the specific saturation capacities for the two types of adsorption sites of the adsorbent. If we compare eqns. 5a, 5b, 7a and 7b, we see that, formally, the bilayer adsorption model corresponds to a two-types-of-sites model with $q_{s2} = 0$ and $q = 2q_{s1}$.

Associative–bilayer adsorption isotherm

In the bilayer model of adsorption, the solute molecules of the second layer compete for adsorption on the molecules adsorbed in the first layer. This is a form of loose association. We can consider another model of association of the adsorbed molecules. As a first approximation, if the association is due primarily to dispersive (or hydrophobic) interactions, the adsorption of a molecule on the primary adsorbed layer does not change much the number of the adsorption sites available, as the area this molecule exposes to the mobile phase is approximately equal to the area it occupies when sorbed in the first layer. In such a case, the rate of adsorption on the second layer is not limited by the number of molecules adsorbed on the first layer as it is in the formulation of eqn. 3a and the equation for the adsorption rate now reads

$$\frac{dq_2}{dt} = k_1^*Cq_1 \quad (8)$$

The same procedure used above yields the following adsorption isotherm equation:

$$q = \frac{A_1C + A_2C^2}{1 + B_1C} = \frac{a_1C}{1 + bC} + a_2C \quad (9)$$

and the parameters A_1, A_2 and B_1 in eqn. 9 are given by

$$A_1 = \frac{k_1}{k_2} \cdot q_s \tag{10a}$$

$$A_2 = \frac{k_1}{k_2} \cdot \frac{k_1^*}{k_2^*} q_s \tag{10b}$$

$$B = \frac{k_1}{k_2} \tag{10c}$$

with the relationships

$$a_1 = A_1 - \frac{A_2}{B}; \quad a_2 = \frac{A_2}{B}; \quad b = B \tag{11}$$

Eqn. 9 is another particular case of the quadratic isotherm equation, different from eqns. 4 and 6. It can be rewritten as the combination of a linear and a Langmuir isotherm. If the association rate constant $k_1^* = 0$, eqn. 9 becomes the equation of the classical Langmuir isotherm.

The actual association process can be intermediate between a free association and the competition for the adsorption sites on the primary layer. In this case, the number of adsorption sites in the second layer would be equal to the number of molecules adsorbed in the first layer minus the number of molecules adsorbed in the second layer multiplied by a coefficient p, between 0 (bilayer–association model) and 1 (bilayer model). Eqn. 3a, for the adsorption rate on the second layer, would read

$$\frac{dq}{dt} = k_1^*(q_1 - pq_2) \tag{12}$$

and the adsorption isotherm becomes

$$q = \frac{\frac{k_1}{k_2} \cdot q_s C + \frac{k_1}{k_2} \cdot \frac{k_1^*}{k_2^*} \cdot q_s(1+p)C^2}{1 + \left(\frac{k_1}{k_2} + \frac{k_1^*}{k_2^*} p\right)C + \frac{k_1}{k_2} \cdot \frac{k_1^*}{k_2^*} \cdot pC^2} \tag{13}$$

Eqn. 13 is the general equation of a quadratic isotherm, with four parameters, k_1/k_2, k_1^*/k_2^*, q_s and p. Eqn. 13 becomes eqn. 9 for $p = 0$ and eqn. 4 for $p = 1$. The actual value of p should obviously depend on the solute and the phase system.

Limited solubility isotherm

Another complicating factor in the sorption process may be the limited solubility of the studied compound in the mobile phase. A provision for this effect can be included in the adsorption model. We can set a limiting condition on the number of available "sites" in the bulk liquid phase in the equation giving the desorption rate. This is done by analogy to the limitation of the adsorption rate by the saturation capacity, q_s (eqn. 1a):

$$-\frac{dq_1}{dt} = k_2 q_1(C_x - C) \tag{14a}$$

$$-\frac{dq_2}{dt} = k_2^* q_2(C_x - C) \tag{14b}$$

where C_x is the limiting solubility concentration of the solute in the bulk liquid phase.

With this solubility limitation, the same derivation procedure as above leads to the following equation for the monolayer (Langmuir) adsorption isotherm:

$$q = \frac{\frac{k_1}{k_2} \cdot q_s \cdot \frac{C}{C_x}}{1 + \left(\frac{k_1}{k_2} - 1\right)\frac{C}{C_x}} = \frac{aC}{1 + bC} \tag{15}$$

Eqn. 15 is formally the same as the classical Langmuir isotherm equation, but it shows that in the case of a limited solubility the sorption capacity q_s can no longer be calculated as the ratio of the two isotherm coefficients a and b. The maximum stationary phase concentration which can be reached in such a system is obtained by setting $C = C_x$ in eqn. 15 (then $q = q_s$). Eqn. 15 cannot be used for the solutes which have an unlimited solubility in the bulk liquid phase.

A limited solubility of the studied component in the bulk liquid is a sign of a lack of compatibility between this solute and the solvent, *i.e.*, of a moderate energy of interaction between their molecules. When the absolute value of the energy of the solute–solvent molecular interactions is smaller than the energy of the solute–solute molecular interactions, a poor solubility is likely to be observed, and to be accompanied by association between the sorbed molecules and by multi-layer adsorption.

If we take into account eqn. 12 for the adsorption rate on the second layer, together with a limited solubility in the bulk liquid, we can modify the isotherm eqn. 14 to read

$$q = \frac{\frac{k_1}{k_2} \cdot q_s \cdot \frac{C}{C_x} + \frac{k_1}{k_2} \cdot q_s \left[\frac{k_1^*}{k_2^*}(1+p) - 1\right]\frac{C^2}{C_x^2}}{1 + \left(\frac{k_1}{k_2} + \frac{k_1^*}{k_2^*} \cdot p - 2\right)\frac{C}{C_x} + \left(\frac{k_1}{k_2} - 1\right)\left(\frac{k_1^*}{k_2^*} \cdot p - 1\right)\frac{C^2}{C_x^2}} \quad (16)$$

Eqn. 16 describes another particular case of the quadratic isotherm, with the coefficients A_1, B_1, A_2 and B_2 defined otherwise than the coefficients in eqns. 4, 6 and 9. Eqn. 16 depends on five parameters, C_x, k_1/k_2, k_1^*/k_2^*, p and q_s.

It results from eqn. 16 that, at equilibrium with a saturated solution ($C = C_x$), the solute concentration in the stationary phase is given by $q = q_s(1 + p)/p$. Hence q should be twice the monolayer capacity when only competitive adsorption takes place in the second layer. On the other hand, q should increase indefinitely with decreasing $C - C_x$ if pure association with already adsorbed solute molecules is expected. The latter case would appear unrealistic, as it assumes that the number of adsorbed layers is unlimited. Experimental data confirm that, when the liquid-phase concentration becomes close to the saturation limit, there is no equivalent in liquid–solid adsorption to the pore condensation observed in gas–solid adsorption when the partial pressure approaches the vapor pressure.

In conclusion, if molecular association does take place, the proportionality constant p should be positive and values of q larger than double the monolayer saturation capacity q_s could be expected.

Fowler isotherm

The Fowler isotherm [5] is another three-parameter isotherm which takes into account the adsorbate–adsorbate molecular interactions through the use of an empirical interaction energy parameter χ. Except for these interactions, the same assumptions are made in the derivation of this model as for the Langmuir model. The Fowler isotherm equation is written as

$$bC = \frac{q}{q_s - q} \cdot e^{\chi \cdot \frac{q}{q_s}} \quad (17a)$$

or

$$q = \frac{bq_sC\, e^{-\chi \cdot \frac{q}{q_s}}}{1 + bC\, e^{-\chi \cdot \frac{q}{q_s}}} \quad (17b)$$

The Fowler isotherm equation was originally derived by statistical thermodynamics [5].

Data handling

The coefficients of the Langmuir isotherms were derived by linear regression of the plots of C/q *versus* C, derived from the experimental data [3]. The computations were performed on an IBM (Boca Raton, FL, USA) Model 50 Z personal computer. The VAX 8650 computer (Digital Equipment, Marlboro, MA, USA) of the Computer Center of the University of Tennessee and the SAS software were used for fitting all the other isotherm equations to the experimental data, using non-linear regression.

EXPERIMENTAL

Instrumentation

An HP 1090M liquid chromatograph (Hewlett-Packard, Palo Alto, CA, USA), equipped with a DR solvent delivery system, an automatic sample injector with a 250-μl sample loop, a temperature-controlled column compartment, a diode-array UV detector and a data workstation was used to acquire the data necessary for the determination of the equilibrium isotherms.

Stainless-steel columns (250 mm × 4.6 mm I.D.) were packed in the laboratory with the following adsorbents, using a high-pressure slurry technique: Impaq RG2010-C_{18} (PQ Corp.), 10-μm C_{18}-bonded silica, silica average pore size 200 Å, surface area 246 m^2/g, amount of bonded material 16.85% C, bonding density 3.65 μmol/m^2, surface area after derivatization 139 m^2/g, dead volume V_M = 3.12 ml, phase ratio ϕ = 0.331, packing density 0.5 kg/l; and Nucleosil 500-C_{18} (Macherey–Nagel, Düren, Germany), 7-μm C_{18}-bonded silica, pore size 500 Å, surface area 35 m^2/g, V_M = 3.17 ml, ϕ = 0.308.

Solutes

Cholesterol, cholestanone, cholesteryl acetate and cholesteryl formate (all 99+% grade, Sigma, St. Louis, MO, USA) were dissolved in the mobile phases used for the determination of the isotherms, at concentrations approximately 10% below the solubility limits to avoid possible precipitation in the instrument lines.

Mobile phases

Spectroscopic-grade acetonitrile, dichloromethane, *n*-propanol and *n*-hexane (Burdick & Jackson, Muskegon, MI, USA) were used to prepare the mobile phases by mixing in the appropriate ratios. *n*-Hexane was dried and stored over molecular sieves 3A. All the solvents were filtered through a 0.45-μm filter (Millipore, Milford, MA, USA) before the preparation of the mobile phase. The mobile phase and the sample solution used for the determination of the adsorption isotherm were degassed continuously in the liquid chromatograph by stripping with helium. The mobile phase flow-rate was set at 1–3 ml/min, depending on the solute retention.

Determination of equilibrium isotherms

The equilibrium isotherms were measured using the frontal analysis method as described previously [14,15]. The mobile phase was stored in one of the solvent flasks of the solvent-delivery system, the solution of the solute under study, in a solvent of same composition as the mobile phase, in another flask. The gradient-delivery system was used to pump and mix the solutions needed for the frontal analysis experiments.

The ratio of the flow-rates of the two solutions controls the concentration of the solute delivered continuously to the column. It was adjusted from 0 to 100% in successive 10% steps. Time was allowed for the stabilization of the detector signal after each concentration change. The flow-rate and the column temperature (35°C) were kept constant during all the experiments.

In each experiment the solute concentration in the stationary phase was determined from the integral mass balance equation, using the experimental retention volume (inflection point of the breakthrough curve), corrected for the volume of the tubing between the mixing point of the liquids pumped in each channel and the column top, as described previously in more detail [15]. All the experiments were repeated at least twice.

The experimental results are presented in table form. All concentrations are in g/l.

RESULTS AND DISCUSSION

The experimental isotherms of the four compounds studied on the Impaq C_{18} column, with pure acetonitrile, and of cholesterol on the Impaq and Nucleosil C_{18} columns, with a series of acetonitrile–dichloromethane and acetonitrile–*n*-hexane mixtures as mobile phases, are shown as symbols in Figs. 1–4. Some of these experimental isotherms appear to be close to straight lines, especially in pure acetonitrile (Fig. 1), but there is a significant curvature at low solute concentrations and the data cannot be fitted accurately to straight lines. This is obvious in Figs. 2 and 3.

We successively fitted the four isotherm equations discussed in the previous section (eqns. 2, 4, 9 and 16) to the experimental results, in an attempt to find the equation having the smallest number of parameters that would fit these data. We discuss the sets of parameter values obtained with each model to show the extent of their agreement and/or their inconsistencies with these models.

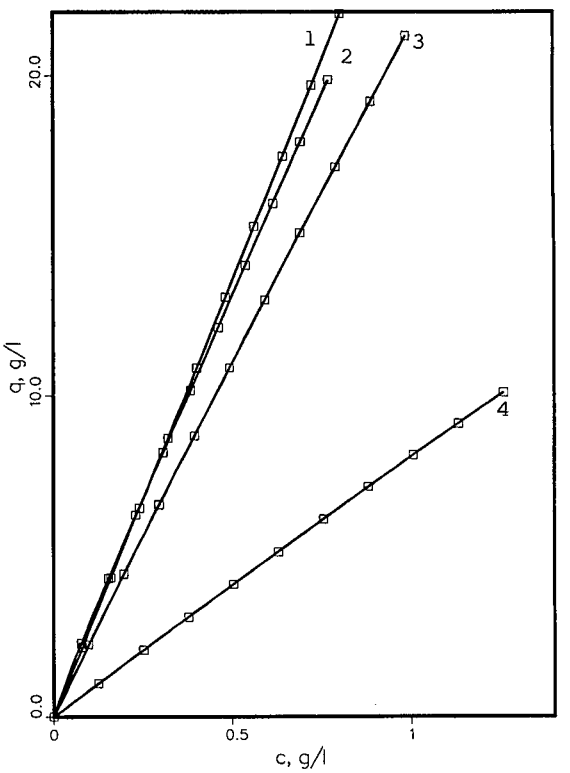

Fig. 1. Isotherms of (1) cholesteryl formate, (2) cholesterol, (3) cholestanone and (4) cholesteryl acetate on an Impaq RG2010-C_{18} column in pure acetonitrile at 35°C. Symbols, experimental data measured by frontal analysis; solid lines, best fits to the three-parameter quadratic isotherm (eqn. 9). c, q = Concentrations of the solutes in the mobile and stationary phase, respectively.

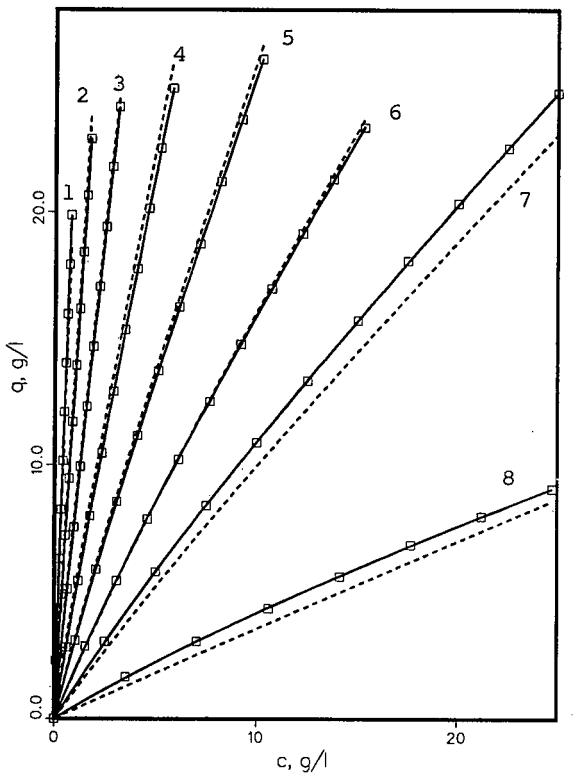

Fig. 2. Isotherms of cholesterol on an Impaq RG2010-C_{18} column in solutions containing (1) 0%, (2) 10%, (3) 20%, (4) 30%, (5) 40%, (6) 50%, (7) 60% and (8) 80% dichloromethane in acetonitrile at 35°C. Symbols, experimental data measured by frontal analysis; solid lines, best fits to the three-parameter quadratic isotherm (eqn. 9); dashed lines, isotherms calculated using the relationships derived in this work between the parameters A_1, A_2 and B of this isotherm and the concentration of dichloromethane in the mobile phase (from Table VII).

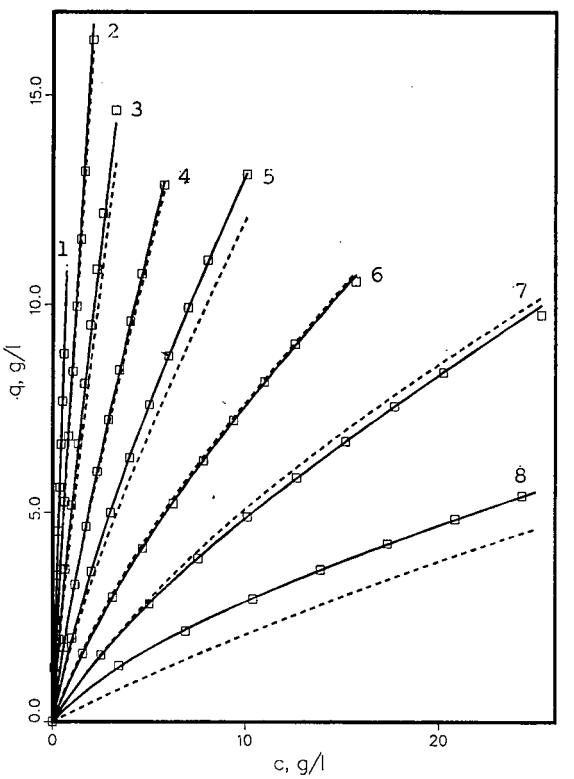

Fig. 3. Isotherms of cholesterol on a Nucleosil 500-C_{18} column in solutions containing (1) 0%, (2) 10%, (3) 20%, (4) 30%, (5) 40%, (6) 50%, (7) 60% and (8) 80% dichloromethane in acetonitrile at 35°C. Symbols, experimental data measured by frontal analysis; solid lines, best fits to the three-parameter quadratic isotherm (eqn. 9); dashed lines, isotherms calculated using the relationships derived in this work between the parameters A_1, A_2 and B of this isotherm and the concentration of dichloromethane in the mobile phase (from Table VII).

Langmuir isotherm

Although this isotherm equation broadly describes the main features of the experimental results, the shape of the Langmuir isotherm (eqn. 2) deviates significantly from the profile of the experimental isotherms, making an accurate fit impossible. The correlation coefficients of the fitted Langmuir equations were between 0.82 and 0.98 and the mean relative error of the values of q predicted from the best-fit Langmuir isotherm was between 1 and 3%. The best values of the parameters a and b of the Langmuir isotherms fitted to the experimental data on the two C_{18} columns with acetonitrile–dichloromethane as mobile phases are given in the Tables I (Impaq RG2010-C_{18}) and II (Nucleosil 500-C_{18}).

The parameter b of the Langmuir isotherm for cholesteryl formate in pure acetonitrile is negative, which does not make any physical sense within the framework of the Langmuir model. The reason for this behavior is that, differing from all other isotherms, the experimental isotherm of this compound is convex downwards, which explains the negative value for b and is inconsistent with the Langmuir model.

The data in Tables I and II show that the parameters a and b of the Langmuir isotherm of cholesterol decrease with increasing concentration of dichloromethane in acetonitrile. This is in agreement with the reversed-phase retention mechanism. Increasing the concentration of a less polar solvent

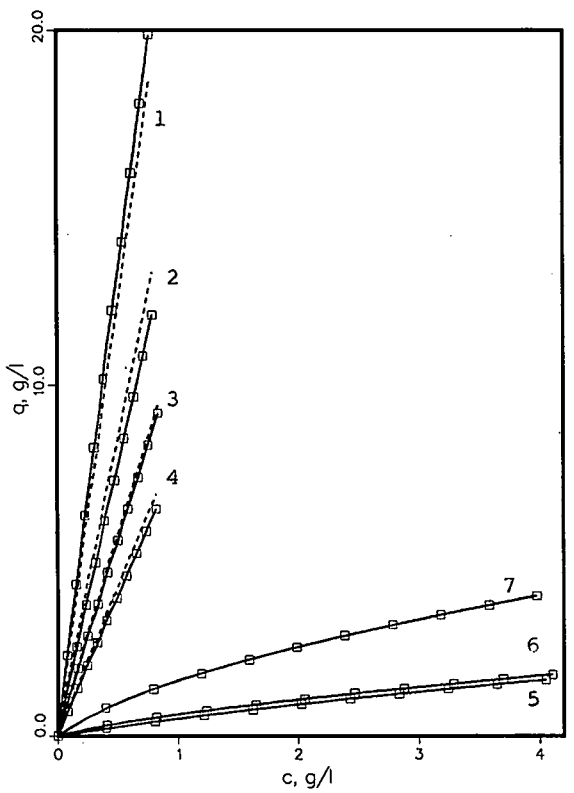

Fig. 4. Isotherms of cholesterol on an Impaq RG2010-C_{18} column in solutions containing (1) 0%, (2) 5%, (3) 10%, (4) 13.6%, (5) 98%, (6) 99% and (7) 100% *n*-hexane in acetonitrile at 35°C. Symbols, experimental data measured by frontal analysis; solid lines, best fits to the three-parameter quadratic isotherm (eqn. 9); dashed lines, isotherms calculated using the relationships derived in this work between the parameters A_1, A_2 and B of this isotherm and the concentration of dichloromethane in the mobile phase (from Table VII).

in a more polar solvent increases the solubility and decreases the retention of hydrophobic molecules such as the steroids studied here, and hence decreases the ratio of the adsorption and desorption rate constants, k_1/k_2.

A comparison of the dependence of the isotherm parameters on the composition of the mobile phase for the two C_{18}-bonded silica columns shows that the values of the parameter a of the Langmuir isotherm are always higher for the Impac C_{18} than for the Nucleosil C_{18}, whereas the opposite holds true for the parameter b (Tables I and II). The larger retention volume and the higher specific saturation capacity for Impaq C_{18} than for Nucleosil C_{18} are in agreement with the higher specific surface area of the former stationary phase.

We expect the specific surface area to have little effect on the rate constants of adsorption and desorption, whereas the saturation capacity should be proportional to this area. The large variation of the apparent specific saturation capacity ($q_s = a/b_L$) with increasing dichloromethane concentration in Tables I and II does not seem compatible with the

TABLE I

REPRESENTATION OF THE EXPERIMENTAL DATA WITH THE LANGMUIR ISOTHERM

Stationary phase, Impac RG2010-C_{18}. n.a. = Not applicable.

Solute[a]	φ[b]	a	b	q_s (mg/ml)
1	0	22.78	0.064	356
2	0	8.66	0.078	111
3	0	25.45	−0.031	n.a.
4	0	28.79	0.179	161
4	10	14.29	0.063	227
4	20	8.25	0.028	295
4	30	4.8	0.023	209
4	40	2.97	0.018	165
4	50	1.85	0.015	123
4	60	1.21	0.010	121
4	80	0.46	0.010	46

[a] Solutes: 1 = cholestanone; 2 = cholesteryl acetate; 3 = cholesteryl formate; 4 = cholesterol.
[b] Solvent composition (% dichloromethane in acetonitrile).

TABLE II

REPRESENTATION OF THE EXPERIMENTAL DATA WITH THE LANGMUIR ISOTHERM

Stationary phase, Nucleosil 500-C_{18}.

φ[a]	a	b	q_s (mg/ml)
0	17.26	0.264	65
5	11.67	0.168	69
10	9.16	0.114	80
30	3.21	0.083	39
40	1.96	0.055	36
50	1.05	0.038	28
60	0.63	0.027	23

[a] Solvent composition (% dichloromethane in acetonitrile).

Langmuir model assumptions. The surface area occupied by one adsorbed molecule on the surface should not depend to that extent on the solvent composition, even if the values of the saturation capacity at high dichloromethane concentrations are not considered, because of their relative lack of accuracy (too small a retention).

One can calculate that a saturation capacity of 100 mg/ml for cholesterol (MW = 386.64) corresponds to 0.26 mol/l. With a packing density of 0.5 kg/l and a surface area of 139 m^2/g, this would give a surface area of 45 $Å^2$ per cholesterol molecule, a small value for this flat molecules, but still a likely order of magnitude. An estimate of the maximum saturation capacity with a Langmuir isotherm can be derived from the surface area, assuming spherical molecules with a density of 1.5 (thus, packing to a fluid of 0.90 density). The diameter of such a molecule would be 9.35 Å. A dense monolayer (hexagonal distribution) of such spheres on the silica surface (area 69.5 m^2/ml) would include $9.1 \cdot 10^{19}$ molecules for a mass of 58 mg. Because a dense packing is impossible, some pores are not accessible to cholesterol and this molecule is flat and may be solvated, a saturation capacity of the order of 10–30 mg/ml would be more reasonable. The values in Tables I and II are unrealistically high, confirming the failure of the Langmuir model.

Three-parameter eqn. 9

The results of a fit of the three-parameter quadratic isotherm (eqn. 9) to all the experiment data sets is shown by the solid lines in Figs. 1–4. The agreement is much better than with the Langmuir model, with an average relative difference (model error) between the experimental values of q and the values calculated from the best-fit three-parameter quadratic isotherm between 0.05 and 0.8%. The best values obtained for the parameters a_1, a_2 and b of this isotherm equation (eqn. 9) when fitted to our experimental data are given in the Tables III (Impaq RG2010-C_{18}) and IV (Nucleosil 500-C_{18}). Also included in these tables are the values of A_1, A_2, the adsorption capacity, q_s, and the ratio of the second-layer association and desorption rate constants, k_1^*/k_2^*, derived from the values of a_1, a_2 and b (eqns. 10a–c and 11).

The values of the parameter b of the three-parameter quadratic isotherm equation are all positive, but they differ significantly between the individual compounds. For all the solutes, except cholesteryl formate, the ratio of the first layer adsorption and desorption rate constants ($b = k_1/k_2$) is greater than the corresponding rate constant ratio for the association in the second layer (k_1^*/k_2^*). The opposite behavior of cholesteryl formate results in a negative value for the parameter a_1 (but positive values for

TABLE III

REPRESENTATION OF THE EXPERIMENTAL DATA WITH THE THREE-PARAMETER QUADRATIC ISOTHERM

Stationary phase, Impaq RG2010-C_{18}. See eqn. 10, with $q_s = A_1/B = (a_1 + a_2)/b$, $k_1/k_2 = B$ and $k_1^*/k_2^* = A_2/A_1 = a_2 b/(a_1 + a_2)$.

Solute[a]	φ^b	a_1	a_2	b	q_s (mg/ml)	A_1	A_2	k_1^*/k_2^*
1	0	2.93	20.12	1.11	21	23.05	22.3	0.97
2	0	1.51	7.67	3.13	2.9	9.2	24.0	2.62
3	0	−11.3	36.77	0.076	335	25.5	2.79	0.11
4	0	12.89	25.11	22.50	1.70	38.0	565.0	14.9
4	10	3.19	12.64	3.82	4.1	15.8	48.3	3.05
4	20	1.34	7.42	1.48	5.9	8.8	11.0	1.25
4	30	1.05	3.97	0.40	12.6	5.0	1.60	0.32
4	40	0.86	2.28	0.22	14.3	3.14	0.50	0.16
4	50	0.66	1.27	0.10	19.3	1.93	0.13	0.07
4	60	0.47	0.78	0.05	25	1.25	0.04	0.03
4	80	0.23	0.25	0.04	12	0.48	0.01	0.02

[a] Solutes: 1 = cholestanone; 2 = cholesteryl acetate; 3 = cholesteryl formate; 4 = cholesterol.
[b] Solvent composition (% dichloromethane in acetonitrile).

TABLE IV

REPRESENTATION OF THE EXPERIMENTAL DATA WITH THE THREE-PARAMETER QUADRATIC ISOTHERM

Stationary phase, Nucleosil 500-C_{18}. See eqn. 10, with $q_s = A_1/B = (a_1 + a_2)/b$, $k_1/k_2 = B$ and $k_1^*/k_2^* = A_2/A_1 = a_2b/(a_1 + a_2)$.

φ^a	a_1	a_2	b	q_s (mg/ml)	A_1	A_2	k_1^*/k_2^*
0	6.96	13.92	11.64	1.8	20.9	162.0	7.76
5	5.17	9.92	7.45	2.0	15.1	73.9	4.90
10	4.26	7.56	4.47	2.6	11.8	33.8	2.86
30	1.62	1.76	0.43	7.85	3.4	0.75	0.22
40	1.06	0.96	0.25	8.1	2.02	0.24	0.12
50	0.69	0.45	0.13	8.8	1.14	0.06	0.05
60	0.57	0.24	0.16	5.1	0.81	0.04	0.04

[a] Solvent composition (% dichloromethane in acetonitrile).

A_1, A_2 and B) and in an isotherm which is slightly concave upward, whereas the isotherms of all the other compounds tested are slightly convex upward, as normally expected.

The data in Tables III and IV show that the parameters a_1, a_2 and b_T of the three-parameter quadratic isotherm of cholesterol decrease with increasing concentration of dichloromethane in acetonitrile, and so does the ratio k_1^*/k_2^*. As explained above in the case of the Langmuir isotherm, this is in agreement with the reversed-phase retention mechanism. Increasing the concentration of a less polar solvent in a more polar solvent not only increases the solubility and decreases the retention of this hydrophobic molecule by decreasing the ratio of the first-layer adsorption and desorption rate constants, k_1/k_2. At the same time as the solubility of cholesterol in the mobile phase increases, we expect that the ratio of the second-layer association rate constants, k_1^*/k_2^*, should decrease with increasing compound solubility in the bulk liquid phase. This is what we observe in the Tables III and IV.

However, we expect the model to give comparable values of the specific saturation capacities for the four steroids whose molecules have comparable sizes, and a nearly constant value for the specific saturation capacity of cholesterol when the dichloromethane concentration is increased. The experimental results are certainly not in agreement with this prediction. The order of magnitude is reasonable except at very low dichloromethane concentrations where the isotherm is nearly linear and the coefficients inaccurate. The increase in the saturation capacity with increasing dichloromethane concentration could be explained by a decreasing degree of solvation of the cholesterol molecule and an increasing solubility of the bonded alkyl chains in the mobile phase. More investigations are needed in this area.

Comparing Tables III and IV, we see that the parameters a_1 and a_2 are higher on Impaq C_{18} than on Nucleosil C_{18}, whereas the values obtained for the parameters b and k_1^*/k_2^* on the two phases are close, with the exception of the data measured with pure acetonitrile as the mobile phase. We expect the specific surface area to have little effect on the ratios of the rates of adsorption and desorption in the first and second adsorption layers but to affect to a greater extent the adsorption capacity, which is the result observed. The saturation capacity for Nucleosil 500-C_{18} is between two and three times smaller than for Impac C_{18}, in agreement with the four times smaller specific surface area and the 2.5 times larger average pore size, making the adsorbent surface more accessible.

We attempted to fit the Fowler isotherm equation (eqn. 17) to the experimental data sets for the C_{18} columns. These attempts were unsuccessful, probably because, at a given adsorption capacity and initial isotherm slope, the initial curvature of the isotherm increases with increasing value of χ, while the comparison between the results obtained with the Langmuir and the three-parameter isotherm shows that experimental results are better repre-

sented by an equation which has a smaller initial curvature than the Langmuir isotherm.

Four-parameter isotherms

Not surprisingly, a fit of the four-parameter quadratic isotherm equation (eqn. 4) to the experimental data sets, using non-linear regression, gave better results than those obtained with the three-parameter equation (eqn. 9). The values of the parameters A_1, A_2, B_1 and B_2 of this isotherm for the four solutes and the different stationary and mobile phases investigated are reported in the Tables V and VI, together with the parameters A_1, A_2 and B of the three-parameter isotherm (eqn. 9) calculated from the values of the parameters a_1, a_2 and b in Tables III and IV, using eqn. 10a–c.

The values calculated for the parameters A_1 and A_2 of the three- and four-parameter isotherm equations are generally close. In contrast, the values obtained for the parameters B_1 of the four-parameter isotherm equation differ significantly from the value of the parameter b in the Tables III and IV. For this reason, we used the parameter B_1 of the four-parameter isotherm instead of the parameter b in eqns. 10a–11 for the calculation of the coefficient A_2 of the three-parameter isotherm in Tables V and VI. A comparison between these tables and the Tables III and IV shows the extent of the differences.

Variation of isotherm parameters with mobile phase composition

Like the parameters a_1, a_2 and b, the parameters A_1, A_2 and B_1 of either the three- or the four-parameter isotherms decrease with increasing dichloromethane concentration in the mobile phase. By analogy with the well known dependence of the retention factors on the mobile phase composition in reversed-phase systems [16], we can expect the following empirical relationships to describe properly the ratios k_1/k_2 and k_1^*/k_2^* as a function of the concentration of dichloromethane in the mobile phase, φ:

$$\frac{k_1}{k_2} = k_0 e^{-\kappa\varphi} \quad (18a)$$

$$\frac{k_1^*}{k_2^*} = k'_0 e^{-\kappa'\varphi} \quad (18b)$$

where κ is a numerical coefficient.

If these empirical equations apply, we can expect an exponential decrease in the parameters A_1, A_2 and B of the three-parameter isotherm (eqn. 9) with increasing mobile phase concentration of dichloromethane. For the four-parameter isotherms (eqns. 13 and 16), a similar dependence is expected for A_1 and A_2. The results of the linear regressions of the logarithms of the isotherm parameters of cholesterol

TABLE V

REPRESENTATION OF THE EXPERIMENTAL DATA WITH THE THREE-PARAMETER (EQN. 9) AND THE FOUR-PARAMETER QUADRATIC (EQNS. 4 AND 16) ISOTHERMS

Stationary phase, Impaq RG2010-C_{18}; mobile phase, acetonitrile–dichloromethane. Solutes and φ as in Table I; A_1 (T) and A_2 (T) were calculated from eqn. 10a–c using the parameters a_1 and a_2 of the isotherm (eqn. 9) from Table III and the values of B_1 for b.

Solute	φ	A_1	A_2	B_1 (l/g)	B_2 [(l/g)^2]	A_1(T)	A_2(T)
1	0	23.11	33.61	1.62	0.019	23.11	32.56
2	0	9.12	19.60	2.59	−0.014	9.17	19.86
3	0	25.48	2.35	0.07	−0.007	25.43	2.44
4	0	34.49	292.2	11.94	−0.254	37.99	299.9
4	10	15.72	43.15	3.43	−0.006	15.83	43.38
4	20	8.75	10.28	1.39	−0.001	8.77	10.31
4	30	5.14	3.36	0.80	0.004	5.02	3.16
4	40	3.30	1.56	0.61	0.003	3.14	1.40
4	50	2.11	0.90	0.56	0.004	1.93	0.71
4	60	1.42	0.55	0.50	0.003	1.25	0.39
4	80	0.56	0.14	0.35	0.002	0.48	0.09

TABLE VI

REPRESENTATION OF THE EXPERIMENTAL DATA WITH THE THREE-PARAMETER (EQN. 9) AND THE FOUR-PARAMETER QUADRATIC (EQNS. 4 AND 16) ISOTHERMS

Stationary phase, Nucleosil 500-C_{18}; mobile phase, acetonitrile–dichloromethane. Solutes and φ as in Table II; isotherm parameters as in Table V.

φ	A_1	A_2	B_1 (l/g)	B_2 [(l/g)^2]	A_1(T)	A_2(T)
0	20.43	134.77	9.73	−0.216	20.88	135.48
5	14.88	64.30	6.37	−0.110	15.09	63.16
10	11.30	39.36	5.30	−0.064	11.82	40.03
30	3.96	3.15	1.32	0.039	3.38	2.33
40	2.58	1.54	1.05	0.023	2.02	1.01
50	1.27	0.91	0.98	0.023	1.41	0.44
60	0.95	0.40	0.81	0.012	0.81	0.19

on the concentration of dichloromethane in the mobile phase are reported in Table VII. These results are in general agreement with our other conclusions. The correlation coefficients are best for A_1, acceptable for A_2 and poor for B_1. No such dependence is observed for B_2.

The dashed lines in Figs. 2 and 3 show the three-parameter quadratic isotherms (eqn. 9) calcu-

TABLE VII

DEPENDENCE OF THE ISOTHERM PARAMETERS ON THE MOBILE PHASE COMPOSITION

Slopes (s) and intercepts (i) of the regression equations relating the mobile phase composition (φ) and the natural logarithms of the parameters A_1, A_2, B_1 and B_2 of the four-parameter quadratic isotherm (eqns. 4 and 16) and of the parameters A_1 and A_2 of the three-parameter quadratic isotherm (eqn. 9) of cholesterol. Isotherm parameters as in Table III; R^2 = correlation coefficient. Columns: I = Nucleosil 500-C_{18}; II = Impaq RG2010-C_{18}. Solvents: ACN = acetonitrile; DCM = dichloromethane; HEX = n-hexane; %HEX = 0–13.6%; %ACN = 0–2%.

Column	Mobile phase	φ	Parameter	Intercept	Slope	R^2
I	ACN–DCM	%DCM	A_1	2.968	−0.0519	0.9961
I	ACN–DCM	%DCM	A_2	4.618	−0.0975	0.9814
I	ACN–DCM	%DCM	B_1	2.039	−0.0430	0.9285
I	ACN–DCM	%DCM	A_1 (T)	2.990	−0.0557	0.9958
I	ACN–DCM	%DCM	A_2 (T)	4.693	−0.1114	0.9884
II	ACN–DCM	%DCM	A_1	3.282	−0.0498	0.9893
II	ACN–DCM	%DCM	A_1	4.623	−0.0905	0.9402
II	ACN–DCM	%DCM	B_1	1.570	−0.0399	0.8021
II	ACN–DCM	%DCM	A_1 (T)	3.347	−0.0527	0.9887
II	ACN–DCM	%DCM	A_2 (T)	4.703	−0.0966	0.9525
II	ACN–HEX	%HEX	A_1	3.542	−0.1009	0.9999
II	ACN–HEX	%HEX	A_2	5.774	−0.1498	0.9118
II	ACN–HEX	%HEX	B_1	2.571	−0.0639	0.6830
II	ACN–HEX	%HEX	A_1 (T)	3.641	−0.1061	0.9998
II	ACN–HEX	%HEX	A_2 (T)	5.798	−0.1500	0.9154
II	ACN–HEX	%ACN	A_1	0.967	−0.7364	0.9274
II	ACN–HEX	%ACN	A_2	0.763	−0.6171	0.8923
II	ACN–HEX	%ACN	B_1	0.804	−0.1535	0.9413
II	ACN–HEX	%ACN	A_1 (T)	0.854	−0.7048	0.9705
II	ACN–HEX	%ACN	A_2 (T)	0.141	−0.2787	0.7887

lated using the values of the parameters A_1, A_2 and B derived from the regression equations in Table VII, *i.e.*, using a single equation to account for the equilibrium isotherm in the whole range of mobile phase composition investigated. The agreement between this general isotherm equation and the experimental data is very good over a broad range of mobile phase compositions, from 0 to 50% dichloromethane. At higher dichloromethane concentrations, the differences between experimental and calculated data are more significant, but are still reasonably small below 80%.

The intercepts of the linear regressions of the logarithm of the parameter A_1 on the dichloromethane concentration in the mobile phase are higher on the Impaq C_{18} column than on the Nucleosil C_{18} column (Table VII). This was expected, as these intercepts depend on the adsorption capacity, which should be higher for Impaq C_{18} which has the larger specific surface area. On the other hand, the intercepts of the regressions for B_1 and the slopes for all three parameters of eqn. 9 do not depend on the saturation capacity and, according to eqns. 10a–c and 18a and b, should be far less affected by the type of C_{18}-bonded silica used. In agreement with these considerations, the values found for the two columns tested are close: -0.052 and -0.050 for the slopes of the A_1 regression, -0.098 and -0.091 for the slopes of the A_2 regression and -0.043 and -0.040 for the slopes of the B_1 regression.

Comparison between the models

The results discussed so far indicate that the four-parameter quadratic isotherm (eqn. 4) gives a very accurate representation of the experimental data. To a first approximation, however, these data are also in good agreement with a model assuming association between sorbed molecules in the second layer, but without competition (three-parameter quadratic isotherm, eqn. 9).

The small difference between the quality of the representation afforded by these two models is explained by the small values of the parameter B_2 in the four-parameter model, generally close to zero. The values of B_2 are lower for Impaq C_{18} than for Nucleosil C_{18}, except for cholesterol in pure acetonitrile. On both columns, the values of B_2 for cholesterol are negative in mobile phases containing 0–20% of dichloromethane in acetonitrile. They increase with increasing concentration of dichloromethane until small positive values are achieved at high concentrations. Because of the systematic character of this variation, it is unlikely that the negative values of B_2 at low concentrations could result from experimental errors or from errors made in fitting the data.

Isotherm model with limited solubility (eqn. 16)

Both four-term quadratic isotherms, whether taking into account full (eqn. 4) or partial (eqn. 13) competition for adsorption in the second layer, predict positive values for all the isotherm parameters and cannot explain negative values of B_2 for cholesterol and its esters in pure acetonitrile or in acetonitrile-rich mobile phases. However, the parameters A_2, B_1 and/or B_2 can be either positive or negative for the four-parameter quadratic isotherm model which takes into account a limited solubility of the solute in the mobile phase (eqn. 16).

The two adsorption–desorption rate constant ratios k_1/k_2 and k_1^*/k_2^* in eqn. 16 cannot be compared directly with the corresponding ratios estimated on the basis of the three-term isotherm (eqn. 9) because in the latter isotherm the ratios do not take into account the influence of the solubility of the solutes in the mobile phase. Considering the experimental solubilities of cholesterol determined recently and published elsewhere [12], we can calculate the values of these two rate constant ratios and of the proportionality constant p, knowing the constants of the four-parameter quadratic isotherm and assuming the validity of eqn. 16. The values obtained are reported in the Table VIII for the Impaq C_{18} column. On the basis of the parameters in this table, the dependence of the constant B_1 on the concentration of dichloromethane in the mobile phase can be explained as follows.

The proportionality constant p in eqn. 16 represents the fraction of molecules sorbed in the second layer which are not available for direct association with other solute molecules in the bulk liquid phase; p can be expected to increase with increasing solubility in the mobile phase, while the two rate constant ratios k_1/k_2 and k_1^*/k_2^* decrease. In mobile phases with low dichloromethane concentrations, the two rate constant ratios of cholesteryl esters and cholesterol are probably significantly higher than unity

TABLE VIII

REPRESENTATION OF THE EXPERIMENTAL DATA WITH THE FOUR-PARAMETER QUADRATIC ISOTHERM (EQN. 16) WHEN SOLUBILITY IS LIMITED

Stationary phase: Impaq RG2010-C_{18}. φ = % dichloromethane in acetonitrile. The values of the parameters k_1/k_2, k_1^*/k_1^*, p and q_s of the quadratic isotherm (eqn. 16) are calculated from the best values of the parameters A_1, A_2, B_1 and B_2 of the quadratic isotherm (eqn. 4), using the experimental solubilities C_x of cholesterol in mixtures of acetonitrile and dichloromethane on the Impaq RG2010-C_{18} column.

φ	C_x (g/l)	k_1/k_2	k_1^*/k_2^*	p	pk_1^*/k_2^*	q_s
0	0.872	11.43	7.40	0.133	0.981	2.631
10	2.241	8.69	6.15	0.162	0.996	4.053
20	3.932	6.46	4.62	0.216	0.998	5.322
30	6.794	6.39	4.42	0.234	1.033	5.465

and the coefficients A_2 and B_1 are positive. If p is low, however, the product pk_1^*/k_2^* can be lower than unity and B_2 is negative. When the concentration of dichloromethane increases, p increases more rapidly than the ratio k_1^*/k_2^* decreases, the product pk_1^*/k_2^* becomes higher than unity and the term B_2 is positive. However, because the solubility C_x also increases, B_2 is close to zero.

Most probably, the proportionality constant p increases with decreasing polarity of the molecule. Since the order of group polarity is keto < ester < hydroxyl, p should be larger for cholestanone than for cholesteryl esters, and larger for these esters than for cholesterol. This could explain why B_2 is positive for cholestanone in pure acetonitrile.

Isotherms with acetonitrile–n-hexane solutions

The results obtained with solutions of either *n*-hexane or dichloromethane in acetonitrile as mobile phases were very similar. The quality of the fit of the different isotherm equations used here to the experimental data measured on the Impaq C_{18} column with mobile phases containing moderate concentrations (below 14%) of *n*-hexane in acetonitrile is similar to that observed with acetonitrile–dichloromethane mobile phases. With these latter solutions, the average errors on the calculated values of q are 0.6–1% for the Langmuir isotherm, 0.06–0.2% for the three-parameter isotherm (eqn. 9) and 0.02–0.08% for the four-parameter quadratic isotherm (eqn. 4).

The average errors with mobile phases containing small concentrations of acetonitrile (below 3%) in *n*-hexane were 1–2.7% for the Langmuir isotherm, 0.3–0.7% for the three-parameter isotherm and 0.05–0.24% for the four-parameter isotherm. It was not possible to measure isotherms in mobile phases containing between 3 and 85% of acetonitrile in *n*-hexane, because these solvents are not miscible in this range of concentrations. In Fig. 4, we show the best three-parameter equation (solid lines) fitted to the experimental data (symbols). Attempts to fit the Fowler isotherm to the experimental data failed as they did with isotherm data obtained with mixtures of acetonitrile and dichloromethane.

In Table IX, we give the values of the parameters a and b_L of the Langmuir isotherm and of the parameters a_1, a_2 and b_T of the three-parameter isotherm (eqn. 9) of cholesterol on Impaq C_{18} with acetonitrile–*n*-hexane mobile phases, together with the ratios of the second layer association–desorption rates k_1^*/k_2^* calculated from eqns. 10 and 11. In mobile phases having a high acetonitrile content, the parameters of both the Langmuir and the three-parameter quadratic isotherms decrease with increasing *n*-hexane concentration, in agreement with the assumptions of the reversed-phase mechanism. On the other hand, in *n*-hexane-rich mobile phases, the isotherm parameters decrease with increasing acetonitrile concentration, which is expected for normal-phase systems. This behavior can probably be attributed to the existence of residual, unshielded silanol groups at the surface of the stationary phase.

TABLE IX

REPRESENTATION OF THE EXPERIMENTAL DATA WITH THE LANGMUIR AND THE THREE-PARAMETER ISOTHERMS

Stationary phase, Impac RG2010-C_{18}; mobile phase, acetonitrile–*n*-hexane. φ = % *n*-hexane in acetonitrile; parameters of the isotherms as in Table I.

φ	a	b_L (l/g)	a_1	a_2	b_T (l/g)	k_1^*/k_2^*
0	28.79	0.179	12.89	25.11	22.50	14.9
10	11.60	0.080	2.52	10.83	18.78	15.2
13.6	8.32	0.082	1.21	7.71	8.22	7.1
98	0.54	0.097	0.35	0.27	0.45	0.19
99	0.88	0.167	0.64	0.37	0.66	0.24
100	2.16	0.304	1.95	0.57	0.87	0.20

In Fig. 4, we show that the isotherms of cholesterol are more strongly curved in mobile phases having a high *n*-hexane concentration (conditions under which the normal-phase mechanism tends to control the retention) than in mobile phases having a high acetonitrile concentration, for which the reversed-phase mechanism applies. The ratio k_1^*/k_2^* should decrease with increasing solubility of cholesterol, *i.e.*, with increasing concentration of *n*-hexane in the mobile phase. This is the result observed.

The comparison of the values of the parameters A_1, A_2 and B calculated from a_1, a_2 and b of the three-parameter isotherm (eqn. 15) with the values of the corresponding parameters determined by fitting the four-parameter quadratic isotherm (eqn. 4) in Table X shows good agreement for A_1, fair agreement for A_2 in acetonitrile-rich mobile phases and poor agreement for A_2 in mobile phases with low concentrations of acetonitrile and for B_1. The parameters of the linear relationship between the logarithm of the isotherm parameters and the mobile phase concentration of *n*-hexane (at high acetonitrile concentrations) or of acetonitrile (at high *n*-hexane concentrations), φ, were in general agreement with eqn. 18. However, the quality of the correlation decreases in the order $A_1 > A_2 > B_1$ (see Table VII). These results are similar to those obtained with acetonitrile–dichloromethane solutions. The slopes of these relationships are steeper for *n*-hexane than for dichloromethane, in agreement with the lower polarity and higher solvent strength of *n*-hexane in non-aqueous reversed-phase systems (Table VII).

TABLE X

REPRESENTATION OF THE EXPERIMENTAL DATA WITH THE THREE-PARAMETER (EQN. 9) AND THE FOUR-PARAMETER QUADRATIC (EQNS. 4 AND 16) ISOTHERMS

Stationary phase, Impaq RG2010-C_{18}; mobile phase, acetonitrile–*n*-hexane. φ = % of *n*-hexane in acetonitrile; isotherm parameters as in Table V.

φ	A_1	A_2	B_1 (l/g)	B_2 [(l/g)^2]	A_1(T)	A_2(T)
0	34.50	292.20	11.944	−0.254	37.99	299.9
10	12.67	103.75	9.72	−0.104	13.35	105.2
13.6	8.72	32.08	4.27	−0.078	8.92	32.9
98	0.68	0.71	1.61	0.077	0.62	0.72
99	0.99	0.90	2.00	0.110	1.01	0.74
100	2.96	2.43	2.19	0.180	2.52	1.25

The dashed lines in Fig. 4 compare the data and the three-parameter isotherms (eqn. 9) calculated with the values of the parameters A_1, A_2 and B derived from the regression equations in Table VII. The degree of agreement achieved between the experimental data at high acetonitrile concentrations and the predictions of this general isotherm whose parameters are obtained as a function of φ is similar to the agreement seen in Figs. 2 and 3 for acetonitrile–dichloromethane mixtures as mobile phases. As with these solutions, the three-parameter quadratic equation is more suitable than the Langmuir isotherm to describe the experimental isotherm of cholesterol on a C_{18} column in acetonitrile–*n*-hexane solutions, but for precise calculations and for the interpretation of the isotherms, the four-parameter quadratic equation (eqn. 4), with a term B_2 different from zero, should probably be preferred.

The values of the parameters B_2 of the four-parameter quadratic isotherm of cholesterol are negative in mobile phases having a high acetonitrile concentration and positive in mobile phases having a high *n*-hexane concentration. This behavior can be explained by considering the isotherm eqn. 16, derived for the case of a limited sample solubility in the mobile phase, such as happens with the acetonitrile–dichloromethane solutions. In solutions having a low *n*-hexane concentration, the ratio of the second-layer adsorption and desorption rate constants is likely to decrease with increasing cholesterol solubility, *i.e.*, with increasing *n*-hexane concentration in the mobile phase, and the proportionality constant p is also expected to be small. Consequently, the product pk_1^*/k_2^* is lower than unity and, because the ratio of the first-layer adsorption and desorption rate constants, k_1/k_2, is obviously larger than unity, the parameter B_2 is negative, as it is with the solutions having a low dichloromethane concentration in acetonitrile (see above).

In solutions having a high *n*-hexane concentration, the cholesterol solubility is higher than in the solutions concentrated in acetonitrile. Consequently, p is higher and k_1^*/k_2^* is lower with these solutions. It remains possible, however, that the effect of the proportionality constant p predominates and that the product pk_1^*/k_2^* is larger than unity, as in the

TABLE XI

ABILITY OF THE MODELS TO ACCOUNT FOR THE EXPERIMENTAL DATA

Solutes as in Table I. Mobile phases: AC = acetonitrile; DCM = dichloromethane; HEX = *n*-hexane. Mean relative errors (%) of the concentrations q of (1) cholestanone, (2) cholesteryl acetate, (3) cholesteryl formate and (4) cholesterol calculated at equilibrium on the Impaq RG2010-C_{18} (1) or Nucleosil 500-C_{18} (2) column when using the Langmuir isotherm (L, eqn. 2), the three-parameter quadratic isotherm (T, eqn. 9) and the four-parameter quadratic isotherm (Q, eqns. 4 and 16).

Column	Mobile phase	φ	Solute	Mean relative error (%)		
				L	T	Q
1	DCM–AC	0% DCM	2	0.7	0.03	0.02
1	DCM–AC	0% DCM	3	0.23	0.06	0.02
1	DCM–AC	0% DCM	4	1.4	0.09	0.03
1	DCM–AC	10% DCM	4	1.1	0.04	0.03
1	DCM–AC	20% DCM	4	0.72	0.02	0.02
1	DCM–AC	30% DCM	4	0.8	0.11	0.04
1	DCM–AC	40% DCM	4	1.1	0.17	0.03
1	DCM–AC	50% DCM	4	1.1	0.28	0.07
1	DCM–AC	60% DCM	4	1.0	0.34	0.09
1	DCM–AC	80% DCM	4	1.3	0.45	0.12
2	DCM–AC	0% DCM	4	1.7	0.08	0.09
2	DCM–AC	5% DCM	4	1.8	0.14	0.07
2	DCM–AC	10% DCM	4	1.7	0.42	0.20
2	DCM–AC	30% DCM	4	1.5	0.41	0.07
2	DCM–AC	40% DCM	4	2.1	0.54	0.17
2	DCM–AC	50% DCM	4	1.7	0.78	0.40
2	DCM–AC	60% DCM	4	2.1	0.51	0.23
1	HEX–AC	10% HEX	4	0.8	0.06	0.01
1	HEX–AC	14% HEX	4	0.6	0.06	0.01
1	AC–HEX	1% AC	4	2.7	0.53	0.24
1	AC–HEX	2% AC	4	1.0	0.31	0.21

solutions of dichloromethane and acetonitrile which are concentrated in dichloromethane.

CONCLUSIONS

Cholesterol and many similar compounds have a limited solubility in most of the mobile phases used in non-aqueous reversed-phase chromatography. The Langmuir isotherm cannot describe successfully the adsorption behavior of these solutes in such chromatographic systems.

As demonstrated by the results obtained by fitting different isotherm equations to the experimental data (Table XI), a three-parameter quadratic isotherm (eqn. 9) accounts fairly well, as a first approximation, for the adsorption behavior of cholesterol and the related compounds studied on C_{18}-bonded phases in non-aqueous reversed-phase systems. This model accounts especially well for the moderate curvature of the experimental isotherms in the low concentration range. The values of the parameters of this isotherm and their variations with the composition of the solution are in qualitative agreement with the model of non-competitive adsorption or association of the solute molecules on the first adsorbed layer.

The four-parameter quadratic equation based on an isotherm model taking into account the limited solubility of the solute in the mobile phase, together with a non-stoichiometric competition of the adsorbate molecules in the second layer for access to the adsorption sites on the first layer, provides a good fit to the experimental data. The variation of the parameters of this isotherm for Impaq C_{18} with the mobile phase composition is in semi-quantitative agreement with the prediction of the model. With other systems, it is possible to explain qualitatively the observed dependencies of the isotherm param-

eters on the composition of the solution.

The experimental results described demonstrate the usefulness of the isotherm model presented here. This model can explain, at least qualitatively, the single-component experimental isotherms of cholesterol and of some related compounds. This model is also most convenient to fit the experimental data. However, the acquisition of a larger amount of such data would be necessary to prove the physical validity of the model and explain the physical meaning of its parameters.

ACKNOWLEDGEMENTS

We acknowledge the generous gift of the Impaq RG2010-C_{18} sample and detailed information regarding this product by Neil T. Miller (PQ Corp., Conshohoken, PA, USA). This work was supported in part by grant CHE-8901382 from the National Science Foundation and by the cooperative agreement between the University of Tennessee and the Oak Ridge National Laboratory. We acknowledge support of our computational effort by the University of Tennessee Computing Center.

REFERENCES

1 A. M. Katti and G. Guiochon, *Adv. Chromatogr.*, 31 (1991) 1.
2 I. Langmuir, *J. Am. Chem. Soc.*, 38 (1916) 2221.
3 J. D. Andrade, in J. D. Andrade (Editor), *Surface and Interfacial Aspects of Biomedical Polymers*, Vol. 2, Plenum Press, New York, 1985, p. 35.
4 R. J. Laub, *ACS Symp. Ser.*, 297 (1986) 1.
5 R. H. Fowler and E. A. Guggenheim, *Statistical Thermodynamics*, Cambridge University Press, Cambridge, 1939.
6 D. M. Ruthven, *Principles of Adsorption and Adsorption Processes*, Wiley, New York, 1984.
7 T. L. Hill, *Introduction to Statistical Thermodynamics*, Addison-Wesley, Reading, MA, 1960.
8 V. Svoboda, *J. Chromatogr.*, 518 (1990) 77.
9 J. Toth, *Acta Chim. Acad. Sci. Hung.*, 69 (1971) 311.
10 J. M. Honig and L. H. Reyerson, *J. Phys. Chem.*, 56 (1952) 140.
11 M. D. Levan and T. Vermeulen, *J. Phys. Chem.*, 85 (1981) 3247.
12 P. Jandera and G. Guiochon, *J. Chromatogr.*, 588 (1991) 1.
13 G. Guiochon, S. Golshan-Shirazi and A. Jaulmes, *Anal. Chem.*, 60 (1988) 1856.
14 E. Cremer and J. F. K. Huber, *Angew. Chem.*, 73 (1961) 461.
15 S. Golshan-Shirazi, S. Ghodbane and G. Guiochon, *Anal. Chem.*, 60 (1988) 2630.
16 P. Jandera and J. Churáček, *Gradient Elution in Column Liquid Chromatography*, Elsevier, Amsterdam, 1985.

Journal of Chromatography, 605 (1992) 19–31
Elsevier Science Publishers B.V., Amsterdam

CHROM. 24 205

Optimization of the mobile phase for the liquid chromatographic separation of modafinil optical isomers on a Chiral-AGP column

J. E. Drouin and M. Broquaire

Centre de Recherche du Laboratoire L. Lafon, 19 Avenue du Professeur Cadiot, 94701 Maisons-Alfort (France)

(First received January 9th, 1992; revised manuscript received March 24th, 1992)

ABSTRACT

Optical isomers of modafinil were separated by chiral liquid chromatography on a Chiral-AGP column. Optimization of the mobile phase was undertaken in order to obtain a complete resolution of the two isomers. Two buffers, sodium dihydrogenphosphate and ammonium acetate, were studied and the influence of ionic strength and pH was investigated. The results showed that ionic strength was not a major parameter for optimization but that pH was. Ammonium acetate was a considerably better buffer than sodium dihydrogenphosphate. Different organic modifiers, ethanol, 1-propanol, 2-propanol, 1-butanol and 1-pentanol were studied with the two buffers. The best separations were obtained with 1-butanol and 1-pentanol.

INTRODUCTION

Modafinil, 2-[(diphenylmethyl)sulphinyl]acetamide, is an awakening drug [1], recently developed as the racemate; its structure contains an asymmetric sulphur atom. In order to study separately the different properties of pure optical isomers, they were synthesized and an analytical method was needed to assess their optical purity. This method might also be usable for pharmacokinetic studies. The best techniques to achieve these objectives seemed to be chromatographic methods, but gas chromatography failed because of the thermal lability of modafinil. Only liquid chromatography produced satisfactory results.

Different assays using a column packed with *d*-phenylglycine bound to silica gel were attempted using normal-phase high-performance liquid chromatography (HPLC) but failed; the best value of the separation factor was 1.03 for k' values around 20 [2]. Better results were obtained using a column packed with human α-1-acid glycoprotein bounded to silica gel and eluted with a mixture of potassium dihydrogenphosphate buffer and 1-propanol [2]. These chromatographic conditions, coupled with UV detection, were suitable for optical purity assessment, the purpose for which they were developed, but failed for pharmacokinetic purposes because of the lack of sensitivity and selectivity.

In order to circumvent these limitations, the different parameters which could improve a chromatographic separation were investigated bearing in mind that, for modafinil, the sensitivity and selectivity could be increased by using mass spectrometry (MS) with a thermospray (TSP) interface as a detector [3]. For this reason, potassium dihydrogenphosphate buffer was replaced with ammonium acetate buffer and different organic modifiers were tried.

This paper reports the optimization of the two mobile phases (dihydrogenphosphate and acetate) and their comparison.

Correspondence to: Dr. M. Broquaire, Centre de Recherche du Laboratoire L. Lafon, 19 Avenue du Professeur Cadiot, 94701 Maisons-Alfort, France.

0021-9673/92/$05.00

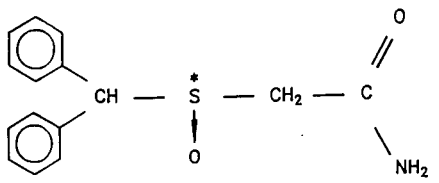

Fig. 1. Formula of modafinil.

EXPERIMENTAL

Standards

Modafinil, the structure of which is given in Fig. 1, and its two optical isomers CRL 40982 (−) and CRL 40983 (+), were synthesized in the research laboratories of Laboratoire L. Lafon (Maisons-Alfort, France). Standards solutions were prepared by dissolving separately 20 mg of modafinil and 10 mg of each isomer in 20 ml of methanol followed by 1:40 dilution 0.01 *M* KH_2PO_4. The volume of each solution injected was 20 μl, representing injected amounts corresponding to 0.9 nmol of each isomer.

Reagents and solvents

The reagents used to prepare buffer solutions, ammonium acetate, potassium dihydrogenphosphate and dipotassium hydrogenphosphate, were of analytical-reagent grade and were purchased from Prolabo (Paris, France). Acetic acid was purchased from UCB (Leuven, Belgium). Alcohols, used as organic modifiers, were of analytical-reagent or HPLC grade and were purchased from Prolabo and Merck (Darmstadt, Germany).

Equipment

The liquid chromatograph consisted of an SP 8780 autosampler equipped with a 20-μl loop, an SP 8800 ternary HPLC pump, an SP 8490 UV–visible programmable spectrophotometer operating at 220 nm and 0.2 a.u.f.s. and a Data Jet integrator, connected together through a Labnet Network (Spectra-Physics, Les Ulis, France). Chromatograms and data could be stored and treated on a Winner station (Spectra-Physics).

A Chromtech Chiral α AGP chromatographic column (10 cm × 4.6 mm I.D.) (Interchim, Montluçon, France) was thermostated with a Crococil insulated thermoregulated oven (Cluzeau, Ste. Foy la Grande, France). The flow-rate through the column was maintained at 1.0 ml/min and the temperature in the oven at 40°C throughout the study.

Experimental variables

Two different buffers were investigated: Potassium dihydrogenphosphate, which is recommended by the manufacturer of the Chiral α AGP column (but which is unusable in LC–TSP-MS, and ammonium acetate, which is usable with a TSP interface.

For each buffer, the following parameters were investigated, in this order: pH of the mobile phase; salt concentration; and nature and concentration of the organic modifier. The organic modifiers investigated were: ethanol, 1-propanol, 2-propanol, 1-butanol and 1-pentanol. Acetonitrile and methanol were found to be inefficient in separating optical isomers of modafinil in a previous study [2].

Measured parameters

For each set of chromatographic conditions, the column was equilibrated at a flow-rate of 1.0 ml/min until stable retention times were obtained for modafinil standard solution. The discrimination factor, d_0[a] [4] was measured from the chromatogram obtained, then CRL 40982 and CRL 40983 standard solutions were successively injected and the following parameters were measured simply with a millimetre graduated ruler: d_{R0}, "dead volume" distance of the chromatographic system, d_R, retention distance of the compound, and $b_{0,5}$, width at half-height.

From these values, the following parameters were calculated: k'_1, capacity factor of CRL 40982; k'_2, capacity factor of CRL 40983; α, separation factor, $\alpha = k'_2/k'_1$; R_s, resolution between CRL 40982 and CRL 40983; N_1, number of theoretical plates per metre for CRL 40982; and N_2, number of theoretical plates per metre for CRL 40983.

The values of N (and to a lesser extent R_s) must be treated with caution, as they were calculated from

[a] The discrimination factor, d_0, between two consecutive peaks was defined by El Fallah and Martin [4] as $d_0 = (h_p - h_v)/h_p$, where h_p is the distance from the top of the smallest peak to the baseline and h_v is the distance from the bottom of the valley between the two peaks to the baseline.

$b_{0.5}$ values for which the relative accuracy varied between 2 and 5%; consequently the relative accuracy of N and R_s ranged between 4 and 10% at least. For this reason, only variations of N and R_s larger than 15% should be considered.

RESULTS

During previous studies with potassium dihydrogenphosphate, we noticed that the efficiency of Chiral-AGP columns could drastically decrease because of the occurrence of a hole at the top of the column. Pouring in a small amount of Chiral-AGP slurry, to complete the bed of stationary phase, restored the column efficiency. Therefore, at the end of each study of the influence of one parameter, the column was re-equilibrated with the mobile phase used at the beginning of that study and standard solution was injected; if the values of d_R and $b_{0.5}$ had changed, the column was carefully checked, repacked if necessary and the experiments were repeated. If no hole was observed, the column was changed. In the phosphate buffer study, such a change was needed after the study of ionic strength. With acetate buffer, a change would occur after having studied the influence of basic pH, but this was done only after the ionic strength study.

Phosphate buffer

Influence of pH. Variations of mobile phase pH were obtained by mixing in different ratios a 0.01 *M* aqueous solution of KH_2PO_4 and a 0.01 *M* aqueous solution of K_2HPO_4, each solution containing 0.5% of 1-butanol as organic modifier. The ratios and corresponding pH values are listed in Table I.

Variations in k', α, R_s, d_0 and N *versus* pH are displayed in Fig. 2A–E, respectively. Small variations in the acidic or basic range did not influence the k' values but there was a net break around pH 7; the k' values for both compounds decreased by about 30%. Larger differences in k' values between CRL 40982 and CRL 40983 were obtained between pH 6 and 7. The break, described for k', was not observed for α values. To a first approximation, within the experimental accuracy, α increased linearly with pH from 1.05 to 1.17; the slope of the linear regression, calculated from experimental data, was equal to $3.31 \cdot 10^{-2}$ k' unit per pH unit.

TABLE I

INFLUENCE OF pH USING 0.01 *M* PHOSPHATE BUFFER: COMPOSITION OF THE MOBILE PHASE

Each KH_2PO_4–K_2HPO_4 mixture contained 0.5% of 1-butanol.

KH_2PO_4:K_2HPO_4	pH	KH_2PO_4:K_2HPO_4	pH
100:0	4.90	50:50	7.06
90:10	6.09	40:60	7.09
80:20	6.43	20:80	7.49
70:30	6.68	15:85	7.62
60:40	6.76	10:90	7.79

In the same way, R_s and d_0 increased linearly with pH in the acidic range but remained fairly constant in basic media. At pH 4.9, d_0 was equal to 0 as there was insufficient separation between CRL 40982 and CRL 40983 [4]. The highest values of R_s (0.79) and of d_0 (0.5) were obtained at pH 7.06. The number of theoretical plates varied in the opposite direction to k'. Variations of N *versus* pH showed complicated curves in which minimum values (about 5000 plates/m) occurred in acidic medium, and maximum values (about 12 000 plates/m) were observed at pH 7.5.

Influence of phosphate concentration. Variations of phosphate concentration were obtained by dilution of a 0.03 *M* aqueous solution of PO_4^{2-} at pH 7.06 with water. The PO_4^{2-} solution was a 50:50 mixture of a 0.03 *M* solution of KH_2PO_4 and a 0.03 *M* solution of K_2HPO_4. The final concentrations of PO_4^{2-} were 0.03, 0.02, 0.01 and 0.005 *M*. Each solution contained 0.5% of 1-butanol as organic modifier.

Variations in k', α, R_s, d_0 and N versus phosphate concentration are displayed in Fig. 3A–E, respectively.

The k' values decreased slowly, from 3.45 to 3.18 for CRL 40982 and from 3.96 to 3.68 for CRL 40983, when the phosphate concentration increased from 0.005 to 0.03 *M*. α (mean value 1.16), R_s (mean value 0.63) and d_0 (mean value 0.4) were independent of phosphate concentration. Variations in the number of theoretical plates were of the same order of magnitude as the experimental accuracy.

Influence of organic modifiers. The mobile phase used to study the influence of organic modifiers was 0.02 *M* phosphate solution (pH 7.06), prepared as

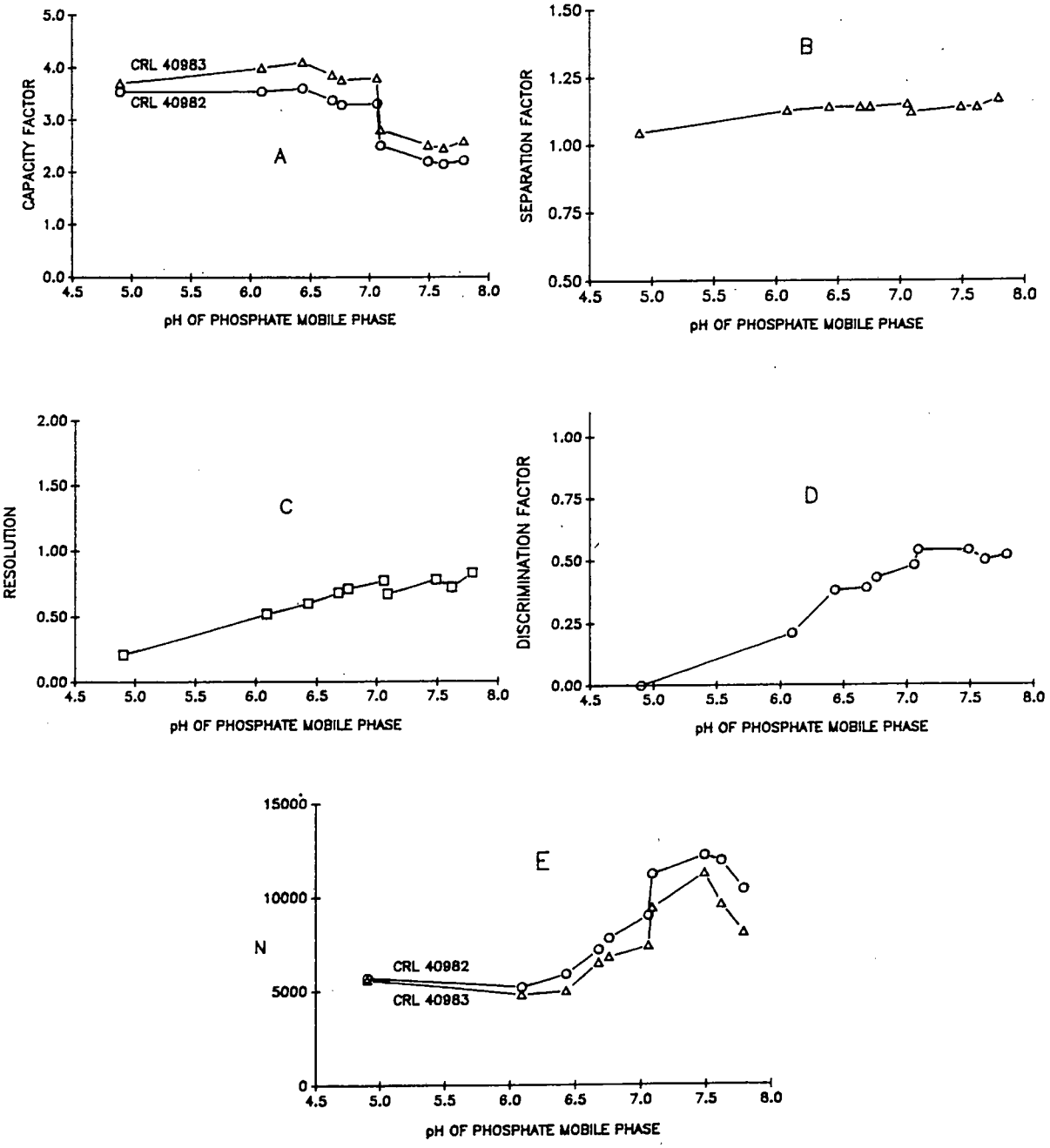

Fig. 2. Phosphate buffer: influence of pH on chromatographic parameters: (A) k'; (B) α; (C) R_s; (D) d_0; (E) N. Mobile phase, 0.5% 1-butanol in 0.01 M phosphate buffer (for composition, see text); flow-rate, 1.0 ml/min; column temperature, 40°C.

described above. In order to have sufficient accuracy, the amounts of organic modifiers were weighed and converted to volume using a density value of 0.8.

Variations in k' values with organic modifier concentration are displayed in Fig. 4A. The elution order was the same, CRL 40982 being eluted before

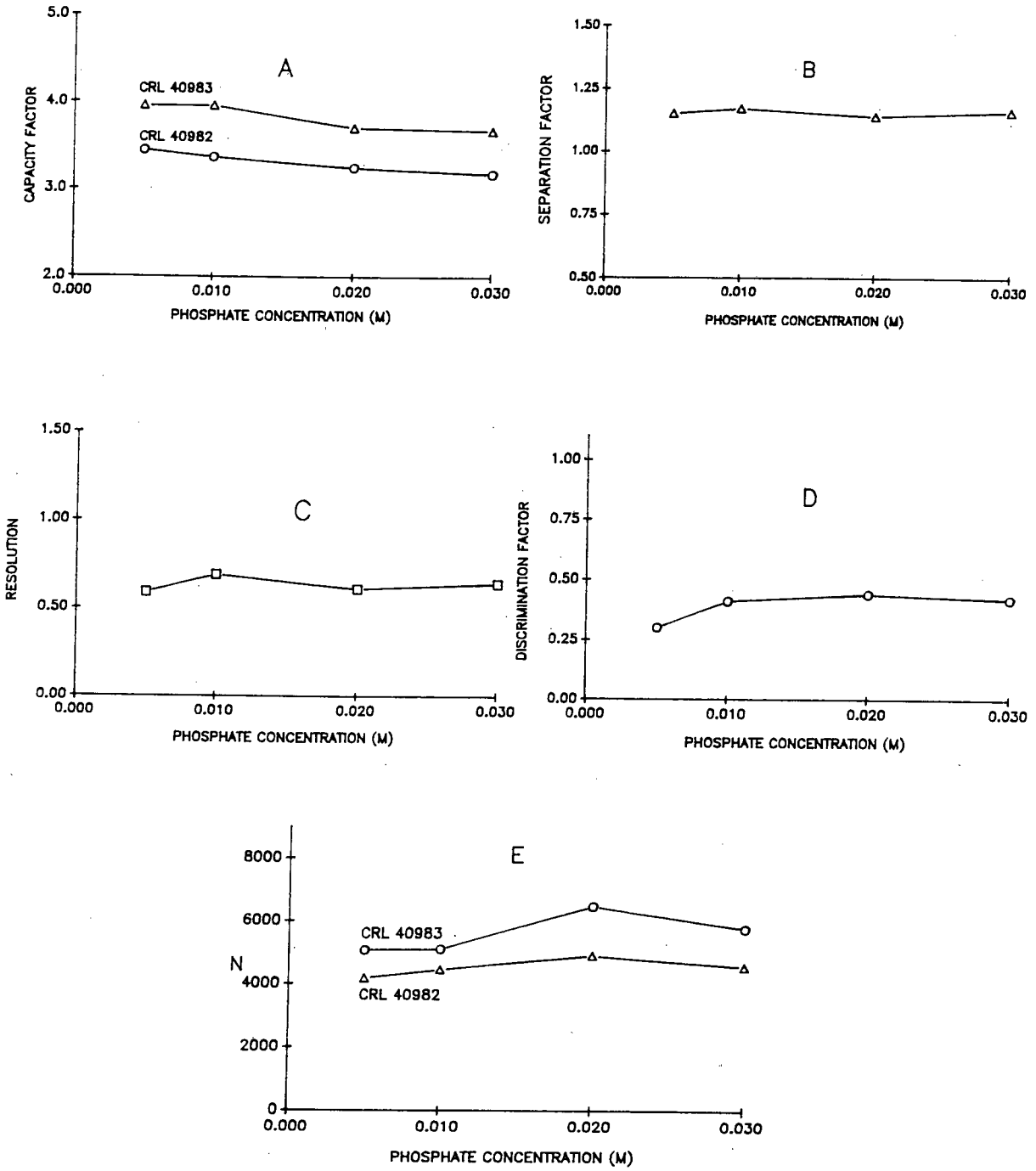

Fig. 3. Phosphate buffer: influence of phosphate concentration on chromatographic parameters. (A)–(E) as in Fig. 2. Mobile phase, 0.5% 1-butanol in phosphate buffer (pH 7) (for composition, see text); flow-rate, 1.0 ml/min; column temperature, 40°C.

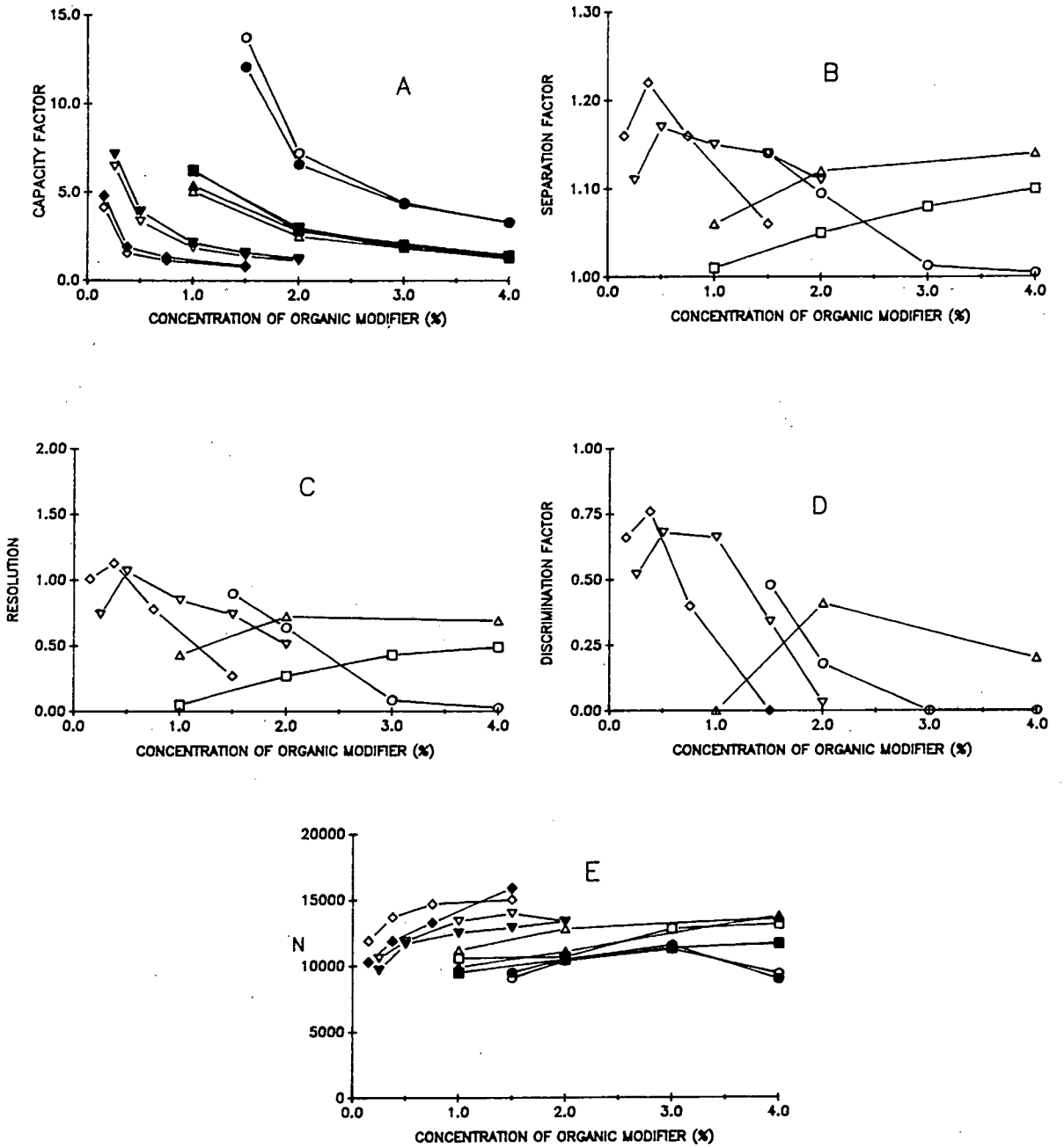

Fig. 4. Phosphate buffer: influence of nature and concentration of organic modifier on chromatographic parameters. (A)–(E) as in Fig. 2. Buffer of mobile phase: 0.02 *M* phosphate (pH 7); flow-rate, 1.0 ml/min; column temperature, 40°C. Open symbols, CRL 40982; closed symbols, CRL 40983. ○, ● = Ethanol; △, ▲ = 1-propanol; □, ■ = 2-propanol; ▽, ▼ = 1-butanol; ◇, ◆ = 1-pentanol.

CRL 40983 whatever the organic solvent, except with ethanol, for which the elution order was reversed. In each instance, the difference between the k' values of CRL 40982 and CRL 40983 was small, so the α values (Fig. 4B) ranged from 1.005 (4% ethanol) to 1.22 (0.375% 1-pentanol). The shape of the α curves varied with the nature of the modifier: for ethanol, the α values decreased from 1.14 to 1.005 when the ethanol concentration increased from 1 to 4%. For 1- and 2-propanol, the α values increased from 1.06 to 1.14 and from 1.01 to 1.10, respectively, when the modifier concentration increased from 1 to 4%. With 1-butanol as organic modifier, the α values reached a maximum (1.17) at 0.5% 1-butanol and then decreased slowly at higher concentrations. The same pattern was observed with 1-pentanol (maximum 1.22 at 0.375% 1-pentanol), but the decrease was faster.

The variations in R_s (Fig. 4C) followed the same kind of profile as described for α, except with 1-propanol, for which a maximum was reached at 2%. The observed R_s values were higher than 1.0 in only three cases: 1.07 for 0.5% 1-butanol and 1.01 and 1.13 for 0.15 and 0.375% 1-pentanol, respectively. The d_0 values (Fig. 4D), when they were different from zero, followed the same kind of pattern as R_s. In any case for 2-propanol, d_0 was equal to zero as no valley occurred between CRL 40982 and CRL 40983.

To a first approximation and in the studied range, the numbers of theoretical plates increased with increasing organic modifier concentration (Fig. 4E) but for ethanol, 1-propanol and 2-propanol their variations remained below or equal to the experimental accuracy. The variations in N values were greatest for 1-butanol and 1-pentanol. The highest values of N of 15 000 and 15 800 plates/m, respectively, for CRL 40982 and CRL 40983 were obtained with 1.5% 1-pentanol.

Acetate buffer

Influence of pH. Variations of mobile phase pH were obtained by mixing in different ratios a 0.1 M aqueous solution of ammonium acetate ($AcONH_4$) with a 0.1 M aqueous solution of acetic acid (AcOH), each solution containing 0.75% of 1-butanol as organic modifier. The pH of a 0.1 M aqueous solution of ammonium acetate being 6.75, higher values of pH were obtained by adding a few drops of concentrated ammonia solution to the 0.1 M ammonium acetate solution. The composition of the mobile phase and the corresponding pH values are listed in Table II.

Experimentally, pH was varied from 6.75 to 5.55 then, after re-equilibration, from 6.75 to 7.6.

The variations in k', α, R_s, d_0 and N with pH are displayed in Fig. 5A–E, respectively. The break in k' and N values observed in phosphate buffer at pH $\approx$ 7 did not occur in acetate buffer; in the studied range of pH, the k' of CRL 40982 was independent of pH (mean value 2.98) and the k' of CRL 40983 increased linearly with pH. Consequently, the α values increased linearly with pH; the slope of the linear regression, calculated from experimental results, was $5.82 \cdot 10^{-2}$ k' unit per pH unit.

To a first approximation, d_0 increased linearly with increasing pH, from 0.87 to 0.96. The R_s values also increased with pH, from 1.4 to 2.3. In contrast to the other parameters, the variations in the number of theoretical plates were almost independent of pH until pH 7.1 (mean value 22 000 plates/m for both CRL 40982 and CRL 40983).

At pH 7.6, the efficiency of the column began to decrease, indicating partial destruction of the col-

TABLE II

INFLUENCE OF pH USING 0.1 M ACETATE BUFFER: COMPOSITION OF THE MOBILE PHASE

Each mixture contained 0.75% of 1-butanol.

Component	Proportion (%)						
0.1 M $AcONH_4$	100	100	100	97.5	95	92.5	90
0.1 M AcOH	0	0	0	2.5	5	7.5	10
Conc. NH_3	$1 \cdot 10^{-4}$	$0.5 \cdot 10^{-4}$	0	0	0	0	0
pH	7.6	7.1	6.75	6.1	5.8	5.65	5.55

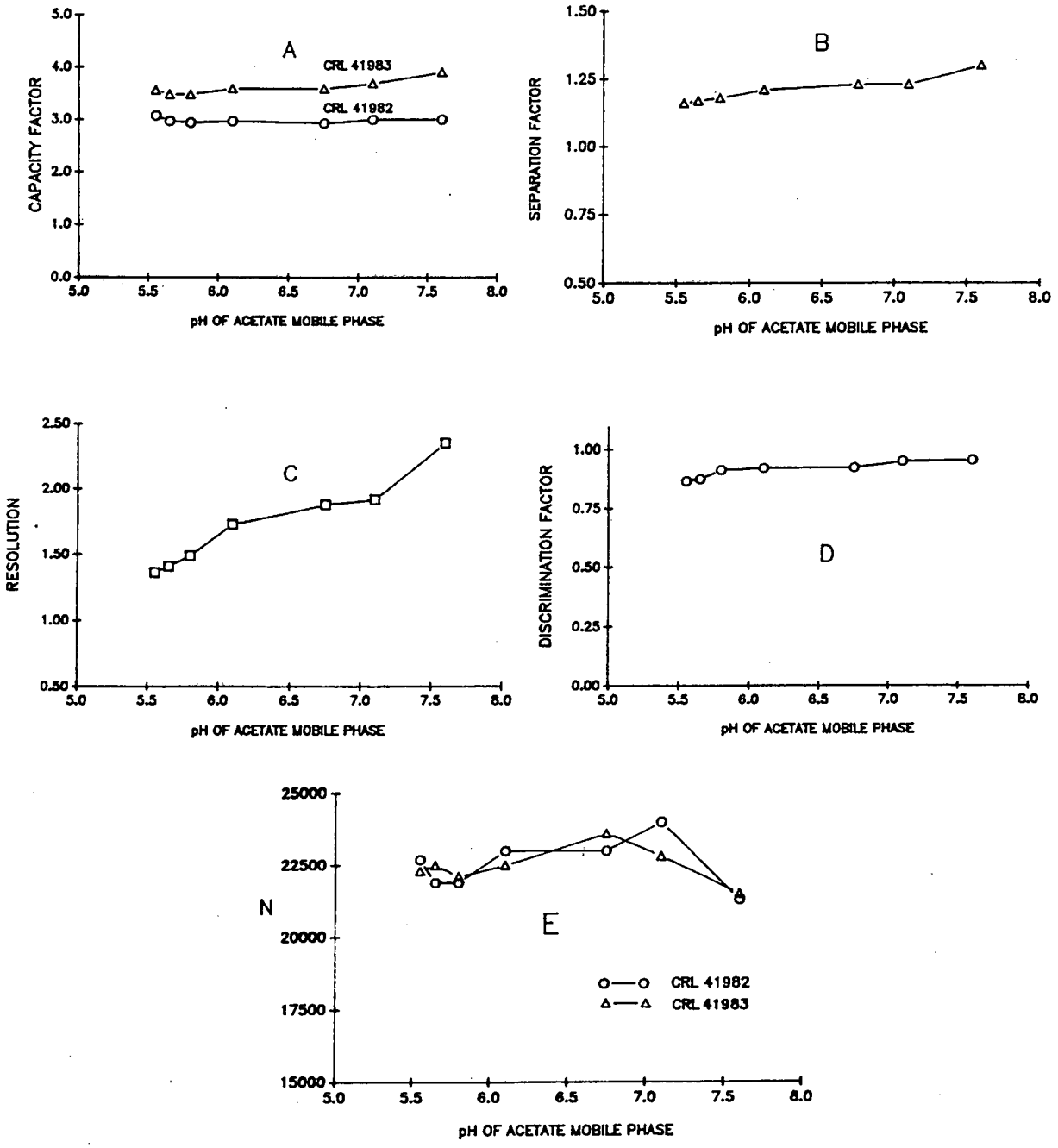

Fig. 5. Acetate buffer: influence of pH on chromatographic parameters. (A)–(E) as in Fig. 2. Mobile phase, 0.75% 1-butanol in 0.1 *M* acetate buffer (for composition, see text); flow-rate, 1.0 ml/min; column temperature, 40°C.

umn's qualities, observed at pH 7.8 (results at this pH were not reported because they were insignificant). The decrease in efficiency was irreversible even after a long re-equilibration with a mobile phase of acidic pH. Such a partial destruction was not observed with phosphate buffers, for which the

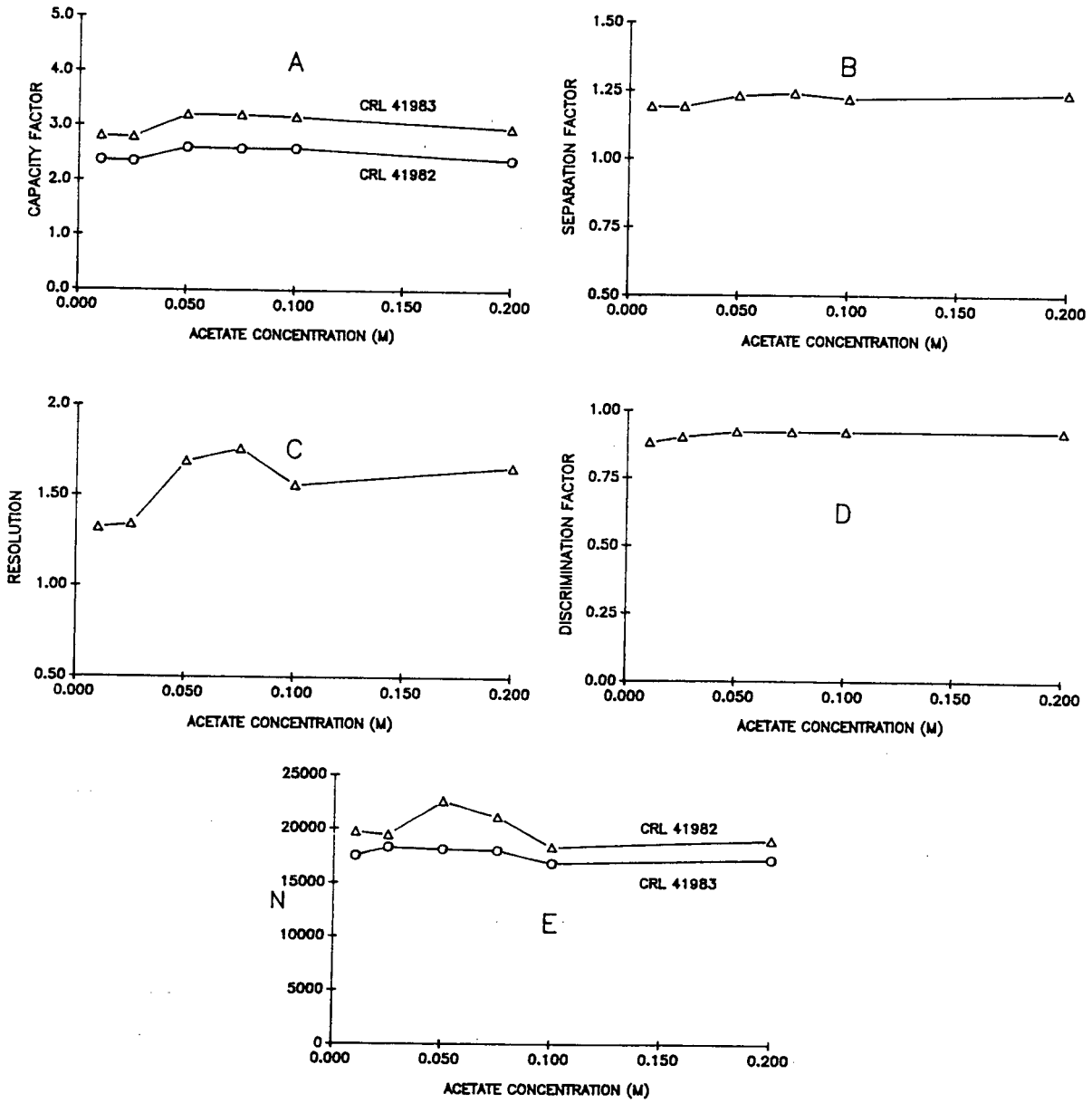

Fig. 6. Acetate buffer: influence of acetate concentration on chromatographic parameters. (A)–(E) as in Fig. 2. Mobile phase, 0.75% 1-butanol in ammonium acetate (pH 6.75); flow-rate, 1.0 ml/min; column temperature, 40°C. Symbols as in Fig. 4.

N values were higher at basic than at acidic pH.

Influence of acetate concentration. Variations of acetate concentration were obtained by dilution of 0.2 M aqueous ammonium acetate solution at pH 6.75 with water. The studied concentrations were 0.2, 0.1, 0.075, 0.050, 0.025 and 0.01 M, each solution containing 0.75% of 1-butanol.

Variations in k', α, R_s, d_0 and N values with acetate concentration are displayed in Fig. 6A–E, respectively. Except for N and R_s, for which some variations occurred for acetate concentration of 0.05 and 0.075 M, all the other parameters were indepen-

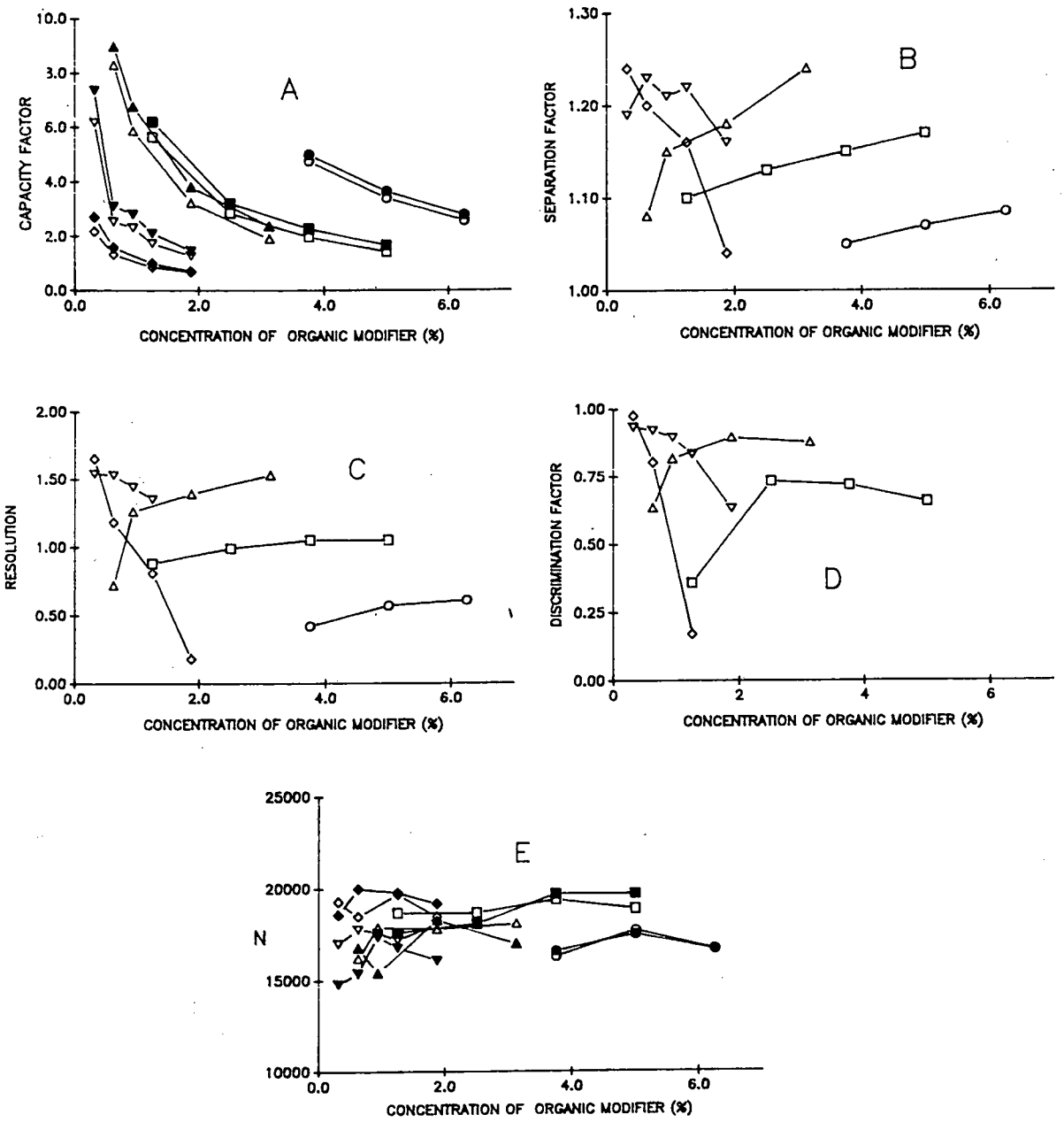

Fig. 7. Acetate buffer: influence of nature and concentration of organic modifier on chromatographic parameters. (A)–(E) as in Fig. 2. Buffer of the mobile phase, 0.1 *M* ammonium acetate (pH 6.75); flow-rate, 1.0 ml/min; column temperature, 40°C. Symbols as in Fig. 4.

dent of the acetate concentration. Because of the partial destruction of the column during the pH study, some results, obtained under the same analytical conditions, were different from those described above; nevertheless, the variations in the chromatographic parameters observed in this study remained meaningful as they were obtained with a column that was still able to separate the two optical isomers.

Influence of organic modifier. The mobile phase

was 0.1 *M* ammonium acetate aqueous solution at pH 6.75 to which various amounts of different organic modifiers were added. In order to have sufficient accuracy, the amount of organic modifiers was weighed and converted to volume using a density value of 0.8. Variations of k' values with organic modifier concentration are displayed in Fig. 7A. The elution order was always the same, CRL 40982 being eluted before CRL 40983 whichever organic solvent was used. The inversion of elution order observed with ethanol in phosphate buffer did not occur with ammonium acetate. In each instance, the difference between k' values of CRL 40982 and CRL 40983 was small, so the extreme α values (Fig. 7B) were 1.04 (1.875% 1-pentanol) and 1.24 (0.3% 1-pentanol). In the range of organic modifier concentrations used in this study, the α values increased in relation to the concentration of ethanol, 1-propanol and 2-propanol, were nearly independent of 1-butanol concentration, and decreased with 1-pentanol concentration.

The R_s values (Fig. 7C) were almost independent of the concentration of ethanol (0.4–0.6) and 2-propanol (0.9–1.05) and increased from 0.72 to 1.53 for 1-propanol and decreased slowly for 1-butanol from 1.54 to 0.88 and rapidly for 1-pentanol from 1.65 to 0.18.

The d_0 values (Fig. 7D) were zero for ethanol at any concentration and for 1-pentanol at 1.875%. For 1- and 2-propanol they reached a maximum (0.9 for 1-propanol at 1.875% and 0.74 for 2-propanol at 2.5%). The d_0 values slowly decreased for 1-butanol (from 0.94 to 0.63) and very rapidly for 1-pentanol (from 0.95 to 0.17).

Regarding variations in the numbers of theoretical plates (Fig. 7E), no trends could be observed. The N values ranged from 15 000 to 20 000 plates/m.

DISCUSSION

Choice of buffer

The amounts of organic modifier used for studying the influence of buffers were derived from preliminary results and were chosen to obtain approximately the same values of k' at neutral pH in each buffer for both CRL 40982 and CRL 40983. The significant variations in chromatographic parameters reported above were principally obtained more for pH modifications than for ionic strength.

Variations in k', indicating variations in thermodynamic equilibrium between the solute and the chromatographic system, were significant only *versus* pH variations in phosphate buffer and could not be used for optimization of the separation as both the compounds were affected in the same way by pH variations. The thermodynamic changes were due not only to pH but also to a more complex phenomenon as they did not occur in acetate buffer in the same range of pH. The influence of pH was more effective on α values: for both the buffers, the linear variation of α with pH indicated a better separation of the two isomers at neutral or basic pH (but basic pH was precluded because of instability of the column in acetate buffer). The effect of pH variations was more important in acetate buffer (slope of linear regression $= 5.82 \cdot 10^{-2}$ k' unit per pH unit) than in phosphate buffer (slope of linear regression $= 3.31 \cdot 10^{-2}$ k' unit per pH unit).

The ionic strength of the buffer did not exhibit any thermodynamic effect as, for both buffers, no variation in k' with salt concentration was significant. In the same way, the kinetic modifications, showed by variations in R_s, d_0 and N (if the k' values remained constant) due to ionic strength variations were small: only N variations $<25\%$ and R_s variations $<15\%$ were reported.

The kinetic influence of pH was stronger particularly for phosphate buffer: d_0 and R_s increased almost linearly from pH 5 to 7 then remained constant; the d_0 values were increased 2.5-fold between pH 6 and 7 and the R_s values doubled between pH 6 and 7.1. For acetate buffer, only increases in R_s values were really significant, being 1.4-fold between pH 5.55 and 6.75.

Whereas the influence of pH appeared to be weaker in acetate buffer than in phosphate buffer, the absolute values of all the measured chromatographic parameters (for the same k' values) were always larger for acetate buffer than for phosphate buffer. At neutral pH and with the same values of k' and α, in terms of R_s, d_0 and N, the benefit was equal to factors of 2.4, 1.7 and 2.1, respectively. Consequently, ammonium acetate is to be preferred to sodium dihydrogenphosphate as the buffer in order to optimize the separation of modafinil optical isomers.

From a practical point of view, equilibration volumes for Chiral-AGP columns were lower with phosphate buffer (15–20 ml of mobile phase) than with acetate (at least 30 ml), but the lifetime of the column was considerably longer with acetate. In routine work using phosphate buffer as the mobile phase, one needed to add a small amount of Chiral-AGP slurry to the top of the column at least once a week, because of the occurrence of a void volume. Such an occurrence of a void volume had not been observed using acetate buffer, even after 4 months of constant use.

Choice of organic modifier

The results obtained in the study of the influence of organic modifiers confirmed the interest in using ammonium acetate as buffer: for each organic modifier used at the same concentration, values of the chromatographic parameters indicated a better separation using ammonium acetate than sodium dihydrogenphosphate.

To a first approximation, the thermodynamic and kinetic effects of each organic modifier were similar for both buffers. A more detailed examination of the results showed some differences for ethanol which

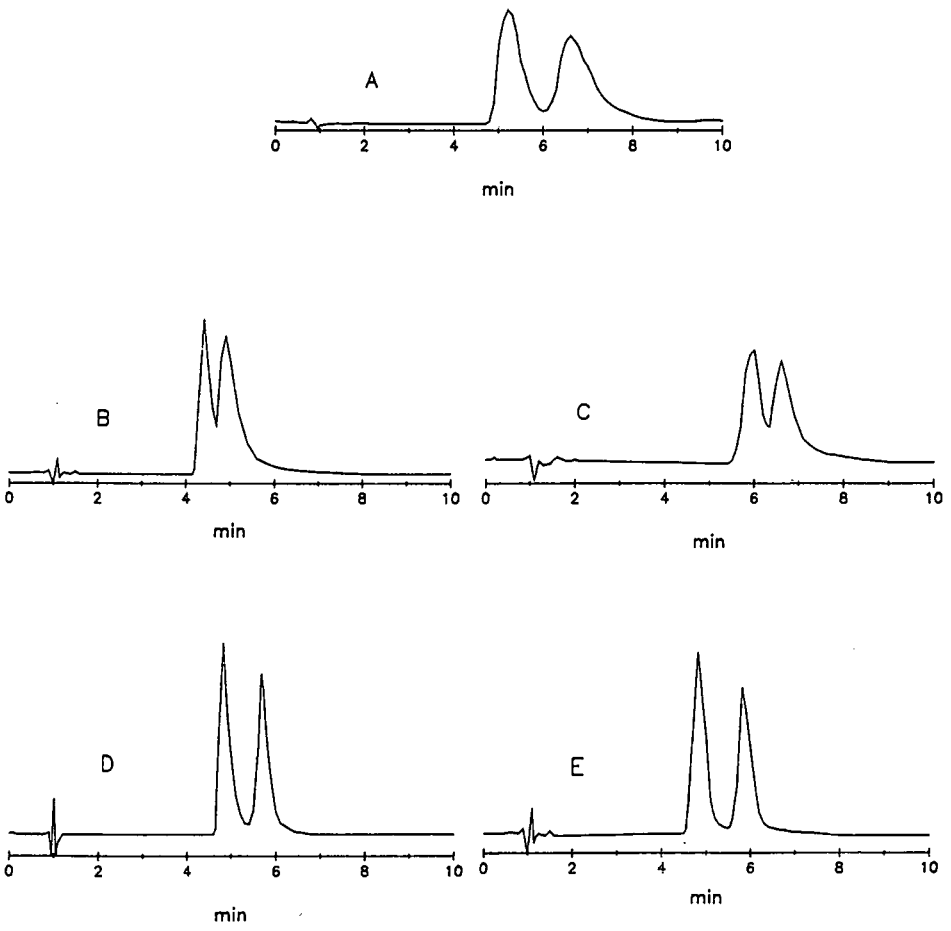

Fig. 8. Chromatograms of Modafinil optical isomers. Chiral AGP column (100 × 4.6 mm I.D.); flow-rate, 1.0 ml/min; temperature, 40°C; detection wavelength, 267 nm [except (A), 220 nm]. (A) 1.5% 1-propanol in 0.03 *M* phosphate buffer (pH 7); (B) 0.5% 1-butanol in 0.02 *M* phosphate buffer (pH 7); (C) 0.15% 1-pentanol in 0.02 *M* phosphate buffer (pH 7); (D) 0.5% 1-butanol in 0.1 *M* acetate buffer (pH 6.75); (E) 0.1% 1-pentanol in 0.1 *M* acetate buffer (pH 6.75).

were probably due to the inversion of the retention order observed for ethanol in phosphate buffer. For both buffers, the eluotropic order was 1-pentanol > 1-butanol > 1-propanol > 2-propanol > ethanol. For acetate buffer the decreasing order of maximum values of α, d_0 and R_s was the same. For phosphate buffer, the order was 1-pentanol > 1-butanol > ethanol > 1-propanol > 2-propanol. Because of drastic variations in the chromatographic parameters with any small variation in the amount of 1-pentanol in the mobile phase, the use of this organic modifier in routine work is not recommended. For this purpose, the use of 1-butanol, for which the consequences of variations were less important, is to be preferred.

CONCLUSIONS

The chromatograms in Fig. 8 highlight the improvement in the separation of modafinil optical isomers obtained after the optimization study of the mobile phase. The use of ammonium acetate as buffer and of 1-butanol as organic modifier allowed real benefits in terms of selectivity, resolution and sensitivity. The use of this kind of mobile phase has already been extended in our laboratory to the separation of other optical isomers, always with the same result: a better resolution and a longer lifetime of the chromatographic column.

Replacement of potassium phosphate buffer by ammonium acetate makes the use of the Chiral AGP column in LC–TSP-MS analysis possible. Consequently, pharmacokinetics studies of Modafinil optical isomers could be considered.

ACKNOWLEDGEMENTS

The authors are grateful to J. Beurier, G. Glauert and P. Leproust, who synthesized the pure optical isomers of modafinil.

REFERENCES

1 J. Duteil, F. A. Rambert, J. Pessonnier, J. F. Hermant, R. Gombert and E. Assous, *Eur. J. Pharmacol.*, 180 (1990) 49–58.
2 M. Broquaire, unpublished results.
3 Th. Becue and M. Broquaire, *J. Chromatogr.*, 557 (1991) 489–494.
4 M. Z. El Fallah and M. Martin, *Analusis*, 16 (1988) 241–248.

Journal of Chromatography, 605 (1992) 33–39
Elsevier Science Publishers B.V., Amsterdam

CHROM. 24 220

Separation of propafenone enantiomers by liquid chromatography with a chiral counter ion

Michel Prevot and Michel Tod

Department of Pharmacotoxicology, Avicenne Hospital, 125 Route de Stalingrad, 93000 Bobigny (France)

Josef Chalom

Eurobio, ZA Courtaboeuf, 7 Avenue de Scandinavie, 91953 Les Ulis (France)

Patrick Nicolas and Olivier Petitjean

Department of Pharmacotoxicology, Avicenne Hospital, 125 Route de Stalingrad, 93000 Bobigny (France)

(First received December 9th, 1991; revised manuscript received March 30th, 1992)

ABSTRACT

Propafenone is a class Ic antiarrhythmic drug with complex pharmacological and pharmacokinetic profiles due to the existence of an asymmetric carbon that is only available as a racemic mixture. A liquid chromatographic method for the determination of propafenone enantiomers using N-benzyloxycarbonylglycyl-L-proline as the chiral selector in the mobile phase is described. Studies on the retention behaviour of both propafenone and propranolol (internal standard) enantiomers with different mobile phase compositions permitted the determination of the optimum conditions. The best resolution for propafenone enantiomers was 2.3. Application to plasma samples with a simple sample preparation is also presented. The method was linear up to 2500 ng/ml of racemic propafenone and the limit of detection was 100 ng/ml for each enantiomer.

INTRODUCTION

Propafenone (PFN) is a class Ic antiarrhythmic drug with weak β-blocking action; its weak calcium-blocking action has also been described [1–4]. PFN contains a chiral centre and is available only as a racemate in therapeutic formulations. The major difference in the pharmacological action of (*R*)-(−)-PFN and (*S*)-(+)-PFN is their affinity to β-receptors, which is 50–100 times greater for the latter [5,6]. The pharmacokinetic profile of the two enantiomers is also different, as hydroxylation, which is the major route of metabolism, is stereoselective and favours (*R*)-(−)-PFN [5]. The hydroxylation of PFN is related to debrisoquin oxidation polymorphism, and stereoselectivity seems to be abolished in poor metabolizers [7]. This issue is important as 5-hydroxy-PFN is an active metabolite which possibly contributes to the clinical activity of the drug [4].

Few chromatographic methods have been devised to separate and determine PFN enantiomers and these methods were based on chiral derivatization [5,8]. A derivatization procedure with (−)-naphthylethyl isocyanate afforded a low detection limit (below 6.25 ng/ml) [8] and Kroemer *et al.* [5] obtained a detection limit of 100 ng/ml after a multi-step extraction procedure and derivatization with 2,3,4,5-tetra-O-acetyl-β-D-glucopyranosyl isothiocyanate. However, even with highly optically pure reagents, racemization may occur before or

Correspondence to: Dr. M. Tod, Department of Pharmacotoxicology, Avicenne Hospital, 125 Route de Stalingrad, 93000 Bobigny, France.

0021-9673/92/$05.00

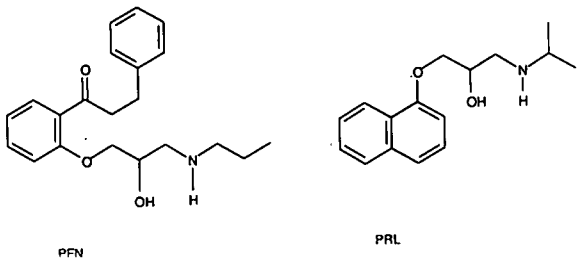

Fig. 1. Structures of propafenone (PFN) and propranolol (PRL).

during the reaction, leading to erroneous results [9–11].

As the structure of PFN is similar to that of β-blocking agents (Fig. 1), a high-performance liquid chromatographic (HPLC) method described by Pettersson and Josefsson [12] for amino alcohols was assessed. This method was reported to give high enantioselectivity for propranolol (α = 1.35) and related structures, and is based on the formation of diastereoisomeric ion pairs with N-benzyloxycarbonylglycyl-L-proline (ZGP) in the mobile phase. Our results on PFN enantiomer separation are presented and discussed in this paper.

EXPERIMENTAL

Instrumentation

A Shimadzu LC 6A pump, a Rheodyne Model 7125 valve injector with a 20-μl sample loop, a Shimadzu SPD 6A detector operating at 300 nm and a Shimadzu CR 5A integrator, purchased from Touzart et Matignon (Vitry, France), were used.

Chemicals

Racemic PFN hydrochloride was obtained from Sigma (St. Louis, MO, USA), (+)- and (−)-propranolol (PRL) hydrochloride, (*Z*)-glycyl-L-proline (ZGP), 0.4-nm molecular sieves and optically active di-*O,O'*-*p*-toluyltartaric acids were obtained from Fluka (Buchs, Switzerland). Dichloromethane without preservative (OSI, Paris, France) was stored desiccated at room temperature; the water content, as measured by the Karl Fisher method, was 120 ppm. Ethanol (Carlo Erba, Rueil, France), 1-pentanol (Merck, Darmstadt, Germany) and triethylamine (TEA) (Prolabo, Paris, France) were of analytical-reagent grade and used without further purification. N-Succinimido-(*Z*)-glycyl-L-proline was a gift from Eurobio (Les Ulis, France). Silica thin-layer chromatographic (TLC) plates (2.5 × 7.5 cm) were obtained from Whatman (Maidstone, UK).

Three liquid chromatographic columns were used: Nucleosil diol (7 μm) (250 × 4.6 mm I.D.) and Nucleosil cyano (5 μm) (250 × 4.6 mm I.D.) columns were obtained from SFCC (Neuilly Plaisance, France) and a Brownlee Labs. Spheri 5 cyano column (250 × 4.6 mm I.D.) was obtained from Touzart et Matignon.

Preparation of PFN enantiomers

PFN enantiomers were obtained by fractional crystallization of diastereoisomeric salts with D- and L-di-*O,O'*-*p*-toluyltartaric acids [13]. Each salt was recrystallized three times. The yields were 68 and 56% for (−)- and (+)-PFN (expressed as bases), respectively.

Column preparation

Before use, each column was washed with 100 ml of dry dichloromethane. Before each manipulation, the mobile phase was recirculated through the column using a volume equal to 100 times the dead volume of the system. Then a new mobile phase was introduced and arranged for recirculation. Separations were carried out at room temperature.

Composition of the mobile phases

Mobile phases were prepared extemporaneously with dried dichloromethane containing $2 \cdot 10^{-4}$–$5 \cdot 10^{-3}$ *M* ZGP and $2 \cdot 10^{-4}$–$2 \cdot 10^{-3}$ *M* TEA, with various amounts of 1-pentanol and water to control retention. The flow-rate was always 1 ml/min.

Calculation

The efficiency of the column was calculated using the peak width at half-height (ω) given by the integrator according to [14]

$$N = 5.54 \frac{t_R^2}{\omega^2}$$

where t_R is the retention time. The resolution (R_s) was expressed as a classical function of the capacity factor of the second-eluted peak (k'_2), enantioselectivity (α) and efficiency (N) according to [14]

$$R_s = \frac{1}{4} \cdot \frac{\alpha - 1}{\alpha} \cdot \frac{k'_2}{k'_2 + 1} \cdot \sqrt{N}$$

Determination of PFN in plasma

Plasma samples (2 ml) were spiked with 60 μl of 10^{-4} *M* (*S*)-(−)-PRL as the internal standard in centrifuge tubes and 200 μl of 1 *M* sodium hydroxide solution and 4 ml of toluene–*n*-butanol (95:5) were added. The tubes were agitated on a horizontal shaker (Toulemonde, Paris, France) for 30 min and centrifuged at 2500 *g* for 15 min. The organic layer, after transfer into a new glass tube and addition of 10 μl of acetic acid, was evaporated to dryness in a block heater (45°C) under a stream of air. The residue was dissolved in 100 μl of chloroform before analysis.

RESULTS AND DISCUSSION

Optical punity of PFN enantiomers: TLC and HPLC

For assessment of optical purity, a rapid semi-quantitative TLC system was used. Samples were derivatized with a 100% excess of N-succinimido-ZGP in dimethylformamide (12 h at room temperature) and were then spotted on silica gel plates and developed at room temperature with dichloromethane–ethanol (10:1) as mobile phase. Spots were revealed with a 254-nm UV lamp or by spraying with 2,4-dinitrophenylhydrazine. Under these conditions, the R_F values for (+)- and (−)-PFN were 0.62 and 0.64, respectively. Thus the optical purity was evaluated as more than 90% in both instances.

The HPLC method with a chiral counter ion allowed the measurement of optical purity. After three crystallizations it was 98.7% for (−)-PFN and 98.6% for (+)-PFN (Fig. 2).

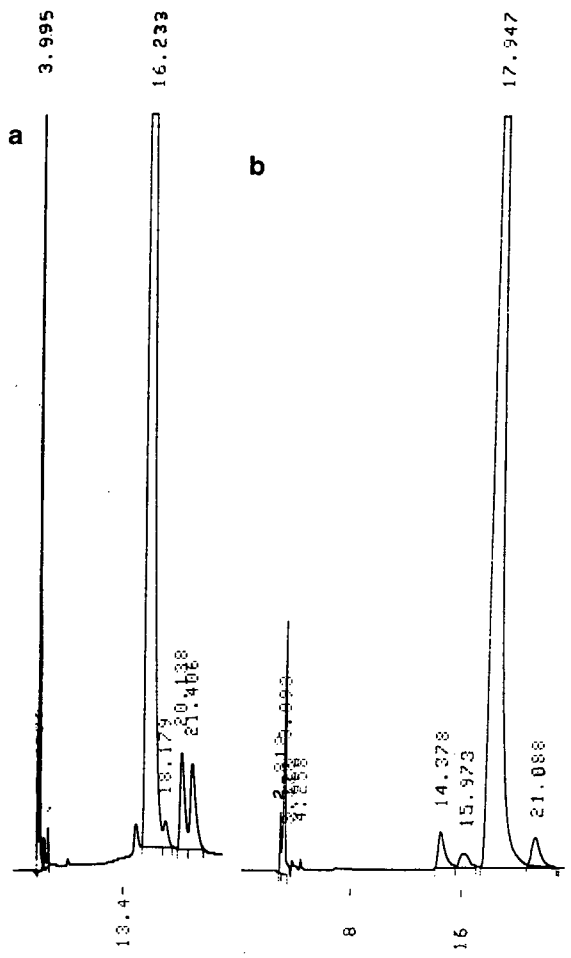

Fig. 2. Optical purity after three recrystallizations. Stationary phase, Nucleosil 5 cyano; mobile phase, dichloromethane–1-pentanol (100:1, v/v)–2.5 · 10^{-3} *M* ZGP–1.5 · 10^{-3} *M* TEA; solutes, PFN enantiomers (10^{-4} *M*); detection, 0.32 a.u.f.s.; detection wavelength, 300 nm; flow-rate, 1 ml/min. (a) $k'_{(+)\text{-PFN}}$ = 4.78 (retention time 16.2 min); $k'_{(-)\text{-PFN}}$ = 5.47 (retention time 18.2 min); enantiomeric excess (ee) = 97.3. (b) $k'_{(+)\text{-PFN}}$ = 4.68 (retention time 16 min); $k'_{(-)\text{-PFN}}$ = 5.39 (retention time 17.9 min); ee = 97.5. Peaks at 14.3, 20 and 21 min are unidentified.

Choice of stationary phase

The three columns were checked for efficiency in the normal-phase system. Nucleosil diol, Spheri 5 cyano and Nucleosil cyano gave 6000, 18 000 and 18 000 theoretical plates, respectively, for nitrobenzene.

The Nucleosil diol column demonstrated poor efficiency and yielded highly asymmetric peaks; the best R_s was 0.78 for PRL enantiomers despite a selectivity factor of 1.42. The system failed to separate PFN enantiomers.

The two cyano-bonded silica columns exhibited similar selectivities for PFN (between 1.10 and 1.20). However, with the Spheri 5 cyano column, short retention times were only obtained with large amounts of 1-pentanol in the mobile phase leading to poor efficiency and incomplete resolution (*cf.*, Table I). In contrast, on the Nucleosil cyano support, short retention times without 1-pentanol in the mobile phase yielded good separations of PFN enantiomers (R_s up to 2.3). The resolutions of PFN enantiomers by methods based on chiral derivatization were similar. Therefore, this stationary phase was used for further studies.

TABLE I

EFFECT OF 1-PENTANOL ON RETENTION AND RESOLUTION OF PFN ENANTIOMERS

Stationary phase, Spheri 5 cyano; mobile phase, dichloromethane–1-pentanol (variable ratio)–$2.5 \cdot 10^{-3}$ *M* ZGP–10^{-3} *M* TEA.

Parameter	Dichloromethane–1-pentanol			
	95:5	93.5:7.5	90:10	85:15
k'^{a}	25	15	14.3	7.5
α	1.13	1.14	1.13	1.14
R_s	1.19	1.2	1.09	0.61

[a] k' = Capacity factor of the last-eluted enantiomer.

Optimization of separation on Nucleosil cyano column

Because application to biological fluids requires internal standardization, PRL and PFN enantiomer separations were investigated concomitantly. The effect of the proportion of each mobile phase component on retention, selectivity and resolution was also evaluated.

Effect of 1-pentanol. Addition of a small percentage of 1-pentanol to the mobile phase always led to shorter retention times associated with a decrease in column efficiency. Unexpectedly, the effects on enantioselectivity differed for PFN and PRL (Fig. 3). The results for resolution were opposite, with an increase for PFN enantiomers and a decrease for PRL enantiomers. The hydrogen donor capacity of 1-pentanol may explain these results: on retention by masking the free silanols of the stationary phase; on selectivity by displacing PRL from ion pairs with ZGP. The absence of a decreased PFN enantioselectivity may be due to steric hindrance.

Effect of ZGP concentration. The concentration of ZGP in the mobile phase affected mainly the enantioselectivity, efficacy of the column and thus resolution. On the other hand, only a minor effect on retention was observed. This unusual behaviour implies a complex elution mechanism of diastereoisomeric ion pairs in this system.

In both instances retention reached a maximum for a ZGP concentration of 10^{-3} *M* (Table II). The column efficiency increased with the increasing concentration of ZGP, as usual in ion-pair chromatography. However, the effects on enantioselectivity were different for PRL and PFN, as described by Petterson and Josefsson [12] for alprenolol and 8-hydroxy-2-(di-*n*-propylamino)tetralin. For PRL, the enantioselectivity increased with increasing concentration of ZGP and no separation occurred when the ZGP concentration was lower than that of TEA, showing a competitive action of TEA towards ion pairs. For PFN, the enantioselectivity and resolution increased for concentrations of ZGP up to 10^{-3} *M* and then decreased. These results remain unexplained.

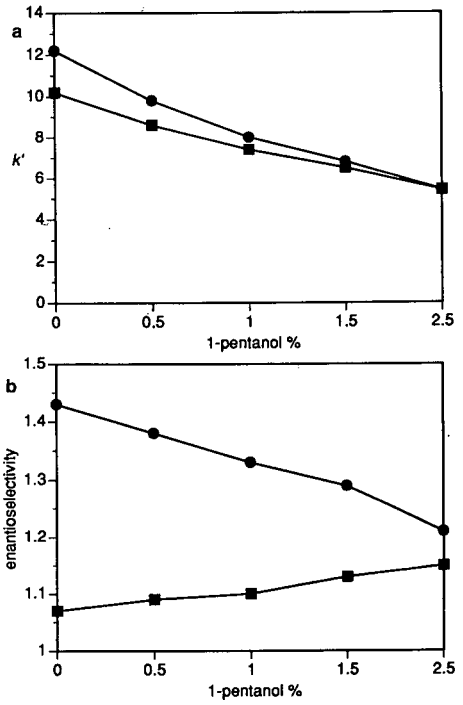

Fig. 3. Effects of 1-pentanol on (a) retention and (b) enantioselectivity. ■ = PFN; ● = PRL. Stationary phase, Nucleosil 5 cyano; mobile phase, dichloromethane–1-pentanol (variable ratio)–$2.5 \cdot 10^{-3}$ *M* ZGP–$5 \cdot 10^{-4}$ *M* TEA. k' = Capacity factor of the last-eluted enantiomer.

Effect of triethylamine. As for 1-pentanol, TEA led to shorter retention times (Fig. 4), but addition of TEA never resulted in a decrease in the efficiency of the system. However, the effects on enantioselectivity were still opposite; for PRL enantiomers the selectivity decreased when the ZGP/TEA ratio decreased, whereas for PFN enantiomers TEA did not significantly affect the selectivity over a wide range

TABLE II

EFFECTS OF ZGP CONCENTRATION ON RETENTION AND SEPARATION OF PFN AND PRL ENANTIOMERS

Stationary phase, Nucleosil 5 cyano; mobile phase, dichloromethane–ZGP (variable)–10^{-3} *M* TEA–200 ppm water.

Enantiomer	Parameter	ZGP concentration (*M*)						
		$2.5 \cdot 10^{-4}$	$5 \cdot 10^{-4}$	$1 \cdot 10^{-3}$	$1.5 \cdot 10^{-3}$	$2.5 \cdot 10^{-3}$	$3.75 \cdot 10^{-3}$	$5 \cdot 10^{-3}$
(−)-PFN	k'^a	7.1	7.7	8.9	7.8	7.2	5.6	4.7
	N	2030	2580	4080	4110	4660	4420	4050
	α	1.13	1.17	1.19	1.15	1.13	1.09	1.07
	R_s	1.14	1.63	2.29	1.85	1.72	1.16	0.86
(−)-PRL	k'	9.85[b]	11.0[b]	12.8	10.7	9.0	6.4	5.0
	N	–	–	–	1360	1600	2300	2140
	α	1	1	1.05	1.21	1.32	1.42	1.44
	R_s	–	–	–	1.46	2.18	3.07	2.95

[a] k' = Capacity factor of the last-eluted isomer.
[b] Enantiomers not resolved.

of concentrations. Hence TEA is suitable for retention adjustment.

Effect of water content. In both instances, amounts of water in the mobile phase ranging from 200 to 1500 ppm resulted in slightly decreased retention times and increased column efficiency (Table III).

The selectivity still differed between the two compounds; no effects on the separation of PFN enantiomers was observed, whereas a slight decrease in enantioselectivity of PRL enantiomer separation was noted.

Comments

It seems that the two racemic compounds studied behave differently in this chromatographic system. PRL enantiomers give highly selective diastereoisomeric ion pairs; PFN enantiomers do not allow enantioselectivity greater than 1.2, probably because their side-chain in the *ortho* position causes steric hindrance.

Modifiers seem to induce opposite effects. Enhancing the solubility of ion-pair components in the mobile phase or coating of the stationary phase silanols increased the efficiency, whereas changing the ion-pair equilibria led to lower selectivity. The resulting effect depends on the lability of ion pairs

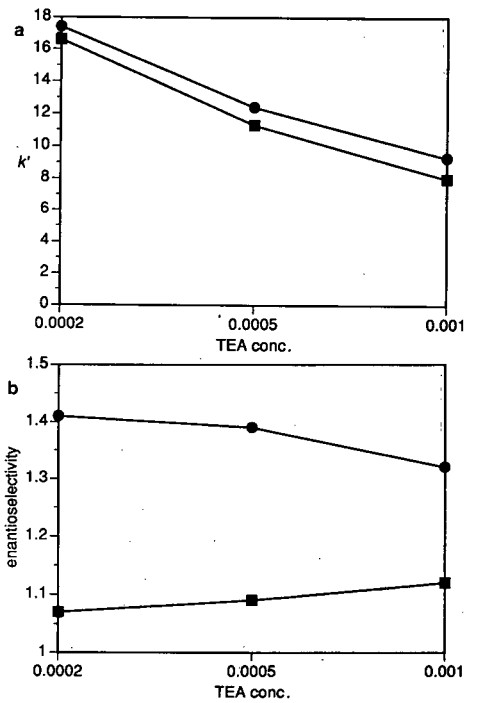

Fig. 4. Effects of TEA concentration (*M*) on (a) retention and (b) enantioselectivity. ■ = PFN; ● = PRL. Stationary phase, Nucleosil 5 cyano; mobile phase, dichloromethane–$2.5 \cdot 10^{-3}$ *M* ZGP–TEA (variable). k' = Capacity factor of the last-eluted enantiomer.

TABLE III

EFFECTS OF SMALL AMOUNTS OF WATER ON RETENTION AND SEPARATION OF PFN AND PRL ENANTIOMERS

Stationary phase, Nucleosil 5 cyano; mobile phase, dichloromethane–2.5 · 10^{-3} *M* ZGP–10^{-3} *M* TEA–water (variable).

Enantiomer	Parameter	Water content (ppm)				
		0	200	500	1000	1500
(−)-PFN	k'^a	8.1	7.2	6.9	6.4	6.2
	N	3460	4660	4620	6180	6690
	α	1.10	1.13	1.13	1.12	1.12
	R_s	1.19	1.72	1.69	1.77	1.83
(−)-PRL	k'	10.6	9.0	8.0	7.1	6.6
	N	1060	1600	2230	3560	4250
	α	1.39	1.32	1.35	1.29	1.26
	R_s	2.08	2.18	2.7	2.93	2.87

[a] k' = Capacity factor of the last-eluted isomer.

and on steric effects. With PRL, the modifiers used to regulate retention always led to a decrease in enantioselctivity. With PFN, the observed effects seem to be due mainly to interactions with the stationary phase.

Application to biological samples

Preliminary studies on the extraction of PFN showed a loss of PFN during evaporation of the organic layer which resulted in irreproducible yields. Therefore, the extracted PFN base was acidified with acetic acid before evaporation. Under these extraction conditions, a yield of at least 85% was obtained. The calibration graphs were linear up to 2500 ng/ml of the racemate in plasma. The equation of the mean four-point calibration graph (n = 3) was (y = PFN-to-PRL area ratio; x = PFN concentration in ng/ml) $y = 2.46 \cdot 10^{-4} x + 0.019$ with r = 0.998 (range 0.997–0.999) for (+)-PFN and $y = 2.48 \cdot 10^{-4} x + 0.018$ with r = 0.998 (range 0.9980–0.9988) for (−)-PFN. The limit of detection (signal-to-noise ratio = 3) was less than 100 ng/ml for each enantiomer in plasma. Typical chromatograms are shown in Fig. 5. Further, in our experience, the acetic acid remaining after incomplete evaporation of the organic phase led to a system peak during elution of (+)-PFN and thus peak compression as shown in Fig. 6. Such interference may be used to enhance the limit of detection.

CONCLUSION

Propafenone and propranolol enantiomers, despite their similar structures, exhibited different behaviours in their chiral resolution when the chromatographic conditions were altered. Thus, chiral counter-ion chromatography, as described by Petterson and Josefsson [12], seems to be a method of general applicability for β-amino alcohols, but the conditions must be carefully defined in each instance. Once optimized, the method provides a simple way to separate propafenone enantiomers. Hence this chromatographic method with one-step sample preparation may be useful for evaluating PFN enantiomer hydroxylation and for assessing steady-state concentrations in patients undergoing PFN therapy.

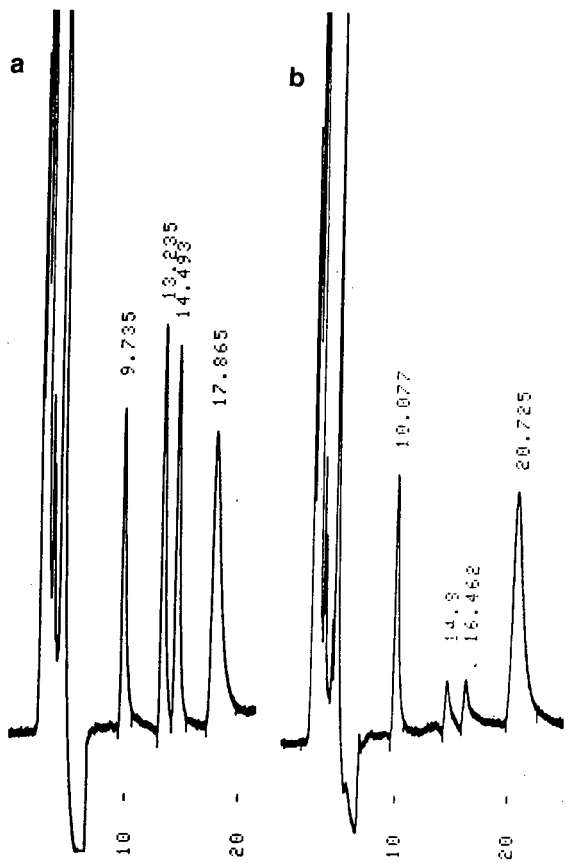

Fig. 5. Chromatograms obtained after extraction of spiked plasmas containing (a) $7.5 \cdot 10^{-6}$ *M* of racemic PFN (1250 ng/ml of each enantiomer) and (b) $8.8 \cdot 10^{-7}$ *M* of racemic PFN (150 ng/ml of each enantiomer). Internal standard, (−)-PRL ($3 \cdot 10^{-6}$ *M*); stationary phase, Nucleosil 5 cyano; mobile phase, dichloromethane–$3 \cdot 10^{-3}$ *M* ZGP–$1.5 \cdot 10^{-3}$ *M* TEA–250 ppm water; detection, 0.04 a.u.f.s.; detection wavelength, 300 nm; flow-rate, 1 ml/min. $k'_{(+)\text{-PFN}} = 4.37$ (retention time 14.7 min); $k'_{(-)\text{-PFN}} = 4.97$ (retention time 16.4 min); $k'_{(-)\text{-PRL}} = 6.57$ (retention time 20.8 min). The peak at 10 min is an endogenous compound.

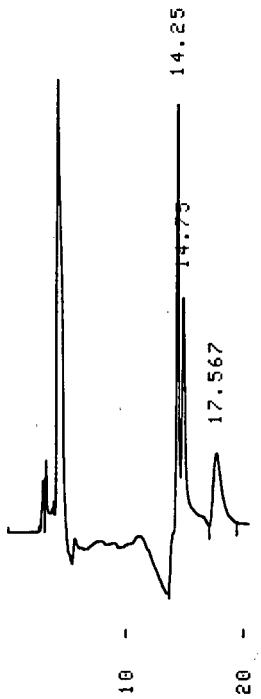

Fig. 6. Effect of system peak on elution of (+)-PFN. Stationary phase, Nucleosil 5 cyano; mobile phase, dichloromethane–$3 \cdot 10^{-3}$ *M* ZGP–$1.5 \cdot 10^{-3}$ *M* TEA–250 ppm water; solute: racemic PFN ($5 \cdot 10^{-5}$ *M*) and (−)-PRL ($2 \cdot 10^{-5}$ *M*); detection, 0.16 a.u.f.s.; detection wavelength, 300 nm; flow-rate, 1 ml/min. $k'_{(+)\text{-PFN}} = 4.09$ (retention time 14.2 min), $N = 16\,400$; $k'_{(-)\text{-PFN}} = 4.27$ (retention time 14.7 min), $N = 2710$; $k'_{(-)\text{-PRL}} = 5.27$ (retention time 17.6 min).

REFERENCES

1 D. W. G. Harron and R. N. Brodgen, *Drugs*, 34 (1987) 617.
2 M. S. S. Chow, C. Lebsack and D. Hilleman, *Clin. Pharm.*, 7 (1988) 869.
3 C. Funck-Brentano, H. K. Kroemer, J. T. Lee and D. M. Roden, *N. Engl. J. Med.*, 322 (1990) 518.
4 J. T. Y. Hii, H. J. Duff and E. D. Burgess, *Clin. Pharmacokinet.*, 21 (1991) 1.
5 H. K. Kroemer, C. Funck-Brentano and D. J. Silberstein, *Circulation*, 79 (1989) 1068.
6 K. Stoschitzky, W. Klein, G. Stark, U. Stark, G. Zernig, I. Graziadei and W. Lindner, *Clin. Pharmacol. Ther.*, 47 (1990) 740.
7 E. Brode, H. Müller-Peltzer and M. Hollmann, *Methods Find. Exp. Clin. Pharmacol.*, 10 (1988) 717.
8 R. Mehvar, *J. Chromatogr.*, 527 (1990) 79.
9 K. Imai, *Adv. Chromatogr.*, 27 (1987) 215.
10 C. Pettersson, A. Karlsson and C. Gioeli, *J. Chromatogr.*, 407 (1987) 217.
11 W. Lindner, in M. Zief and L. J. Crane (Editors), *Chiral Chromatographic Separations (Chromatographic Science Series*, Vol. 40), Marcel Dekker, New York, 1988, p. 91.
12 C. Pettersson and M. Josefsson, *Chromatographia*, 21 (1986) 321.
13 G. Blaschke and B. Walter, *Liebigs Ann. Chem.*, 1987 (1987) 561.
14 R. Rosset, M. Caude and A. Jardy, *Chromatographie en Phase Liquide*, Masson, Paris, 1982.

Journal of Chromatography, 605 (1992) 41–48
Elsevier Science Publishers B.V., Amsterdam

CHROM. 24 218

Identification and determination of the flavonoids from *Ginkgo biloba* by high-performance liquid chromatography

A. Hasler and O. Sticher

Department of Pharmacy, Swiss Federal Institute of Technology (ETH) Zurich, CH-8092 Zurich (Switzerland)

B. Meier

Zeller AG, CH-8590 Romanshorn (Switzerland)

(First received December 12th, 1991; revised manuscript received March 3rd, 1992)

ABSTRACT

Qualitative and quantitative reversed-phase high-performance liquid chromatographic methods have been developed for the separation and determination of the flavonoids found in the leaves and therapeutically used extracts of *Ginkgo biloba*. The first method includes hydrolysis of the flavonoids and subsequent quantitative chromatographic assay of the obtained aglycones and qualitative analysis of the biflavones. The second method is a "fingerprint" procedure to identify unambiguously 33 flavonoids of *Ginkgo biloba*.

INTRODUCTION

Extracts of the leaves of *Ginkgo biloba* L. are used as phytomedicines to increase peripheral and cerebral blood flow. The Ginkgo extracts contain as active compounds flavonoids and terpene lactones (ginkgolides and bilobalide). They show effects on vascular and cerebral metabolic processes and they inhibit platelet-activating factor [1–3].

There have been only a few investigations on the separation and determination of flavonoids in *Ginkgo biloba*. Briançon-Scheid and co-workers [4,5] and with superior results Pietta *et al.* [6] reported high-performance liquid chromatographic (HPLC) separations of biflavones. According to present knowledge, the biflavones represent characteristic markers for the identification of Ginkgo leaves, but they do not show the desired activity and are therefore not suitable for standardization.

The great variety of genuine flavonoid glycosides can be reduced by hydrolysis to the three major aglycones isorhamnetin, kaempferol and quercetin. The minor flavonoids in Ginkgo, apigenin, luteolin and myricetin, can also be identified, if necessary, by our previously described method [7]. The efficient chromatographic procedure is advantageous compared with a similar method described by Wagner *et al.* [8], especially for serial analyses in quality control and stability tests of herbal remedies. The reduction of the genuine compounds by hydrolysis has already been established in the quality control of phytopharmaceuticals, *e.g.*, for the standardization of willow preparations [9].

To identify extracted plant material as a Ginkgo preparation, the erstwhile proposed quantification [7] is, owing to the omnipresent flavonoid aglycones, not sufficient. Therefore, we have developed a chromatographic procedure to determine the

Correspondence to: Dr. O. Sticher, Department of Pharmacy, Swiss Federal Institute of Technology (ETH) Zürich, CH-8092 Zürich, Switzerland.

0021-9673/92/$05.00

aglycones and to qualify the characteristic biflavones of *Ginkgo biloba* in one run. To obtain more information about the genuine flavonoid pattern of *Ginkgo biloba* we have also elaborated a "fingerprint" analysis. Fingerprint chromatography was introduced, and subsequently accepted by WHO [10], several years ago for the quality control of herbal medicines. The possibility of on-line diode-array detection offered real progress in fingerprint chromatography [11]. Wagner *et al.* [8] described a fingerprint HPLC separation of Ginkgo leaves. Twenty peaks were detected within 55 min but only two flavonoids (rutin and astragalin) and the four biflavones (bilobetin, ginkgetin/isoginkgetin and sciadopitysin), ginkgol, shikimic acid and 6-hydroxykynurenic acid could be assigned. Recently, Pietta *et al.* [12] reported an HPLC method for the separation of fifteen known Ginkgo flavonoids within 50 min. The assignment was done with reference compounds for six flavonoids. The other flavonoid glycosides were assigned by their UV–VIS spectra using a diode-array detector, although their absorptions were less than 10 milliabsorption units (mAU). Such assignments, without any other investigations, are very speculative. In both methods the separation and identification of the flavonoids are not very developed and not complete. Lobstein *et al.* [13] used gradient elution with acetonitrile and 0.1 *N* phosphoric acid to separate flavonoids and biflavones within 50 min. No diode-array detector was coupled to the HPLC system. Additionally, the lack of reference compounds prevented complete peak assignment. Kaempferol and quercetin 3-O-coumaroyl glucorhamnoside and the biflavones in leaves were determined. A small study of seasonal variations was carried out.

In summary, there are strategies, but no satisfactory method, for the determination of flavonoids in Ginkgo leaves and Ginkgo preparations for research teams and pharmaceutical companies. These are necessary to fulfil the demands of new guidelines for the assessment of herbal medicines, as proposed by the WHO in Munich in 1991, for example [10]. The isolation of 22 flavonoids, five of which have not been described previously and three others which have not been previously detected in Ginkgo leaves, during our research with *Ginkgo biloba* [14,15] stimulated us to develop effective HPLC methods. In this paper we describe the HPLC determination of flavonols after hydrolysis together with the separation of biflavones in one run and the fingerprint HPLC separation of 33 flavonoids in leaves and in therapeutically used extracts of *Ginkgo biloba.*

EXPERIMENTAL

Plant materials and plant extracts

Ginkgo leaves were purchased from several different dealers (Dixa, St. Gallen, Switzerland; Hänseler, Herisau, Switzerland; Siegfried, Zofingen, Switzerland) and collected from a female tree in Zurich (Mythenquai) from mid-May to mid-November, 1988. Plant extracts were either bought from Flachsmann (Zurich, Switzerland) or provided by Zeller (Romanshorn, Switzerland).

Drying

After collection, the leaves were immediately dried, for 72 h at 35°C in a Salvis TSK2 HL dryer (Salvis, Emmenbrücke, Switzerland) with forced ventilation.

Standards and solvents

The isolation and structure elucidation of all the flavonoid glycosides were carried out in our laboratory [14,15]. The aglycones (Rotichrom HPLC grade) were purchased from Roth (Karlsruhe, Germany) and the biflavones were provided by Dr. Willmar Schwabe (Karlsruhe, Germany). All the organic solvents used were of HPLC grade (Romil Chemicals, Shepshed, UK). Orthophosphoric acid (analytical-reagent grade) was obtained from Fluka (Buchs, Switzerland). Pure water was delivered by a NANOpure Cartridge System (Skan, Basle-Allschwil, Switzerland). Bond Elut C_{18} (500 mg) disposable extraction columns (Analytichem International, Harbor City, CA, USA) were used for sample clean-up.

Instrumentation and columns

All separations were carried out with a Hewlett-Packard system (Model 79994A Analytical Workstation, Model 1090 liquid chromatograph, Model 1040 diode-array detector). A Knauer (Berlin, Germany) prepacked column cartridge (100 × 4 mm I.D.) filled with Nucleosil 100-C_{18}, 3 μm (Machery–Nagel, Düren, Germany) was used.

TABLE I

MOBILE PHASE GRADIENT IN METHOD A

Time (min)	Solvent A (%)	Solvent B (%)	Solvent C (%)
0.01	22.5	22.5	55.0
9.50	22.5	22.5	55.0
9.51	25.0	25.0	50.0
17.00	25.0	25.0	50.0
17.01	30.0	30.0	40.0
20.00	30.0	30.0	40.0

Chromatographic procedures

Method A. The mobile phase consisted of solvent A (methanol), solvent B [tetrahydrofuran (THF)] and solvent C (0.5% orthophosphoric acid) with the gradient shown in Table I. The flow-rate was 1 ml/min, the column temperature 30.0°C, the injection volume 10 μl and detection was effected at 370 nm.

Method B. The mobile phase consisted of solvent A [isopropanol–THF (25:65)], solvent B (acetonitrile) and solvent C (0.5% orthophosphoric acid) with the gradient shown in Table II. The flow-rate was 1 ml/min, the column temperature 30°C, the injection volume 10 μl and detection was effected at 350 nm.

Sample preparation

Method A. A 4-g amount of dried and pulverized plant material or a 2-g amount of dried plant extract was refluxed with 70 ml of methanol and 10 ml of 25% hydrochloric acid for 60 min. After cooling, the solution was filtered through a glass filter (G3, pore size 16–40 μm; Schott, Jena, Germany) covered with a filter-paper (LS 14, pore size 4.4 μm; Schleicher & Schüll, Feldbach, Switzerland). The supernatant was washed with 100 ml of methanol. The solution was evaporated under vacuum to about 80 ml and then diluted to 100 ml with methanol in a volumetric flask. A 5-ml volume of this solution was filtered through a Bond Elut C_{18} cartridge that was equilibrated with methanol. The cartridge was washed with 4 ml of methanol and the solution was diluted to 10 ml with methanol in a volumetric flask. A 10-μl volume of this solution was injected into the HPLC system.

TABLE II

MOBILE PHASE GRADIENT IN METHOD B

Time (min)	Solvent A (%)	Solvent B (%)	Solvent C (%)
0.01	15.0	1.5	83.5
7.00	15.0	1.5	83.5
7.01	12.0	5.0	83.0
12.00	12.0	5.0	83.0
16.00	15.0	13.0	72.0
20.00	5.0	25.0	70.0
20.01	5.0	30.0	65.0
24.00	8.0	42.0	50.0
24.01	0.0	48.0	52.0
30.00	0.0	78.0	22.0

Method B. A 4-g amount of dried and pulverized plant material or a 2-g amount of dried plant extract was extracted using a Polytron PT-MR 3000 high-speed mixer (20 000 rpm) (Kinematica, Littau, Switzerland) with 50 ml of 80% ethanol for 2 min. The solution was filtered through a glass filter (G3, pore size 16–40 μm; Schott) covered with a filter-paper (LS 14, pore size 4.4 μm; Schleicher & Schüll). The supernatant was extracted with the Polytron a second time with 30 ml of 80% ethanol for 1 min and then washed with 20 ml of 80% ethanol. The solution was evaporated under vacuum to about 40 ml and then diluted to 50 ml with 80% ethanol in a volumetric flask. A 5-ml volume of this solution was filtered through a Bond Elut C_{18} cartridge that was equilibrated with 80% ethanol. The cartridge was washed with 4 ml of methanol and the solution was diluted to 10 ml with 80% ethanol in a volumetric flask. A 10 μl-volume of this solution was injected into the HPLC system.

Identification and purity of peaks

The identification of the peaks was carried out with automated library search software (Hewlett-Packard, operating software, Rev. 5.03, 1988). In the library the standards were saved with their retention times (Table III) and their UV spectra.

Determination of the aglycones

The determination of the aglycones was established with external standards. Each sample was injected three times for HPLC. The linearity of the determination of the threee flavonols was verified by regression analysis. The correlation coefficients

TABLE III

THE GRADIENT ELUTION PROFILE OF THE NATURALLY OCCURRING FLAVONOIDS OF *GINKGO BILOBA* L.

Compound No.	t_R (min)	Flavonoid
1	3.21	3-O-{2-O-[6-O-(*p*-Hydroxy-*trans*-cinnamoyl)-β-D-glucosyl]-α-L-rhamnosyl}-7-O-(β-D-glucosyl)quercetin
2	3.47	3-O-[2-O, 6-O-Bis(α-L-rhamnosyl)-β-D-glucosyl]quercetin
3	4.09	3-O-[2-O, 6-O-Bis(α-L-rhamnosyl)-β-D-glucosyl]isorhamnetin
4	4.71	3-O-[2-O, 6-O-Bis(α-L-rhamnosyl)-β-D-glucosyl]kaempferol
5	4.97	3-O-[6-O-(α-L-Rhamnosyl)-β-D-glucosyl]myricetin
6	5.96	3-O-[6-O-(α-L-Rhamnosyl)-β-D-glucosyl]-3′-methylmyricetin
7	6.53	3-O-(2-O-{6-O-[*p*-(β-D-Glucosyl)oxy-*trans*-cinnamoyl]-β-D-glucosyl}-α-L-rhamnosyl)quercetin
8	7.19	3-O-[6-O-(α-L-Rhamnosyl)-β-D-glucosyl]quercetin
9	8.73	3-O-(2-O-{6-O-[*p*-(β-D-Glucosyl)oxy-*trans*-cinnamoyl]-β-D-glucosyl}-α-L-rhamnosyl)kaempferol
10	8.73	3-O-[6-O-(α-L-Rhamnosyl)-β-D-glucosyl]isorhamnetin
11	9.68	3-O-(β-D-Glucosyl)quercetin
12	10.37	3-O-[6-O-(α-L-Rhamnosyl)-β-D-glucosyl]kaempferol
13	10.74	3-O-[2-O-(β-D-Glucosyl)-α-L-rhamnosyl]quercetin
14	11.39	3-O-(β-D-Glucosyl)isorhamnetin
15	13.00	3-O-(β-D-Glucosyl)kaempferol
16	13.58	7-O-(β-D-Glucosyl)apigenin
17	14.58	3-O-[2-O-(β-D-Glucosyl)-α-L-rhamnosyl]kaempferol
18	15.22	3-O-(α-L-Rhamnosyl)quercetin
19	16.65	3′-O-(β-D-glucosyl)luteolin
20	17.05	3-O-(α-L-Rhamnosyl)kaempferol
21	17.60	3-O-{2-O-[6-O-(*p*-Hydroxy-*trans*-cinnamoyl)-β-D-glucosyl]-α-L-rhamnosyl}quercetin
22	18.51	3-O-{2-O-[6-O-(*p*-Hydroxy-*trans*-cinnamoyl)-β-D-glucosyl]-α-L-rhamnosyl}kaempferol
23	18.76	Myricetin
24	20.60	Luteolin
25	21.50	Quercetin
26	22.22	Apigenin
27	22.76	Isorhamnetin
28	22.91	Kaempferol
29	24.02	Amentoflavon
30	25.06	Bilobetin
31	27.00	Ginkgetin
32	27.17	Isoginkgetin
33	29.35	Sciadopitysin

were 0.994 for isorhamnetin, 0.998 for kaempferol and 0.999 for quercetin. Standard solutions for calibration showed a very high stability with a loss of <4% within 12 months and storage at 8°C in a refrigerator. Seven different weight ratios from 0.2 to 2.0 μg (injected, resulting peak heights 250–2200 mAU) of the three flavonols were used. Known amounts of the aglycones dissolved in methanol were submitted three times to the sample preparation process and the recovery was determined: isorhamnetin = 99.8, kaempferol = 101.5 and quercetin = 100.6%.

Reproducibility of the fingerprint method

The reproducibility of the fingerprint method was demonstrated with columns from several batches and with the successful application in the laboratories of Zeller, where the analyses were carried out on an HP 1090 liquid chromatograph with a PV5 system (ternary solvent-delivery system controlled by a proportioning valve) instead of a DR5 system (three low-pressure pumps) on which the separation was developed in the laboratories of the ETH.

RESULTS AND DISCUSSION

Hydrolysis of the glycosides followed by a spectrophotometric determination of the aglycones as an aluminium chelate complex is the current method in several pharmacopeias to determine the concentration of flavonoids in herbal drugs. In the case of Ginkgo leaves this method was not reproducible [14], propably owing to the large amount of disturbing proanthocyanidines. Further, a detailed determination of the qualitative and quantitative composition of the obtained aglycones is not possible.

For more than 10 years, HPLC has been the method of choice for qualitative and especially quantiative analyses of flavonoids. It is logical to combine the well-established hydrolysis in the pharmacopeias with the modern technique of HPLC. The kinetics of hydrolysis were tested with rutin. It decomposed completely to the calculated amount of quercetin within 60 min. The separation of the aglycones on a reversed-phase (RP) column can be realized with complete resolution and different elution orders with two different solvents (method A and ref. 7). The work-up procedure consists of two steps: extraction and hydrolysis of the glycosides, and sample clean-up. Extraction and hydrolysis are performed by refluxing the pulverized plant material or a plant extract with 10 ml of hydrochloric acid (25%) in 70 ml of methanol for 60 min, while sample clean-up is carried out using C_{18} solid-phase extraction cartridges. An aliquot of the resulting final solution is then injected into the HPLC system. Isorhamnetin, kaempferol and quercetin can easily be determined by RP-HPLC using a gradient with 0.5% (v/v) orthophosphoric acid in water and methanol [7] or a methanol–THF mixture and UV detection at 370 nm. The elution profile of isorhamnetin and kaempferol is inverted on using THF as organic solvent.

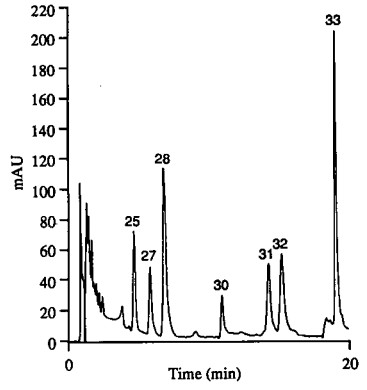

Fig. 1. Chromatogram of a leaf extract from *Ginkgo biloba* after hydrolysis, using Nucleosil 100-C_{18} (3 μm) with method A. Peak numbering as in Table III. Aglycones for quantitative assay and biflavones for identification are detected.

TABLE IV

CONVERSION OF THE FLAVONOID AGLYCONE CONTENT INTO A "GINKGO FLAVONE" GLYCOSIDE CONTENT

The conversion factors for the aglycones isorhamnetin (MW 316.27), kaempferol (MW 286.24) and quercetin (MW 302.2) are determined with the molecular weight of flavonol coumaroyl ester glycosides, *e.g.*, 3-O-{2-O-[6-O-(*p*-hydroxy-*trans*-cinnamoyl)-β-D-glucosyl]-α-L-rhamnosyl}quercetin (MW 756.7).

Compound	Conversion factor[a]
Isorhamnetin	2.39
Kaempferol	2.64
Quercetin	2.51
Average	2.51

[a] Calculation: $\sum$(aglycones) · 2.51 = concentration of "Ginkgo flavone" glycosides.

The analytical validation of methods used for the determination of phytopharmaceuticals is part of the modern documentation ordered by the national regulatory authorities. The specification, precision and accuracy have to be documented. To determine the accuracy of the determination of flavonoids, method A was developed in addition to the earlier described method [7]. Identical values resulted for both methods (Table V). In addition, method A can be used for the identification of the crude drug: the three main aglycones (**25–28**) and the characteristic and therefore specific biflavones (**30–33**) were separated in the same run (Fig. 1). The ubiquitous aglycones alone are not specific enough to identify Ginkgo. This method cannot be applied to special extracts like EGb 761 (Dr. Willmar Schwabe), where the biflavones have been removed.

In the standardization of phytomedicines, direct determination of the naturally occurring active principles would be desirable. The complex flavonoid profile of *Ginkgo biloba* demands a reduction

TABLE V

DETERMINATION OF THE FLAVONOID AGLYCONES IN GINKGO LEAVES AND EXTRACTS

Values in parentheses are relative standard deviations (%) (n = 3)

Harvest month, 1988	Isorhamnetin (%)		Kaempferol (%)		Quercetin (%)		∑(Aglycones) (%)	
	A	C[a]	A	C[a]	A	C[a]	A	C[a]
May	0.13 (2.5)	0.14 (2.5)	0.38 (2.8)	0.38 (1.8)	0.18 (2.2)	0.18 (1.2)	0.70	0.70
June	0.06 (3.5)	0.06 (3.2)	0.17 (3.0)	0.18 (2.5)	0.09 (3.3)	0.09 (2.0)	0.32	0.33
July	0.05 (3.1)	0.06 (2.1)	0.16 (3.6)	0.17 (2.6)	0.08 (3.0)	0.08 (1.7)	0.29	0.31
August	0.06 (1.9)	0.07 (2.1)	0.17 (1.6)	0.17 (2.0)	0.09 (1.9)	0.09 (0.9)	0.32	0.33
September	0.06 (2.5)	0.06 (2.5)	0.16 (2.8)	0.17 (2.8)	0.08 (1.2)	0.09 (1.2)	0.30	0.32
October	0.06 (2.0)	0.06 (3.0)	0.16 (2.0)	0.16 (3.0)	0.07 (2.2)	0.07 (2.2)	0.29	0.29
November[b]	0.07 (2.8)	0.07 (2.8)	0.17 (3.2)	0.17 (3.2)	0.08 (2.8)	0.08 (2.8)	0.32	0.32
Commercial sample								
Hänseler 912050	0.04 (3.0)	0.05 (0.8)	0.10 (2.8)	0.10 (3.1)	0.09 (3.1)	0.10 (3.2)	0.25	0.25
Dixa 38747	0.04 (2.8)	0.04 (3.1)	0.13 (2.7)	0.13 (2.7)	0.10 (3.0)	0.10 (2.7)	0.27	0.27
Siegfried 147974-02	0.04 (1.8)	0.05 (3.8)	0.11 (2.2)	0.11 (2.8)	0.09 (2.0)	0.09 (3.6)	0.24	0.25
Extract								
Flachsmann 6 L 035	0.10 (2.2)	0.10 (2.5)	0.39 (2.5)	0.39 (2.8)	0.50 (2.3)	0.51 (3.0)	0.99	1.00
Zeller 32/89	0.14 (3.0)	0.14 (2.9)	0.42 (2.8)	0.42 (1.9)	0.55 (2.8)	0.55 (2.8)	1.11	1.11

[a] The values in column C were obtained with the earlier described method [7].
[b] Yellow and fallen leaves.

to the basic principles, because most reference compounds are not commercially available and a complete analysis for all compounds is tedious. However, the aglycone content obtained can be correlated with the total flavonoid glycoside content (Table IV). This is done in accordance with the practice in the pharmaceutical industry. The producers of Ginkgo preparations convert the obtained aglycone content into a "Ginkgo flavone" glycoside content. As "Ginkgo flavone" glycosides, the flavonol coumaroyl ester glycosides **21** and **22** (Table III) with an average molecular weight of *ca.* 760 are documented (the described interglycosidic linkage [16,17] has to be revised from 1→4 to 1→2 owing to new NMR investigations [14,15]).

Typical HPLC results for a hydrolysed Ginkgo extract have been presented previously [7]. Generally, kaempferol and quercetin are the main peaks and the concentration of isorhamnetin is approximately five times lower. The very small minor peaks represent further aglycones, *e.g.*, apigenin and luteolin. They could also be determined if they occurred at higher concentration levels. Our investigations have shown that dried Ginkgo leaves obtained commercially contain an aglycone content of 0.2–0.4% (w/w), corresponding to a calculated "Ginkgo flavone" glycoside content of 0.5–1% (w/w) (Table V). Green leaves are considered to be of better quality. However, concerning the total flavonoid content we could not see any significant differences in our ontogenetic studies between June and November 1988. The self-collected and self-dried leaves show a higher concentration of flavonoids than the commercially available leaves and the ratio of kaempferol to quercetin is different (Table V). Ginkgo full extracts contain about 2–4% (w/w) and enriched extracts (*e.g.*, EGb 761) about 24–27% (w/w) of "Ginkgo flavone" glycosides [3].

Further characterization of Ginkgo extracts is possible with the fingerprint analysis of the flavonoids. A chromatographic system (method B) was developed to separate the isolated flavonoids of *Ginkgo biloba*. Owing to the complex mixture of very polar (triglycosides), polar (mono- and diglycosides) and apolar (biflavones) flavonoids, the proposed separation within 30 min requires a sophisticated HPLC procedure including a three-pump system and a diode-array detector. It is possible to identify unambiguously 22 flavonoid glycosides, six flavonoid aglycones and five biflavones in leaves

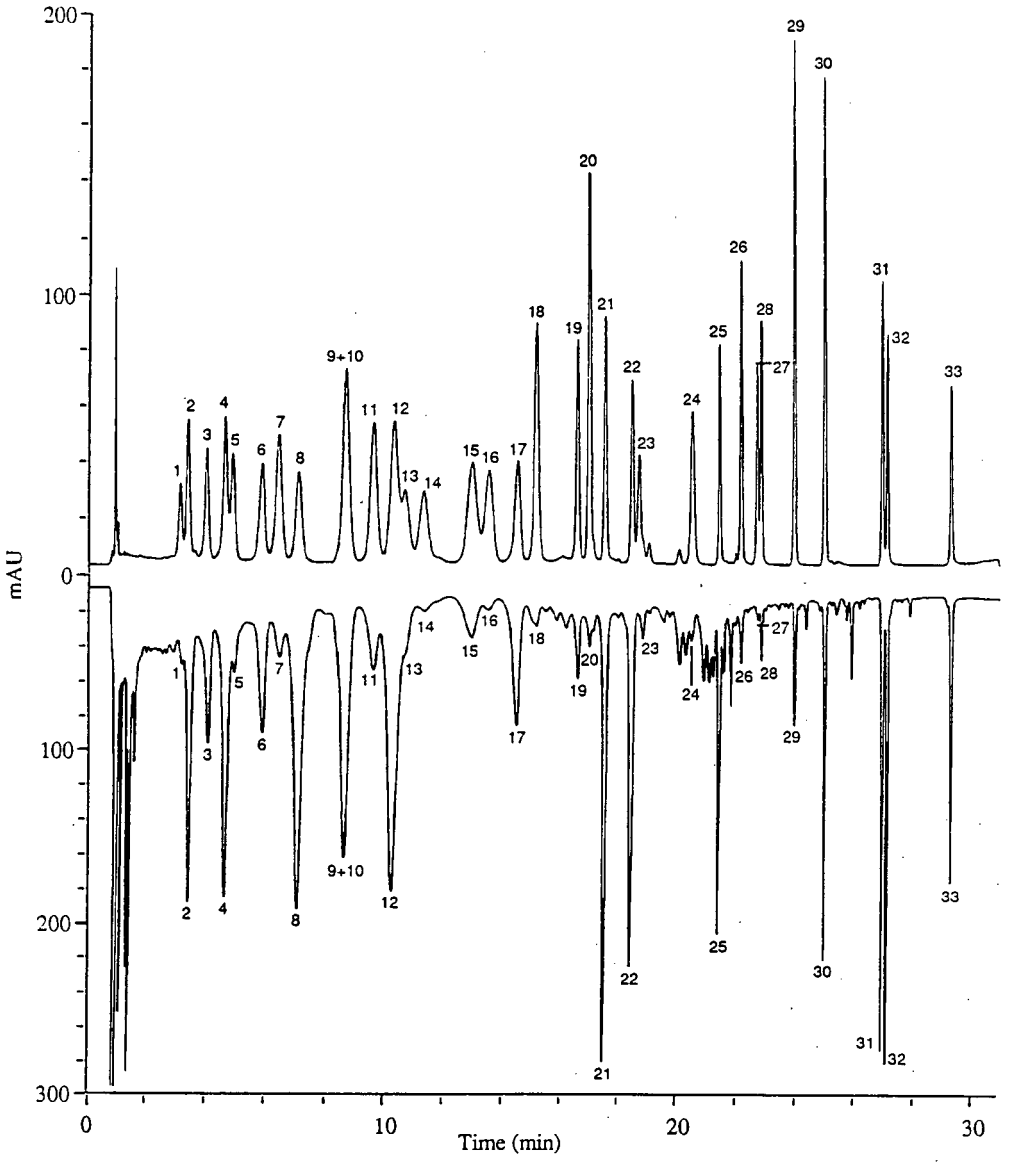

Fig. 2. (Top) chromatogram of the pure reference flavonoids from *Ginkgo biloba* and (bottom) fingerprint chromatogram of a therapeutically used dry extract of the leaves from *Ginkgo biloba* (Zeller, Lot-No. 32/89), using Nucleosil 100-C_{18} (3 μm). Peak numbering as in Table III.

and extracts from the elution order and UV spectra. An elution profile and the chromatographic results of the separation of reference compounds and of an extract used for herbal remedies produced by Zeller are shown in Table III and Fig. 2. The reference run has been stored together with UV spectra in the data system and can be used for peak assignment.

The fingerprint analysis is especially useful in stability tests. It can be shown that the flavonoid glycosides and the biflavones are stable and that the ratio of the compounds does not change. This is a demand of the EEC guideline 75/318 "Quality of Herbal Drugs" [18]. An increase in the aglycones and a decrease in the glycosides would indicate an

undesirable degradation process in the extract. The fingerprint analysis especially allows us to identify the very typical flavonol coumaroyl ester glycosides **21** and **22**. Both are well separated from each other and from other compouds. A more selective system is required in order to separate **9** and **10**. However, the UV spectra of the tested extracts showed a dominance of **10**.

CONCLUSION

New guidelines for herbal medicines demand ever better developed analytical methods to describe the quality of phytopharmaceuticals. *Ginkgo biloba* produces a large number of flavonoids in leaves, mainly derivatives of isorhamnetin, kaempferol and quercetin. The flavonoid assay can be controlled by the determination of the aglycones. The flavonols are commercially available as standards. The standardization of extracts is normally based on this assay. The presented HPLC fingerprint separation for checking the identity and the stability of products is applicable. The assignment can be done from the on-line UV spectra and elution profile. The analysis of a second group of compounds with therapeutic value, the assay of ginkgolides and bilobalide, has been described recently [19]. Analytical methods to guarantee a constant quality of Ginkgo products are now available.

ACKNOWLEDGEMENTS

Financial support from Zeller, Romanshorn, Switzerland, is gratefully acknowledged. We also thank Dr. Willmar Schwabe, Karlsruhe, Germany, for kindly providing the biflavones.

REFERENCES

1 E. W. Fünfgeld (Editor), *Rökan, Ginkgo biloba, Recent Results in Pharmacology and Clinic*, Springer, Berlin, 1988.
2 Special Issue on Extract of *Ginkgo biloba* (EGb 761), *Presse Méd.*, 15, No. 31 (1986) 1464–1604.
3 O. Sticher, A. Hasler and B. Meier, *Dtsch. Apoth. Ztg.*, 131 (1991) 1827.
4 F. Briançon-Scheid, A. Guth and R. Anton, *J. Chromatogr.*, 245 (1982) 261.
5 F. Briançon-Scheid, A. Lobstein-Guth and R. Anton, *Planta Med.*, 49 (1983) 204.
6 P. Pietta, P. Mauri and A. Rava, *J. Chromatogr.*, 437 (1988) 453.
7 A. Hasler, B. Meier and O. Sticher, *J. Chromatogr.*, 508 (1990) 236.
8 H. Wagner, S. Bladt, U. Hartmann, A. Daily and W. Berkulin, *Dtsch. Apoth. Ztg.*, 129 (1989) 2421.
9 B. Meier, O. Sticher and A. Bettschart, *Dtsch. Apoth. Ztg.*, 125 (1985) 341.
10 World Health Organization, *Guidelines for the Assessment of Herbal Medicines, Munich, 28.6.1991*, WHO, Geneva, 1991.
11 B. Meier and O. Sticher, *Pharm. Ind.*, 48 (1986) 87.
12 P. Pietta, P. Mauri, A. Bruno, A. Rava, E. Manera and P. Ceva, *J. Chromatogr.*, 553 (1991) 223.
13 A. Lobstein, L. Rietsch-Jako, M. Haag-Berrurier and R. Anton, *Planta Med.*, 57 (1990) 430.
14 A. Hasler, *Thesis*, No. 9353, ETH Zurich, Zurich, 1990.
15 A. Hasler, G.-A. Gross, B. Meier and O. Sticher, *Phytochemistry*, 31 (1992) 1391.
16 C. Nasr, M. Haag-Berruier, A. Lobstein-Guth and R. Anton, *Phytochemistry*, 25 (1986) 770.
17 C. Nasr, A. Lobstein-Guth, M. Haag-Berrurier and R. Anton, *Phytochemistry*, 26 (1986) 2869.
18 *Qualität von pflanzlichen Arzneimitteln, Erläuternde Hinweise zur geänderten Richtlinie 75/318/EWG*, in K. Feiden (Editor), Arzneimittelrichtlinien, Wissenschaftliche Verlagsgesellschaft, Stuttgart, 1990 Ch. 2.74,4.
19 T. A. van Beek, H. A. Scheeren, T. Rantio, W. Ch. Melger and G. P. Lelyveld, *J. Chromatogr.*, 543 (1991) 375.

Journal of Chromatography, 605 (1992) 49–62
Elsevier Science Publishers B.V., Amsterdam

CHROM. 24 180

Investigation of γ-irradiation of α-tocopherol and its related derivatives by high-performance liquid chromatography using a rapid scanning spectrophotometer☆

Imre Molnar

Institute of Applied Chromatography, Blücherstrasse 22, D-1000 Berlin (Germany)

Susanne Koswig

Institute of Food Chemistry, Humboldt University, Berlin (Germany)

(First received November 29th, 1991; revised manuscript received March 10th, 1992)

ABSTRACT

The behaviour of α-tocopherol in differently reactive model systems was investigated immediately after irradiation or chemical reaction by reversed-phase high-performance liquid chromatography with rapid-scanning UV detection. The main advantage of this technique is the generation of the complete spectral and chromatographic information in one experiment. The other advantage of the method is the ability to study α-tocopherol in different environments (solvents) without tedious sample preparation and the characterization of the main primary products. The method is especially well suited for the investigation of α-tocopherol and related substances, which are sensitive to oxidation, which could not be studied with other conventional techniques.

INTRODUCTION

Tocopherols, a group of lipid-soluble compounds, are used as food ingredients and are biochemically interesting compounds. They are achieving increasing attention, due to α-tocopherol revealing among its properties as vitamin E, to be the most important natural antioxidant. It is able to protect lipids in the lipid phase of foods and in the membrane of living cells from autoxidation [1,2]. As irradiation is increasingly used to conserve foods, especially to protect poultry meat, vegetables, fruits

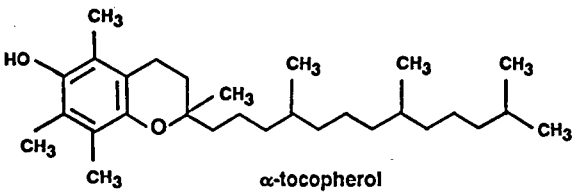

α-tocopherol

and spices from decomposition by various mechanisms and means [3], we wanted to study the behaviour of α-tocopherol during irradiation processes in different environments.

γ-Irradiation leads to changes in food composition, *e.g.*, owing to oxidation in the lipid phase [4]. Several workers have stated that substantial destruction of α-tocopherol occurs during the irradiation processes [5–9]. Therefore, the effect of irradiation on tocopherols and their capacity to act as antioxidants should be investigated.

Correspondence to: Dr. I. Molnar, Institute of Applied Chromatography, Blücherstrasse 22, D-1000 Berlin. Germany.

☆ Part of this paper was presented at the *15th International Symposium on Column Liquid Chromatography, Basle, June 3–7, 1991.*

0021-9673/92/$05.00

There have been several reports of the determination of tocopherols by high-performance liquid chromatography (HPLC) in different systems, such as foods, pharmaceutical preparations and mixtures containing tocopherols and other components, *e.g.*, vitamin mixtures [10]. However, no methods for dealing with products of α-tocopherol immediately after irradiation have been reported, so we wanted to develop an HPLC technique for this purpose.

Normal- and reversed-phase (RP) HPLC have been applied after the reaction of α-tocopherol with various oxidants [11–14]. Cillard *et al.* [11] separated three different tocopherol dimers by normal-phase HPLC after reaction of α-tocopherol with alkaline hexacyanoferrate(II). Yamauchi and coworkers [12–14] investigated the mixture resulting from the reaction of α-tocopherol with 2,2′-azobis (2,4-dimethylvaleronitrile) on μBondasphere C_{18} or Wakosil C_{18} with methanol, with gradient elution from methanol to methanol–ethyl acetate (3:7, v/v) and with methanol–ethyl acetate (7:3, v/v), respectively.

Yamauchi *et al.* [15] separated trimers and other tocopherol oxidation products in autoxidizing methyl lineolate by RP-HPLC on Wakosil C_{18} with a linear gradient from methanol to methanol–diisopropyl ether (1:1, v/v). Gottstein and Grosch [16] studied the products of autoxidation of linoleic acid in the presence of tocopherol model compounds using normal-phase HPLC.

Ha and Csallany [17] separated a mixture of α-tocopherol and five oxidation products by normal-phase HPLC with hexane–chloroform–2-propanol (95:4.5:0.5) (v/v/v) as the mobile phase. Koskas *et al.* [18] separated tocopherol, tocopherylquinone and a tocopheryl dimer by RP-HPLC on Spherisorb ODS with gradient elution from methanol–water (85:15, v/v) to methanol.

Howell and Wang [19] separated α-tocopherol, α-tocopherol acetate, α-tocopherylquinone, 6-hydroxy-2,5,7,8-tetramethylchroman-2-carboxylic acid and γ-tocopherol by RP-HPLC on Partisil ODS and on Spherisorb ODS in an isocratic mode using methanol–water (87:13, v/v) and gradient elu-

TABLE I

FURTHER HPLC METHODS FOR SEPARATION OF TOCOPHEROL AND TOCOPHERYLQUINONE

Column	Eluent (v/v)	Detection[a]	Compounds[b]	Ref.
Zorbax C_{18}	Methanol–water (98:2)	UV, 265 nm	T-quinone	20
C_{18}	Methanol–water (97.5:2.5)	UV, 280 nm	T-quinone	21
Spherisorb ODS	(a) Methanol–water (85:15) (b) Gradient from methanol–water (85:15) to methanol	UV, 290 nm	α-T, γ-T, T-dimer	22
μBondapak C_{18}	Acetonitrile	UV, 254 nm	Vitamin E Vitamin E quinone	23
C_{18}	Methanol–water (96:4)	UV, 265, 292, 215 nm	α-T, α-Tqu, γ-T, α-Tac, cholesterol	24
Ultrasphere ODS	2-Propanol–acetonitrile–water–triethylamine–acetic acid (60:20:19.4:0.5:0.1)	ED	T, T-quinone	25
Spherisorb ODS	96% methanol with sodium perchlorate (50 m*M*)	ED	T, T-quinone	26
Adsorbosphere C_{18} guard column				
C_{18}	Mixtures of ethanol and methanol containing 50 m*M* $NaClO_4$ and 2 m*M* $HClO_4$	ED	Prenyl quinones	27

[a] ED = Electrochemical detection.

[b] α-T = α-Tocopherol; γ-T = γ-tocopherol; α-Tac = α-tocopheryl acetate; Tqu = tocopheryl quinone; T-dimer = tocopheryl dimer.

tion from methanol–water (88:12, v/v) to methanol, respectively.

Some workers have observed α-tocopherylquinone using RP-HPLC in the presence of α-tocopherol (Table I).

In most HPLC analyses of tocopherols, UV, fluorescence or electrochemical detection techniques were used. The application of diode-array detection was described by Greenspan *et al.* [28] for the analysis of α-tocopherol, retinol, cholesterol and other lipid-soluble substances and by Miller and Yang [29] for a mixture of α-tocopherol with carotenoids.

The application of rapid scanning spectrophotometers has the advantage of protecting unstable compounds, which could be formed after gamma irradiation of α-tocopherol, owing to the use of linear optics, which means the application of less light energy to the sample in the detector cell. The use of such a detector for the study of tocopherol oxidation products has not been described previously, however. In our work we used a BarSpec Chrom-A-Scope rapid-scanning UV spectrophotometer as a detector.

EXPERIMENTAL

Instrumentation

A modular HPLC system was constructed, with a Knauer (Berlin, Germany) Type 64.00 pump, a Rheodyne (Cotati, CA, USA) model 7125 injector, a Nucleosil C_{18} (5 μm) column (250 × 4.6 mm I.D.) (Molnar, Berlin, Germany), a Victor (Frankfurt, Germany) PC 386A computer with Model 387 mathematical coprocessor, an NEC P6 (Berlin, Germany) printer and Chrom-A-Scope rapid-scanning spectrophotometer with a wavelength range from 190 to 370 nm (BarSpec, Rehovot, Israel). The eluent was acetonitrile (HPLC grade, Merck, Darmstadt, Germany) at a flow-rate of 2.0 ml/min.

For the investigation of venritidin HCl we used the following conditions: Column, EnCaPharm 100 RP-18 (5 μm) (120 × 4.6 mm I.D.) (Molnar); eluent, acetonitrile–0.4 *M* phosphate buffer (pH 2.1) (10.5:89.5, v/v); temperature, 60°C; injection volume, 40 μl (1 mg/ml); flow-rate 2.0 ml/min.

γ-Irradiation, ^{60}Co MRCH-τ-100 (Humboldt University, Berlin, Germany), irradiation dose 1.3 kGy, dose rate 64 Gy/min, temperature 293 K. To trap the irradiated state, the samples were frozen by using liquid nitrogen.

Reference substances and chemicals

The reference substances used were α-tocopherol (Merck) and tocopherylquinone (Serva, Heidelberg, Germany).

Formyltocopherol, ethoxymethyltocopherol and tocopherone were isolated with the chromatographic system described above. Fractions were evaporated and characterized by UV, IR and ^1H NMR spectroscopy [30] and identified by comparing the results with literature data [9,31,32]. The spirodimer of α-tocopherol was synthetised by the method of Boguth and Hackel [33], characterized by ^1H NMR, UV and IR spectroscopy [30] and identified by comparison with data from the literature [33].

Acetonitrile and methanol as eluents were of HPLC grade, other chemicals were of analytical-reagent grade (Merck).

RESULTS AND DISCUSSION

Method development

The synthesized spirodimer could not be eluted with methanol in the capacity factor (k') range 1–20. Using propionitrile as an eluent of higher elution strength, however, we could elute tocopherol dimers, but had problems with the reproducibility of the results owing to the high viscosity of this eluent. Mixtures of propionitrile with acetonitrile were also still fairly viscous. Methanol did separate well the polar oxidation products of α-tocopherol, but had a high absorbance below 220 nm. With acetonitrile, however, the irradiation products could be

TABLE II

α-TOCOPHEROL CONTENT (%, ±2.0%) AFTER γ-IRRADIATION IN DIFFERENT SOLVENTS [30,34]

Irradiation dose 1.3 kGy in the presence of air.

Solvent	Initial α-tocopherol concentration (g per 100 ml)		
	0.03–0.05	0.07–0.1	0.9–1.0
Benzene	100.0	100.0	100.0
Acetonitrile	93.5	96.9	100.0
Ethanol	68.0	87.7	–
Hexane	52.1	78.1	97.1
Chloroform	0.0	50.7	96.0[a]

[a] Initially 0.7 g of α-tocopherol per 100 ml.

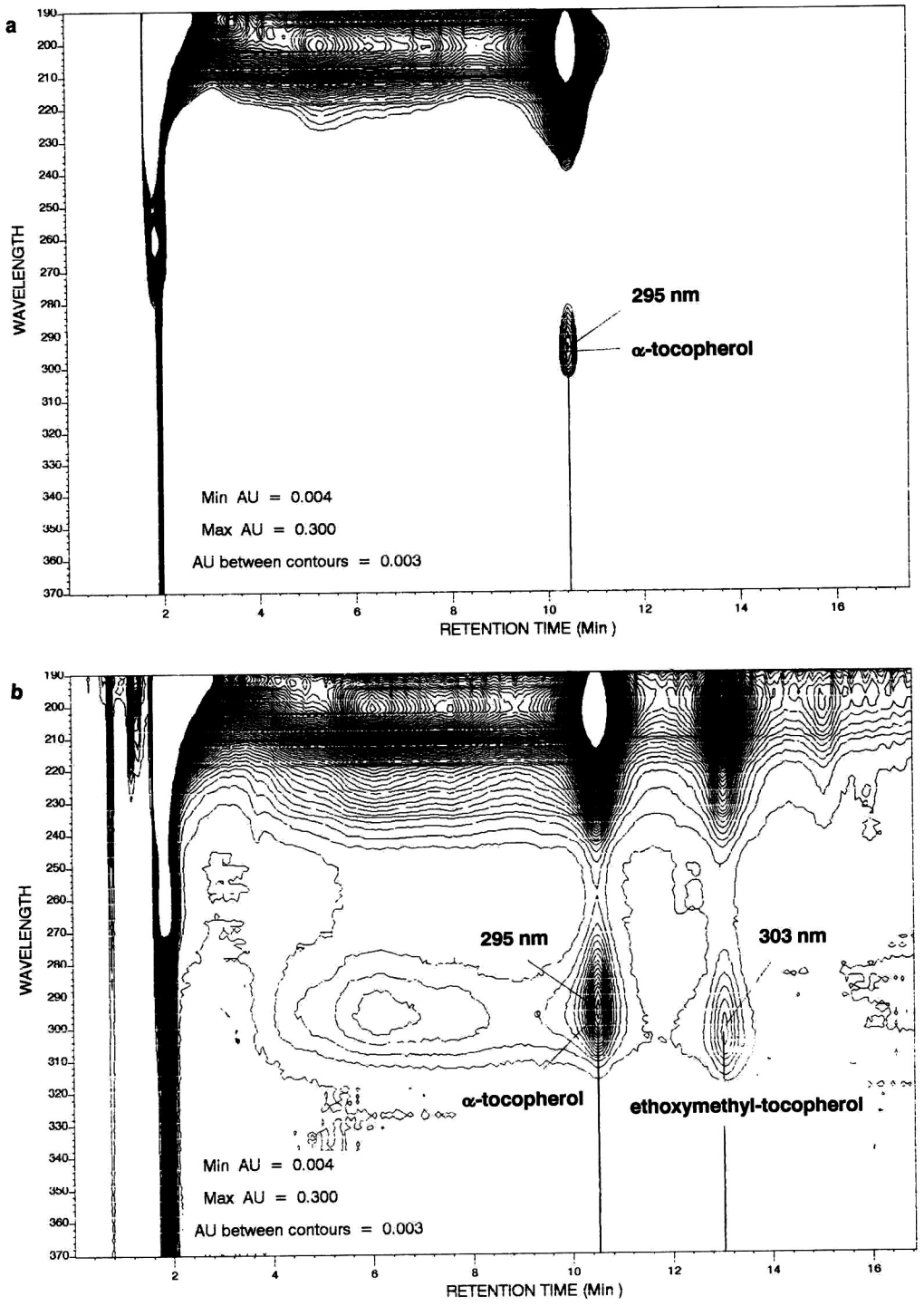
a
WAVELENGTH
RETENTION TIME (Min)
295 nm
α-tocopherol
Min AU = 0.004
Max AU = 0.300
AU between contours = 0.003
b
WAVELENGTH
RETENTION TIME (Min)
295 nm
303 nm
α-tocopherol
ethoxymethyl-tocopherol
Min AU = 0.004
Max AU = 0.300
AU between contours = 0.003

Fig. 1.

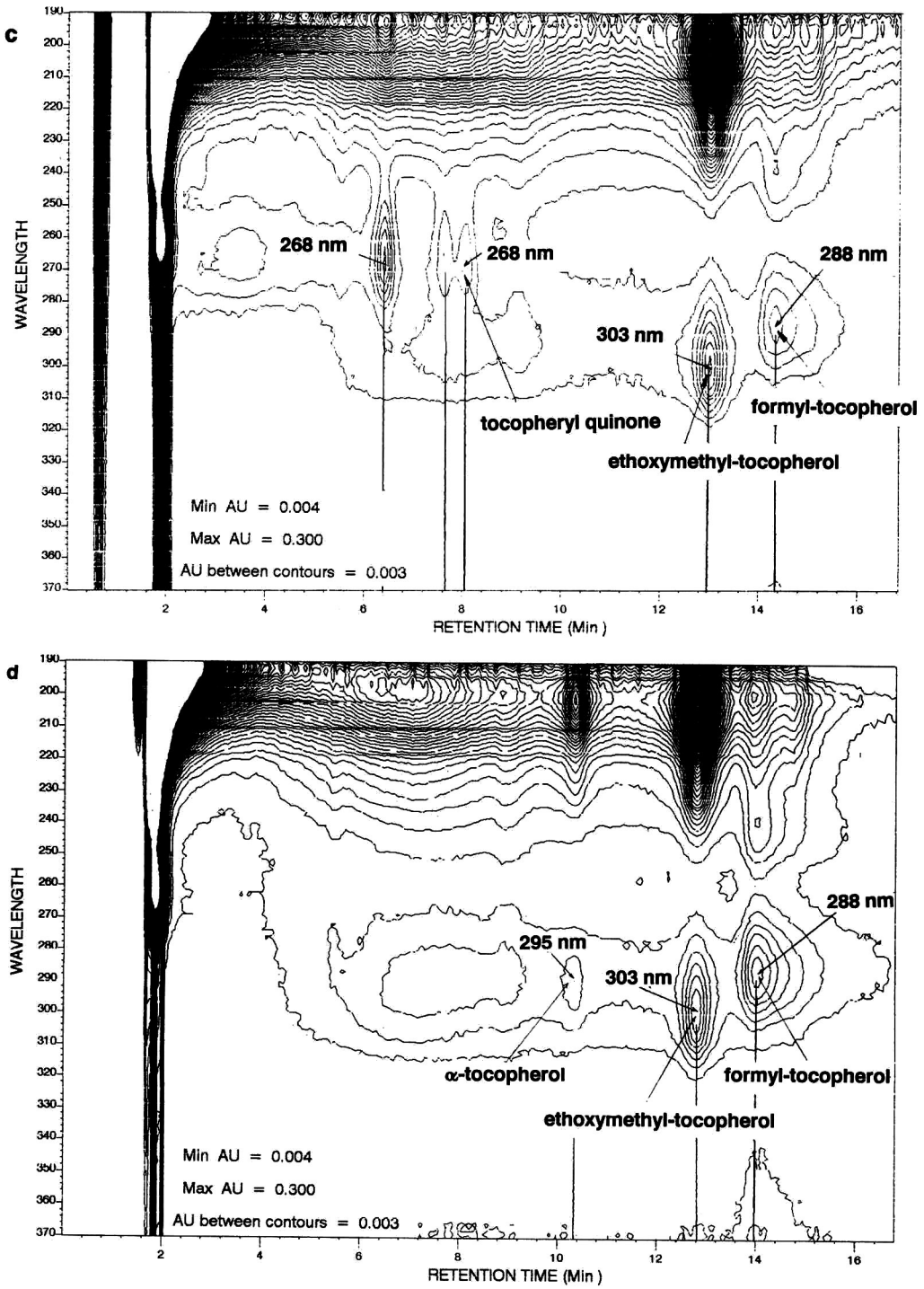

Fig. 1. HPLC contour map of γ-irradiated α-tocopherol in chloroform at low concentration (0.04 g per 100 ml). Injection volume, 100 μl. (a) Without irradiation; (b) *in situ* state after irradiation in the absence of oxygen, under nitrogen; (c) immediately after irradiation in the presence of oxygen; (d) as (c), but after storage for 1 day at 255 K.

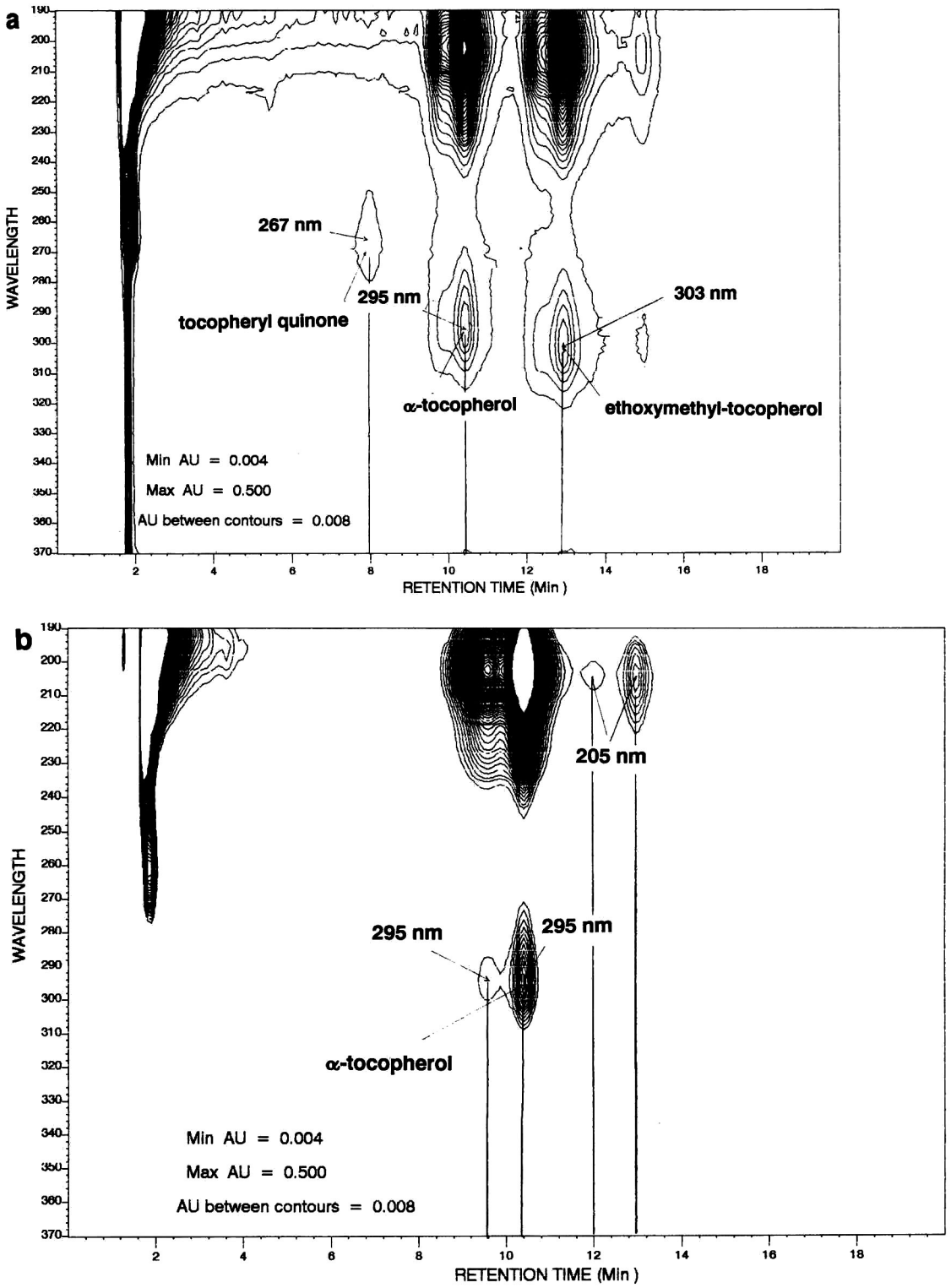
a
WAVELENGTH
RETENTION TIME (Min)
267 nm
295 nm
303 nm
tocopheryl quinone
α-tocopherol
ethoxymethyl-tocopherol
Min AU = 0.004
Max AU = 0.500
AU between contours = 0.008
b
WAVELENGTH
RETENTION TIME (Min)
205 nm
295 nm
295 nm
α-tocopherol
Min AU = 0.004
Max AU = 0.500
AU between contours = 0.008

Fig. 2.

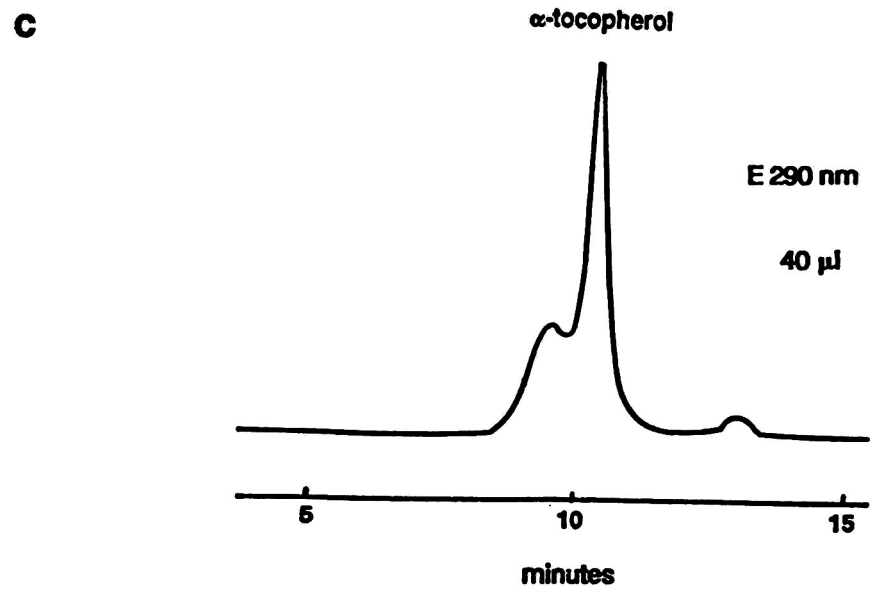

Fig. 2. HPLC and contour map of γ-irradiated α-tocopherol in chloroform at 0.1 g per 100 ml (immediately after irradiation). Injection volume, 40 µl. (a) Irradiation in the presence of oxygen; (b) irradiation in the absence of oxygen, under nitrogen; (c) chromatogram after irradiation under nitrogen (295 nm), from (b).

well separated and detected below 200 nm, making a correlation with the irradiation process possible. This and other investigations in hexane demonstrated further that significant amounts of tocopherol dimers are formed only in irradiated hexane.

Solvent-dependent results of γ-irradiaton

The investigations in different solvent systems revealed that the mechanism (how the reaction products are generated from α-tocopherol) and the degree of α-tocopherol destruction are variable and depend on the reactivity of the radical solvent species formed during the irradiation process (see Table II) [30,34].

Irradiation of the tocopherol molecule in highly reactive media (chloroform, ethanol, hexane) is terminated in oxidation processes and different reaction products are formed: (a) in chloroform, for-

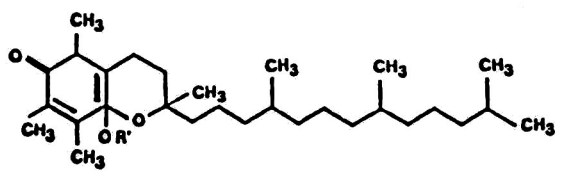

Tocopherone

R = H, OH

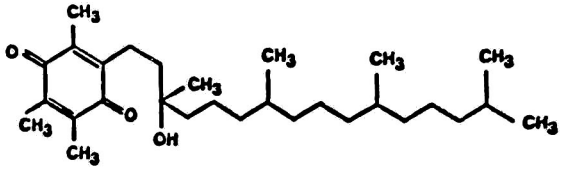

Tocopheryl quinone

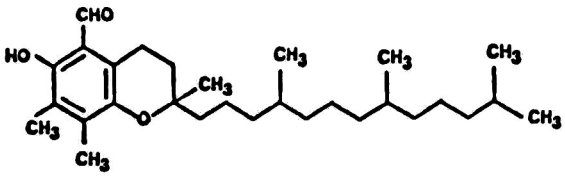

5-Formyl tocopherol

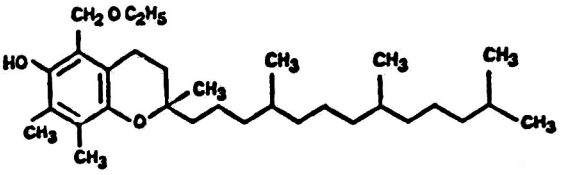

5-Ethoxymethyl tocopherol

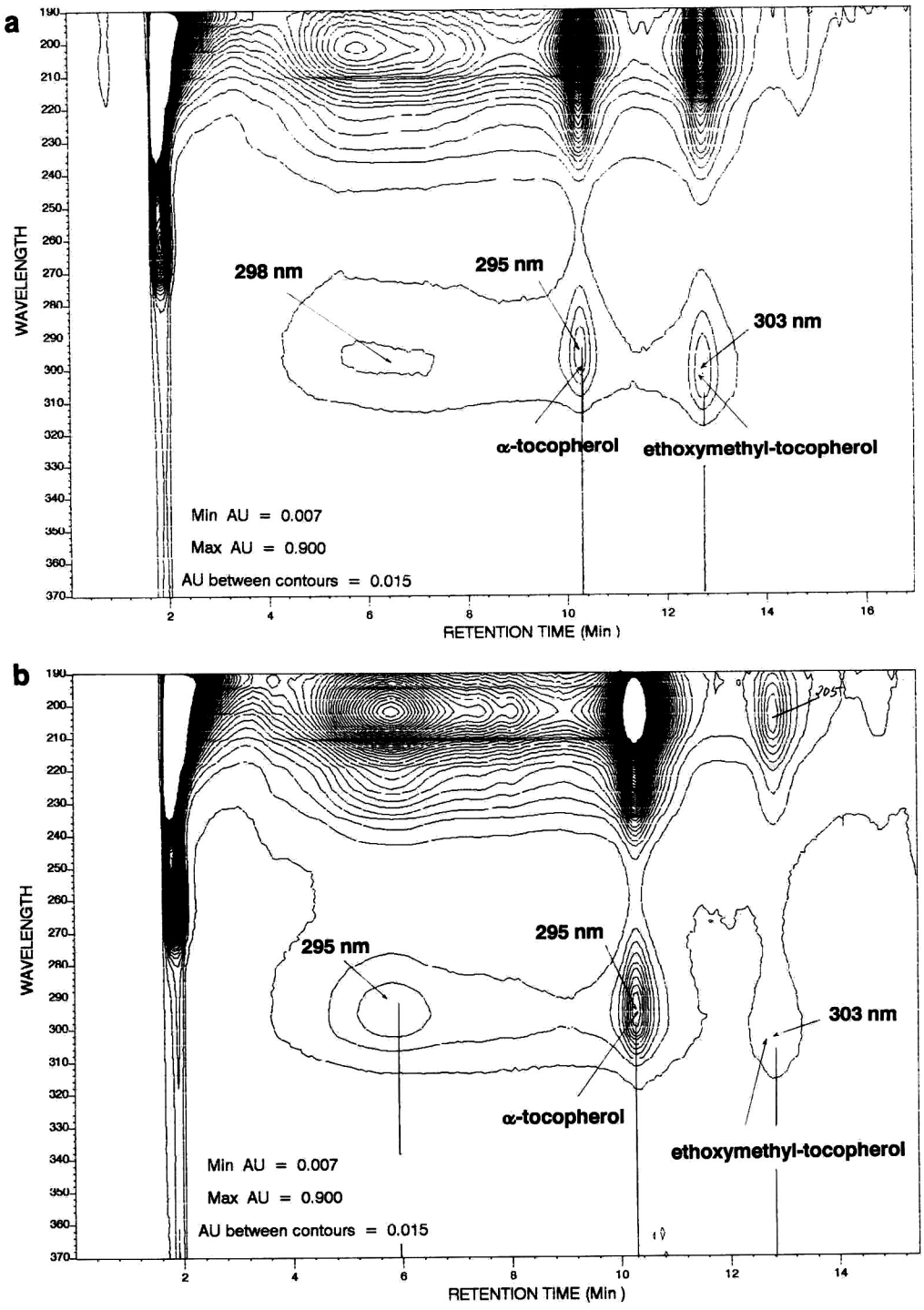
a
WAVELENGTH
RETENTION TIME (Min)
298 nm
295 nm
303 nm
α-tocopherol
ethoxymethyl-tocopherol
Min AU = 0.007
Max AU = 0.900
AU between contours = 0.015
b
WAVELENGTH
RETENTION TIME (Min)
295 nm
295 nm
303 nm
α-tocopherol
ethoxymethyl-tocopherol
Min AU = 0.007
Max AU = 0.900
AU between contours = 0.015

Fig. 3.

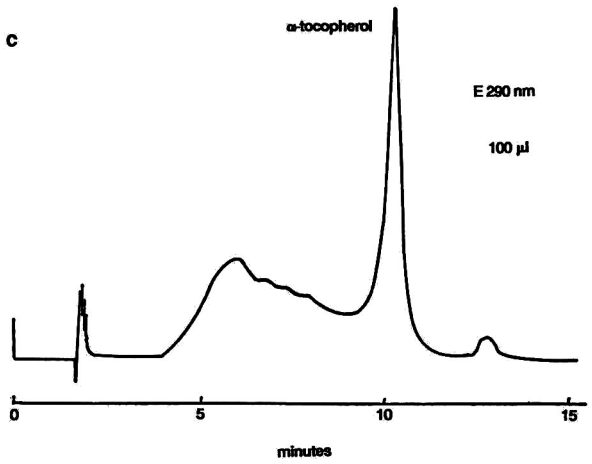

Fig. 3. HPLC and contour map of γ-irradiated α-tocopherol in chloroform at 0.1 g per 100 ml after storage for 1 day at 255 K. Injection volume 100 µl. (a) Irradiation in the presence of oxygen; (b) irradiation in the absence of oxygen, under nitrogen; (c) chromatogram of (b).

myl- and ethoxymethyltocopherol and quinones (Figs. 1–3); (b) in ethanol, tocopherone and tocopherylquinone (Fig. 4); and (c) in hexane, also tocopherylquinone (Fig. 5) and spirodimer (not eluted in Fig. 5), but measured by thin-layer chromatography elsewhere). Formyl-, and ethoxymethyltocopherol are also products of oxidation of α-tocopherol with *tert.*-butyl hydroperoxide in chloroform [31].

Dependence of the irradiation reaction on the presence of oxygen

The investigation showed that the products formed depend on the reactivity of the medium. The solubility of oxygen in the solvent plays an important role in the irradiation process. It is greater in hexane than in chloroform or in ethanol.

Following γ-irradiation in the absence of oxygen, under nitrogen, (a) in chloroform, formyltocopherol and quinones are not formed (Figs. 1–3); (b) in ethanol no products are formed (Fig. 4); and (c) in hexane the same products are formed with or without the presence of dissolved oxygen.

After irradiation in chloroform, an unknown species could be detected which had a shorter retention time and an extremely broad peak form (Figs. 2 and

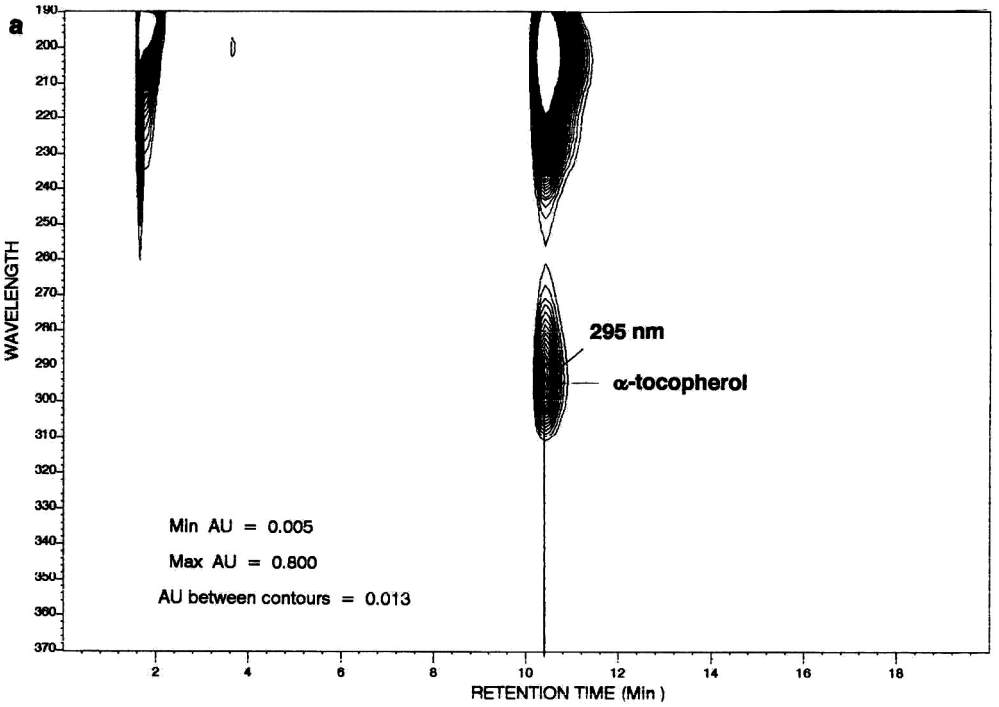

Fig. 4.

(Continued on p. 58)

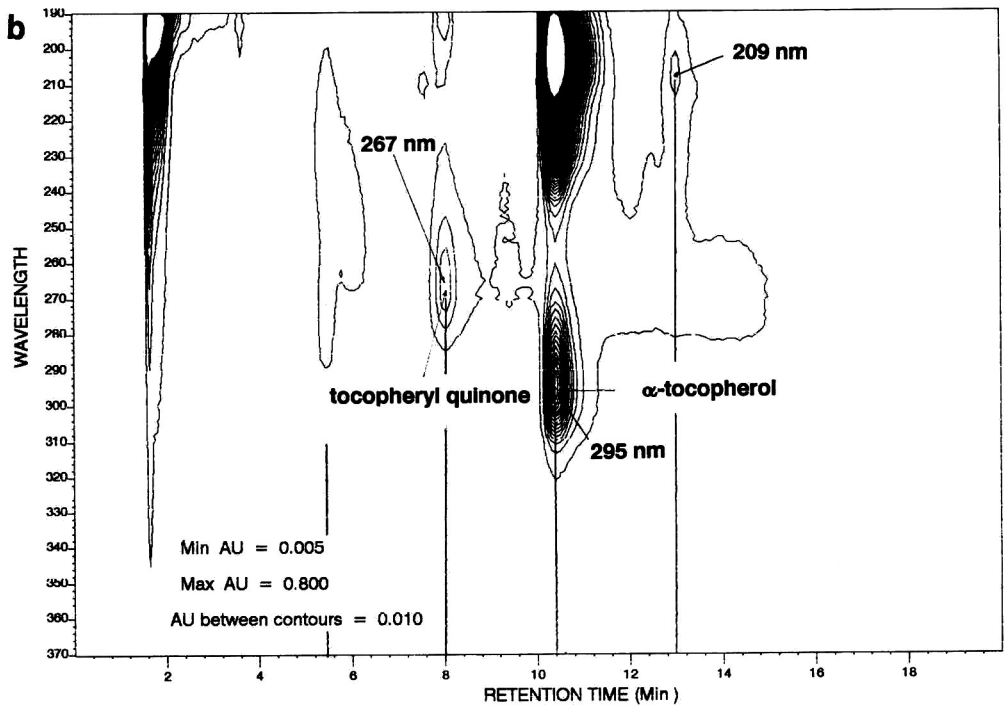

Fig. 4. HPLC contour map of γ-irradiated α-tocopherol in ethanol at 0.05 g per 100 ml (immediately after irradiation). Injection volume, 100 μl. (a) Irradiation in the absence of oxygen, under nitrogen; (b) irradiation in the presence of oxygen.

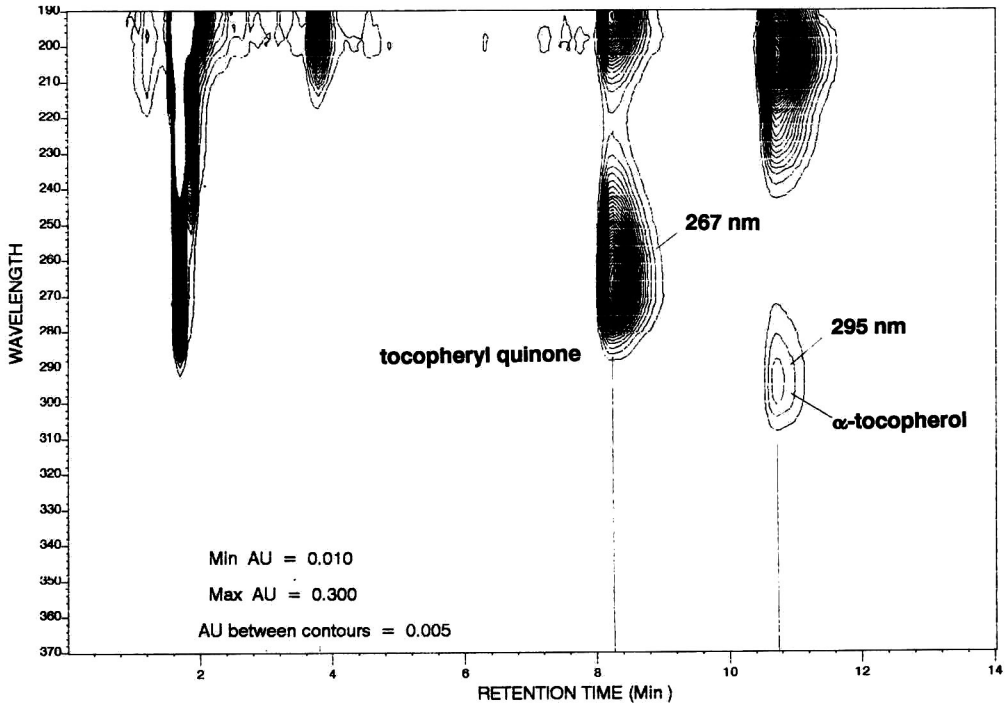

Fig. 5. HPLC contour map of γ-irradiated α-tocopherol in hexane at 0.08 g per 100 ml (*in situ* state). Injection volume, 40 μl.

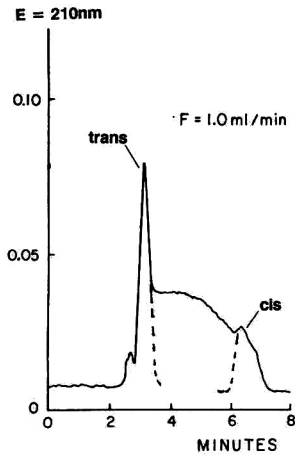

Fig. 6. Chromatogram of the *cis–trans* isomeric mixture of L-alanyl-L-proline as described by Melander *et al.* [36]. Column, LiChrosorb RP-18, 10 μm (250 × 4.6 mm I.D.); eluent, 0.05 *M* phosphate buffer (pH 6.0); flow-rate, 1 ml/min; temperature, 25°C.

3). This type of peak form is known for acid–base equilibria as described in the solvophobic theory of Horváth *et al.* [35]. They found that the ratio of the *k'* values of benzoic, salicylic and homovanillic acids to anions were between 4 and 6, which leads in the absence of buffer to broad peaks, besides protic equilibria. Also *cis–trans* isomers give in RPC in some instances this type of broad peak form, as is the case with L-alanyl-L-proline. Whereas polar and non-polar residues in the *cis* conformation can be placed on opposite sites of a hypothetical plane, no such plane exists for the *trans* conformation, so the *trans* isomer is less retarded (Fig. 6) [36].

Broad peaks are usually observed in RPC for strong bases having a positive charge and also a large solvophobic contact surface area. Similar observations of broad multiple peak formation were found with venritidin, a furane derivative used in ulcer therapy as an H_2-antagonist. At low ionic strength we observed here also instead of one peak, three peaks with an unusual broad peak in the middle. All three peaks have identical UV spectra, which can be seen in the contour map using the rapid scanning spectrophotometer. The three bands probably result from an equilibrium of a *cis–trans* isomer pair similar to L-alanyl-L-proline (Fig. 7) [37].

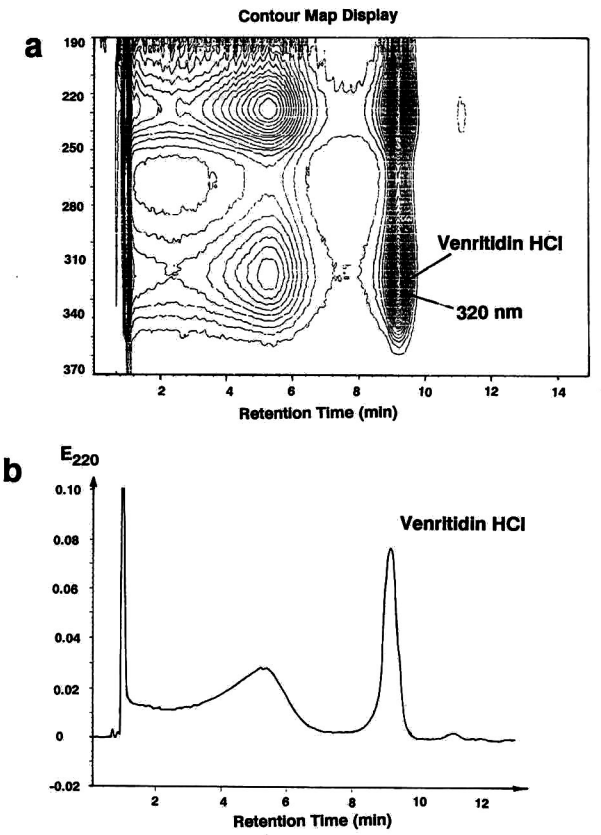

Fig. 7. (a) HPLC contour map of venritidine. (b) The corresponding chromatogram at 205 nm showing three bands: one very polar at t_0, a broad one in the middle and a very sharp third one, all having identical spectral properties. For chromatographic conditions, see Experimental.

The UV spectrum of the broad peak was likewise identical with that of α-tocopherol. After fraction collection of the broad peak in Fig. 3b, concentration by evaporation and re-injection, we found α-tocopherol and some more polar components (Fig. 8). Further work on this aspect is planned.

We assumed that the broad band could represent an equilibrium of the following type:

$$\alpha\text{-tocopherol} \underset{}{\overset{\text{irradiation}}{\rightleftharpoons}} \alpha\text{-tocopherol}^+ + (\text{products})^- \quad (1)$$

Of all the irradiated model solvents that were studied, air-saturated chloroform contained the most reactive short-living radicals, such as the trichloromethaneperoxy radical, $CCl_3OO^\cdot$ (see Table III).

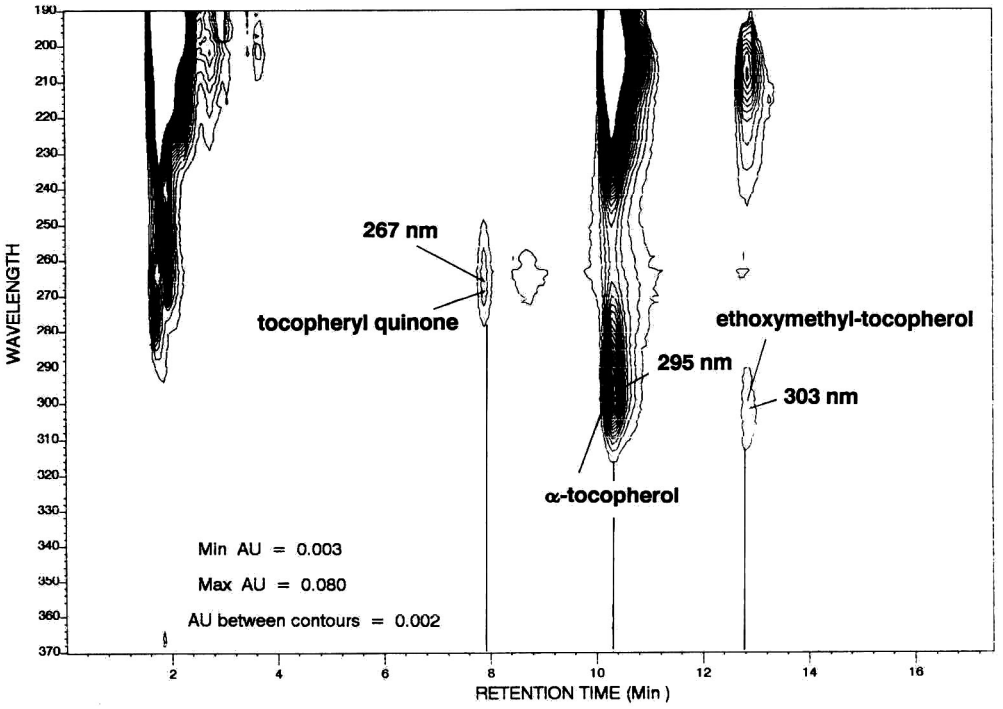

Fig. 8. HPLC contour map of isolated bands with retention times from 5 to 10 min as in Fig. 3b. Concentration of α-tocopherol, 0.1 g per 100 ml; injection volume, 100 μl.

Dependence of the irradiation reaction on the concentration of α-tocopherol

It could be shown that the effect of irradiation on α-tocopherol decreases with increasing concentration in the same solution. Concentration-dependent irradiation in chloroform has shown that formyltocopherol could be formed only at low concentrations, *i.e.*, below 300 ppm α-tocopherol, whereas ethoxymethyltocopherol could be observed at all investigated concentrations (Figs. 1–3).

TABLE III

RATE CONSTANTS FOR THE REACTION ROO· + α-toco–OH → ROOH + α-toco–O·

ROO·	k (l mol^{-1})	Ref.
C_6H_{11}–OO·	$2.3 \cdot 10^7$	38
CCl_3–OO·	$5 \cdot 10^8$	39
CH_3CH–OO·–OH	$9.1 \cdot 10^4$	9
R–OO· from oleic acid	$2.5 \cdot 10^6$	38

To explain the mechanism of tocopherol destruction via γ-irradiation, the dependence on different solvent properties and on the oxygen solubility, α-tocopherol was also chemically oxidized, especially with superoxide anion radical, O_2^{-}·, and Fe^{3+} [30]. The products of the reaction of α-tocopherol with a tenfold excess of O_2^{-}· (Fig. 9) in acetonitrile are similar to the products formed following irradiation of α-tocopherol in ethanol (Fig. 4), so that a correlation between the two mechanisms is possible. The method also allows the investigation of the time-dependent reaction of α-tocopherol with superoxide anion radicals.

Products arising from the reaction of α-tocopherol with Fe^{3+} ions in acetonitrile, *viz.* tocopherylquinone and tocopherone (Fig. 10), are similar to the products of the reaction with superoxide and to the products of the irradiation in ethanol. Both reactions are well documented [40–44].

Concerning electron spin resonance (ESR) studies on different derivatives of α-tocopherol and several tocopherol isomers (α-, β- and γ-tocopherol, to-

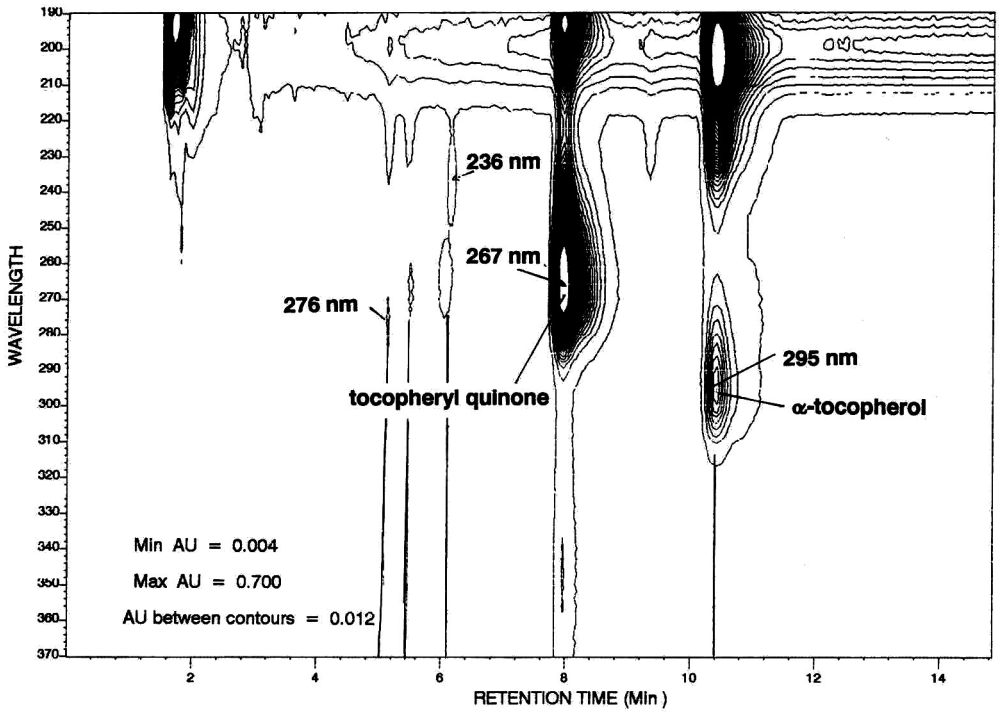

Fig. 9. HPLC contour map of α-tocopherol after oxidation in acetonitrile: $O_2^{-\cdot}$ = 1:8 (mol/mol). Injection volume, 100 μl of a 400 ppm solution of α-tocopherol in acetonitrile.

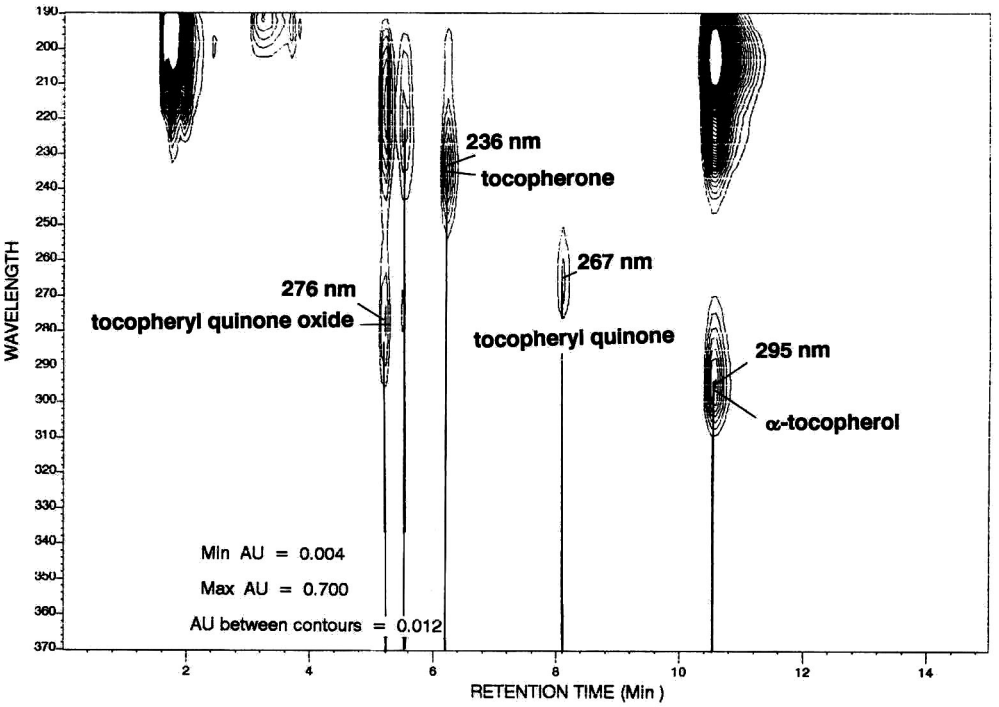

Fig. 10. HPLC contour map of α-tocopherol after oxidation with $FeCl_3$ in acetonitrile at a concentration of 1500 ppm. Injection volume, 40 μl.

col and 2,2,5,7,8-pentamethyl-6-chromanol) [30,45], we concluded that the irradiation process leads in the first step to the formation of a cation radical of α-tocopherol. It could be also observed that the reaction of α-tocopherol with $FeCl_3$ and $O_2^{-}\cdot$ includes in the first step an electron transfer to form Fe^{2+} and O_2^{2-} and an α-tocopherol cation radical, respectively [30,45]. The primary formation of an α-tocopherol cation radical is a possible interpretation to explain the influence of different solvent properties (pH, solvation power, etc.) on tocopherol oxidation and product formation. This cation radical is stabilized to form an α-tocopheryl-radical by releasing a proton.

REFERENCES

1 L. J. Machlin, *Vitamin E—a Comprehensive Treatise*, Marcel Dekker, New York, Basle, 1980.
2 J. Elmadfa and W. Bosse, *Vitamin E*, Wissenschaftliche Verlagsgesellschaft, Stuttgart, 1985.
3 *Food Irradiation: a Technique for Preserving and Improving the Safety of Food*, WHO Report, Geneva, 1988; German translation in SozEp-Hefte, 1 (1991), Institut für Sozialmedizin und Epidemiologie des Bundesgesundheitsamtes, Berlin.
4 P. S. Elias and A. J. Cohen (Editors), *Radiation Chemistry of Major Food Components*, Elsevier, Amsterdam, 1977.
5 E. Bancher, J. Washüttl and R. Schiffauer, *Int. Z. Vitam. Ern. Forsch.*, 43 (1973) 510; 44 (1974) 26.
6 J. F. Diehl, *Z. Lebensm.-Unters.-Forsch.*, 142 (1970) 1; 169 (1979) 276.
7 F. W. Knapp and A. L. Tappel, *J. Agric. Food Chem.*, 9 (1961) 430.
8 P. P. Tobback, in P. S. Elias and A. J. Cohen (Editors), *Radiation Chemistry of Major Food Components*, Elsevier, Amsterdam, 1977, p. 187–220.
9 D. Jore and C. Ferradini, *FEBS Lett.*, 183 (1985) 299.
10 A. P. de Leenheer, W. E. Lambert and M. G. M. de Ruyter (Editors), *Modern Chromatographic Analysis of the Vitamins*, Marcel Dekker, New York, Basle, 1985.
11 J. Cillard, J. Gobaille and P. Cillard, *J. Chromatogr.*, 347 (1985) 434.
12 R. Yamauchi, T. Matsui, Y. Satake, K. Kato and Y. Ueno, *Lipids*, 24 (1989) 204.
13 R. Yamauchi, T. Matsui, K. Kato and Y. Ueno, *Agric. Biol. Chem.*, 53 (1989) 3257.
14 R. Yamauchi, T. Matsui, K. Kato and Y. Ueno, *Lipids*, 25 (1990) 152.
15 R. Yamauchi, K. Kato and Y. Ueno, *Lipids*, 23 (1988) 779.
16 T. Gottstein and W. Grosch, *Fat Sci. Technol.*, 92 (1990) 139.
17 Y. L. Ha and A. S. Csallany, *Lipids*, 23 (1988) 359.
18 J.-P. Koskas, J. Cillard and P. Cillard, *J. Chromatogr.*, 287 (1984) 442.
19 S. K. Howell and Y. M. Wang, *J. Chromatogr.*, 227 (1982) 174.
20 G. T. Vatassery and W. E. Smith, *Anal. Biochem.*, 167 (1987) 411.
21 J. G. Bieri and T. J. Tolliver, *Lipids*, 16 (1981) 777.
22 J.-P. Koskas, J. Cillard and P. Cillard, *J. Chromatogr.*, 287 (1984) 442.
23 G. H. R. Rao, T. P. Krick and J. G. White, *J. Chromatogr.*, 196 (1980) 506.
24 D. D. Stump, E. F. Roth, Jr. and H. S. Gilbert, *J. Chromatogr.*, 306 (1984) 371.
25 M. E. Murphy and J. P. Kehrer, *J. Chromatogr.*, 421 (1987) 71.
26 G. A. Pascoe, Ch. T. Duda and D. J. Reed, *J. Chromatogr.*, 414 (1987) 440.
27 S. Okayama, *Plant Cell Physiol.*, 25 (1984) 1445.
28 M. D. Greenspan, C.-Y. Lee Lo, D. P. Hanf and J. B. Yudkovitz, *J. Lipid Res.*, 29 (1988) 971.
29 K. W. Miller and Ch. S. Yang, *Anal. Biochem.*, 145 (1985) 21.
30 S. Koswig, *Ph.D. Thesis*, Humboldt University, Berlin, 1991.
31 M. Sumarno, E. Atkinson, C. Suarna, J. K. Saunders, E. R. Cole and P. T. Southwell-Keely, *Biochim. Biophys. Acta*, 920 (1987) 247.
32 Y. Ishikawa, *Agric. Biol. Chem.*, 38 (1974) 2545.
33 W. Boguth and R. Hackel, *Int. Z. Vitam. Forsch.*, 38 (1970) 169.
34 S. Koswig and J.-Th. Mörsel, in W. Baltes, T. Eklund, R. Fenwick, W. Pfannhauser, A. Ruiter and H. P. Thier (Editors), *Strategies for Food Quality Control and Analytical Methods in Europe, Proceedings of the 6. European Conference on Food Chemistry, Hamburg, September 22–26, 1991*, B. Behr's Verlag, Hamburg, 1991, pp. 333–337.
35 Cs. Horváth, W. R. Melander and I. Molnar, *Anal. Chem.*, 49 (1977) 142.
36 W. R. Melander, J. Jacobson and Cs. Horváth, *J. Chromatogr.*, 234 (1982) 269.
37 I. Molnar, unpublished results.
38 M. G. Simic, in M. G. Simic and M. Karel (Editors), *Autoxidation in Food and Biochemical Systems*, Plenum Press, New York, 1980, pp. 17–26.
39 J. E. Packer, J. F. Slager and R. L. Willson, *Nature (London)*, 278 (1979) 737.
40 M. Nishikimi and L. J. Machlin, *Arch. Biochem. Biophys.*, 170 (1975) 684.
41 M. Matsuo, S. Matsumoto and Y. Itaka, *J. Org. Chem.*, 52 (1987) 3514.
42 T. Ozawa and A. Hanaki, *Biochem. Biophys. Res. Commun.*, 129 (1985) 461.
43 W. M. Cort, W. Mergens and A. Greene, *J. Food Sci.*, 43 (1978) 797.
44 P. D. Boyer, *J. Am. Chem. Soc.*, 73 (1951) 733.
45 R. Stösser and S. Koswig, in preparation.

Journal of Chromatography, 605 (1992) 63–68
Elsevier Science Publishers B.V., Amsterdam

CHROM. 24 161

Reversed-phase high-performance liquid chromatographic separation of some trace impurities in oxygen-free electronic copper by post-column chelation with 4-(2-pyridylazo)resorcinol and Arsenazo-III

Rajananda Saraswati and T. H. Rao

Defence Metallurgical Research Laboratory, Kanchanbagh P.O., Hyderabad 500 258 (India)

(First received October 9th, 1991; revised manuscript received March 4th, 1992)

ABSTRACT

Trace amounts of impurities such as Al, Cr, Mn, Fe, Co, Ni, Zn, Bi and Pb in oxygen-free electronic copper were separated and determined by reversed-phase high-performance liquid chromatography (HPLC) with spectrophotometric detection using post-column reaction methods. 4-(2-Pyridylazo)resorcinol (PAR) and 2,2'-(1,8-dihydroxy-3,6-disulphonaphthylene-2,7-bisazo)bisbenzenearsonic acid (Arsenazo-III) were used as post-column chelating agents. The requirements for sample preparation, characterization of the post-column reaction and the optimum conditions for the sensitive detection of these trace amounts of metal ions after ion chromatographic separation are discussed. The concentration of PAR, Arsenazo-III and the composition of the eluent were investigated. A baseline separation of these impurities is achieved after 15 min using PAR and at 40 min using Arsenazo-III. The speed of separation was increased by a concentration gradient technique. The detection limits achieved were 1.0, 0.2, 0.1, 2.0, 0.2, 0.6, 2.4, 0.6 and 1.0 ng for Al, Cr, Mn, Fe, Co, Ni, Zn, Bi and Pb, respectively. The results obtained by HPLC methods compare well with those of graphite furnace atomic absorption spectrometry and certified values of MBH.

INTRODUCTION

Studies of the influence of various impurities on the annealing properties and electrical conductivity of oxygen-free electronic copper (OFEC) have shown that the higher the concentrations of impurities the higher the softening temperature and the lower the electrical conductivity [1–6]. For example, every 5 ppm of lead in the range 0–25 ppm reduces the electrical conductivity of copper by about 0.1% IACS (International Annealed Copper Society). Similarly, every 5 ppm increase in the concentration of antimony in the range 0–25 ppm lowers the conductivity by 0.15% IACS. The presence of the order of 0.001% Fe, however, would lead to embrittlement and loss of ductility [1]. The presence of Bi at 0.001% (at a Cu purity of 99.999%) will result in intergranular fractures due to microcracks and micropores as Bi segregates to the grain boundary causing the embrittlement of Cu even at low stress levels. Therefore the accurate determination of trace amounts of impurities in Cu has become increasingly important. Several schemes for systematic analysis have been described previously [7–10]. None of the schemes includes the determination of all impurities in a single sample, although several independent procedures have been proposed. With the advent of atomic absorption spectroscopy (AAS), many procedures for the determination of trace amounts of impurities in copper have been developed. However, the detection limits of AAS procedures have been severely influenced by matrix

Correspondence to: Dr. R. Saraswati, Defence Metallurgical Research Laboratory, Kanchanbagh P.O., Hyderabad 500 258, India.

0021-9673/92/$05.00

effects. In this context, the high-performance ion chromatographic separation and detection technique seems to be one of the most promising tools.

High-performance liquid chromatography (HPLC) is extensively used for the separation of organic compounds. In recent years, this technique has also become an attractive method for the determination of trace amounts of metals [11–13]. In fact, the advances that have taken place in column and detection techniques [14–20] have allowed HPCL to be used to characterize a wider range of anions and cations as individual metals and metal compounds form distinct ions with differing retention times, it is possible to determine several ions in a single run. The separation and simultaneous determination of mixtures of metal ions as their chelates with organic reagents by HPLC has received increasing attention. A wide variety of organic reagents has been used to complex with metal ions before separation [21] and some reagents such as 4-(2-pyridylazo)resorcinol (PAR) and 2,2′-(1,8-dihydroxy-3,6-disulphonaphthylene-2,7-bisazo)bisbenzenearsonic acid (Arsenazo-III) also act as very good post-column reagents.

PAR and Arsenazo-III are azo dyes that have been widely used for complexiметric titrations and spectrophotometric determination of over 40 different metals [22–24]. These reagents can form ionic compounds with metal ions which are water-soluble with unique absorption characteristics. Hence the spectrophotometric determination is usually performed in an aqueous solution. This is one of the features that makes them useful and effective chelating agents for the determination of metals using HPLC with either pre-column or post-column techniques [25].

In previous papers [26,27] we have discussed the separation of transition and rare earth metals which are present in trace amounts in low-alloy steels and transititon metals in stainless steels. This paper describes the determination of the optimum chromatographic conditions for the separation and determination of some of the trace amounts of impurities in OFEC after post-column reaction with PAR and Arsenazo-III.

EXPERIMENTAL

The Waters gradient-control ion chromatographic (IC) system used consists of Model 501 pumps with a Waters U6K injector. A Spherisorb S-5 ODS I separation column was used. A Waters 486 tunable absorbance UV–visible spectometric detector with a 12-μl flow cell was used to monitor the effluent from the column. A Waters post-column reagent mixture module was used together with a Waters maxima 820 chromatography workstation with a printer.

The laboratory equipment was used after conditioning in an ultrasonic cleaner and equilibriating in reagent-grade water (18 Ω resistance) from a Millipore Milli Q water system with total metallic impurities less than 1 ppb.

High-purity "Suprapure" grade chemicals from E. Merck were used. Solvents were further purified using isothermal sub-boiling distillation in a laminar flow fume hood of class 100 condition with the total laboratory facility maintained at class 10 000 level to overcome dust and particulate contamination. Pure metals from Johnson Matthey (JMC) and certified reference materials from MBH were used for the preparation of standards and eluents.

Chromatograms were recorded by injecting 20 μl of standards solutions of ions which were prepared by dissolving known amounts of pure metals and further diluting to the required levels, and elution with 10^{-3} *M* sodium octane-1-sulphonate (54 mg in 250 ml) solution–0.023 *M* tartaric acid at a flow-rate of 1 ml min^{-1}. Standard calibration graphs were obtained with the chosen parameters by injecting standards separately and in mixtures and recording the peak heights of the respective ions.

Sample preparation and matrix separation

A 10-g amount of sample (which had previously been washed with methanol and dried with an infrared lamp) was dissolved in a requisite amount ($\approx$ 40 ml) of nitric acid (1 + 1), covering the beaker and heating to below the boiling point. After the sample had been dissolved, the solution was boiled to remove nitrogen oxides. The solution was cooled and the surface of the dish and the inner walls of the beaker were blow-washed with water. The solution was then diluted to approximately 100 ml.

The sample solution obtained contains lot of copper matrix. This may have detrimental effects on the chromatographic column and the separation of impurities. Therefore the separation of copper is a pre-

requisite for achieving reliable trace element determinations when IC procedures are used with post-column reaction detection. This matrix separation is achieved by subjecting the sample solution to electrolysis at 0.6 A using platinum gauge electrodes and a magnetic stirrer. The solution was covered and heated on an electrothermal plate to concentrate it, and then the solution was diluted to 25 ml in a standard flask and further diluted as required. Aliquots (20 μl) of the solution were used for injection after filtering solution through a 0.45-μm filter.

The concentration gradient technique for elution was used for better resolution and separation. The concentration of the eluent (sodium octane-1-sulphonate–tartaric acid) was varied from 10 to 50% during analysis.

Post-column reaction detection

Good sensitivity for the detection of the individual transition elements Mn, Fe, Co, Ni, Zn, Bi and Pb was obtained with a solution of $2 \cdot 10^{-4}$ *M* PAR and $2.308 \cdot 10^{-2}$ *M* tartrate. The Arsenazo-III ($1 \cdot 10^{-3}$ *M*) solution containing 3 ml l^{-1} ammonia solution was preferred for the detection of Al, Cr, Zn and Pb.

The colour-forming reagents PAR and Arsenazo-III were delivered by the reagent delivery module and mixed with the eluent after passing through the column. The resulting derivative was detected at 533 and 600 nm using the UV–visible spectrophotometric detector.

Instrumental methods

A GBC Model 902 atomic absorption spectrometer was used, equipped with a GBC Model GF 2000 graphite furnace. A deuterium lamp was used for background correction. Visimax II hollow cathode lamps were used as a light source. Solutions were injected by a GBC PAL-2000 autosampler. All absorbances were measured as peak heights and were recorded with an Epson Lx-800 printer. The system was operated by a Philips Model P-3105 data station connected on-line.

A 1-g amount of sample was dissolved in 5 ml of dilute nitric acid (1 + 1) and solution was made up to 100 ml with water and further diluted as required.

RESULTS AND DISCUSSION

The results for four sample materials are presented in Table I. For comparison, the values (%, w/w) obtained by AAS and the certified values from the MBH samples are also given. The agreement between the results is excellent, as are the relative standard deviations.

Several organic solvents such as methanol, ethanol, acetonitrile, tetrahydrofuran, isopropylalcohol and sodium octane-1-sulphonate combined with water were investigated as binary and ternary mobile phases. The sodium octane-1-sulphonate (10^{-3} *M*) and the tartaric acid (0.1 *M*)–water system were found to be satisfactory for the separation of Mn, Fe, Co, Ni, Cu, Zn, Bi, Pb, Al and Cr metal chelates. PAR and Arsenazo-III were found to be good colour-forming post-column reagents. The metal ions Mn^{2+}, Fe^{3+}, Co^{2+}, Ni^{2+}, Cu^{2+}, Zn^{2+}, Bi^{3+} and Pb^{2+} gave stable colours with PAR, whereas Al^{3+}, Cr^{3+}, Zn^{2+} and Pb^{2+} gave good colours with Arsenazo-III. The important factors that influence the sensitivity and resolution of metal ions are the rate of reaction between the reagent and the metal ions, the background absorbance, noise and the efficiency of the mixing cell.

PAR is a tridentate ligand [25] that forms metal chelates which absorb in the visible region. The absorption of these red chelates of metal ions with PAR is influenced by the hydrogen ion concentration. The absorption spectra were recorded under acidic conditions as chromatographic studies were to be performed on silica-bonded phase columns. The absorption due to Al–PAR, Cr–PAR, Mn–PAR, Fe–PAR, Co–PAR, Ni–PAR, Cu–PAR, Zn–PAR, Bi–PAR and Pb–PAR chelates was at a maximum in the pH range 5–6. Below this pH there is a marked decrease in the absorbance of some of the chelates which may be due to protonation equilibria, as was found for the Cr–PAR chelate [28].

The effect of various buffers such as tartrate, oxalate and citrate on the absorbance of these chelates was studied. The maximum absorption was obtained in tartrate buffer. It was also found that the absorption of the metal–PAR chelates was influenced by the concentration of tatrate added. The maximum absorption of M–PAR chelates was obtained when the concentration of tartrate was about $2.308 \cdot 10^{-2}$ mol dm^{-3}. A possible explanation is

TABLE I

COMPARISON OF RESULTS (%, w/w) OBTAINED BY HPLC AND GRAPHITE FURNACE AAS WITH THE CERTIFIED VALUES OF MBH SAMPLES

Values in square brackets were obtained by graphite furnace AAS and values in parentheses are for MBH samples. Results given as mean ± relative standard deviation (%). $n = 5$.

	17867B	17868B	17869B	17870B
Mn	0.008 ± 2.1 [0.008 ± 4.2] (0.009)	0.0215 ± 2.6 [0.0215 ± 6.2] (0.0216)	0.0286 ± 2.0 [0.0288 ± 4.9] (0.030)	0.040 ± 3.8 [0.040 ± 7.8] (0.0405)
Fe	0.0120 ± 4.2 [0.0125 ± 6.1] (0.0125)	0.028 ± 0.8 [0.026 ± 1.2] (0.029)	0.037 ± 1.9 [0.037 ± 7.2] (0.038)	0.053 ± 2.5 [0.055 ± 6.8] (0.055)
Co	0.035 ± 4.5 [0.032 ± 3.8] (0.037)	0.030 ± 1.2 [0.030 ± 5.2] (0.030)	0.016 ± 1.8 [0.018 ± 7.6] (0.016)	0.001 ± 2.5 [0.001 ± 6.6] (0.001)
Ni	0.039 ± 6.1 [0.035 ± 9.8] (0.040)	0.0336 ± 2.9 [0.0333 ± 8.6] (0.0340)	0.020 ± 1:3 [0.021 ± 3.2] (0.020)	0.0048 ± 2.1 [0.005 ± 6.1] (0.005)
Zn	0.030 ± 5.2 [0.035 ± 9.2] (0.030)	0.0241 ± 5.7 [0.0245 ± 10.6] (0.0245)	0.0130 ± 5.0 [0.0130 ± 5.5] (0.0135)	0.0020 ± 1.6 [0.002 ± 12.8] (0.0022)
Bi	0.011 ± 1.1 [0.011 ± 9.6] (0.011)	0.0290 ± 1.8 [0.0290 ± 4.4] (0.0295)	0.035 ± 5.0 [0.038 ± 5.3] (0.0385)	0.054 ± 3.6 [0.055 ± 4.5] (0.055)
Pb	0.012 ± 4.2 [0.015 ± 8.1] (0.013)	0.024 ± 4.0 [0.025 ± 7.6] (0.025)	0.0380 ± 6.9 [0.0389 ± 5.8] (0.0385)	0.046 ± 7.2 [0.049 ± 4.1] (0.048)
Al	0.008 ± 4.2 [0.008 ± 4.6] (0.009)	0.020 ± 1.5 [0.022 ± 3.6] (0.020)	0.031 ± 6.8 [0.035 ± 4.6] (0.034)	0.044 ± 1.2 [0.046 ± 1.4] (0.045)
Cr	0.0045 ± 8.1 [0.0040 ± 2.9] (0.0046)	0.003 ± 7.5 [0.0033 ± 0.6] (0.0034)	0.002 ± 6.9 [0.003 ± 7.8] (0.003)	0.0005 ± 1.8 [0.0006 ± 6.5] (0.0006)

that, in a weakly acidic medium, the concentration of hydroxy groups is low and hence the hydroxy groups coordinated to metal ions could be replaced by tartrate. As a result, coloured ternary M–tartrate–PAR complexes would be formed. Therefore the absorbance increases as the tartrate concentration increases. However, at high concentrations of tartrate, the coordinated PAR would be replaced by tartrate, which would lead to a decrease in the absorbance.

The chromatograms obtained for some of the trace amounts of impurities are illustrated in Fig. 1. The chromatograms were recorded at 533 nm as all the chelates showed significant absorption at this wavelength. Based on the spectrophotometric studies described earlier, the chromatographic separation was performed in tartrate buffer. When the separation of these elements was performed without a solvent programme, 15 min were required to complete the separation (Fig. 1a). Pb was separated at about 3 min 30 s, followed by Fe (4 min 10 s), Bi (4 min 46 s), Cu (5 min 15 s), Ni (5 min 50 s), Zn (6 min 30 s), Co (9 min 40 s) and Mn (15 min 5 s). However, the speed of separation was increased by using a concentration gradient for elution, the concentration of the eluent being increased five-fold (Fig. 1b).

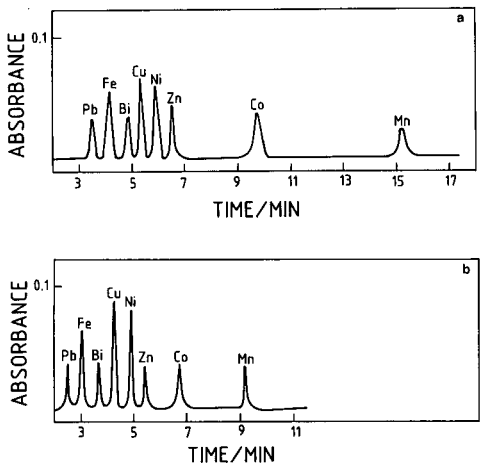

Fig. 1. Separation of some trace amounts of metals in OFEC sample (CRM 17867B) by HPLC using PAR as the post-column reagent. (a) Without solvent programme and (b) with gradient elution using octane-1-sulphonate ($1 \cdot 10^{-3}$ *M*)–tartaric acid (0.123 *M*) as the mobile phase; pH 5.5. Flow-rate 1 ml min^{-1}; PAR ($2.5 \cdot 10^{-4}$ mol dm^{-3}); column length, 300 × 3.9 mm I.D.; detection wavelength, 533 nm.

Al and Cr were not detected using PAR as the post-column reagent, but Arsenazo-III was found to be the preferred reagent for the detection of Al and Cr together with Zn and Pb (Fig. 2).

Arsenazo-III is a weak octabasic acid and is one of the most often used azo dyes, forming metal chelates which absorb in the visible region. It was found that Arsenazo-III ($1 \cdot 10^{-3}$ *M*) solution containing 3 ml l^{-1} NH_3 gives good detection of Al, Cr, Zn and Pb in the pH range 3.5–4 at 600 nm. Pb was detected at about 4 min 8 s followed by Cu (5 min 35 s), Zn (7 min 10 s), Al (12 min 22 s) and Cr (40 min 15 s). The speed of separation of Cr was increased by a concentration gradient, the concentration of the eluent being increased ten-fold (Fig. 2b).

The composition of the eluent was also studied. As mentioned earlier, the absorption characteristics of the chelastes are influenced by the concentration of tartrate and PAR. Therefore the effect of tartrate and PAR on the separation and detection of the chelates was studied by monitoring chromatograms as a function of the reagent concentration in the mobile phase. It was found that the effect of the tartrate concentration in the range $1.2 \cdot 10^{-2}$ to $2.33 \cdot 10^{-2}$ mol dm^{-3} and the PAR concentration in the range $2.0 \cdot 10^{-4}$ to $5.0 \cdot 10^{-5}$ mol dm^{-3} on retention times and the detection of the metal ions Pb^{2+}, Fe^{3+}, Bi^{3+}, Ni^{2+}, Zn^{2+}, Co^{2+} and Mn^{2+} was very slight. The best separation and detection was obtained at tartrate and PAR concentrations of $2.308 \cdot 10^{-2}$ and $2.5 \cdot 10^{-4}$ mol dm^{-3}, respectively.

The results of the spectrophotometric studies indicated that the pH of the chelating medium has a significant effect on the absorption of the metal–PAR complex. The reversed-phase separation was performed on silica-based bonded columns. As the optimum performance of these columns occurs in the pH range 3.5–7.0, the effect of varying the pH of the eluent was carefully studied within this range. It was observed that the retention time increases with decreasing pH. This is because a decreased pH decreases the ionization of tartrate, which in turn decreases the degree of metal complexation, thereby increasing retention times. It was found that a pH of 5.5 gave the best separation and detection.

The peaks that appeared in the chromatograms were identified by spiking with authentic (*i.e.* known) metal ion solutions. Quantitative measurements were carried out by plotting calibration graphs for individual elements, taking the peak

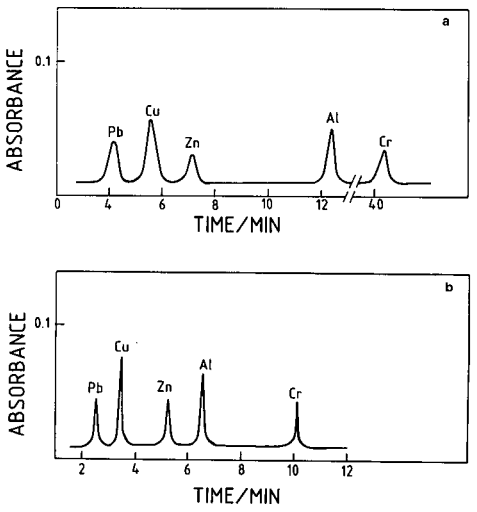

Fig. 2. Separation of some trace amounts of elements in OFEC sample (CRM 1786B) by HPLC using Arsenazo-III as the post-column reagent. (a) Without solvent programme and (b) with gradient elution using octanesulphonate ($1 \cdot 10^{-3}$ *M*)–tartaric acid (0.023 *M*) as the mobile phase; pH 6.0. Flow-rate 1 ml min^{-1}; Arsenazo-III (10^{-3} *M*) containing 3 ml l^{-1} NH_3; column length, 300 × 3.9 mm I.D.; detection wavelength, 600 nm.

heights at different concentrations and comparing the results with those for samples. The absolute detection limits, calculated as the amount injected that gave a signal that was three times the background noise (*i.e.* a signal-to-noise ratio of 3:1), were 1.0, 0.2, 0.1, 2.0, 0.2, 0.6, 2.4, 0.6 and 1.0 ng for Al, Cr, Mn, Fe, Co, Ni, Zn, Bi and Pb, respectively.

The other trace elements that are normally present in OFEC are Se, Te, Mg, As and Sn. Neither PAR nor Arsenazo-III give any detectable colour with these impurities.

No significant change in peak width was observed during the separation of ions using same volume of sample solution, indicating an excellent column performance throughout the analysis.

CONCLUSIONS

By using PAR and Arsenazo-III as post-column chelating agents some of the trace impurities in OFEC have been successfully separated and determined by reversed-phase HPLC on a C_{18} column. This chromatographic method is fairly selective and sensitive and can be used for the simultaneous determination of trace impurities of Al, Cr, Mn, Fe, Co, Ni, Zn, Bi and Pb in OFEC at sub-ppm levels.

ACKNOWLEDGEMENTS

The authors are grateful to Dr. P. Rama Rao, previous Director, DMRL and Shri S.L.N. Acharyulu, Director, for permission to publish this paper.

REFERENCES

1 Y. T. Hsu and B. O. Reilly, *J. Metals*, 12 (1977) 21.
2 *Copper Data, Publication No. 12*, Copper Development Association, London, 1976.
3 S. Nakahara and Y. Okinaka, *Scripta Metal.*, 19 (1985) 517.
4 L. K. Bigelow, *Metal Trans.*, 7B (1976) 661.
5 W. P. Riley and H. V. Maker, *Conserv. Recycl.*, 4 (1986) 315.
6 D. C. Abbas, *Diss. Abstr. Int.*, 38 (1978) 121.
7 Z. Marczenko, *Chem. Anal. (Warsaw)*, 11 (1966) 347.
8 I. M. Kolthoff and P. J. Elving (Editors), *Treatise on Analytical Chemistry*, Part 2, Vol. 3, Interscience, New York, 1961.
9 W. Reichel and B. G. Blaekley, *Anal. Chem.*, 46 (1974) 59.
10 D. E. Leyden and W. Wegscheider, *Anal. Chem.*, 53 (1981) 1059.
11 B. R. Willeford and H. Veening, *J. Chromatogr.*, 251 (1982) 61.
12 G. Nickless, *J. Chromatogr.*, 313 (1985) 129.
13 B. Steinbrech, *J. Chromatogr.*, 10 (1987) 1.
14 F. Vlacil, L. Vins and J. Coupek, *J. Chromatogr.*, 391 (1987) 119.
15 F. Vlacil, L. Vins and J. Coupek, *J. Chromatogr.*, 391 (1987) 133.
16 Yu. E. Pzazukhina, O. A. Shpigun, I. N. Voloschits and M. I. Litvina, *Zh. Anal. Kim.*, 43 (1988) 117.
17 J. S. Fritz, D. T. Gjerde and R. M. Becker, *Anal. Chem.*, 52 (1980) 1519.
18 J. S. Fritz and G. J. Sevenich, *Anal. Chem.*, 55 (1983) 12.
19 J. F. Jen, K. E. Daugherty and J. G. Tarter, *J. Chromatogr.*, 436 (1988) 86.
20 Z. Hu and Y. Tans, *Analyst (London)*, 113 (1988) 179.
21 C.-S. Lin, X.-S. Zhang and X.-Z. Liu, *Analyst (London)*, 116 (1991) 277.
22 R. G. Anderson and G. Nickless, *Analyst (London)*, 92 (1967) 207.
23 S. Ahrland and R. G. Herman, *Anal. Chem.*, 47 (1975) 2422.
24 S. J. Tsai and Y. Lee, *Analyst (London)*, 116 (1991) 615.
25 D. A. Roston, *Anal. Chem.*, 56 (1984) 241.
26 R. Saraswati, N. R. Desikan, S. V. Athavale and T. H. Rao, *Anal. Chim. Acta*, 237 (1990) 325.
27 R. Saraswati and T. H. Rao, *Analyst (London)*, 117 (1992).
28 H. Hoshino and T. Yotsuyanagi, *Anal. Chem.*, 57 (1985) 625.

Journal of Chromatography, 605 (1992) 69–80
Elsevier Science Publishers B.V., Amsterdam

CHROM. 24 188

Evaluation of capillary columns used in the routine determination of methylmercury in biological and environmental materials

E. Rubí, R. A. Lorenzo, C. Casais, A. M. Carro and R. Cela

Departamento de Química Analítica, Nutrición y Bromatología, Facultad de Química, Universidad de Santiago de Compostela, Santiago de Compostela (Spain)

(First received October 17th, 1991; revised manuscript received March 17th, 1992)

ABSTRACT

The factors determining the effective life of the capillary columns commonly used in the determination of organomercury compounds in biological and environmental materials were examined. The effects of pretreatment of these columns with mercury(II) salts on their behaviour and the duration of the treatments in terms of the type of stationary phase considered are discussed, in addition to the influence of the thickness of the stationary phase and the external protective covering of the columns. The use of diphenyldimethylsiloxane columns with a film thickness of 5 μm seems to be the most advantageous option for routine analysis.

INTRODUCTION

Mercury is a widely distributed toxic substance in the environment. Organomercurial compounds are generally more toxic than elemental mercury or its inorganic salts. Among its organic forms, the alkylmercurials and methylmercury in particular are more toxic than the arylmercurials. The changes that have been made in the traditional methods for the analytical evaluation of the mercury content in biological and environmental materials may be attributed to the toxicity of methylmercury and the fact that methylation of inorganic mercury caused by bacteria is a natural process. Consequently, the bioaccumulation of mercury in large marine predators usually occurs as methylmercury owing to its greater lipophilic properties. The present tendency is towards the speciation of mercury, and, preferably, towards the determination of methylmercury present in these materials [1–4].

With these objectives in mind, several methods have been proposed, ranging from titrimetry [5] and thin-layer chromatography [6–9] to inductively coupled plasma mass spectrometry [10–12], and including spectrometric techniques of absorption and fluorescence (cold vapour) [13–19] and emission microwave-induced plasma [20–24], associated, in most instances, with an earlier stage of chromatographic separation or clean-up, allowing for speciation. High-performance liquid chromatography (HPLC) has also been used [25–28]. The literature up to 1971 was critically reviewed by Uthe and Armstrong [29]. However, the most common technique, and the only one being used for routine analysis and quality control, is separation by gas chromatography with species detection using electron-capture detection (ECD) [6–8,30–43]. In this instance, and based on the classical studies by Westöö [6–8], in which columns packed with 10% Carbowax 20M on Chromosorb W were used, several workers have studied the problem of organomercu-

Correspondence to: Dr. R. Cela, Departamento de Química Analítica, Nutrición y Bromatología, Facultad de Química, Universidad de Santiago de Compostela, Santiago de Compostela, Spain.

0021-9673/92/$05.00

rial compounds with completely different stationary phases. Sumino [30,31] studied sixteen stationary phases and concluded that those with the greatest polarity [diethylene glycol succinate (DEGS) and 1,4-butanediol succinate (DBS)] produce the best separations. DEGS has been proposed by several other workers [34,35,44] and is probably the most commonly used stationary phase in packed columns with these objectives, although other phases (*e.g.*, OV-17 [36,37], ethylene glycol adipate [38], Carbowax 20 M [6,7,34] and polyethylene glycol succinate [9]) have also been proposed with apparently equivalent results.

More recently, other workers have studied the use of capillary and semicapillary columns with the same objectives [45–48]. In general, the results appear to be excellent for both polar and non-polar columns, and it is evident that by using these, some of the problems associated with packed columns can be solved (*e.g.*, low response to methyl- and ethylmercury due to supposed interactions with the column and/or decomposition; peak tailing; low efficiency of the column; variable decrease in the areas and heights of methyl- and ethylmercury peaks when injected with extracts of fish and sediment.

The fact that columns having such different polarities gave equivalent results is curious. However, no studies have been carried out on the separation mechanism of these compounds in the column. There is another important fact. Most workers, whether using packed or capillary columns, have stressed the need to carry out pretreatments of the stationary phase, which generally entails the injection of large amounts of mercury(II) chloride or iodide at regular intervals [44,49,50]. No rational explanation have been found to justify this treatment, which has a number of drawbacks (rapid deterioration of the performance characteristics of the columns, progressive and irreversible contamination of electron-capture detectors, dead periods during the operation, which usually take up more time than the periods spent working on the analyses, etc.)

This paper presents the results obtained after trying, for routine purposes, various types of fused-silica semicapillary columns having different polarities (BP-1; dimethylsiloxane, BP-20; polyethylene glycol, BP-5 and AT-5; and 5% diphenyldimethylsiloxane) with external protective layers of polyimide and aluminium.

EXPERIMENTAL

Apparatus and reagents

All the experiments were carried out with a Hewlett-Packard Model 5890A gas chromatograph, equipped with a nickel-63 electron-capture detector using N52 nitrogen as carrier and make-up gas. Chromatographic data was acquired by means of a

TABLE I

COLUMNS STUDIED AND EXPERIMENTAL CONDITIONS

Characteristic	Column			
	BP-1	BP-20	BP-5	AT-5
Type	Bonded-phase	Bonded-phase	Bonded-phase	Bonded-phase
Stationary phase	Dimethylsiloxane	Polyethylene glycol	5% Diphenyl-dimethylsiloxane	5% Diphenyl-dimethylsiloxane
Polarity	Low	High	Low	Low
Length (m)	25	25	12	30
Material	Fused silica	Fused silica	Fused silica	Fused silica
Film thickness (μm)	1.0	1.0	1.0	5.0
Inside diameter (mm)	0.53	0.53	0.53	0.54
Oven temperature (°C)	90	175	90	170
Injector temperature (°C)	200	250	200	250
Detector temperature (°C)	250	250	250	250
Carrier flow-rate (ml/min)	14.2	20	14	10

Hewlett-Packard Model 3396A integrator. Table I shows the characteristics of the columns evaluated and the operating conditions used in each instance.

All reagents were of analytical-reagent grade and solvents were of spectroscopic or HPLC quality. Tests were carried out by injecting methylmercury chloride (Merck) standard solutions of appropriate concentration in toluene. These solutions were prepared by dilution from a 1 g/l stock solution and were kept refrigerated and protected from light. The treatment solution used was 1% mercury chloride (Merck) in toluene.

Column treatment

The treatment of the different columns used evaluated here coincides basically with O'Reilly's [44], except for the temperature, which depended on the column used. Thus, with columns of low polarity (BP-1 and BP-5), injections of the mercury chloride solution were made at an oven temperature of 115°C, whereas with high-polarity columns (BP-20) these injections were made at 200°C. The difference is explained by the temperature at which the separation of the compounds in question is to take place, which must always be higher than the above treatment temperature. With the BP-1 and BP-5 columns the separation temperature is 90°C and with the BP-20 type it is 175°C. According to our experiments, if treatment is carried out at a temperature 25°C higher than the separation temperature, the conditions were found to be more efficient, the system became cleaner sooner and the effect of the treatment lasted longer.

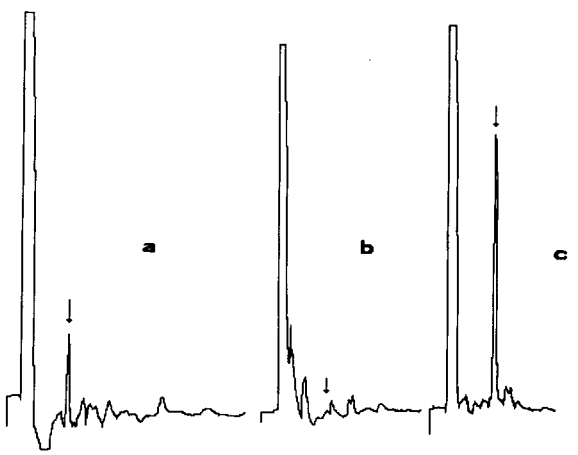

Fig. 1. Chromatograms of (a) toluene after recent treatment of the column, (b) toluene when the column is ready for analysis and (c) standard solution of methylmercury in toluene (all injections made in a BP-1 column).

Procedure for the analysis of real samples

The basic procedure used for the speciation of organomercurials in mussel samples and other materials of biological origin and in samples of marine sediment was described by Hight and Corcoran [42]. The changes made involve the extract volumes in the final stages of the process (four times lower than recommended by Hight and Corcoran), in order to improve the sensitivity, which in this work is *ca.* 50 ng/g expressed as methylmercury chloride (as opposed to 250 ng/g reported by Hight and Corcoran).

RESULTS AND DISCUSSION

Effect of previous treatment of columns

The effect of the previous treatment of the columns is decisive. If it is not applied, the injection of methylmercury chloride in toluene very often do not produce a visible peak on the chromatograms. Curiously, however, when a competely new column was mounted in the chromatograph and conditioned in the usual way as recommended by the supplier, the first injections of methylmercury standard solutions showed a relatively favourable response, especially with BP-5. However, if this or another standard continues to be injected, the height of the methylmercury peak gradually decreased and eventually disappeared. If injections of concentrated solutions of methylmercury were continued to be made, the peak reappeared in the chromatograms, which implies that part of the methylmercury had remained in the column, either retained as such or in a decomposed state, and once a certain level had been achieved, it had an effect similar to the conventional treatment.

On the other hand, after conventional treatment has been applied and once the baseline has been recovered, which takes between 10 and 15 h, during which time the chromatographic system cannot be used, it is necessary to carry out frequent injections of solvent to create a situation in which no trace of the treatment appears in the retention zone of the methylmercury peak. Fig. 1 shows one of these tol-

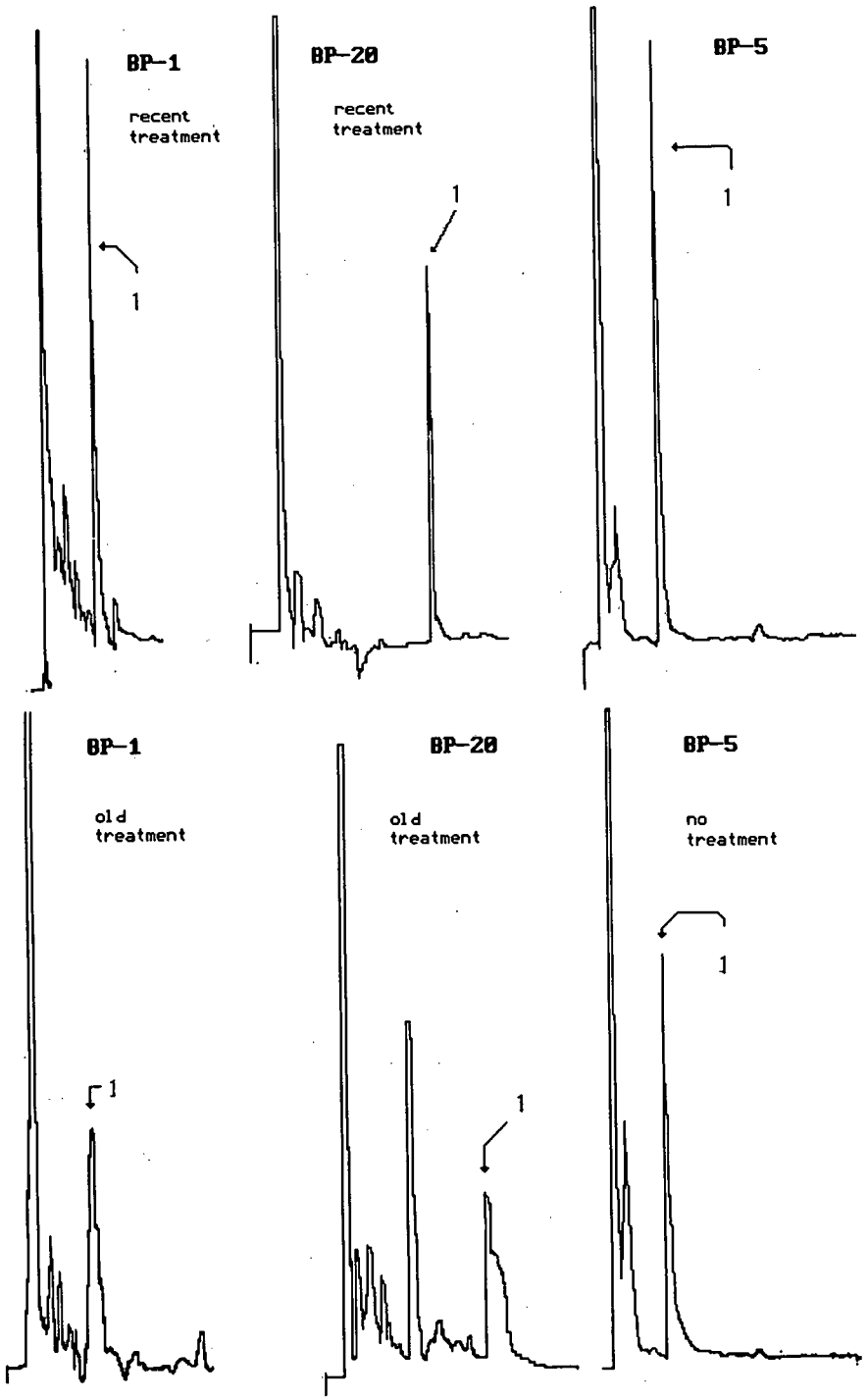

Fig. 2. Response of the different columns to injections of a standard solution of methylmercury (I) in toluene as a function of the column type and the treatment state.

uene injections after treatment, compared with the last in the series of flushing injections (usually 10–12 injections are necessary to obtain an acceptable and reproducible blank) and compared with a chromatogram for methylmercury. It can be seen that the traces of the treatment flushed out by the solvent injections appear at exactly the same retention time as the methylmercury peak, which is surprising, as these species have considerably different vapour pressures. Moreover, it is obvious that we cannot attempt to calibrate the system, which should be carried out without fail after each treatment, until the blanks are reproducible and low, meaning that the chromatograph will be unusable for practical purposes for another 2–3 h. Once the optimum situation for calibration has been attained, this should be carried out and then the series of analyses should be started.

After doing several sample injections, the height of the peaks usually tends to decrease. This effect has been described [44,49,50] and interruption of the sequence of analysis has been suggested, in order to carry out one or two "follow-up" treatment injections, so that the system will recover its analytical capabilities and be able to analyse a few more samples. Logically, this is when the baseline has been recovered and the blanks are acceptable. These "follow-up" treatments are useful for a while, until not only a decrease in peak height with the injections but also a deterioration in peak shape are observed. This means that the treatment has lost its effectiveness and that a completely new treatment is required. Thus, some workers [42] distinguish between "long" and "short" treatments, the latter being the treatments we have termed "follow-up". The chromatograms in Fig. 2 show some of the situations described above.

Some workers [50] even recommend treatment injections before analysing each sample in order to eliminate the variability in the time during which treatments remain effective.

In spite of the numerous objections that may be raised against this methodology, our experience has shown that the nature of the stationary phase used affects the way in which the treatments should be carried out, especially regarding duration and efficiency.

The chromatograms in Fig. 3 show the methylmercury peaks (spiked real mussel samples) obtained using BP-1, BP-5 and BP-20 columns with a polyimide covering after finishing the respective treatments and ensuring the repeatability of the blanks. Here, the three columns are seen to produce excellent separations after treatment. However, the duration of the treatment with the BP-20 columns is much shorter, and in practice, this (long) treatment must be repeated at least once every 48 h, and not more than 20–30 samples could be analysed between treatments.

After several months of work (about every 1000–4000 injections, depending of the type of column used, a number of which will have corresponded to the treatments) the shape of the peaks show that the treatments are no longer efficient and, therefore, the column has been rendered useless. As bonded-phase columns can be washed relatively easily, we attempted to "regenerate" these columns by flushing them with different solvents. The best results were obtained by flushing with acetone, although the quality of the peaks after regeneration was far from satisfactory.

Logically, if we compare the behaviours of the three types of columns considered, it is obvious that the more frequent treatments required by the BP-20 column reduce its effective lifetime. Also, for the same reason, the contamination of the electron-capture detector is much greater when this column is used. This is also a determining factor in the selection of the type of column.

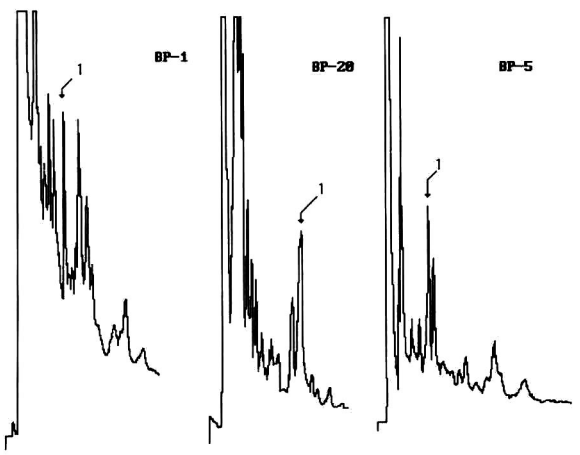

Fig. 3. Chromatograms of a spiked mussel sample as a function of the column type. For chromatographic conditions, see table I. Peak 1 = Methylmercury.

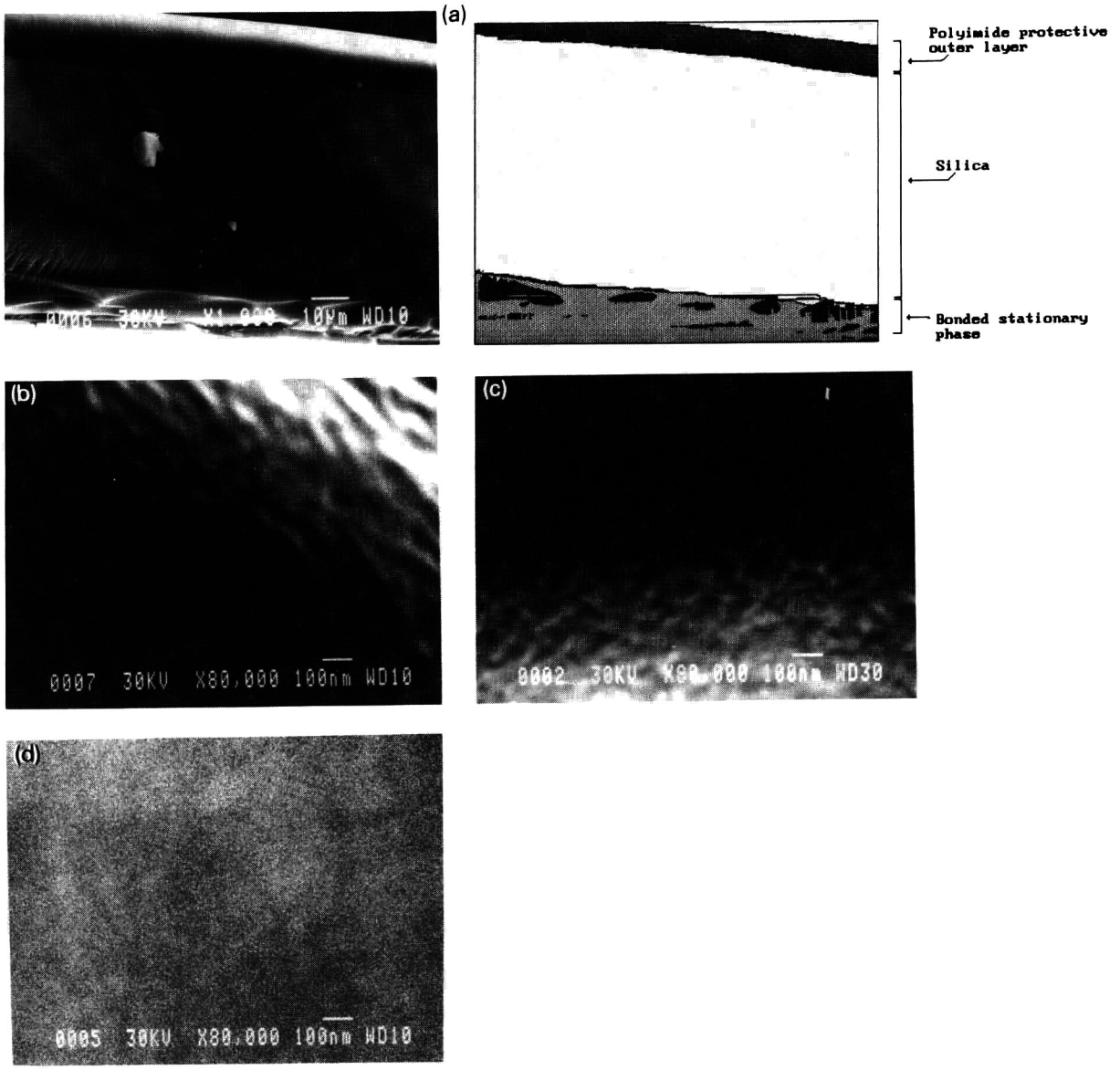

Fig. 4. Electron microscope photographs of (a) cross-section of a new BP-1 column, (b) inner surface of a new BP-1 column, (c) inner surface of a barely used BP-1 column after treatment and (d) inner surface of the same column after several treatments and analyses.

For the purpose of understanding these phenomena, the inner surface of the columns was studied by electron microscopy and the results are shown in Fig. 4. Fig. 4a shows a cross-section of a BP-1 column (bottom of the photograph) where we can observe the appearance of the bonded-phase layer. Fig. 4b, c and d are the corresponding cross-sections of the inner surface of (b) a new BP-1 column never used before, (c) the same column after being subjected to three treatments with mercury(II) chloride for 1 month of work and (d) the same column after having been rejected (useless after numerous treatments). The appearance of the surface of the bonded phase is clearly different in Fig. 4d, al-

though differences are already noticeable between Fig. 4b and c, which implies that the effect of the treatment on the condition of the surface is really noteworthy and is quickly demonstrated.

Based on these results, our hypothesis accepts the fact that there are active points on these columns at which the methylmercury may connect and attach itself irreversibly to the silanol groups on the silica wall of the column (Fig. 2). Logically, when the column is new, the number of active points is relatively small, which allows us to carry out injections and obtain acceptable results without the need for any treatment at all. When the number of active points increases, they must be blocked by means of injections of mercury(II) chloride. However, these injections also destroy the phase, which means that as the column is used more and more, it becomes necessary to carry out treatments at more frequent intervals. Finally (Fig. 4d), the stationary phase is almost non-existent and is seen to be clearly discontinuous, so the effect of the treatments barely last long enough to carry out the calibration injections.

If this hypothesis is correct, it would seem logical to assume that there are two major effects when a particular stationary phase is used: the nature of the phase and its effect on the uniformity of the bonded layer, and the thickness of the bonded layer.

In the first instance, considering the molecular structures of the different phases tested (see Fig. 5), it seems logical to accept an order of efficiency of BP-5 > BP-1 > BP-20 phases. In the latter instance, experiments were done using a BP-5 column with a thicker bonded layer (Alltech Non-Pakd AT-5, 30 m × 0.54 mm I.D., 5.0-μm film thickness). The results obtained with this column were completely satisfactory and so far it has been used in the routine analysis of mussel samples for several months without needing any treatment at all, which confirms the hypothesis that was formulated.

Effect of the external covering of the column

In recent times there has been a tendency to replace fused-silica capillary columns with a protective covering of polyimide with equivalent columns having a protective layer of aluminium. This type of covering has some advantages from a mechanical point of view, and especially when nitrogen–phosphorus detectors are used. In this instance, this type of column was initially used in the determination of organomercurial compounds because it was available in the laboratory at that time. However, the results showed that it was impossible to obtain peaks for methylmercury even after prolonged treatments. After a series of tests, we found that the

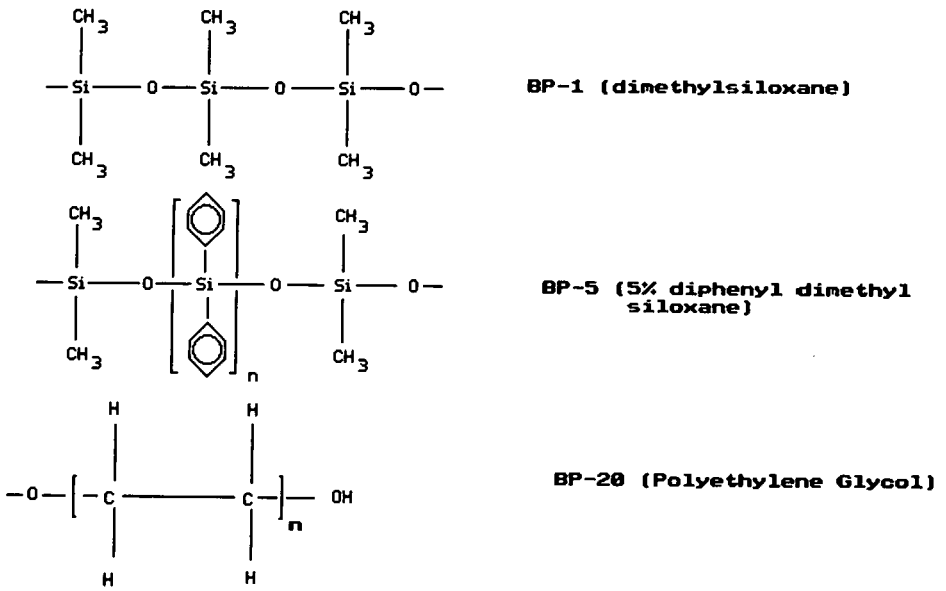

Fig. 5. Structures of the stationary phases considered.

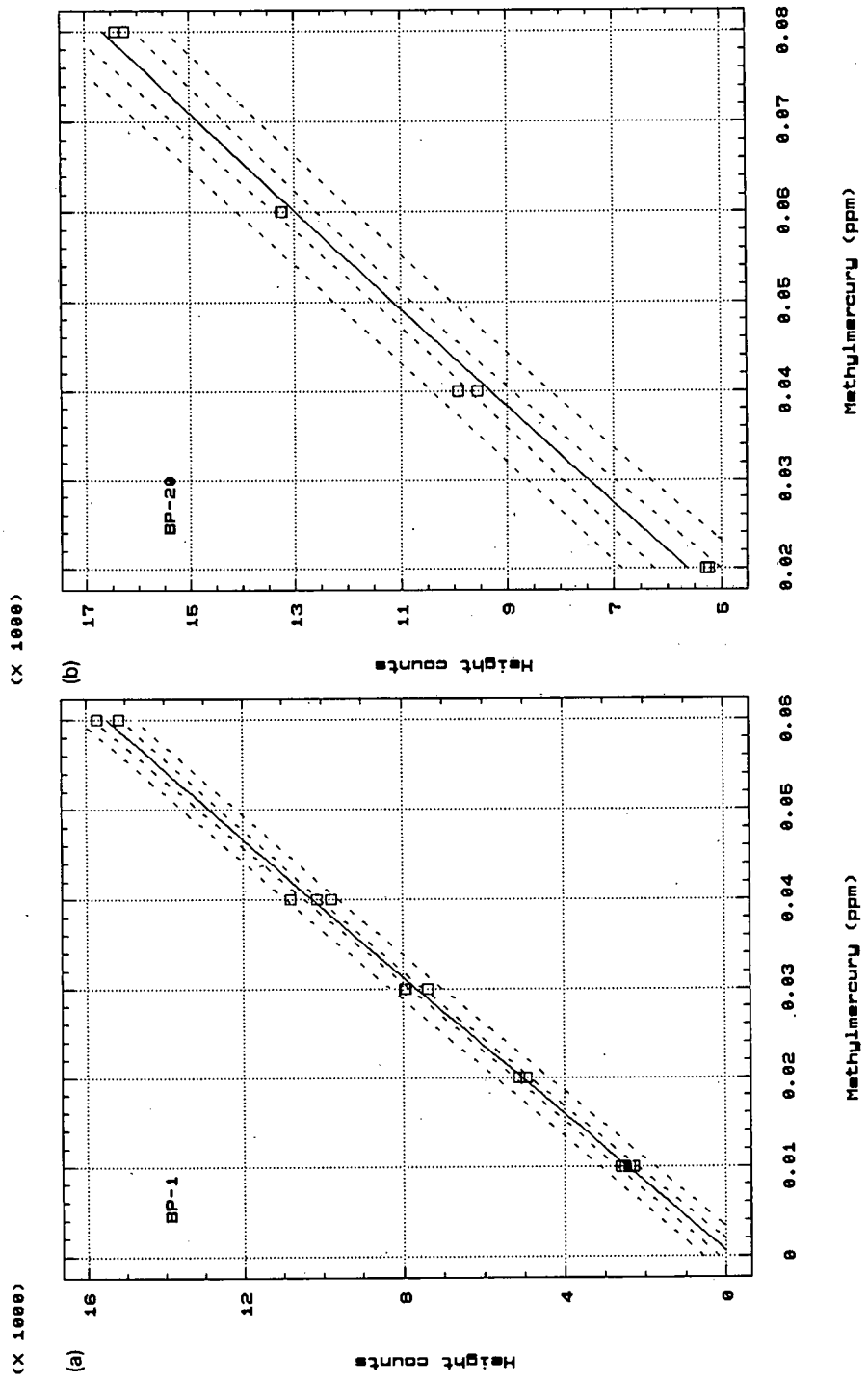
(a)
(X 1000)
Height counts
16
12
8
4
0
BP-1
0 0.01 0.02 0.03 0.04 0.05 0.06
Methylmercury (ppm)
(b)
(X 1000)
Height counts
17
15
13
11
9
7
5
BP-20
0.02 0.03 0.04 0.05 0.06 0.07 0.08
Methylmercury (ppm)

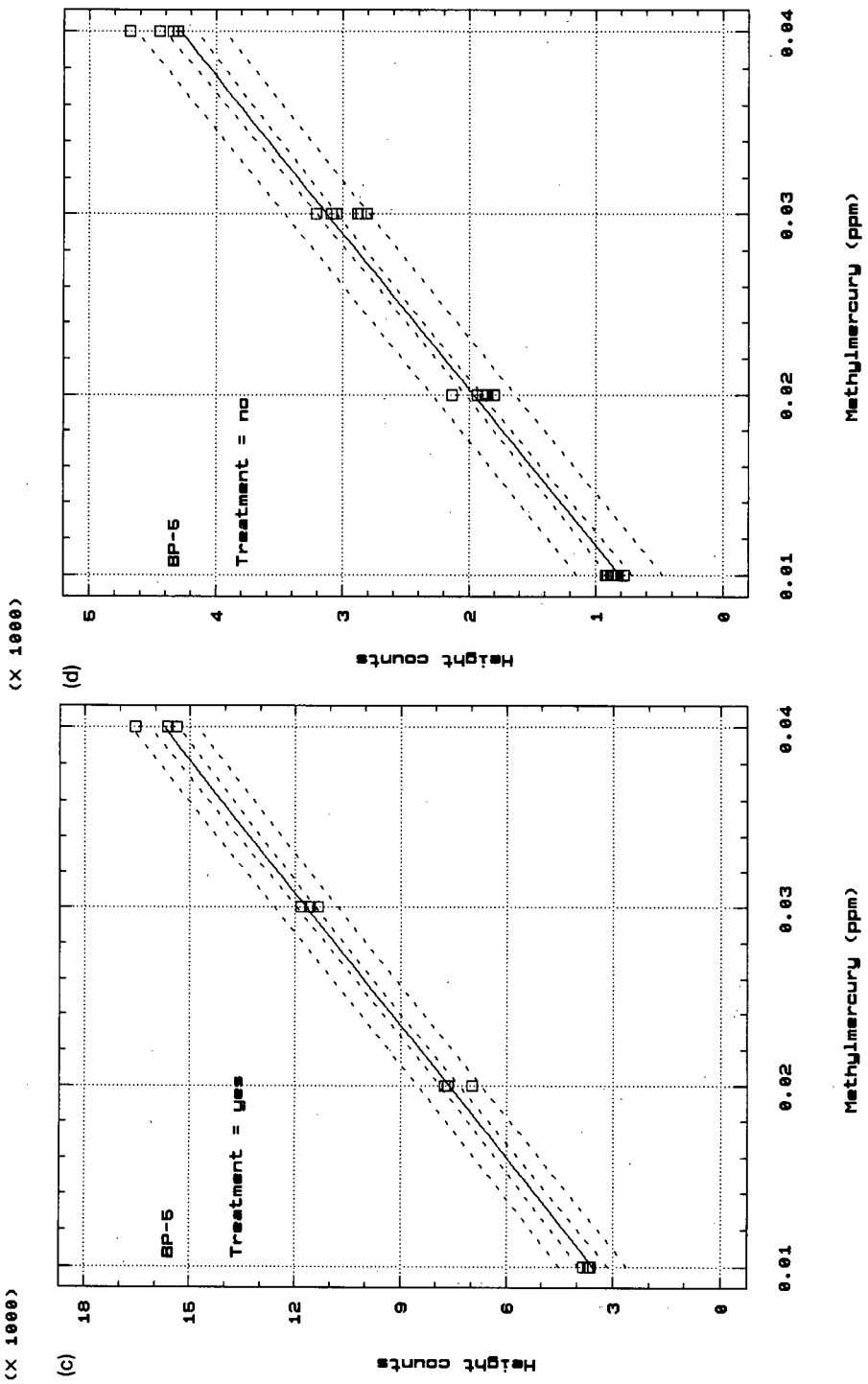

Fig. 6.

(Continued on p. 78)

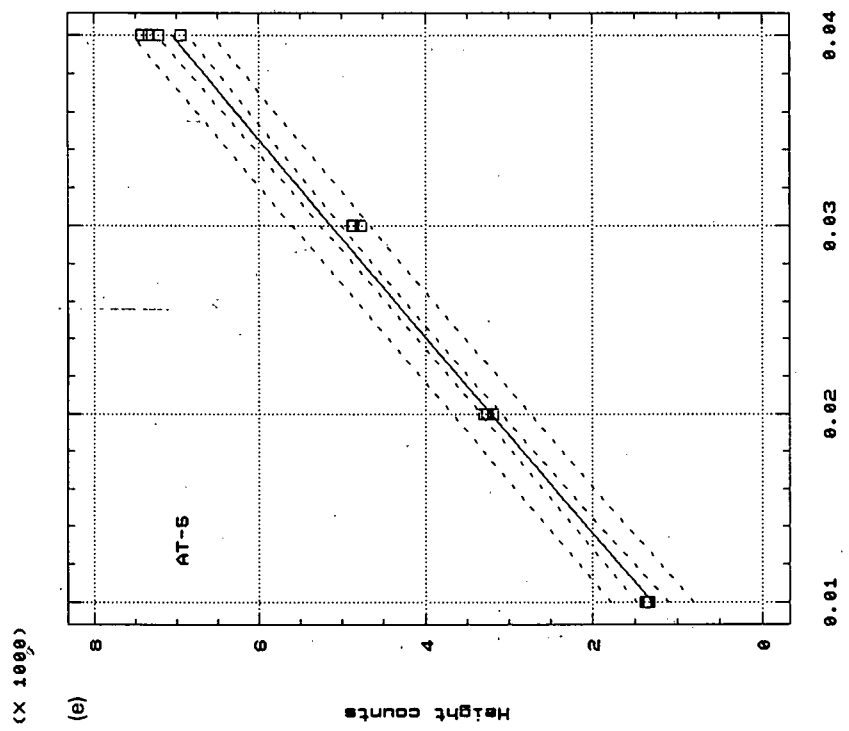

Fig. 6. Calibration graphs for methylmercury as a function of the column type and treatment.

reason for this behaviour resided in the external covering of the column in the length (barely 2 mm) that the column penetrates the injector body. The presence of metallic aluminium at high injector temperatures causes all mercury compounds in the injector to be reduced to metallic mercury, which means that no peaks are observed. Consequently, the use of this type of column was concluded to be impossible in analyses for compounds containing mercury.

Effect of the type of column on the response linearity of the chromatographic system

In addition to the practical reasons for the selection of a particular stationary phase or column type explained earlier, another study was carried out on the effect on the linearity of response of the system.

In order to do this, a multi-level point-to-point calibration (external standard method) was carried out. In Fig. 6 the respective calibration graphs are shown (together with 95% confidence and predictions bands) for the columns tested. With the BP-5 column, there is also a calibration graph corresponding to its first few days of life, when the column has not undergone any treatment. It can be seen that a linear calibration graph can be obtained also in this situation. The regression coefficients are BP-1 0.9981, BP-20 0.9960, BP-5 (no treatment) 0.9930, BP-5 (with treatment) 0.9970 and AT-5 0.9958. Hence, when treatment was administered, the different types of columns tested showed almost identical results in terms of linearity of response. On the other hand, on comparing the calibration graphs for the BP-5 column, it can be appreciated that the absolute response to methylmercury is higher when treatment had been applied. Note also that the linearity range is greater when using the BP-1 and BP-20 columns. This is because the response to methylmercury in these columns was lower than with the BP-5 column, enabling a larger dynamic range to be used. As the AT-5 column shows identical results, and for the reasons cited earlier, it must be concluded that this type of column is the most suitable for routine analysis.

CONCLUSIONS

The results presented here suggest that columns having a substantial stationary phase thicknesses must be used in the determination of organomercurial compounds by gas chromatography. When more common columns used in the laboratory (1.0-μm phase thickness) are applied, they must undergo frequent treatments with mercury(II) salts in order to obtain satisfactory separations and reproducible results. Among these, heavy phases of low polarity may behave better than polar phases in terms of the effect and duration of the treatments, for which reason they are recommended for use in occasional analyses for these compounds. However, this type of treatment has negative effects on the effective life of the columns and on the contamination of electron-capture detectors.

ACKNOWLEDGEMENT

The authors thank the Electron Microscopy Service of the University of Cádiz for producing the photographs presented in this paper.

REFERENCES

1 International Programme for Chemical Safety (IPCS), *Environmental Health Criteria 101: Methylmercury*, World Health Organization, Geneva, 1990.
2 J. Gavis and J. F. Fergusson, *Water Res.*, 6 (1972) 989–1008.
3 W. H. Schroeder, *Trends Anal. Chem.*, 8 (1989) 339–342.
4 Y. Thibaud and D. Cossa, *Appl. Organomet. Chem.*, 3 (1989) 257–266.
5 J. C. Gage, *Analyst*, 86 (1961) 457–459.
6 G. Westöö, *Acta Chem. Scand.*, 20 (1966) 2131–2137.
7 G. Westöö, *Acta Chem. Scand.*, 21 (1967) 1790–1800.
8 G. Westöö, *Acta Chem. Scand.*, 22 (1968) 2277–2280.
9 J. O'G. Tatton and P. J. Wagstaffe, *J. Chromatogr.*, 44 (1969) 284–289.
10 D. Beauchemin, K. W. M. Siu and S. S. Berman, *Anal. Chem.*, 60 (1988) 2587–2590.
11 D. S. Bushee, *Analyst (London)*, 113 (1988) 1167–1170.
12 S. S. Berman, K. W. M. Siu, P. S. Maxwell, D. Beauchemin and V. P. Clancy, *Fresenius' Z. Anal. Chem.*, 333 (1989) 641–644.
13 L. Magos, *Analyst (London)*, 96 (1971) 847–853.
14 I. M. Davies, *Anal. Chim. Acta*, 102 (1978) 189–194.
15 R. Capelli, C. Fezia, A. Franchi and G. Zanichi, *Analyst (London)*, 104 (1979) 1197–1200.
16 M. Fujita and E. Takabatake, *Anal. Chem.*, 55 (1983) 454–457.
17 A. Paudyn and J. C. Van Loon, *Fresenius' Z. Anal. Chem.*, 325 (1986) 369–376.
18 N. Bloom and W. F. Fitzgerald, *Anal. Chim. Acta*, 208 (1988) 151–161.
19 N. Bloom, *Can. J. Fish. Aquat. Sci.*, 46 (1989) 1131–1140.
20 C. A. Bache and D. J. Lisk. *Anal. Chem.*. 43 (1971) 950–952.

21 K. Chiba, K. Yoshida, K. Tanabe, H. Haraguchi and K. Fuwa, *Anal. Chem.*, 55 (1983) 450–453.
22 D. A. Ballantine, Jr. and W. H. Zeller, *Anal. Chem.*, 56 (1984) 1288–1293.
23 G. Decadt, W. Baeyens, D. Bradley and L. Goeyens, *Anal. Chem.*, 57 (1985) 2788–2791.
24 P. Lansens and W. Baeyens, *Anal. Chim. Acta*, 228 (1990) 93–99.
25 W. A. McCreham, R. A. Durst and J. M. Bellama, *Anal. Lett.*, 10 (1977) 1175–1188.
26 W. A. McCreham, *Anal. Chem.*, 53 (1981) 74–77.
27 I. S. Krull, D. S. Bushee, R. G. Schleicher and S. B. Smith, Jr., *Analyst (London)*, 111 (1986) 345–349.
28 O. Evans and G. D. McKee, *Analyst*, 112 (1987) 983–988.
29 J. F. Uthe and F. A. J. Armstrong, in L. Frieberg and J. Vostal (Editors), *Mercury in the Environment*, CRC Press, Cleveland, OH, 1972, pp. 21–53.
30 K. Sumino, *Kobe J. Med. Sci.*, 14 (1968) 115–130.
31 K. Sumino, *Kobe J. Med. Sci.*, 14 (1968) 131–148.
32 S. Nishi, Y. Horimoto and Y. Umezawa, *Bunseki Kagaku*, 19 (1970) 1646–1651; *C.A.*, 74 (1971) 134799d.
33 S. Nishi and Y. Horimoto, *Bunseki Kagaku*, 20 (1971) 16–20, *C.A.* 75 (1971) 58434j.
34 J. F. Uthe, J. Solomon and B. Grift, *J. Assoc. Off. Anal. Chem.*, 55 (1972) 583–589.
35 J. O. Watts, K. W. Boyer, A. Cortez and E. R. Elkins, Jr., *J. Assoc. Off. Anal. Chem.*, 59 (1976) 1226–1233.
36 C. J. Cappon and J. C. Smith, *Anal. Chem.*, 49 (1977) 365–369.
37 C. J. Cappon and J. C. Smith, *Bull. Environm. Contam. Toxicol.*, 19 (1978) 600–607.
38 L. Goolvard and H. Smith, *Analyst (London)*, 105 (1980) 726–729.
39 S. C. Hight and S. G. Capar, *J. Assoc. Off. Anal. Chem.*, 66 (1983) 1121–1128.
40 G. H. Alvarez, S. C. Hight and S. G. Capar, *J. Assoc. Off. Anal. Chem.*, 67 (1984) 715-717.
41 S. Aygun, M. A. Seckin and O. Y. Ataman, *Mikrochim. Acta*, III (1985) 307–317.
42 S. C. Hight and M. T. Corcoran, *J. Assoc. Off. Anal. Chem.*, 70 (1987) 24–30.
43 M. Horvat, A. R. Byrne and K. May, *Talanta*, 37 (1990) 207–212.
44 J. E. O'Reilly, *J. Chromatogr.*, 238 (1982) 433–444.
45 R. Dumarey, R. Dams and P. Sandra, *J. High Resolut. Chromatogr. Chromatogr. Commun.*, 5 (1982) 687–689.
46 C. J. Cappon and T. Y. Toribara, *LC·GC*, 4 (1986) 1012–1014.
47 A. G. F. Brooks, E. Bailey and R. T. Snowdon, *J. Chromatogr.*, 374 (1986) 289–296.
48 G.-B. Jiang, Z.-M. Ni, S.-R. Wang and H.-B. Han, *Fresenius' Z. Anal. Chem.*, 334 (1989) 27–30.
49 L. R. Kamps and B. McMahon, *J. Assoc. Off. Anal. Chem.*, 55 (1972) 590–595.
50 M. L. Schafer, U. Rhea and J. E. Campbell, *J. Agric. Food Chem.*, 23 (1975) 1079–1083.

Journal of Chromatography, 605 (1992) 81–86
Elsevier Science Publishers B.V., Amsterdam

CHROM. 24 234

Gas chromatography–electron-capture detection investigation of trihalomethanes produced by chlorination of humic acid in the presence of bromide

M. P. Italia* and P. C. Uden

Department of Chemistry, University of Massachusetts, Amherst, MA 01003 (USA)

(First received November 14th, 1991; revised manuscript received March 31st, 1992)

ABSTRACT

Concern over the production of hazardous trihalomethanes (THMs) as byproducts of the chlorination of drinking water prompted the examination of the chlorination of naturally occurring aquatic humic acid in the presence of bromide ion. The effect on THM production of varying reaction conditions such as pH, chlorine-to-bromine ratio, and reaction time was investigated using gas chromatography–electron-capture detection. THMs were formed under all conditions examined, the production of highly brominated compounds being favored.

INTRODUCTION

There is an increasing awareness of the possible dangers inherent in chlorinated drinking water. There are a number of toxic and mutagenic compounds formed in the chlorination process [1,2]. While most studies have concentrated on the detection of chlorinated products, recent research has been directed towards the investigation of alternative reactions occurring due to the presence of other chemical factors in the environment.

Bromide ion, present in aquatic systems at levels of approximately 10 mg/l in ground water and possibly exceeding 100 mg/l in surface water [3], can be considered as a possible coreactant with chlorine. Bromide ion can react with hypochlorous acid to produce hypobromous acid, which then reacts with organic substrates in a manner analogous to hypochlorite [4]. Thus, as Bunn *et al.* [5] have shown, there is the possibility for formation of trihalomethanes containing bromine, which are considered to be more hazardous to human health than their solely chlorinated analogs.

This study concerned the effect of bromide ion upon the products of the reaction of hypochlorite with a humic acid. Conditions of pH, reaction time and chlorine-to-bromine ratios were examined.

EXPERIMENTAL

Materials

Humic acid was obtained from B. Matvienko (Universidad de Sao Paulo, Sao Carlos, Brazil). This material had been obtained from a tropical aquatic source and was extensively purified by a procedure following that of Thurman and Malcolm [6]; this involved adsorption from filtered water on XAD-8 resin, elution with base, reacidification and reconcentration on XAD-8, a second base elution and precipitation at pH 1. Elemental analysis of this humic acid showed 35.08% carbon, 4.51% hydrogen and 7.33% nitrogen. The nitrogen level is great-

Correspondence to: Dr. P. C. Uden, Department of Chemistry, University of Massachusetts, Amherst, MA 01003, USA.

* Present address: Knoll Pharmaceuticals, Whippany, NJ 07981, USA.

0021-9673/92/$05.00

er than typically seen in non-tropical source materials.

Potassium bromide (certified ACS grade) was obtained from Fisher Scientific (Pittsburg, PA, USA). Diethyl ether, ACS reagent grade (Fisher) was double distilled before use. Commerical "Chlorox" was used as the source of HOCl; prior to use it was standardized by sodium thiosulfate-idoine titration. Buffer solutions were prepared from ACS-certified-grade sodium phosphate (Fisher).

Gas chromatography

The gas chromatograph used was a Hewlett-Packard 5730 (Avondale, PA, USA) with an electron-capture detector. The carrier gas was nitrogen, with a detector temperature of 320°C and an injection temperature of 225°C. The temperature program involved an initial temperature hold of 2 min at 40°C, followed by a temperature ramp of 5°C/min to a final temperature of 180°C with a final hold of 1 min.

The column used was 30 m × 0.25 mm internal diameter DB-5 fused-silica capillary column (J &W Scientific, Folsom, CA, USA) with an inlet split ratio of 50:1. The output was to a Perkin-Elmer (Norwalk, CT, USA) Sigma 100 recorder/integrator.

Chlorination/bromination procedures

Halogenated compound formation studies vs. pH. Humic acid samples were prepared at pH values 4–9 in phosphate buffer (0.1 *M*), containing 400 mg/l of KBr. Samples of humic acid (100 mg) were added to each of five different water sampling jars equipped with crimp top seals. Approximately 160 ml of the buffer solution and 3.5 ml of HOCl (175 mg Cl) were placed in a beaker and the pH adjusted with small amounts of NaOH or HCl; this solution was then added to the 165 ml sampling jar which was then crimp sealed. This procedure ensured that each sample received the defined dose of HOCl and contained an equal amount of bromide ion. It also ensured that the hypochlorite and hypobromite had attained equilibrium before addition to the humic material. After reagent addition, the mixture was allowed to react for 24 h (except for the time-dependent study), then quenched, extracted and analyzed for trihalomethanes (THMs).

For analysis, the sample jar was opened and 25–50 mg of sodium thiosulfate were added to quench residual reactivity of remaining HOCl and HOBr. A 4-ml aliquot of the solution was then removed, placed in a small vial and extracted with two 2-ml aliquots of diethyl ether. From this extract, 1 ml was diluted into 4 ml of diethyl ether and 2 μl samples were gas chromatographed (with a 50:1 inlet split). THM levels in the various analyzed samples were in the 10–100 ppm range; in all studies reagent and full method blanks were examined and predictably no measurable trihalomethanes were found.

THM formation vs. time. The procedure involved adding 100 mg humic acid, 25 mg KBr and 160 ml of 0.1 *M* pH 6 phosphate buffer to a 165-ml crimp top vial fitted with a resealable septum top. After adding 3.5 ml of HOCl, the vial was sealed and shaken. In sampling for gas chromatographic quantitation of THMs, 100-μl aliquots were removed and added to 4 ml of diethyl ether which contained 25–50 mg of sodium thiosulfite to quench the reaction. Sampling times during the reaction were after 4 min, 22 min, 45 min, 1.25 h, 2 h, 2.5 h, 5 h and 21 h.

THM formation vs. concentration of bromide ion. Studies were carried out with *ca.* 100-ml volumes of solutions in pH 6 phosphate buffer (0.1 *M*), using 165-ml crimp top vials. The total halogen level was kept at 0.021 *M* and the different molar ratios of Cl/Br were 1:1, 10:1, 50:1 and 100:1; the chlorine-to-carbon ratio was maintained at 5:1 to ensure complete reaction. The appropriate amount of humic acid was added to each of the vials followed by the calculated amount of bromide ion and HOCl, and the sample was allowed to react. After 24 h, 100-μl aliquots were removed and added to 4 ml of diethyl ether containing 25–50 mg of sodium thiosulfate.

RESULTS AND DISCUSSION

Standard compound analysis

Standards of the expected THMs were gas chromatographed to check for retention time (Fig. 1) and linearity of detector. Fig. 2 shows linear responses for the THM standards over the required experimental range.

Compound formation vs. pH

The results from the pH variation study are shown in Fig. 3. It can be seen that at low pH,

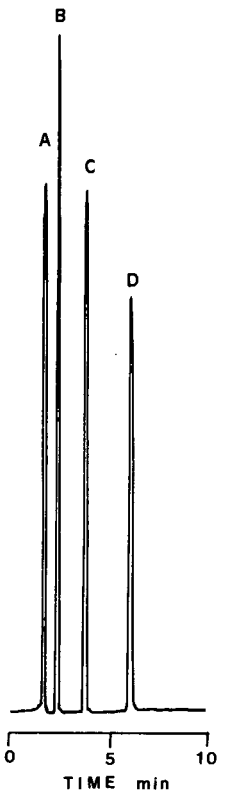

Fig. 1. Gas chromatography (GC)–electron-capture detection (ECD) chromatogram of the standard mixture of (A) chloroform, (B) bromodichloromethane, (C) chlorodibromomethane and (D) bromoform. GC conditions as given in the text. All compounds are at approximately 100-μg/l level.

chloroform formation predominates. As pH is increased, bromoform formation begins to increase and eventually becomes dominant, to the point where it contributes more than 90% of the total trihalomethanes formed. This observation is in contrast to other studies which show chloroform formation to increase with increasing pH [7,8], but these involved only reaction of hypochlorous acid with the humic molecule and did not consider bromide and the impact of the additional hypochlorous/hypobromous equilibrium:

$$HOCl \rightarrow H^+ + OCl^- \quad pK = 7.5\ [9]$$

$$+$$

$$Br^- \quad \text{rate constant} = 1.77 \cdot 10^5\ \text{l/mol minute}$$

$$\downarrow$$

$$HOBr \rightarrow H^+ + OBr^- \quad pK = 8.7\ [9]$$

Wong and Davidson [10] showed that this reaction is so predominant that when hypochlorite is added to a bromide-containing mixture in a ratio of less than 1:1, all HOCl is converted to HOBr in under 2.5 min. It has been shown that the reaction of hypobromous acid with many compounds is faster than the hypochlorous acid reaction with the same species [11].

THM formation vs. time. As can be seen in Fig. 4, chloroform was produced to the greatest extent within the first few minutes of reaction, with other THMs being slower to form. However, the formation of each THM then follows the general path of the chloroform formation, with some early reduction in measure levels which is probably due to measurement imprecision, and maintains a constant but lower level for the remaining time period of the study. The order of amount formed is bromoform, chlorodibromomethane and bromodichloromethane. As can be seen, there are no relative changes in compound ratios, implying that once the THM is formed it is not a precursor to further compound formation.

Bromide concentration study

Fig. 5 shows the results of the bromide concentration study. At high levels of bromide ion (Cl as HOCl/Br ratio = 1) bromoform and chlorodibromomethane formation dominate. This is consistent with the hypochlorite-to-hypobromite transformation, producing more hypobromite than hypochlorite. As the concentration of bromide is lowered (increase in Cl/Br ratio) there is a significant drop in the di- and tribrominated species, the chlorinated compounds beginning to predominate. It is noteworthy that the levels of these chlorinated compounds (expressed as mole percents) do not rise to the levels of the brominated compounds. This is presumably because, even when a small amount of bromide is present, the system equilibrium enhances hypobromite production, thus favoring brominated products.

CONCLUSIONS

With the concern over the availability of clean drinking water, and the equal need to determine the level of pollutants in the water supply, it has be-

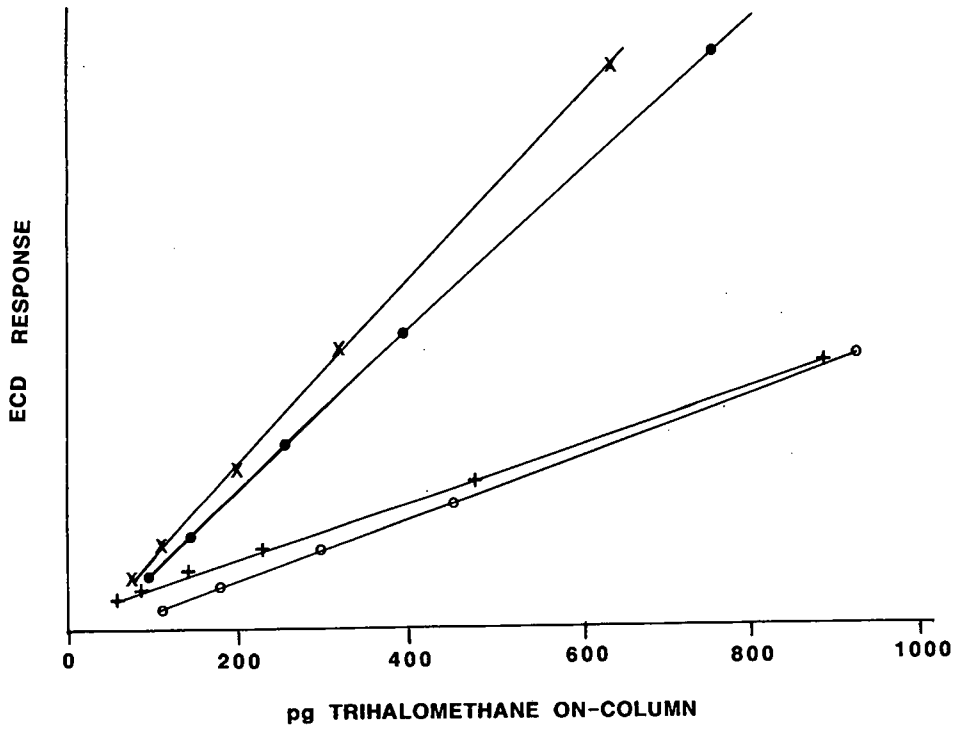

Fig. 2. GC–ECD linearity study and calibration curves for standards: chloroform (+), bromodichloromethane (×), chlorodibromomethane (●) and bromoform (○). All chromatographic conditions are as in the text.

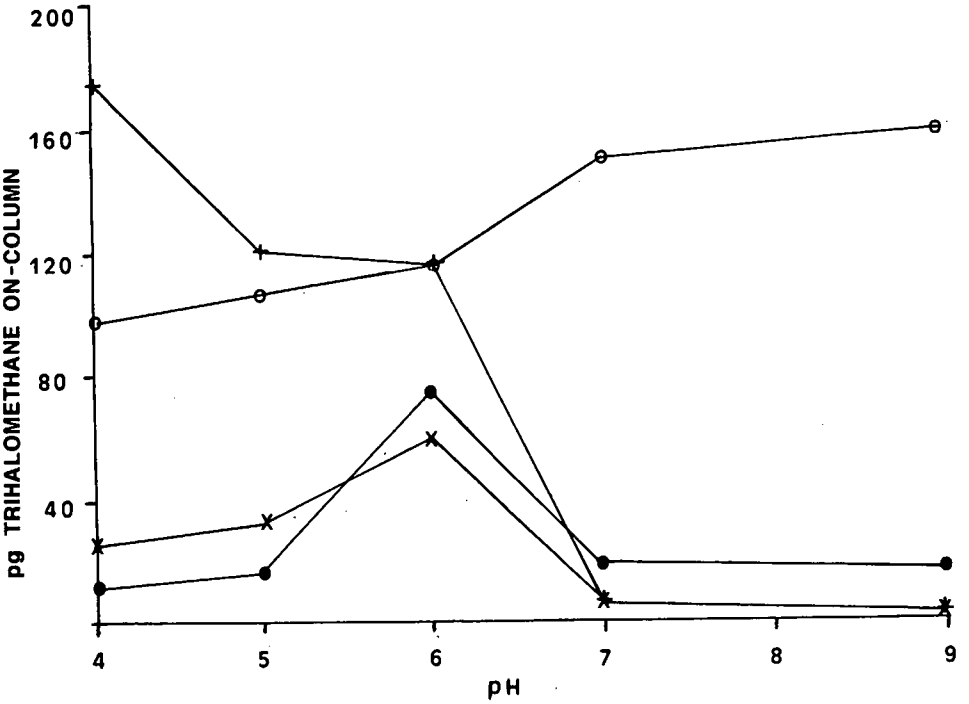

Fig. 3. Study of trihalomethane formation with respect to pH. Plot is of detected quantities of chloroform (+), bromodichloromethane (×), chlorodibromomethane (●) and bromoform (○). Quantitation was performed using GC–ECD with all chromatographic conditions as in the text.

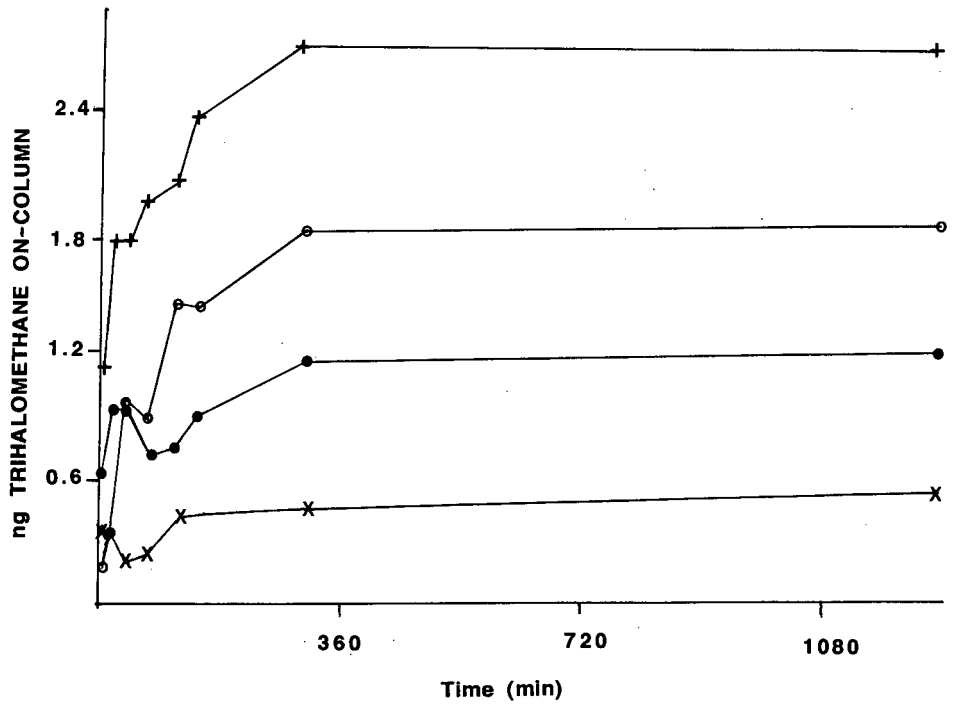

Fig. 4. Time-dependent study of trihalomethane formation with respect to the halogenation of aquatic humic acid. Symbols: + = chloroform; × = bromodichloromethane; ● = chlorodibromomethane; ○ = bromoform. Quantitation was performed using GC–ECD with all chromatographic conditions as in the text.

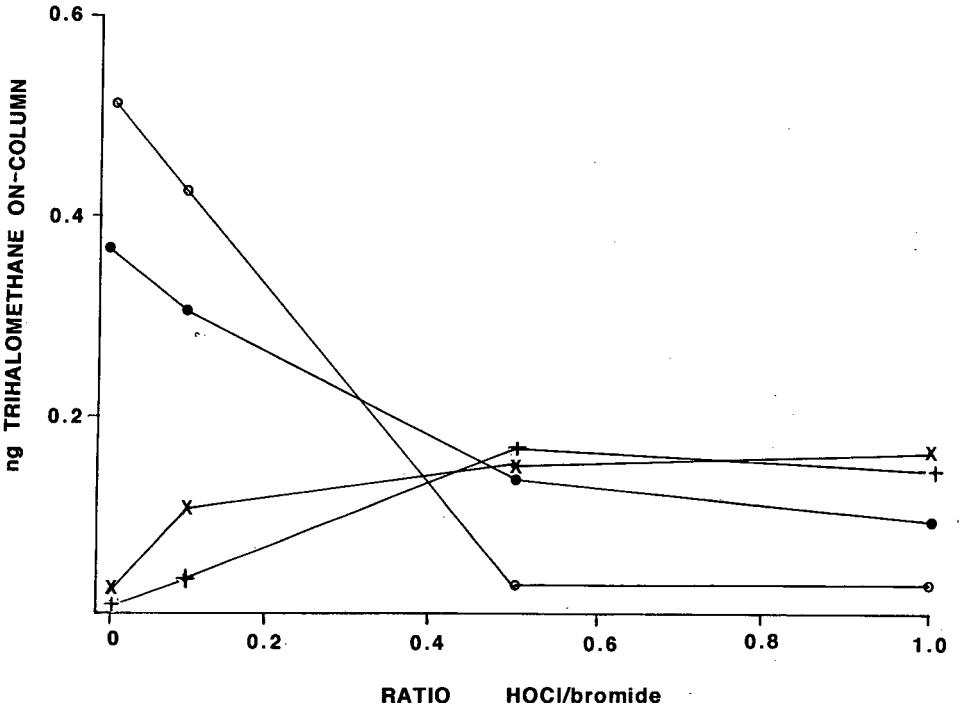

Fig. 5. Chlorine (as HOCl)-to-bromide ratio (*M*/*M*) study of trihalomethane formation from the halogenation of humic acid. Symbols: + = chloroform; × = bromodichloromethane; ● = chlorodibromomethane; ○ = bromoform. Quantitation was performed using GC–ECD with all chromatographic conditions as in the text.

come important to identify which pollutants are present from a waste disposal process and which ones may have occurred due to the water purifying process itself. It has long been known that the chlorination process itself is capable of producing chlorinated organic byproducts when water is cleansed. It appears that brominated compounds, which are detrimental to human health, are formed faster than and preferentially to chlorinated compounds. It is also important to note that these compounds are formed in the pH range at which drinking water chlorination occurs.

ACKNOWLEDGEMENTS

This research was supported in part by the Geological Survey, US Department of the Interior through the Massachusetts Water Research Institute, by the 3M Corporation and by the Dow Chemical Company.

REFERENCES

1 J. J. Rook, *Water Treat. Exam.*, 23 (1974) 234.
2 J. Symons, T. A. Bellar, J. K. Carswell, J. DiMarco, K. L. Kropp, G. G. Robek, D. R. Seeger, C. J. Slocum, B. L. Smith and A. A. Stevens, *J. Am. Water Works Assoc.*, 67 (1975) 634.
3 T. Luong, C. Peters and R. Perry, *Environ. Sci. Technol.*, 16 (1982) 473.
4 J. Morris, in R. L. Jolley (Editor), *Water Chlorination: Environmental Impact and Health Effects*, Vol. 1, Ann Arbor Sci. Publ., Ann Arbor, MI, 1977, pp. 21–35.
5 W. W. Bunn, B. B. Hass, E. R. Deane and R. D. Kleopfer, *Environ. Lett.*, 10 (1975) 205.
6 E. Thurman and R. Malcolm, *Environ. Sci. Technol.*, 15 (1981) 463.
7 J. W. Miller, *Ph. D. Dissertation*, University of Massachusetts, Amherst, MA, 1982.
8 J. C. Morris and B. Baum, in R. L. Jolley, H. Gorchev and D. H. Hamilton Jr. (Editors), *Water Chlorination: Environmental Impact and Health Effects*, Vol. 2, Ann Arbor Sci. Publ., Ann Arbor, MI, 1977, pp. 29–48.
9 R. C. Weast (Editor), *CRC Handbook of Chemistry and Physics*, CRC Press, Boca Raton, FL, 64th ed., 1985, p. D-167.
10 G. T. F. Wong and J. A. Davidson, *Water Res.*, 11 (1977) 971.
11 W. J. Cooper, L. M. Meyer, C. C. Bofill and E. Cordal, in R. L. Jolley, W. A. Brings and R. B. Cumming (Editors), *Water Chlorination: Environmental Impact and Health Effects*, Vol. 3, Ann. Arbor Sci. Publ., Ann Arbor, MI, 1979, pp. 285–296.

Journal of Chromatography, 605 (1992) 87–94
Elsevier Science Publishers B.V., Amsterdam

CHROM. 24 192

Development of directly coupled supercritical fluid chromatography with packed capillary column–mass spectrometry with atmospheric pressure chemical ionization

Kozo Matsumoto, Satoru Nagata, Hideo Hattori and Shin Tsuge

Department of Applied Chemistry, School of Engineering, Nagoya University, Furo-Cho, Chikusa-Ku, Nagoya 464 (Japan)

(First received November 6th, 1991; revised manuscript received March 18th, 1992)

ABSTRACT

Semi-micro packed column supercritical fluid chromatography was combined with atmospheric pressure chemical ionization mass spectrometry through a vacuum nebulization interface originally developed for high-performance liquid chromatography (HPLC)–mass spectrometry. High-purity carbon dioxide (99.999%) used as the mobile phase was delivered through a conventional HPLC pump to the semi-micro packed capillary column maintained at 100°C in an oven. The injected samples were introduced into the ion source with the aid of the nebulizing gas. To obtain the optimum results, the effects of various experimental parameters of the system were studied using Triton X-100 as a test sample. Under the optimum conditions, polyethylene glycol 400, polystyrene A-300, fat-soluble vitamins and polycyclic aromatic hydrocarbons were analysed.

INTRODUCTION

Compared with gas chromatography (GC), supercritical fluid chromatography (SFC) can be applied to less volatile compounds and compared with high-performance liquid chromatography (HPLC) it can be applied to the compounds with a shorter separation time and with a high resolving power. On the other hand, mass spectrometry (MS) possesses outstanding characteristics for the identification of isolated compounds with extremely high sensitivity. SFC–MS systems combining the characteristics of both techniques have been developed [1–6]. Many SFC–MS systems developed use capillary separation columns and chemical ionization (CI) or electron impact (EI) ionization in MS. With capillary separation columns, in general, hardly any drop in pressure is observed and the number of theoretical plates is larger than that of packed separation columns. In a capillary column, however, only a small sample size can be loaded and a splitter is usually installed after the injector. In additon, the analysis time with capillary columns is longer than that with packed columns.

In a previous paper, we reported an SFC–MS system with a capillary column and the CI mode with a vacuum nebulization interface [6]. In this system, a restrictor at the end of the capillary separation column was inserted into the ion source. Therefore, fluctuations of the flow-rate of the mobile phase caused changes in the ion source pressure and affected the observed mass chromatograms. In addition, mobile phase pump pressures above 300 atm could not be used to maintain a low vacuum in the ion source of the quadrupole mass spectrometer.

On the other hand, when atmospheric pressure ionization (API) is used with the SFC–MS system, API can ionize sample molecules at ambient pres-

Correspondence to: Dr. K. Matsumoto, Department of Applied Chemistry, School of Engineering, Nagoya University, Furo-Cho, Chikusa-Ku, Nagoya 464, Japan.

0021-9673/92/$05.00

sure without affecting the high vacuum of the mass spectrometer even if fluctuations of the flow-rate of the mobile phase occur and the mobile phase elutes into the ion source, as both the SFC and MS instruments can be operated almost independently of intervention by the API source. Huang *et al.* [7] reported a packed column SFC–APCI-MS system, using a common HPLC packed column (100 mm × 4.6 mm I.D.), a direct liquid introduction interface with a 20-μm pinhole and a triple quadrupole mass spectrometer [7]. They succeeded in the analysis of steroids extracted from equine urine.

In this study, a packed column SFC–API-MS system was developed, in which a semi-micro packed column was used as a separation column to attain splitless injection of samples for large sample loads and more rapid separation than with capillary columns. In this system, the vacuum nebulizing interface originally developed for HPLC–MS coupling was modified and incorporated into the nebulizer for transferring the SFC effluent to the API source. As API is a "soft" and highly efficient ionization method, it is suitable for the analysis of thermally unstable and oligomeric compounds which are amenable to SFC. The optimum conditions for the SFC–API-MS system were examined by using Triton X-100 as a test sample. The system was then applied to the analysis of various samples such as polyethylene glycol, polystyrene, vitamins and polycyclicaromatic hydrocarbons.

EXPERIMENTAL

The packed-column SFC–API-MS system used is shown schematically in Fig. 1. It is composed of three main parts: a supercritical fluid chromatograph, a nebulizing interface and a mass spectrometer. High-purity carbon dioxide was delivered to the packed separation column (5) through the pump of a Shimadzu Model LC-5A high-performance liquid chromatograph (2) which was operated in the pressure-programmed mode. The pump head was cooled to about 0°C with a micro-cooler (Netsudenshi). A fused-silica capillary tube (18 cm × 0.53 mm I.D.) packed with Kaseisorb LC ODS-300-5 3 (5 μm) (Tokyo Kasei) was used as the separation column, which was heated to 100°C in an oven (4). An integral-type restrictor with a 20-μm pinhole was connected to the end of the separation column through a stainless-steel transfer line (6) (1 m × 0.1 mm I.D.) heated at the same temperature of the oven. For modification of the mobile phase, methanol was added at a flow-rate of 10 μl/min with another HPLC pump (9). The mass spectrometer used was a Hitachi Model M-2000 double-focusing instrument equipped with an API system for HPCL–MS. The operating conditions were accelerating voltage 4 kV, ion-multiplier voltage 1.5 kV, scan rate 8 s from m/z = 0 to 1875 and corona discharge current 10 μA.

A vacuum nebulizing interface developed for

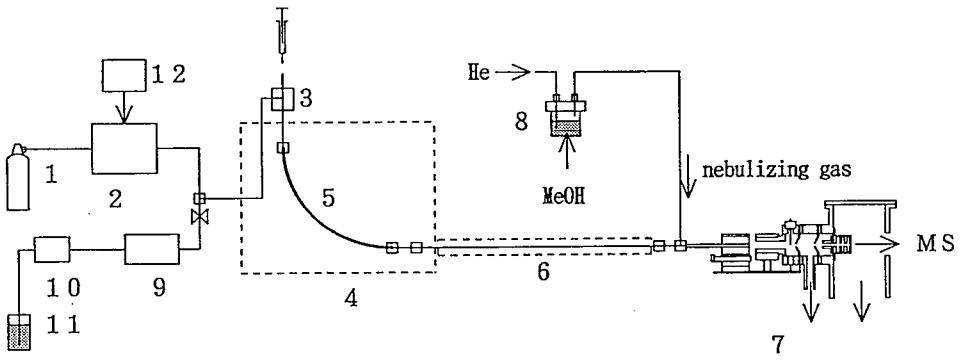

Fig. 1. Schematic diagram of the packed column SFC–API-MS system. 1 = CO_2 reservoir; 2 = HPLC pump modified for SFC; 3 = loop injector (0.5 μl); 4 = oven; 5 = semi-micro packed column; 6 = heated transfer line; 7 = API-MS interface; 8 = bubble saturator; 9 = HPLC pump for modifier; 10 = degasser; 11 = modifer reservoir; 12 = pressure programming controller.

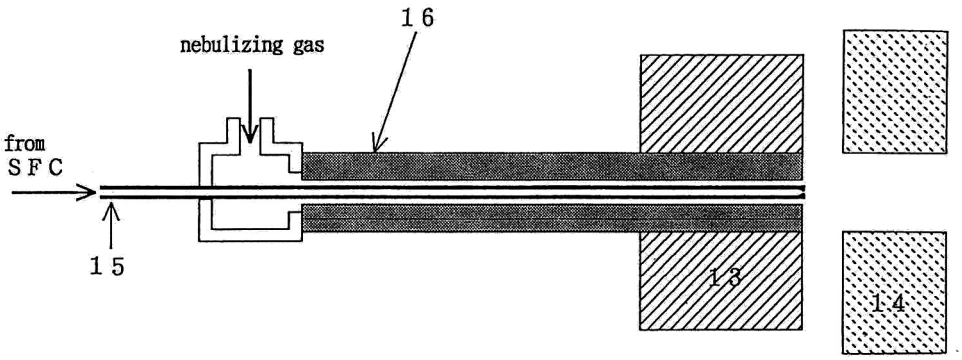

Fig. 2. Schematic diagram of the nebulizer nozzle. 13 = Nebulizer heater; 14 = desolvation chamber; 15 = restrictor (20 cm × 0.375 mm O.D. × 50 μm I.D.); 16 = stainless-steel sheath (13 cm × 1/16 in. O.D. × 0.41 mm I.D.).

HPLC–MS was applied in this SFC–MS system. Fig. 2 shows the modified interface for the SFC–MS system used in this work. The expansion of the supercritical fluid carbon dioxide at the outlet of the restrictor involves an endothermic effect under atmospheric pressure. As a result, the tip of the restrictor was cooled until it was covered with frost. Therefore, to attain stable and continuous nebulization, a nebulizing gas was supplied around the nozzle, the temperature of which was maintained between 200 and 400°C. The nebulizing gas (helium) saturated with methanol contained in a bubble saturator was introduced through the coaxial space between the restrictor and a stainless-steel sheath (13 cm × 1/16 in. O.D. × 0.41 mm I.D.). The desolvation chamber was also heated independently to 400°C to promote the desolvation of the sample molecules.

RESULTS AND DISCUSSION

In order to determine the optimum experimental conditions, various factors such as the temperatures of the nebulizer and the desolvation chamber, position of the nozzle tip, the species and the flow-rate of the nebulizing gas and the drift voltage for the API source were studied.

Effect of nebulization temperature

Fig. 3 shows reconstructed total ion current (RTIC) chromatograms of Triton X-100 obtained at various nebulization temperatures. Except for the nebulization temperature, the SFC–MS system was operated under the same experimental conditions: oven temperature 100°C, pressure programming mode from 150 to 350 kg/cm^2 at a rate of 10 kg/cm^2 · min, desolvation temperature 400°C, nebulizing gas flow-rate 200 ml/min and drift voltage 50 V. An aliquot (0.5 μl) of Triton X-100 solution disolved in methanol (3%) was injected through a loop injector. The three chromatograms A, B and C were obtained at nebulization temperatures of 200, 350 and 400°C, respectively. The chromatogram at 200°C (A) shows disturbed peaks and a lower peak intensity at higher molecular regions compared

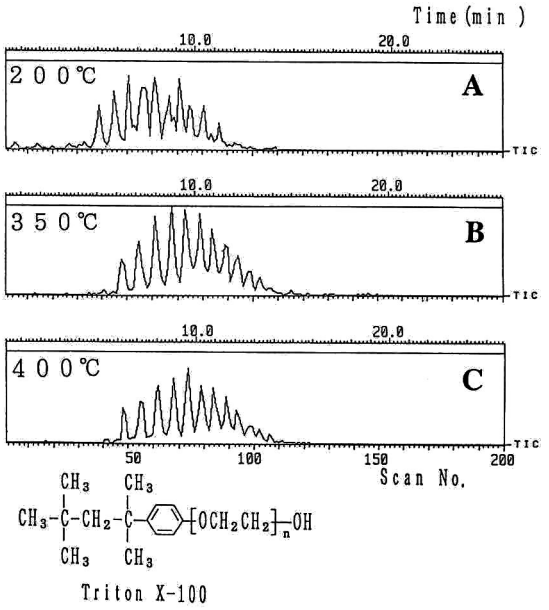

Fig. 3. Effect of nebulizer heater temperature on reconstructed total ion current (RTIC) chromatograms of Triton X-100. (A) 200°C; (B) 350°C; (C) 400°C.

with that obtained at 350°C (B). This effect is due to unstable nebulization caused by an insufficient heat supply to the nebulizer tip. On the other hand, the chromatogram at 400°C (C) gives lower intensity peaks than that at 350°C, but their shapes are very similar. This result suggests that the sample is partly decomposed by overheating. The nebulization temperature of 350°C was empirically decided to be the optimum for this sample.

Effect of the desolvation chamber temperature

When the desolvation temperature was kept at about 200°C, intense cluster ions of methanol and water and adduct ions of the sample molecules with methanol and water were observed in the mass spectrum, where the molecular and/or quasi-molecular ion peaks of the sample molecules were very difficult to identify. To reduce the cluster and adduct ions, the temperature of the desolvation chamber was kept at 400°C, which was the maximum temperature of this mass spectrometer.

Position of the nozzle tip

The position of the nozzle tip was varied under the optimum experimental conditions determined above. When the tip was located out of the nebulizing sheath, the observed peaks on the chromatograms became broad especially at longer retention times because of the insufficient heat supply. On the other hand, when the tip was withdrawn into the sheath, the peak heights of the chromatograms became lower because of the partial thermal decomposition of the sample molecules. Therefore, in this work, the position of the nozzle tip was adjusted to meet the edge of the nebulizing sheath.

Flow-rate of nebulizing gas

No significant influence of the flow-rate of the nebulizing gas below 400 ml/min was observed on the resulting mass chromatograms. However, without the nebulizing gas, the nebulization became unstable and the peak intensities on the chromatogram became weaker. On the other hand, at flow-rate above 400 ml/min, the observed peak intensities became smaller because of the shorter residence time of the sample molecules in the ion source. Therefore, in this work, the flow-rate of the nebulizing gas was fixed at about 200 ml/min. In addition, methanol saturation of the nebulizing gas (helium) was effective in to attaining "softer" ionization compared with pure helium.

Drift voltage

For the HPLC–API-MS system, a drift voltage of 150 V is usually used to obtain stronger (protonated) molecular peaks. In this SFC–API-MS system, a lower voltage, *e.g.*, 50 V, proved to be suitable to attain "soft" ionization because of the presence of carbon dioxide used as the mobile phase (*ca.* 200 ml/min at NTP).

Applications

Fig. 4 shows the mass chromatograms of Triton X-100 observed under the optimum conditions: nebulization temperature 350°C, desolvation chamber temperature 400°C, nebulizing gas flow-rate 200 ml/min, drift voltage 50 V, column oven temperature 100°C and column head pressure 150–350 atm at a programming rate of 10 atm/min. The components were eluted within 15 min and gave clearly separated peaks on the chromatograms. As shown in Fig. 5, identification of the components (degree of polymerization, *DP*) was performed with the corresponding mass spectra on which protonated molecular peaks, MH^+, appeared as the main peaks with some adduct ions. The components from *DP* = 3 to 15 for this sample were identified. Takeuchi

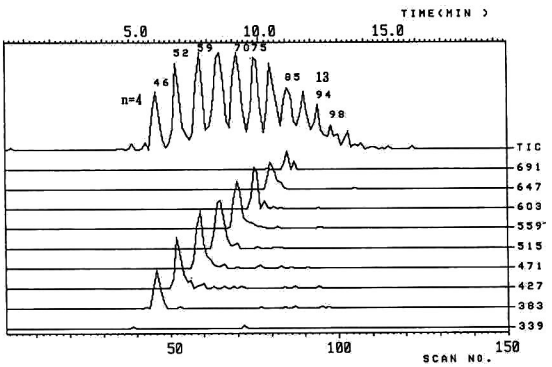

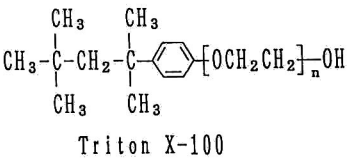

Triton X-100

Fig. 4. RTIC and reconstructed ion current (RIC) chromatograms of Triton X-100.

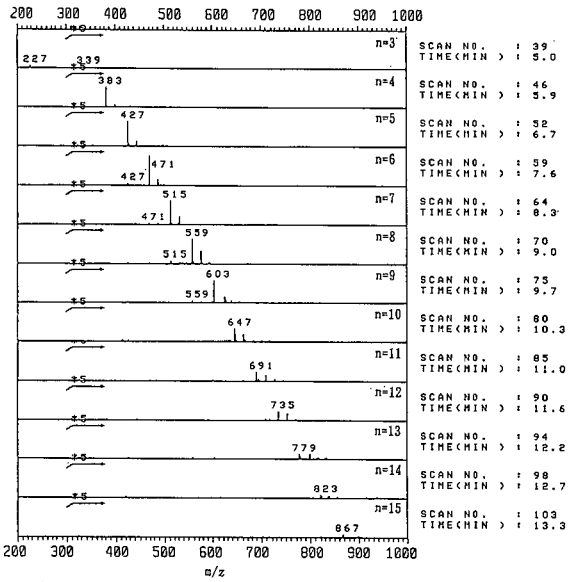

Fig. 5. Mass spectra of Triton X-100.

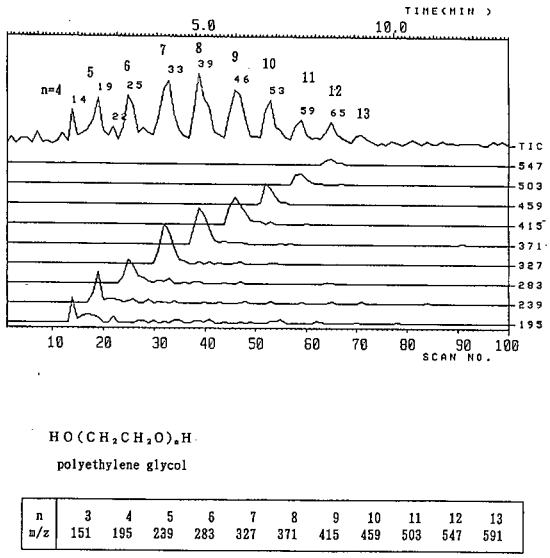

Fig. 6. RTIC and RIC chromatograms of polyethylene glycol 400.

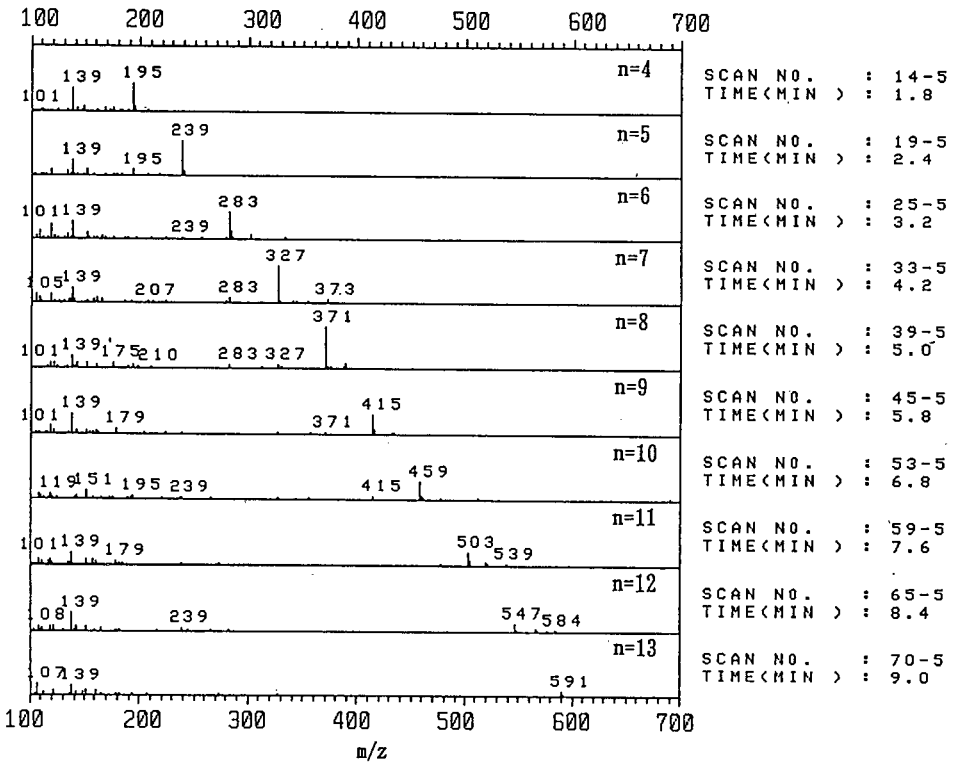

Fig. 7. Mass spectra of polyethylene glycol 400.

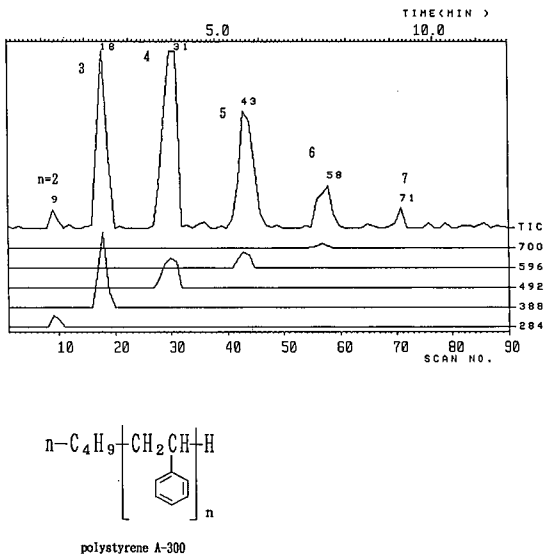

Fig. 8. RTIC and RIC chromatograms of polystyrene A-300.

et al. [8] reported the analysis of oligomers of DP = 3–14 by use of capillary HPLC–fast atom bombardment MS.

Fig. 6 shows mass chromatograms of polyethylene glycol 400 obtained under the same experimental conditions as in Fig. 4 except for the lower nebulization temperature of 300°C for the thermally labile Triton-X. The components were clearly resolved within 10 min. The identification of the peaks was also peformed with the corresponding mass spectra shown in Fig. 7, on which strong protonated molecular peaks were observed.

Fig. 8 shows the observed mass chromatograms of polystyrene A-300. The experimental conditions were the same as in Fig. 6, but the pressure was programmed from 200 to 350 atm at 10 atm/min. The components of the sample were eluted within 10 min, giving symmetrical and smooth peaks. As shown in Fig. 9, the identification of the components was performed from the mass spectra, on which aduct ions, $[MH + CH_3OH - CH_3]^+$, appeared in higher mass regions at m/z 284, 388, 492, 596, 700 and 804 for n = 2, 3, 4, 5, 6 and 7, respectively. In addition, fragmentation is observed, giving peaks of $[MH - C_6H_5]^+$ and $[MH - (C_6H_5 + C_6H_6)]^+$, *e.g.*, at m/z 293 and 215 for n = 3.

Fig. 10 shows the mass chromatograms of a mixture of fat-soluble vitamins (vitamin K_1, E and D_3 and vitamin A acetate) obtained under the same conditions as in Fig. 8. The samples were dissolved in methanol (0.25% each). All the components were eluted within 5 min. Although vitamin D_3, E and K_1 were not separated under these conditions on the RTIC chromatogram, they were discriminated on the RIC chromatograms. As shown in Fig. 11, they gave protonated molecular peaks, $[MH]^+$, on the mass spectra. Vitamin A acetate, however, gave a fragment peak of $[MH - AcOH]^+$ at m/z 269 without giving the protonated molecular peak on the mass spectrum.

Finally, polycyclic aromatic hydrocarbons

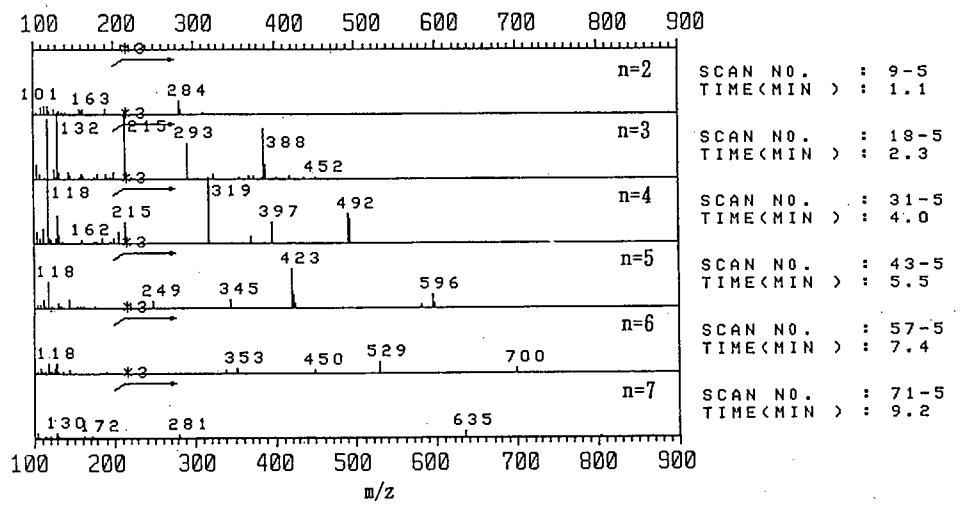

Fig. 9. Mass spectra of polystyrene A-300.

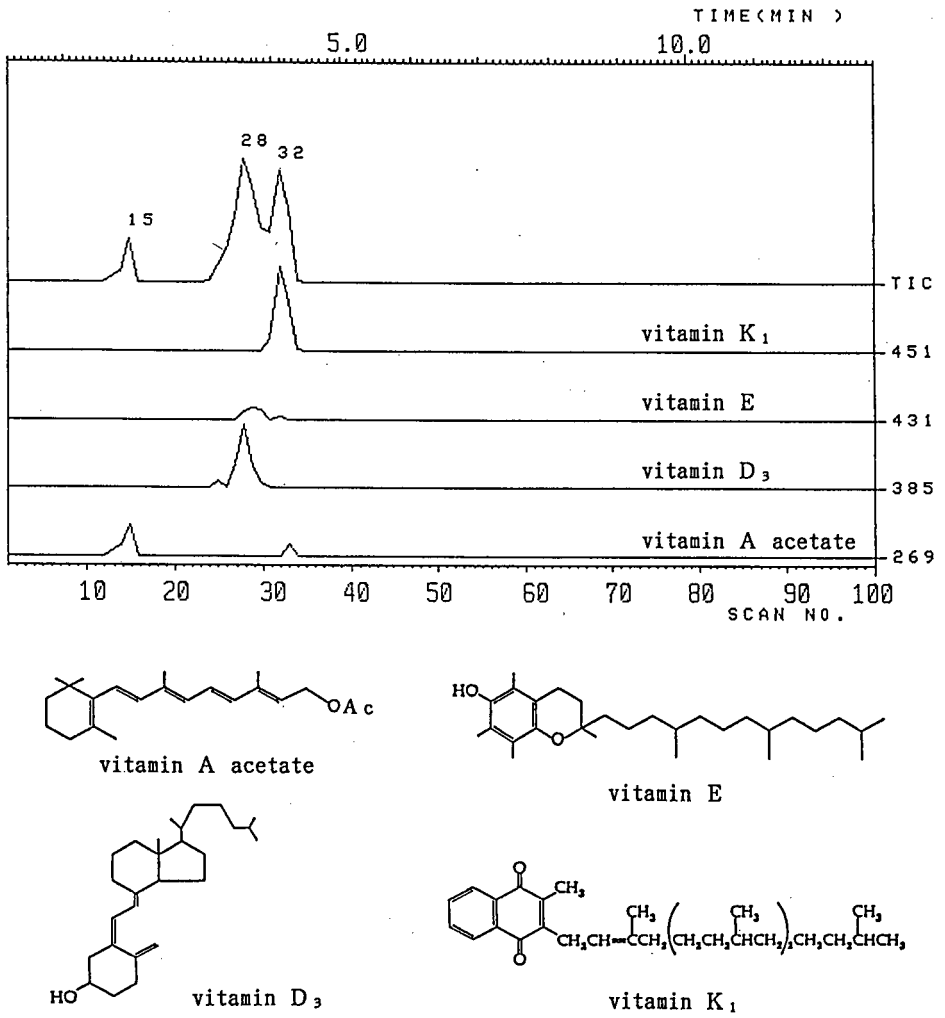

Fig. 10. RTIC and RIC chromatograms of the vitamin mixture.

(PAHs) are chosen as test samples which are not suitable for ordinary API detection because of their low polarity [9]. However, as shown by the following results, PAHs could be analysed using SFC–API-MS with the methanol-saturated helium as the nebulizing gas, which assisted the ionization of PAHs.

Fig. 12 shows the mass chromatograms of PAHs under the same conditions as in Fig. 6 except for the starting pressure of 100 atm. Samples (naphthalene, MW = 128; acenaphthylene, MW = 152; fluorene, MW = 166; anthracene, MW = 180; fluoranthene, MW = 202; pyrene, MW = 202; chrysene, MW = 228; and benzo[*e*]pyrene, MW = 252) dissolved in benzene (0.2% each) were analysed. These compounds gave $[M]^+$ and $[MH]^+$ ions of comparable intensity on their mass spectra without any appreciable fragment peaks. For naphthalene, its $[M]^+$ (*M/z* 128) was recorded on the RIC chromatogram, because the protonated molecular peak, $[MH]^+$, overlapped with the methanol tetramer peak, $[(CH_3OH)_4 + H]^+$, at *m/z* 129.

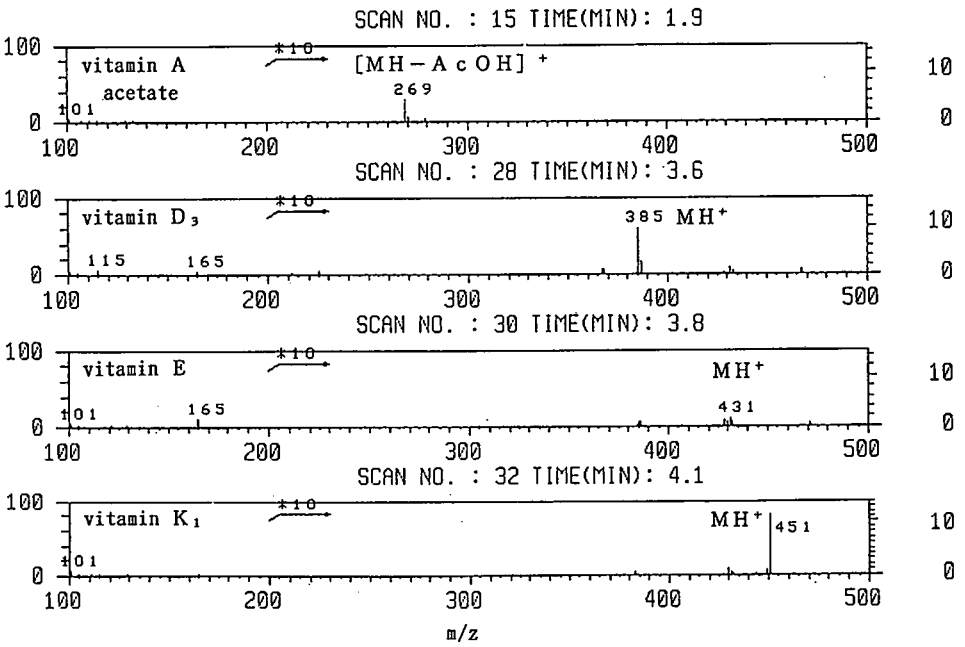

Fig. 11. Mass spectra of the vitamin mixture.

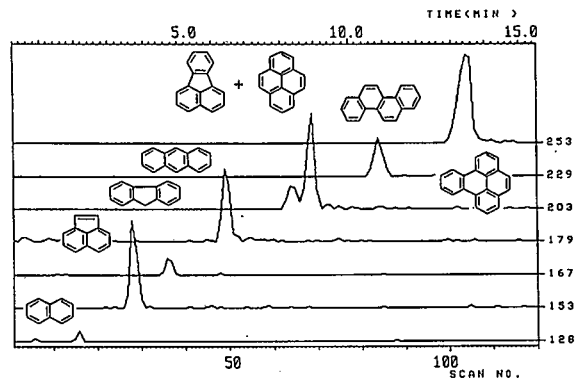

Fig. 12. RIC chromatogram of the PAH mixture. *m/z* 128 = Naphthalene; 153 = acenaphthylene; 167 = fluorene; 179 = anthracene; 203 = fluoranthene and pyrene; 229 = chrysene; 253 = benzo[*e*]pyrene.

CONCLUSIONS

A packed column SFC–APCI-MS system was developed with the use of a modified vacuum nebulization interface. The analysis of the thermally labile compounds such as Triton X-100, polyethylene glycol 400, polystyrene A-300 and fat-soluble vitamins was performed. Polycyclic aromatic hydrocarbons, for which conventional HPLC–APCI-MS did not give any appreciable sensitivity because of their low polarity, could be analysed with this system with the aid of a methanol-saturated nebulizing gas.

REFERENCES

1 S. M. Sheeley and V. N. Reinhold, *J. Chromatogr.*, 474 (1989) 83.
2 E. C. Huang, B. J. Jackson, K. E. Markides and M. L. Lee, *Anal. Chem.*, 60 (1988) 2715.
3 V. N. Reinhold, D. M. Sheeley, J. Kuei and G. Her, *Anal. Chem.*, 60 (1988) 2720.
4 H. T. Kalinoski and L. O. Hargiss, *J. Chromatogr.*, 474 (1989) 69.
5 J. D. Pinkston, D. J. Bowling and T. E. Delaney, *J. Chromatogr.*, 474 (1989) 97.
6 K. Matsumoto, N. Sato, S. Tsuge and M. Taguchi, *Mass Spectrosc.*, 39 (1991) 43.
7 E. Huang, J. Henion and T. R. Covey, *J. Chromatogr.*, 511 (1990) 257.
8 T. Takeuchi, S. Watanabe, N. Kondo, M. Goto and D. Ishii, *Chromatographia*, 25 (1988) 523.
9 *Hitachi Technical Data*, MS No. 43, Hitachi, Naka.

Journal of Chromatography, 605 (1992) 95–101
Elsevier Science Publishers B.V., Amsterdam

CHROM. 24 179

Packed column subcritical fluid chromatography of underivatized amino acids

V. Camel, D. Thiébaut and M. Caude

Laboratoire de Chimie Analytique des Processus Industriels, ESPCI, 10 Rue Vauquelin, 75231 Paris Cedex 5 (France)

M. Dreux

Laboratoire de Chimie Analytique, Université d'Orléans, B.P. 6559, Orléans Cedex 2 (France)

(First received November 25th, 1991; revised manuscript received March 13th, 1992)

ABSTRACT

Packed column subcritical fluid chromatography of underivatized amino acids is described. Using pyridine (or ethylene glycol)–methanol–water–triethylamine as modifier in the carbon dioxide, mixtures of amino acids can be separated on diol-bonded silica and detected without derivatization using evaporative light-scattering detection. Pyridine and ethylene glycol are shown to impregnate the stationary phase and to improve efficiency. The results demonstrate the wide potential of packed column subcritical fluid chromatography for the determination of polar compounds.

INTRODUCTION

Many different methods have been used to separate amino acids by liquid chromatography (LC); in most instances, precolumn or postcolumn derivatization is required to allow UV absorptiometry or fluorescence detection and to mask reactive functions. Thus, the use of reagents such as *o*-phthaldialdehyde (OPA) [1–3], 9-fluorenylmethylchloroformate (FMOC) [4] and phenyl isothiocyanate (PITC) to form phenylthiohydantoin (PTH) derivatives [5] has been extensively investigated and apparatus involving these techniques has been automated.

In contrast, to our knowledge, only four references are devoted to supercritical fluid chromatography (SFC) of amino acids [6–9]. They involve precolumn derivatization with PITC or FMOC on bare silica [6,9] or on cyanopropyl-bonded silica [7,8] and separations require a high modifier content in the carbon dioxide to dissolve amino acids in combination with an elution gradient. Derivatization was used to advantage for detection and mainly to reduce the polarity of amino acids by masking their polar functions. Employing a high percentage of a modifier means that the mobile phase was subcritical instead of supercritical. Thus, under these conditions, the kinetic advantages of subcritical fluid chromatography (SubFC) are reduced owing to the lower diffusion coefficients.

The SubFC separation and detection of amino acids without derivatization were a challenge: clearly the polarity of CO_2 is too low to dissolve amino acids without adding a high concentration of modifiers. The mobile phase has to be strong enough to elute them from a packed column while keeping the selectivity high enough to obtain a good resolution. This requires the stationary phase to be chosen with care in order to retain and elute the amino acids: with a low-polarity stationary phase, they would

Correspondence to: Dr. D. Thiébaut, Laboratoire de Chimie Analytique des Processus Industriels, ESPCI, 10 Rue Vauquelin, 75231 Paris Cedex 5, France.

0021-9673/92/$05.00

elute without retention; with a polar stationary phase, amino acids would have too strong interactions to permit elution under reasonable conditions, *i.e.*, with a modifier content in the CO_2 lower than 30%. After selecting a suitable stationary phase, the mobile phase must control the retention and solubility of the solutes. On packed columns, this can be done by adding polar modifiers to the CO_2 and varying their contents or, for small amounts of modifiers, by varying the CO_2 density [10]. Hence very polar modifiers have been used to separate polyhydroxybenzoic acids and benzenepolycarboxylic acids [11,12], phenols [13], imidazole derivatives [14], opium alkaloids [15] and various chiral species such as β-blocking drugs [16,17]. It has been demonstrated that polar modifiers improve peak shapes and promote the elution of polar compounds by clustering together: the solvent strength in the clusters where the solutes are localized is much higher than that in the bulk mobile phase [12]. Hence it is necessary to add modifiers to the mobile phase, but selecting the modifiers is not trivial with regard to amino acids.

From the detection point of view, the challenge was solved using the experience gained in our laboratory with evaporative light-scattering detection (ELSD) coupled to SubFC [18–21] or, in some experiments, by adding copper ions to the polar modifier to obtain complexes of amino acids giving suitable UV absorption at 254 nm [22].

It should be borne in mind that this work was undertaken mainly to show the extreme limits of packed column CO_2 SubFC for the separation of very polar compounds, and not to compete with LC.

EXPERIMENTAL

SubFC with UV detection

A newly developed prototype of supercritical fluid chromatograph (Gilson Villiers-le-Bel, France) was coupled to a Varian (Orsay, France) Model 2550 UV detector. It consists of a Model 305 piston pump (main pump) with its head cooled to 0°C to deliver the CO_2, a Model 306 piston pump (slave pump) for the modifiers, a Model 811 B mixing chamber (two-stage dynamic mixing, 1.5 ml total volume) connected to the pulse damper module, a Rheodyne injection valve equipped with a 20-μl loop, a column oven and a manometric module combined with a pulse damper and a first-stage back-pressure regulator. This new module provides column inlet and outlet pressures to the main pump. The outlet pressure can be monitored using the main pump software, allowing pressure gradients in combination with modifier gradients by increasing the modifier flow-rate. A Tescom back-pressure regulator set at 80 bar ensured final expansion of the mobile phase. The chromatograms were stored in a Shimadzu Model C-R6A integrator (Touzart et Matignon, Vitry-sur-Seine, France).

SubFC with evaporative light-scattering detection (ELSD)

A liquid chromatograph modified for packed column SFC (Varian Model 2500 M) was used without modification. It consists of two Model 2510 piston pumps that allow programming of composition gradients, a dynamic mixing chamber (Gilson, Model 811B) and a Valco injection valve equipped with a 20-μl loop. The column was placed in a heated bath and connected to the interface of the ELSD (Sédex 45, Sédéré, Alfortville, France) designed for SFC. This interface replaces the LC interface and allows both expansion and nebulization of the mobile phase prior to detection using a calibrated fused-silica restrictor housed in stainless steel. In contrast to the LC device, the glass part connecting the interface to the evaporation tubing (set at 45°C) is thermoregulated at 70°C to avoid freezing. As usual [18,19], air supplies the SFC interface (pressure 1 bar) and the detection cell (pressure 2 bar) to improve nebulization and vaporization of the mobile phase and to reduce band broadening in the detection cell [18,19]. A Kipp & Zonen Model BD 40 plotter (Touzart et Matignon) was used to record the chromatograms.

Columns

The columns used for these experiments (Table I) were (1) 50, (2) 150 or (3) 250 × 4.6 mm I.D.

Solvents and solutes

CO_2 (industrial quality) was purchased from l'Air Liquide (Paris, France). Methanol and triethylamine were of high-performance liquid chromatographic grade from Prolabo (Paris, France). Pyridine, formic, citric and trifluoroacetic acid, eth-

TABLE I

STATIONARY PHASES USED FOR SubFC OF AMINO ACIDS

Column dimensions: (1) 50 × 4.6 mm I.D.; (2) 150 × 4.6 mm I.D.; (3) 250 × 4.6 mm I.D.

Stationary phase	Column	Diameter of particles (μm)	Company
Ultrabase UB 225 (C18)	3	5	SFCC Shandon, Eragny, France
Intersphère 1000 Å	3	7	Interchim, Montluçon, France
Intersphère-NH_2	2	5	Interchim
Nucleosil-NH_2	2	5	SFCC Shandon
LiChrospher 100 CN	2	5	Merck, Paris, France
Hypersil Deltabond CN	2	5	Touzart et Matignon
LiChrosorb diol	2	5	Interchim
LiChrosorb diol	1	5	SFCC Shandon

ylene glycol, glycerol, 2-propanol and propylamine were of analytical-reagent grade from Prolabo and Merck.

Amino acids were purchased from Prolabo and Merck. Samples to be injected were prepared by dissolving the amino acids in water–methanol (90:10, v/v) and then diluting them in the modifier to obtain 10^{-2} *M* solutions.

RESULTS AND DISCUSSION

Using the results obtained in the laboratory for the separation of alkaloids, imidazole derivatives and chiral species [14,15], we selected methanol–water–aliphatic amine as the main modifier to begin the experiments. In this slightly basic medium, amino acids were in the anionic form. To deal with positively charged amino acids, some experiments were also carried out with trifluoroacetic acid, citric acid or formic acid instead of triethylamine. The retention of amino acids on non-polar and polar stationary phases was first investigated to obtain rapid screening.

Preliminary experiments

Non-polar stationary phase. Experiments were carried out on Ultrabase end-capped octadecyl-bonded silica. Using 5–20% of methanol–water–triethylamine (or trifluoroacetic acid) (95.2:4.75:0.05, v/v/v) in CO_2, amino acids were not retained.

Polar stationary phases. Bare silica and amino-propyl-, nitrile- and diol-bonded phases were studied using similar mobile phases to those used with non-polar phases.

For a modifier content ranging from 10 to 20% in CO_2, the capacity factors of the amino acids vary (according to their polarity) from 0.5 to more than 30. Nevertheless, the efficiency is too low [less than 400 theoretical plates (TP)] to resolve mixtures of amino acids (elution peaks exhibit strong tailing).

Using acid modifiers, retention on the amino-bonded phase is too high to elute proline, used as a medium polarity test amino acid. In contrast, retention on Deltabond CN is very low and no separation of amino acids can be expected with this type of stationary phase and mobile phase. The best selectivity is obtained on LiChrospher CN and LiChrosorb diol-bonded silica but, unfortunately, the efficiency is still very low (less than 1000 TP).

Using a basic modifier, the results are almost the same: again, the greatest selectivity is obtained with the LiChrosorb diol but the efficiency remains very low.

As has already been demonstrated, the Deltabond CN phase is very deactivated and allows the elution of very polar compounds without adding modifiers [23–25]. For SubFC of amino acids, a minimum content of *ca.* 10% of modifier is required to dissolve samples in the mobile phase. With lower contents, the elution peaks exhibit strong front tailing. It appears that with such an amount of polar compounds in CO_2, retention of amino acids cannot be obtained on Deltabond CN. This means that

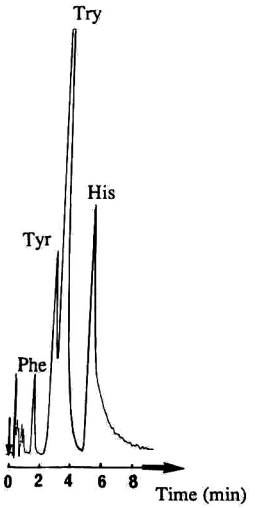

Fig. 1. SubFC of a mixture of four amino acids. Column, 150 × 4.6 mm I.D. LiChrosorb diol, 5 μm; mobile phase, CO_2–polar modifier (70:30, v/v); flow-rate, 2.8 ml/min (at 0°C); polar modifier, methanol–water–triethylamine (95:4.95:0.05, v/v/v); inlet pressure, 307 bar; outlet pressure, 250 bar; temperature, 30°C; UV detection at 225 nm, 0.08 a.u.f.s.

the amount of bonded CN groups is very low and/or the retention on other cyano-bonded phases used came from residual silanol groups.

Consequently, for further experiments, the basic modifier combined with LiChrosorb diol was chosen because partial resolution of mixtures of amino acids could be obtained and the efficiency was enhanced (Fig. 1). As described in the Introduction, subcritical conditions are only reached with 10–20% modifier.

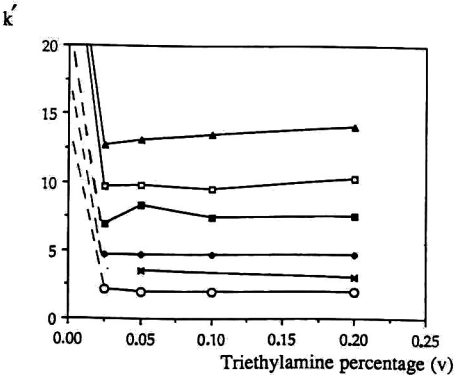

Fig. 2. Influence of triethylamine content in mobile phase on the retention of amino acids. Conditions as in Fig. 1, except CO_2–polar modifier (80:20, v/v); polar modifier, methanol–water–triethylamine (95 − *x*:5:*x*, v/v/v); UV detection at 254 nm; amount injected, 20 μl at 10^{-2} *M*. ○ = Leu; × = Val; ◇ = Pro; ■ = Ala; □ = Thr; ▲ = Hyp.

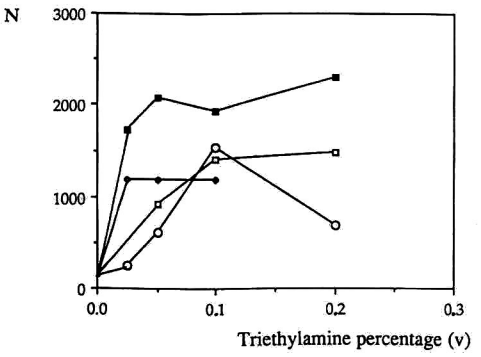

Fig. 3. Influence of triethylamine content in the mobile phase on the retention of amino acids. Conditions as in Fig. 2. ○ = Leu. ◇ = Pro; ■ = Ala; □ = Thr.

Improvement of separation efficiency on diol-bonded silica

Alcohol modifier. Methanol and 2-propanol were compared. Methanol was preferred although the chromatographic behaviour of the two alcohols were similar, the solubility of amino acids was higher in methanol.

Water modifier. The amount of water in the modifier between 1.5 and 11% (v/v) was investigated. No modification of solute retention with varying amount of water in the modifier could be observed. The percentage of water was fixed at 5%, mainly to

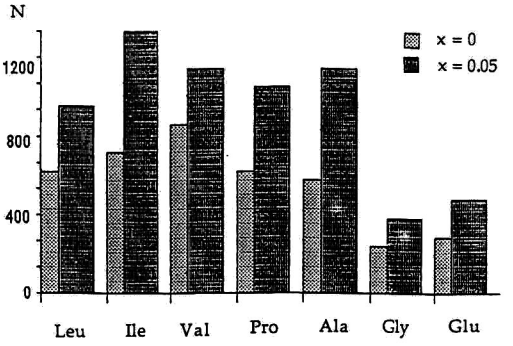

Fig. 4. Influence of triethylamine content in the mobile phase on column efficiency with pyridine modifier. Conditions as in Fig. 1 except CO_2–modifier (67:33, v/v); polar modifier, methanol–water–triethylamine–pyridine (82.8 − *x*:7.2:*x*:10, v/v); flow-rate, 4.5 ml/min (at 0°C); inlet pressure, 265 bar; detection, ELSD.

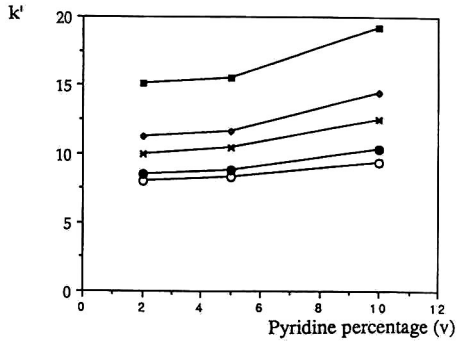

Fig. 5. Influence of pyridine content in the mobile phase on the retention of amino acids. Conditions as Fig. 1 except polar modifier, methanol–water–triethylamine–pyridine (93 − *x*:7:0.05:*x*, v/v); flow-rate, 5 ml/min (at 0°C); detection, ELSD. ○ = Leu; ● = Ile; × = Val; ◇ = Pro; ■ = Ala.

ensure solubility of amino acids in the mobile phase without demixing of the mobile phase.

Basic component. Experiments were carried out to study the influence of basic additives on retention, selectivity and efficiency; propylamine and pyridine were compared with triethylamine.

Propylamine exhibits almost the same behaviour as triethylamine (Fig. 2). Addition of a small amount (0.05%, v/v) of amine to the mobile phase greatly decreases the retention (by more than a factor of 2), this effect being more pronounced with triethylamine, whereas the selectivity does not vary. The influence of the amount of amine in the mobile phase on the efficiency is important, as shown in

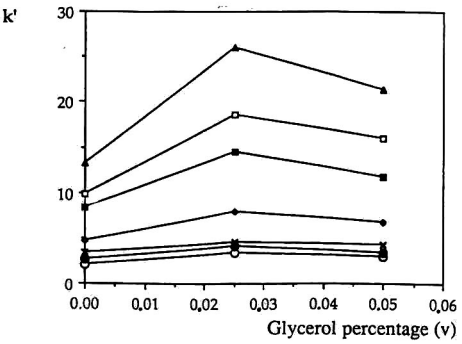

Fig. 6. Influence of glycerol content in the mobile phase on the retention of amino acids. Conditions as in Fig. 1, except polar modifier, methanol–water–triethylamine–glycerol (95.2 − *x*: 4.75:0.05:*x*, v/v); flow-rate, 4 ml/min; temperature, 40°C; outlet pressure, 200 bar; UV detection at 254 nm. ○ = Leu; ● = Ile; × = Val; ◇ = Pro; ■ = Ala; □ = Thr; ▲ = Hyp.

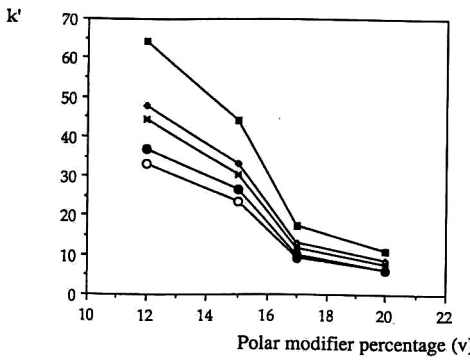

Fig. 7. Variation of capacity factors of amino acids with the amount of modifier in the mobile phase. Column, 50 × 4.6 mm I.D. LiChrosorb diol, 5 μm; mobile phase, CO_2–polar modifier (100 − *x*:*x*, v/v); flow-rate, 3 ml/min (at 0°C); polar modifier, methanol–water–triethylamine–pyridine (88:6.95:0.05:5, v/v); inlet pressure, 135 bar; temperature, 30°C; detection, ELSD. ○ = Leu; ● = Ile; × = Val; ◇ = Pro; ■ = Ala.

Fig. 3; the efficiency increases from a few hundred to 2000 TP by adding 0.05% (v/v) amine to the mobile phase.

When triethylamine is replaced with pyridine, the percentage of the latter must be seven times higher to obtain a similar separation. The efficiency is improved by a factor of 2 if triethylamine is also added (Fig. 4); this indicates (i) the possibility of very strong interactions between the amino acids and the residual silanol groups and (ii) an easier separation of negatively charged amino acids, both requiring a more basic additive than pyridine. Fig. 5 indicates that the retention increases as the pyridine content in the mobile phase increases, in the presence of triethylamine. The latter observation is consistent

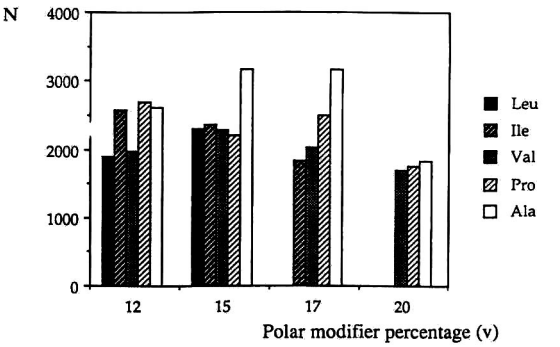

Fig. 8. Variation of efficiency with the amount of modifier in the mobile phase. Conditions as in Fig. 7.

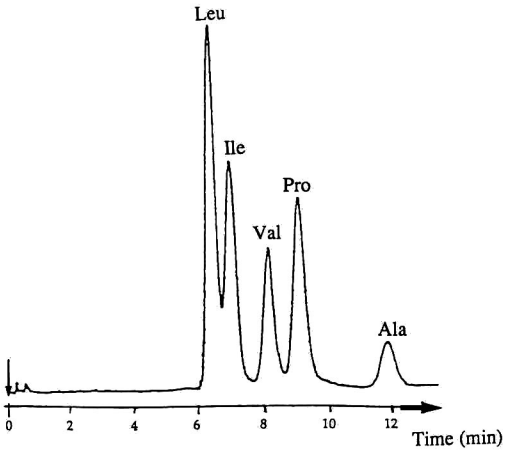

Fig. 9. SubFC of a standard mixture of five amino acids. Conditions as in Fig. 7, except CO_2–modifier (85:15, v/v); modifier, methanol–water–triethylamine–pyridine (87.95:7:0.05:5, v/v); flow-rate, 2.5 ml/min (at 0°C); inlet pressure, 107 bar.

with Janicot *et al.*'s results indicating impregnation of the stationary phase by the amine component of the modifer [15]. Here, both pyridine and triethylamine impregnate the diol-bonded silica. A similar effect is also obtained when ethylene glycol or glycerol [0–0.2% (v/v) in the mobile phase] is added to

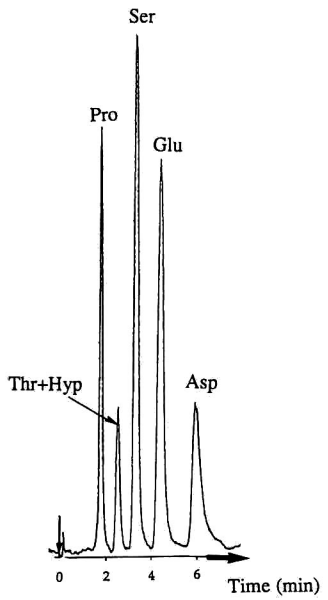

Fig. 10. SubFC of diacidic and hydroxy amino acids. Conditions as in Fig. 9, except CO_2–modifier (80:20, v/v); flow-rate, 5 ml/min (at 0°C); inlet pressure, 230 bar.

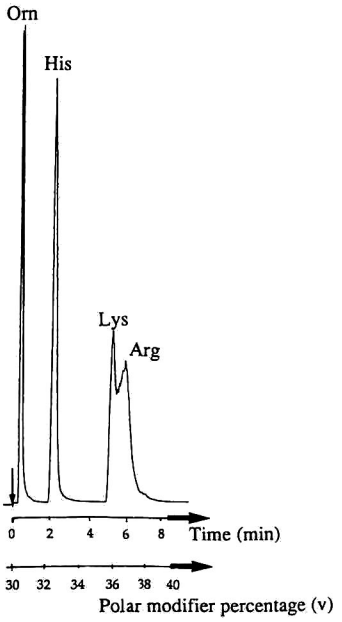

Fig. 11. SubFC of dibasic amino acids. Conditions as in Fig. 10, except modifier gradient from 30 to 40% (v/v) in CO_2.

the modifier instead of pyridine; the efficiency and selectivity are not modified and the efficiency ranges from 1000 to 2200 TP. Modification of the stationary phase is also evident from the curves showing an increase in retention with increasing amount of glycerol added (Fig. 6). Similar results were reported recently by Smith [26].

In conclusion, the following quaternary mixture was chosen as the "modifier": methanol–water–triethylamine–pyridine (87.95:7:0.05:5, v/v). It provides good efficiency [3.5 (at 2.5 ml/min) $< h <$ 10, h = reduced plate height] and acceptable retention of amino acids.

Examples of separations

By varying the content of the modifier in the CO_2, the retention (Fig. 7) and efficiency (Fig. 8) can be adjusted to maximize the column efficiency and to obtain a good separation.

Thus, using a short column and a CO_2–modifier mixture (85:15, v/v), less polar amino acids can be easily resolved (Fig. 9). The elution order and the polarity (Rekker indices) are well correlated.

Increasing the modifier content to 20% permitted the separation of more polar amino acids including

diacids (glutamic and aspartic acid, Fig. 10). Under these conditions threonine and hydroxyproline co-elute without any possibility of resolving them by varying the proportions of the modifier or the CO_2 density.

Elution of dibasic amino acids can even be obtained by packed column SubFC but it requires a gradient elution from 30% to 40%. With this high modifier content, arginine is still very difficult to elute and the peak exhibits strong front tailing (Fig. 11).

Owing to the short length of the column used and the high linear velocity of the mobile phase, the analysis times remain low in spite of the retention of the amino acids (the k' values always exceed 10). Fast re-equilibration of the column was observed in accordance with Steuer *et al.*'s data [27] (10–30 column volumes, *ca.* 5 min). No regeneration test of the columns was undertaken.

CONCLUSIONS

SubFC–ELSD allows separations of amino acids without any derivatization step on diol-bonded silica. Various stationary and mobile phases were investigated to enhance the efficiency, which was the major problem with which we had to deal. It requires impregnation of the stationary phase with basic additives or polyols. Samples containing five or six amino acids have been partially resolved. Using a modifier gradient, resolution of more than ten amino acids could certainly be obtained in less than 10 min.

These results cannot compete with LC coupled with modern derivatization techniques, but they highlight the wide potential of SubFC on packed columns for the separation of medium polarity molecules. These can be separated more easily than amino acids by LC or SubFC using conventional modifiers, the latter being much faster and cheaper owing to the time saved and the lower price of industrial CO_2 in comparison with LC solvents. Hence there is no major reason why routine analyses of medium polarity solutes could not be done by SubFC rather than LC.

ACKNOWLEDGEMENTS

The authors thank Rexim for initiating and financially supporting this work and Gilson France for the loan of the prototype supercritical fluid chromatograph.

REFERENCES

1 M. Roth, *Anal. Chem.*, 43 (1971) 880.
2 M. Roth and A. Hampai, *J. Chromatogr.*, 83 (1973) 353.
3 H. Umagat, P. Kucera and L.-F. Wen, *J. Chromatogr.*, 239 (1982) 463.
4 S. Einarsson, B. Josefsson and S. Lagerkvist, *J. Chromatogr.*, 282 (1983) 609.
5 C. L. Zimmerman, *Anal. Biochem.*, 75 (1976) 77.
6 D. Games, *Lab. Pract.*, February (1987) 45.
7 T. A. Berger, J. F. Deye, M. Ashraf-Khorassani and L. T. Taylor, *J. Chromatogr. Sci.*, 27 (1989) 105.
8 M. Ashraf-Khorassani, M. G. Fessahaie, L. T. Taylor, T. A. Berger and J. F. Deye, *J. High Resolut. Chromatogr. Chromatogr. Commun.*, 11 (1988) 352.
9 J.-L. Veuthey, M. Caude and R. Rosset, *Chromatographia*, 27 (1989) 105.
10 A. Villermet, D. Thiébaut, M. Caude and R. Rosset, *J. Chromatogr.*, 557 (1991) 85.
11 T. A. Berger and J. F. Deye, *J. Chromatogr. Sci.*, 29 (1991) 26.
12 T. A. Berger and J. F. Deye, *J. Chromatogr. Sci.*, 29 (1991) 141.
13 T. A. Berger and J. F. Deye, *J. Chromatogr. Sci.*, 29 (1991) 54.
14 D. Parlier, D. Thiébaut, M. Caude and R. Rosset, *Chromatographia*, 31 (1991) 293.
15 J.-L. Janicot, M. Caude and R. Rosset, *J. Chromatogr.*, 437 (1988) 351.
16 N. Bargmann, L. Siret, M. Caude and A. Tambuté, *Chirality*, in press.
17 C. Lee, J.-P. Porziemsky, M.-C. Aubert and A. Krstulovic, *J. Chromatogr.*, 539 (1991) 55.
18 P. Carraud, D. Thiébaut, M. Caude, R. Rosset, M. Lafosse and M. Dreux, *J. Chromatogr. Sci.*, 25 (1987) 395.
19 D. Nizery, D. Thiébaut, M. Caude, R. Rosset, M. Lafosse and M. Dreux, *J. Chromatogr.*, 467 (1989) 49.
20 M. Dreux and M. Lafosse, *Spectra 2000*, 153 (1990) 24.
21 M. Lafosse, C. Elfakir, L. Morin-Allory and M. Dreux, *J. High Resolut. Chromatogr.*, in press.
22 W. S. Hancock, *Handbook of HPLC for the Separation of Amino Acids, Peptides and Proteins*, Vol. I, CRC Press, Boca Raton, FL, 1984.
23 M. Ashraf-Khorassani, L. T. Taylor and R. A. Henry, *Chromatographia*, 28 (1989) 569.
24 P. J. Schoenmakers, L. G. M. Uunk and H.-G. Janssen, *J. Chromatogr.*, 506 (1990) 563.
25 L. T. Taylor and H.-C. K. Chang, *J. Chromatogr. Sci.*, 28 (1990) 357.
26 R. M. Smith, presented at the *15th International Symposium on Column Liquid Chromatography, Basle, 1991.*
27 W. Steuer, M. Schindler and F. Erni, *J. Chromatogr.*, 454 (1988) 253.

Journal of Chromatography, 605 (1992) 103–107
Elsevier Science Publishers B.V., Amsterdam

CHROM. 24 175

Direct enantiomeric separation of phenylalanine, DOPA and their intermediates by supercritical fluid chromatography

Xianwen Lou, Xueliang Liu, Yufong Sheng and Liangmo Zhou

Dalian Institute of Chemical Physics, Chinese Academy of Sciences, Dalian 116012 (China)

(First received December 6th, 1991; revised manuscript received March 12th, 1992)

ABSTRACT

Phenylalanine (Phe), 3-(3,4-dihydroxyphenyl)alanine (DOPA) and their corresponding intermediates [N-acyl alkyl esters of Phe, DOPA, 3-(3,4-dimethoxylphenyl)alanine, 3-(3-methoxyl-4-hydroxyphenyl)alanine and 3-(3,4-methylenedioxyphenyl)alanine] were enantiomerically separated by supercritical fluid chromatography with carbon dioxide as the mobile phase in a cross-linked polycyanoethyl vinyl siloxane, L-Val-*tert.*-butylamide fused-silica capillary column. The effects of substituents in the benzene ring and the acyl and alkyl groups of the intermediates or derivatives of Phe and DOPA on enantioselectivity were investigated. The optical purities of some intermediates of Phe and DOPA were determined.

INTRODUCTION

Phenylalanine (Phe) is an important amino acid and can be used as a nutriment and food additive [1–3]. Many of its substituted optically active isomers are of great importance in pharmacology; L-DOPA, for example, can be used to treat Parkinson's disease [4]. These optically active compounds can be obtained by asymmetric hydrogenation [5] and then normal hydrolysis [6], as shown below.

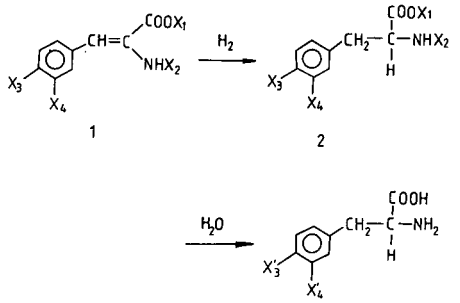

1 2

Correspondence to: Dr. L. Zhou, Dalian Institute of Chemical Physics, Chinese Academy of Sciences, Dalian 116012, China.

The key step in the synthesis is the asymmetric hydrogenation of a prochiral alkene (**1**) to a specific optical isomer of Phe or a substituted Phe derivative (**2**) [7]. The selectivity of the key step can be determined by the enantiomeric excess of intermediate **2** [8]. The enantiomeric separation of compound **2** is of great significance in pharmacology, asymmetric synthesis and biochemistry. In intermediate, **2**, X_1 is usually a methyl or ethyl group and x_2 an acetyl (Ac) or benzoyl (Bz) group [9,10]. Most of the intermediates are of low volatility and are not suitable for separation by gas chromatography (GC). Supercritical fluid chromatography (SFC) with chiral stationary phases (CSPs) can be used to separate enantiomers of low volatility under mild conditions and with a higher enantioselectivity (α value) than GC [11,12].

The use of several CSPs in SFC with carbon dioxide as the mobile phase was reviewed by Macaudiere *et al.* [13]. Immobilized Chirasil-Dex [14] and Chirasil-Val [15] have been reported for the separation of enantiomers by SFC.

In this work, the SFC separation of Phe, DOPA

and their corresponding intermediates with cross-linked polycyanoethyl vinyl siloxane-L-Val-*tert.*-butylamide was investigated.

EXPERIMENTAL

Chemicals and materials

Phe was obtained from Sigma, and DOPA and the N-acyl alkyl esters of (substituted) Phe isomers were kindly supplied by Dr. X. Liu. Blank fused-silica capillary tubes were from Yongnian Optical Fibre Manufacturer.

Chromatographic conditions

The cross-linked polycyanoethyl vinyl siloxane-L-V-*tert.*-butylamide fused-silica capillary column (10 m × 70 μm I.D.) was prepared as described previously [16]. The SFC experiments were carried out with a laboratory-made SFC chromatograph equipped with a flame ionization detector [17]. Phe and DOPA were derivatized as N-trifluoroacetyl (TFAc) isopropyl ester according to the method of McKenzie and Tenaschuk [18].

RESULTS AND DISCUSSION

In SFC with carbon dioxide as the mobile phase, the density of the mobile phase has no influence on the separation factors (α) of the solutes [11]. The capacity factors (k') and separation factors (α) of *N*-TFAc-Phe isopropyl ester and N-Ac-Phe isopropyl ester at different pressures are given in Table I.

The classical method of derivatization of Phe for separation by GC and SFC is their conversion into N-perfluoroacyl alkyl esters [19]. Replacing TFAc by pentafluoropropionyl or heptafluorobutyryl has little effect on the α and k' values in GC [20]. Other acylation reagents have not yet been fully investigated.

The α and k' values of the solutes tested in SFC are given in Table II.

For Phe, the α value of *N*-TFAc-Phe isopropyl ester is much greater than N-Bz-Phe isopropyl ester but much lower than N-Ac-Phe isopropyl ester; that is, the α values of Phe are greatly changed by replacing TFAc with Ac or Bz. The k' value of N-TFAc-Phe isopropyl ester increased significantly

TABLE I

α AND k' VALUES OF N-TFAc-Phe ISOPROPYL ESTER AND N-Ac-Phe ISOPROPYL ESTER AT DIFFERENT PRESSURES IN SFC (60°C)

Solute	13.0 MPa		14.0 MPa		15.0 MPa	
	α	k'	α	k'	α	k'
N-TFAc-Phe isopropyl ester	1.17	0.48	1.17	0.11	–	–
N-Ac-Phe isopropyl ester	–	–	1.21	0.40	1.22	0.13

TABLE II

α AND k' VALUES OF N-ACYL-(SUBSTITUTED) Phe ALKYL ESTERS IN SFC (65°C)

Solute	α	k'	Pressure (MPa)
N-TFAc-Phe isopropyl ester	1.16	0.23	14.0
N-Ac-Phe isopropyl ester	1.19	0.56	14.0
N-Ac-Phe methyl ester	1.16	0.67	14.0
N-Bz-Phe methyl ester	1.09	0.88	16.0
N-Ac-3-(3,4-dimethoxyphenyl)alanine ethyl ester	1.17	0.31	16.0
N-Bz-3-(3,4-dimethoxyphenyl)alanine isopropyl ester	1.14	0.77	16.0
N-Bz-3-(3,4-dimethoxyphenyl)alanine methyl ester	1.11	0.89	16.0
N-Bz-3-(3,4-methylenedioxyphenyl)alanine methyl ester	1.09	0.96	16.0
N-Bz-3-(3-methoxy-4-hydroxyphenyl)alanine methyl ester	1.12	1.17	16.0
N-TFAc-DOPA isopropyl ester	1.16	0.32	14.0

TABLE III

ENANTIOMERIC EXCESS OF SOME SYNTHESIZED N-ACYL-(SUBSTITUTED) Phe ALKYL ESTERS DETERMINED BY SFC

	PNNP[a] (%)	PMEO[b] (%)
N-Ac-Phe-methyl ester	–	78
N-Ac-3-(3,4-dimethoxyphenyl)alanine ethyl ester	71	75
N-Bz-Phe-methyl ester	55	–
N-Bz-3-(3,4-dimethoxyphenyl)alanine methyl ester	–	92
N-Bz-3-(3,4-methylenedioxyphenyl)alanine methyl ester	67	–
N-Bz-3-(3-methoxy-4-hydroxyphenyl)alanine methyl ester	71	–

[a] Enantiomeric excess of D-enantiomers with PNNP [N,N′-bis(*S*-1-phenylethyl)-N,N′-bis-(diphenylphosphino)ethylenediamine] as the chiral ligand of rhodium catalyst.

[b] Enantiomeric excess of L-enantiomers with PMEO [N,N′-bis(*R*-1-(*p*-methoxyphenyl)ethyl-N,N′-bis(diphenylphosphino)ethylenediamine] as the chiral ligand of rhodium catalyst.

when N-TFAc was replaced with N-Ac and increased further when replaced with N-Bz.

The α values of isopropyl esters of N-acyl-(substituted)-Phe are greater than their corresponding methyl esters as reported in separation by GC [21]. The retention behaviour of methyl esters of N-acyl-(substituted)-Phe and their corresponding isopropyl esters in GC and SFC was also compared. In GC, methyl esters usually elute before their corresponding isopropyl esters [21], whereas in SFC the elution order of the tested samples is changed, *i.e.* methyl esters elute after their corresponding isopropyl, esters (Table III and Fig. 1). According to Matire and Boehm [22], the solute capacity factor (k value) in SFC can be represented by

$$\ln k = \ln k^0 + F(T_R, \rho_R) \quad (1)$$

where T_R and ρ_R are the reduced temperature and reduced density of the mobile phase and K^0 is the capacity factor corresponding to ideal GC. The change of elution order of the tested methyl and isopropyl esters of N-acyl-(substituted)-Phe is probably due to their difference in solubility in carbon dioxide. When the benzene ring of Phe is substituted with 3,4-dimethoxyl or 3-methoxy-4-hydroxy or 3,4-methylenedioxy, the α values were slightly increased.

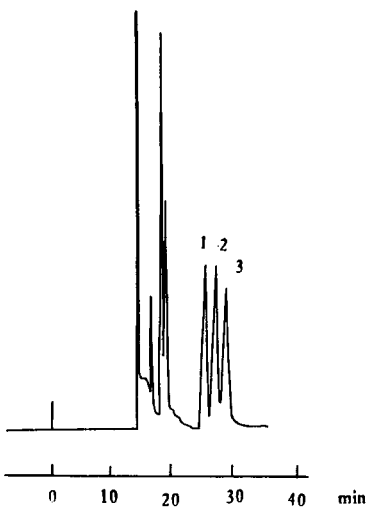

Fig. 1. Chromatogram of D,L-N-Ac-Phe isopropyl ester and L-excess D,L-N-Ac-Phe methyl ester by SFC. Column, cross-linked polycyanoethyl vinyl siloxane-L-Val-*tert.*-butylamide (10 m × 70 μm); temperature, 60°C; mobile phase, carbon dioxide, 13.5 MPa; detector, flame ionization. Peaks: 1 = D-N-Ac-Phe isopropyl ester; 2 = L-N-Ac-Phe isopropyl ester + D-N-Ac-Phe methyl ester; 3 = L-N-Ac-Phe methyl ester.

From these results, the following conclusions can be made. (1) Both the acyl and alkyl groups of N-acyl-(substituted)-Phe isopropyl esters have considerable effects on the α and k' values. Replacing TFAc with the Ac or Bz group, the changes in α values are large; (2) The substituents in the benzene ring of Phe have some effect on the α values. The substituted isomers tested do not have α values lower than their corresponding N-acyl-Phe alkyl esters.

The enantiomeric excesses of some synthesized N-acyl-(substituted)-Phe alkyl esters determined by SFC are given in Table III.

Fig. 2 is a chromatogram of the enantiomeric

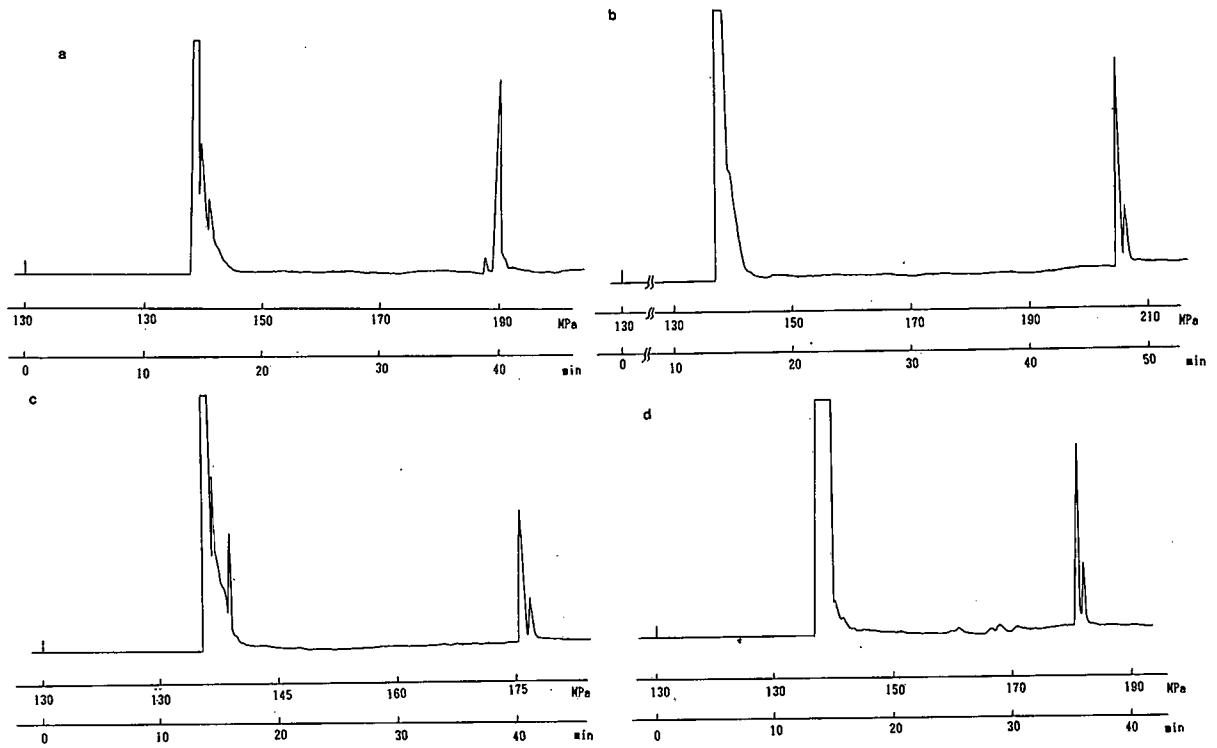

Fig. 2. Enantiomeric separation of some intermediates of Phe and DOPA by SFC. Chromatographic conditions as in Fig. 1. (a) N-Bz-3-(3,4-dimethoxyphenyl)alanine methyl ester; (b) N-Bz-3-(3-methyoxy-4-hydroxyphenyl)alanine methyl ester; (c) N-Bz-3-(3,4-methylenedioxyphenyl)alanine methyl ester; and (d) N-Bz-Phe methyl ester. D-enantiomers eluted first.

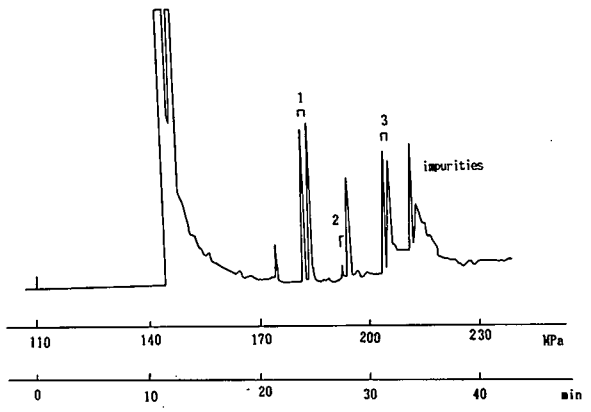

Fig. 3. Chromatogram of some N-acyl-(substituted)-Phe alkyl ester enantiomers by SFC. Chromatographic conditions as in Fig. 1 with mobile phase carbon dioxide (11.0 MPa) increased at 0.3 MPa/min. Peaks: 1 = D,L-N-TFAc-Phe isopropyl ester; 2 = D,L-N-Ac-Phe methyl ester; 3 = D,L-N-Ac-3-(3,4-dimethoxyphenyl)alanine methyl ester. D-enantiomers eluted first.

separation of some intermediates by SFC with pressure programming.

The enantiomeric separation of some N-acyl-(substituted)-Phe alkyl esters with pressure programming by SFC is shown in Fig. 3.

CONCLUSIONS

The acyl groups, alkyl groups and substituents in the benzene ring of N-acyl-(substituted) Phe alkyl esters have considerable effects on both α and k' values. When TFAc is replaced with Ac or Bz, the α values of the solutes tested were greatly changed.

ACKNOWLEDGEMENTS

We thank Professors Daoqian Zhu, Qinghai Wang and Yafong Guang for technical help and valuable discussions. This work was supported by the National Natural Science Foundation of China

and Youth Science Foundation of Dalian Institute of Chemical Physics.

REFERENCES

1 R. Noyori, *Science*, 248 (1990) 1194.
2 M. Fiorini and G. M. Giongo, *J. Mol. Catal.*, 7 (1980) 411.
3 H. B. Kagan, *Bull. Chim. Soc. Fr.*, (1988) 846.
4 W. S. Knowles, *Acc. Chem. Res.*, 16 (1983) 106.
5 W. S. Knowles, *J. Chem. Educ.*, 63 (1986) 222.
6 W. S. Knowles, *J. Chem. Soc., Chem. Commun.*, (1968) 1146.
7 G. W. Parshall and W. A. Nugent, *Chemtech*, March (1988) 184.
8 A. Nakamura, A. Konishi, Y. Tatsuno and S. Otsuka, *J. Am. Chem. Soc.*, 100 (1978) 3443.
9 R. M. Herbst and D. Shemin, *Org. Synth., Coll.*, 2 (1943) 1.
10 J. S. Buck and W. S. Ide, *Org. Synth., Coll.*, 2 (1943) 55.
11 X. Lou, Y. Sheng and L. Zhou, *J. Chromatogr.*, 514 (1990) 253.
12 W. Röder, F.-J. Ruffing, G. Schomburg and W. H. Pirkle, *J. High Resolut. Chromatogr. Chromatogr. Commun.*, 10 (1987) 665.
13 P. Macaudiere, M. Caude, R. Rosset and A. Tambute, *J. Chromatogr. Sci.*, 27 (1989) 383.
14 V. Schuring, Z. Juvancz, G. J. Nicholson and D. Schmalzing, *J. High Resolut. Chromatogr. Chromatogr. Commun.*, 14 (1991) 58.
15 G. Lai, G. Nicholson, U. Muhleck and E. Bayer, *J. Chromatogr.*, 540 (1991) 217.
16 X. Lou, Y. Liu and L. Zhou, *J. Chromatogr.*, 552 (1991) 153.
17 L. Zhou, Q. Wang and H. Jiang, *Fenxi Huaxue*, 18 (1990) 1149.
18 S. L. McKenzie and D. Tenaschuk, *J. Chromatogr.*, 173 (1979) 53.
19 V. Schurig, *Angew. Chem. Int. Ed. Engl.*, 23 (1984) 747.
20 R. Liardon and S. Ledermann, in W. Bertsch, W. G. Jennings and R. E. Kaiser (Editors), *Recent Advances in Capillary Gas Chromatography*, Hüthig, Heidelberg, 1982, p. 429.
21 I. Abe, T. Kohno and S. Musha, *Chromatographia*, 11 (1978) 393.
22 D. E. Matire and R. E. Boehm, *J. Phys. Chem.*, 91 (1987) 2433.

Journal of Chromatography, 605 (1992) 109–113
Elsevier Science Publishers B.V., Amsterdam

CHROM. 24 246

In situ extraction and derivatization of pentachlorophenol and related compounds from soils using a supercritical fluid extraction system

Hing-Biu Lee and Thomas E. Peart

Research and Applications Branch, National Water Research Institute, Environment Canada, P.O. Box 5050, Burlington, Ontario L7R 4A6 (Canada)

Robert L. Hong-You

Wastewater Technology Centre Laboratory, P.O. Box 5050, Burlington, Ontario L7R 4A6 (Canada)

(First received January 28th, 1992; revised manuscript received April 7th, 1992)

ABSTRACT

An *in situ* supercritical fluid extraction and derivatization procedure for the determination of pentachlorophenol (PCP) and related compounds from soil samples is described. Phenols are extracted from soil and acetylated *in situ* with supercritical carbon dioxide in the presence of triethylamine and acetic anhydride at a temperature of 80°C. Quantitative recovery of di-, tri-, tetra- and penta-chlorophenols was obtained by a 10-min extraction with carbon dioxide at 37.2 MPa (365 bar, 0.8 g/ml density) from soil samples fortified to 0.5 and 5 μg/g levels. In a comparison study, the supercritical fluid extracton and the steam distillation methods both produced very similar results for pentachlorophenol and other chlorophenols in a reference sample. When this method is applied to contaminated soils samples collected in a wood treatment plant, results for chlorophenols in a sample can be obtained in approximately 90 min.

INTRODUCTION

Abnormal discoloration of wood, commonly referred to as sapstain, is caused by fungi which derive nourishment from wood cells. Other than by kiln-drying, sapstain and mold on the surface of lumber can be prevented by treatment of wood with anti-sapstain chemicals. Due to their effectiveness, pentachlorophenol (PCP) and its derivatives have been the most widely used anti-sapstain chemicals in Western Canada over the last 50 years. Recently, the application of PCP by the sawmilling and forestry industries has become an environmental concern since PCP is toxic to fish and mammals and technical grades of PCP are known to contain the highly toxic chlorinated dibenzo-*p*-dioxins and furans. In response to these concerns, the use of PCP as a wood preservative in British Columbia has mostly been phased out. However, this chemical is still being used in wood-treatment plants in other parts of Canada for special applications.

PCP in soils or sediments can be traditionally determined by solvent extraction techniques (*e.g.* Soxhlet) [1] or by a steam distillation approach [2,3]. In both cases, the extraction process takes a few hours or longer. In the case of solvent extraction, a large amount of solvent must be used and a great deal of coextractives are produced. The latter often create a problem in the subsequent cleanup and chromatographic analysis. If the extracted PCP is to be analyzed by gas chromatography in the form of

Correspondence to: Dr. H.-B. Lee, Research and Applications Branch, National Water Research Institute, Environment Canada, P.O. Box 5050, Burlington, Ontario L7R 4A6, Canada.

0021-9673/92/$05.00

an acetyl, methyl or pentafluorobenzyl derivative, extra time is required for the additional derivatization step.

Supercritical fluid extraction (SFE) has been proven to be a more efficient alternative than existing solvent extraction techniques for most solid samples. It has been successfully applied to the determination of polychlorinated biphenyls [4], chlorobenzenes [5], polycyclic aromatic hydrocarbons [4,6], dioxins [7], resin and fatty acids [8] in sediment and other matrices and the list is growing rapidly. Because of the non-polar nature of supercritical carbon dioxide, extraction recovery of polar parameters is low unless a modifier such as methanol is added to the system. SFE of free pentachlorophenol from a soil sample has also been reported [9]. More recently, the possibility of combined SFE and derivatization of polar compounds has been explored [10–13]. This latter approach further reduces sample preparation time and at the same time enhances the extractability of polar compounds since derivatives are in general less polar than their parent compounds. Our work on resin and fatty acids [8] demonstrated that this one-step technique can be applied to the rapid screening of the acids in sediment samples. In this report, we shall describe a rapid and quantitative method using an *in situ* extraction/derivatization technique for the determination of PCP and other chlorophenols in soils contaminated by the wood-preserving chemical.

EXPERIMENTAL

All chlorophenol standards were supplied by Supelco. Acetic anhydride and triethylamine were purchased from Aldrich. The anhydride was triple-distilled and the fraction of b.p. 138–140°C was collected and used. Distilled-in-glass solvents were supplied by Burdick & Jackson. Carbon dioxide (SFE grade) with a helium head pressure of 10.5 MPa was obtained from Scott Specialty Gases and Linde.

Stock solutions of individual chlorophenols at 1000 μg/ml were prepared in acetone. Mixtures of the 14 chlorophenols (Table I) at 10 and 50 μg/ml were prepared for the spiking of soil samples and the preparation of calibration standard. A mixture of 2,4-dibromophenol and 2,4,6-tribromophenol at 10 μg/ml, also in acetone, was prepared as a surrogate standard.

TABLE I

PRECISION AND ACCURACY OF THE *IN SITU* SFE/DERIVATIZATION PROCEDURE FOR THE DETERMINATION OF CHLOROPHENOLS IN SPIKED SAMPLES

Mean and standard deviation of six replicate determinations.

Chlorophenol	Recovery (%)	
	0.5 μg/g	5.0 μg/g
2,6-Dichlorophenol	97 ± 7	93 ± 5
2,4-Dichlorophenol	92 ± 7	93 ± 6
3,5-Dichlorophenol	96 ± 8	97 ± 6
2,3-Dichlorophenol	87 ± 6	89 ± 5
3,4-Dichlorophenol	98 ± 6	89 ± 6
2,4,6-Trichlorophenol	93 ± 7	102 ± 5
2,3,6-Trichlorophenol	91 ± 6	97 ± 4
2,3,5-Trichlorophenol	101 ± 4	98 ± 4
2,4,5-Trichlorophenol	101 ± 6	101 ± 5
3,4,5-Trichlorophenol	94 ± 3	90 ± 4
2,3,5,6-Tetrachlorophenol	90 ± 6	95 ± 5
2,3,4,6-Tetrachlorophenol	101 ± 7	103 ± 5
2,3,4,5-Tetrachlorophenol	104 ± 4	93 ± 4
Pentachlorophenol	96 ± 6	102 ± 5

For consistency, all samples were prepared in the following manner prior to extraction. Two layers of Whatman GF/C filters cut to the diameter of the extraction thimble were placed on top of the bottom thimble cap to minimize contamination and plugging of the frit. The 7-ml thimble was then filled with 200 mg of Celite followed by 1 g of sample, which was previously mixed and ground. A 50-μl volume of the above surrogate solution and 30 μl of triethylamine were spiked to the soil sample. If the soil was completely dry, 50 μl of water (equivalent to a moisture content of 5%, w/w) was also added directly to the sample. The thimble was shaken on a vortex mixer for 15 s after addition of each liquid. The sample was topped by another 200 mg of Celite and 30 μl of acetic anhydride were added before it was subject to supercritical carbon dioxide extraction. In the case of recovery experiments, samples were prepared as described above except that the surrogate solute also contained a known amount of the 14 chlorophenols.

All extractions were performed by a Hewlett-Packard 7680A SFE module using supercritical carbon dioxide of a density of 0.8 g/ml (37.2 MPa) and a flow-rate of 2.0 ml/min. Static and dynamic

extractions of 5 min each were carried out and the extraction chamber temperature was maintained at 80°C during this time. An octadecylsilane (ODS) trap, used for the collection of sample extracts, was kept at 15 and 45°C, during the extraction and rinsing stages, respectively. SFE extracts from the trap were eluted by hexane in two 1.2-ml fractions.

The derivatized extract was partitioned with 3 ml of 1% potassium carbonate solution by vortexing in a centrifuge tube for 1 min. This step removed the acetic acid formed in the acetylation reaction and the excess acetic anhydride reagent: both of them could lead to chromatographic problems if the uncleaned extracts were analyzed. The hexane extract was then transferred to a short (3 cm) anhydrous sodium sulfate column and a 5 cm 5% deactivated silica gel column prepared in tandem using disposable Pasteur pipettes for further cleanup. The columns were first eluted with 5 ml of hexane and this fraction was discarded. The acetyl derivatives of chlorophenols were removed from the column by elution with 10 ml of light petroleum (b.p. 30–60°C)–dichloromethane (1:1). This was followed by solvent exchange into 5 ml or other suitable volume of iso-octane.

For comparison of SFE results, steam distillation of soil samples was also performed. A 1-g amount of soil was stirred with 50 ml of a 1% solution of potassium carbonate for 10 min in a 500-ml round-bottom flask. A 1-ml volume of acetic anhydride was added and stirred for another 10 min. The mixture was steam distilled for 1 h into 3 ml of hexane in the condenser according to the method developed by Veith and Kiwus [2]. The acetates were then cleaned up as described anbove except that the silica gel column cleanup was omitted. A commercial standard reference soil sample (SRS 103–100) supplied by Fisher Scientific was used in the comparison study.

Chromatographic analysis was carried out with a Hewlett-Packard 5890 Series II gas chromatograph equipped with an electron-capture detector and a split-splitless injection port. Splitless injection (1 μl) was made by a HP 7673 autosampler onto a 25 m × 0.2 mm I.D. HP-5 fused-silica column. The initial oven temperature was 70°C (0.75 min hold) and it was programmed to 120°C at 30°C/min and then to 200°C at 2°C/min. Splitless time was 0.75 min. Hydrogen was the carrier gas and the column head pressure was 105 kPa. Instrument control and data acquisition were achieved by a personal computer running the HP 3365 ChemStation software in the Microsoft Windows environment.

To calibrate the instrument, a concentrated mixture of the acetyl derivatives of chlorophenols was prepared by an aqueous acetylation of a known amount of chlorophenols according to established procedures [1,14]. Quantitation of chlorophenols in soil samples was performed by an external standard method, using appropriate dilutions of the above mixture with iso-octane.

RESULTS AND DISCUSSION

In a recent report, free PCP was extracted from soil in 60 min using supercritical carbon dioxide at 31.0 MPa and 70°C [9]. In this case, 10% (w/w) of water was added to the sample as a modifier. Quantitative recovery of PCP from soil was obtained in our laboratory by a 15-min extraction with carbon dioxide at 37.2 MPa and 80°C, in the presence of the same amount of modifier. Also, we found that the same approach applied to the extraction of the di-, tri- and tetrachlorophenols as well although the recovery of the less chlorinated phenols were low (60 to 80%) under such conditions. Since chlorophenols are routinely analyzed by electron-capture detection in the form of acetyl derivatives in our laboratories, the above SFE approach would require an off-line derivatization step. The disadvantage of having an extra step in the procedure can be eliminated if the extraction and derivatization steps can be combined into one.

Chlorophenols in water samples can readily be converted into stable acetyl derivative by an *in situ* acetylation using acetic anhydride and a base such as a carbonate or bicarbonate [14]. Acetyl derivatives of chlorophenols with two or more chlorine atoms are sensitively detected by an electron-capture detector and are more amenable to column cleanup than the free phenols. For these reasons as well as the fact that the acetyl derivatives are easily formed and stable under the SFE conditions, they are the most appropriate choice for this work.

Similar to the aqueous reaction, derivatization of chlorophenols under SFE conditions also required a base. Although the *in situ* acetylation of chlorophenols was working with an aqueous solution of potassium carbonate, quantitative derivatization of

TABLE II

RESULTS OF PCP AND OTHER CHLOROPHENOLS (μg/g) IN A REFERENCE SOIL SRS 103-100 by SFE AND STEAM DISTILLATION

N.D. = No data.

Chlorophenol	Steam distillation (this work) (n = 3)	SFE (this work) (n = 6)	SFE (ref. 9) (n = 3)
2,3,5-Tri-	0.40 ± 0.01	0.36 ± 0.01	N.D.
2,3,5,6-Tetra-	14.4 ± 0.4	13.9 ± 0.3	N.D.
2,3,4,6-Tetra-	20.6 ± 0.4	20.2 ± 0.3	N.D.
2,3,4,5-Tetra-	1.9 ± 0.1	1.8 ± 0.1	N.D.
PCP	1499 ± 67	1483 ± 93	1361

all phenols could only be achieved in the presence of triethylamine. Presumably, the inorganic base is less effective than the organic base since the former is less soluble in supercritical carbon dioxide and thus less available for the reaction. In order to have the highest recovery of the acetyl derivatives, approximately equal volumes of acetic anhydride and triethylamine should be used. A large excess (250 μl or more) of the two reagents was found to be detrimental to the recovery of the derivatives. A chamber temperature of 80°C was chosen since, at this temperature, a 10-min extraction was enough for the complete recovery of the chlorophenols in soil. On the contrary, only 60 and 90% of the PCP could be recovered in 10 min if the chamber temperature was set at 40 and 60°C, respectively.

In order to evaluate the efficiency of the *in situ* SFE/derivatization procedure, the recovery of chlorophenols from clean soil samples fortified at different levels was determined. Basically, recoveries of 90% or above were obtained in the 0.5 and 5 μg/g range for PCP and other chlorophenols (Table I). The results suggested that this method is also applicable to the quantitative determination of di-, tri- and tetrachlorophenols if they are present in the soil samples.

The ruggedness of the SFE method was again tested with a standard reference soil sample (SRS 103-100) naturally contaminated by PCP. In a side-by-side comparison, our results for PCP and other chlorophenols generated by the *in situ* SFE/derivatization procedure for this sample are nearly identical to those obtained by the steam distillation procedure, indicating completeness of extraction and derivatization (Table II). Both techniques also showed similar degree of precision as indicated by

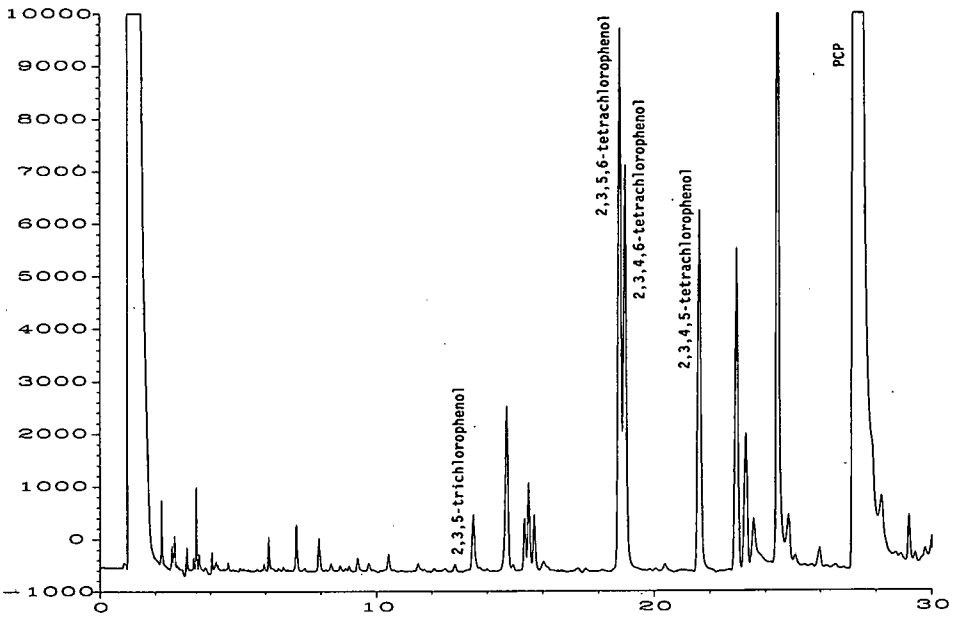

Fig. 1. Gas chromatography–electron-capture detection of the acetyl derivatives of chlorophenols in a contaminated soil sample prepared by *in situ* SFE and derivatization.

the standard deviation in replicate determinations. It should also be noted that our PCP result for this reference sample (1483 μg/g) is more comparable to that obtained by the non-derivatized SFE approach (1361 μg/g) [9] than the rather ambiguous certified value (965 ± 374 μg/g) furnished by the supplier.

This new procedure is being evaluated for the determination of chlorophenols from contaminated soil samples collected in an Ontario site for the preservation of railroad ties and hydro poles. The texture of the samples varied from light color sandy type to dark color loamy soil. Other than PCP, which contributed 90% (w/w) or more of the total chlorophenols in nearly all cases, tetrachlorophenols and a few trichlorophenols were also detected in the samples analyzed. The levels of chlorophenols in these soil samples varied from *ca.* 100 ng/g for some trichlorophenols to over 1000 μg/g for PCP, indicating the method is applicable to a wide range of concentrations. Again, the SFE results were in good agreement with the steam distillation results in the cases where both techniques were used for cross checking. If the surrogates (bromophenols) were less than 75% recovered, the extraction was repeated. Fig. 1 is an ECD chromatogram of a contaminated soil sample after SFE/derivatization and cleanup. The levels of 2,3,5-trichlorophenol, 2,3,5,6-, 2,3,4,6- and 2,3,4,5-tetrachlorophenol and PCP are 0.12, 0.98, 0.71, 0.55 and 57.8 μg/g, respectively, in the sample. The entire analytical sequence (sample preparation, extraction, derivatization, cleanup, solvent replacement, gas chromatographic analysis and report generation) required approximately 90 min.

CONCLUSIONS

The method described here is suitable for the rapid yet quantitative and specific determination of chlorophenols in soil and sediment samples in the ng/g to μg/g range. This procedure is more efficient and has a wider application than the one reported for the SFE of free PCP from soil. The present SFE method is proven to be a reliable alternative to the established steam distillation procedure since they both produce similar results for real-life samples. The simple analytical procedure results in an extremely short sample turn around time and thus it is most valuable under an environmental emergency situation. It also stands out in environmental friendliness since it consumes much less solvents and chemicals than all existing methodologies involving the derivatization step.

ACKNOWLEDGEMENT

We are grateful to Hewlett-Packard (Canada) Ltd. for the generous loan of the HP 7680A SFE module.

REFERENCES

1 H. B. Lee, Y. D. Stokker and A. S. Y. Chau, *J. Assoc. Off. Anal. Chem.*, 70 (1987) 1003.
2 G. D. Veith and L. M. Kiwus, *Bull. Environ. Contam. Toxicol.*, 17 (1977) 631.
3 D. W. Kuehl and R. C. Dougherty, *Environ. Sci. Technol.*, 14 (1980) 447.
4 M. M. Schantz and S. N. Chesler, *J. Chromatogr.*, 363 (1986) 397.
5 H. B. Lee, R. L. Hong-You and T. E. Peart, unpublished results.
6 S. B. Hawthorne and D. J. Miller, *Anal. Chem.*, 59 (1987) 1705.
7 N. Alexandrou and J. Pawliszyn, *Anal. Chem.*, 61 (1989) 2770.
8 H. B. Lee and T. E. Peart, *J. Chromatogr.*, 594 (1992) 309.
9 W. Beckert, V. Lopez-Avioa and S. Cram, *Am. Environ. Lab.*, Oct. (1991) 21.
10 D. J. Miller, S. B. Hawthorne and J. J. Langenfeld, *International Symposium on Supercritical Fluid Chromatography and Extraction, Park City, UT, January 1991,* Abstracts.
11 D. C. White, D. E. Nivens, D. Ringelberg, D. Hedrick and S. B. Hawthorne, *International Symposium on Supercritical Fluid Chromatography and Extraction, Park City, UT, January 1991,* Abstracts.
12 J. W. Hills and H. H. Hill, Jr., *International Symposium on Supercritical Fluid Chromatography and Extraction, Park City, UT, January 1991,* Abstracts.
13 J. M. Levy, A. C. Rosselli, D. S. Boyer and K. Cross, *International Symposium on Supercritical Fluid Chromatography and Extraction, Park City, UT, January 1991,* Abstracts.
14 R. T. Coutts, E. E. Hargesheimer and F. M. Pasutto, *J. Chromatogr.*, 179 (1979) 291.

Journal of Chromatography, 605 (1992) 115–123
Elsevier Science Publishers B.V., Amsterdam

CHROM. 24 217

Capillary zone electrophoresis of proteins with a dynamic surfactant coating

Influence of a voltage gradient on the separation efficiency

W. G. H. M. Muijselaar, C. H. M. M. de Bruijn and F. M. Everaerts

Laboratory of Instrumental Analysis, Eindhoven University of Technology, P.O. Box 513, 5600 MB Eindhoven (Netherlands)

(First received February 4th, 1992; revised manuscript received March 30th, 1992)

ABSTRACT

In capillary zone electrophoresis of proteins, the adsorption of the proteins on the capillary wall is a considerable problem that seriously impairs the separation efficiency. The use of a dynamic surfactant coating is a possible way to diminish this adsorption. Highly efficient separations were achieved with a cationic fluorinated buffer additive as a dynamic surfactant coating in untreated fused-silica capillaries at neutral pH. The influence of a voltage gradient on the separation efficiency is discussed and a simple relationship is presented to calculate effective mobilities under voltage gradient conditions.

INTRODUCTION

Capillary zone electrophoresis (CZE) has become a widely used separation technique, especially for mixtures of biological compounds such as peptides, proteins and DNA fragments [1,2]. One of the main problems occurring with protein separations is the adsorption of these molecules on the surface of fused-silica capillaries. This phenomenon causes serious peak broadening, resulting in much lower separation efficiencies than theoretically predicted. To eliminate this protein adsorption, various methods have been described: (1) performing the separation under alkaline conditions [3,4]; if the buffer pH is higher than the isoelectric points (p*I*s) of the proteins, both capillary surface and proteins will have a net negative charge and adsorption is diminished by coulombic repulsion; (2) adding salts or zwitterions to the buffer, resulting in a competition between these buffer additives and proteins for the negative silanol groups on the silica surface [5,6]; (3) coating the capillary surface with a neutral hydrophilic compound by a chemical modification in order to shield the silanol groups [7–13]; (4) adding a surfactant to the buffer which forms a dynamic coating on the capillary surface, thus diminishing protein adsorption [14]. This last method has several advantages above the other methods. The buffer pH remains a freely adjustable parameter over a wide range to optimize selectivity and to avoid denaturation of the proteins. A buffer solution with a low ionic strength can be used to minimize Joule heating. No surface pretreatment is required so that the separation can be performed in untreated fused-silica capillaries.

Recently, Emmer *et al.* [14] reported a cationic fluorinated buffer additive as a dynamic surfactant coating. We used this approach for the separation of several proteins. The influence of the buffer pH on both the electroosmotic flow (EOF) and the sep-

Correspondence to: W. G. H. M. Muijselaar, Laboratory of Instrumental Analysis, Eindhoven University of Technology, P.O. Box 513, 5600 MB Eindhoven, Netherlands.

0021-9673/92/$05.00

aration efficiency were studied. Further, the influence of a voltage gradient on the separation efficiency was examined.

THEORETICAL

In CZE, the velocity of a migrating component is given by

$$v = m_{app}E = m_{app}V/l_c \quad (1)$$

where v is the velocity of the component (cm/s), m_{app} the apparent mobility of the component ($cm^2/V \cdot s$), E the electrical field strength (V/cm), V the applied potential (V) and l_c the total length of the capillary (cm). Further,

$$l_d = vt \quad (2)$$

where l_d is the length from the injection to detection point (cm) and t is the migration time measured (s). From eqns. 1 and 2, the apparent mobility of a component can be calculated according to

$$m_{app} = \frac{l_c l_d}{tV} \quad (3)$$

The effective mobility, m_{eff}, of a component is given by

$$m_{eff} = m_{app} - m_{EOF} \quad (4)$$

where m_{EOF} is the "mobility" of the EOF, which can be calculated with the migration time of a neutral compound.

As reported by McCormick [7], the separation efficiency can be increased by using a programmed separation voltage, *i.e.*, the separation voltage is not applied immediately but is reached linearly in a certain programme time. In this instance, however, eqns. 2 and 3 cannot be used, as the separation voltage is not maintained constant during one experiment. In fact, longer migration times will be observed if the programme time is increased. The effective mobility of a component, however, will be constant with a given electrolyte system and can be used for identification [15]. It can be calculated from the measured migration times.

If the separation voltage is a function of time, eqn. 2 should be written as

$$l_d = \int_0^t v(t)\mathrm{d}t \quad (5)$$

If the final separation voltage, V_p, is reached linearly in a programme time t_p, as shown in Fig. 1, combination of eqns. 1 and 5 leads to

$$l_d = \int_0^{t_p} m_{app} \cdot \frac{\alpha t + \beta}{l_c} \cdot \mathrm{d}t + \int_{t_p}^{t} m_{app} \cdot \frac{V_p}{l_c} \cdot \mathrm{d}t \quad (6)$$

where α and β are the slope of the voltage gradient and the initial voltage, respectively. The apparent mobility of a component now can be calculated according to

$$m_{app} = \frac{l_c l_d}{\frac{\alpha}{2} \cdot t_p^2 + \beta t_p + V_p(t - t_p)} \quad (7)$$

Note that for $t_p = 0$ this equation reduces to eqn. 3.

Combination of eqns. 3 and 7, with $\beta = 0$, leads to an expression for τ, the ratio of the migration time with and without a programmed separation voltage. The dimensionless parameter τ is a linear function of the programme time t_p:

$$\tau = \frac{t(t_p \neq 0)}{t(t_p = 0)} = 1 + \frac{1}{2} \cdot \frac{m_{app}V_p}{l_c l_d} \cdot t_p \quad (8)$$

To demonstrate the influence of a voltage gradient on the migration time, τ is shown in Fig. 2 as a function of t_p for different apparent mobilities.

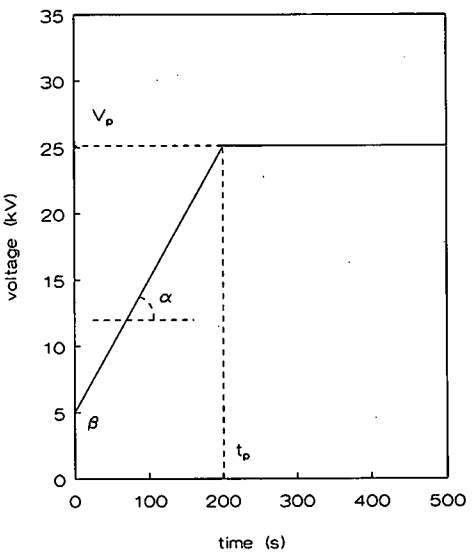

Fig. 1. Separation voltage *versus* time for a linear voltage gradient.

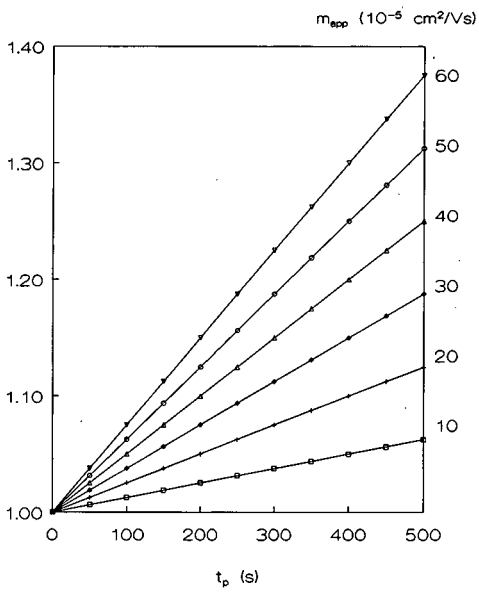

Fig. 2. Calculated graphs of τ *versus* the programme time, t_p, for different apparent mobilities shown on the right-hand ordinate. Capillary, $l_c = l_d = 100.00$ cm. Initial and final separation voltage 0 and 25 kV, respectively.

EXPERIMENTAL

Instrumentation

All experiments were carried out on a laboratory-built CZE apparatus. A computer-controlled high-voltage power supply was used (HCN 35-35000; F.u.G. Elektronik, Rosenheim, Germany). The cathode was positioned at the inlet side and the anode at the outlet side of the capillary, unless indicated otherwise. Capillaries could be flushed by applying vacuum on the outlet side. A Spectra 100 variable-wavelength UV–VIS detector was used (Spectra-Physics, San Jose, CA, USA), equipped with a flow cell for on-column detection. The length of the detection slit was about 0.1 cm. For all protein separations detection was carried out at 200 nm and for the EOF measurements at 254 nm. All experiments were carried out at ambient temperature. Both the high-voltage power supply and the detector were connected with a Tulip SX/AT personal computer via a laboratory-built Multilab-TS interface, to control the separation voltage and to register electropherograms. The laboratory-written data acquisition program CAESAR was used to analyse the electropherograms.

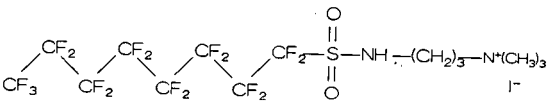

Fig. 3. Structural formula of the cationic surfactant FC135.

Materials and reagents

Fused-silica capillaries of 50 μm I.D.(Siemens, Mülheim, Germany) were used for all experiments. Lysozyme was obtained from Merck (Darmstadt, Germany) and all other proteins from Sigma (St. Louis, MO, USA). The cationic surfactant FC135 (Fig. 3) was kindly donated by 3M (Zoeterwoude, Netherlands). All other reagents were of analytical-reagent grade. Deionized water was used to prepare the buffers and all buffer and sample solutions were filtered through a 0.45-μm filter before use.

Methods

New capillaries were rinsed successively for 20 min with 0.1 *M* KOH, 20 min with water and 20 min with buffer solution before use. If buffer solutions were changed, the capillary was flushed with the new buffer for 10 min. All proteins were dissolved in the separation buffer with a final concentration of 0.1 mg/ml. Mesityl oxide was used as a neutral EOF marker. Injections were carried out by electromigration.

RESULTS AND DISCUSSION

Dynamic surfactant coating

If a sufficient amount of a cationic surfactant is added to the separation buffer, the charge of the capillary surface will be changed from negative to positive. This results in a reversal of the EOF, which will now be directed from the cathode to the anode. By selecting a buffer with a lower pH than the p*I* values of the proteins, both proteins and the capillary surface have a net positive charge and adsorption is diminished by coulombic repulsion. In this way a cationic surfactant can be applied as a dynamic coating in CZE of proteins. With this method, the pH range that can be used to optimize the selectivity is limited by the p*I* values of the proteins being analysed. However, basic proteins can be separated under neutral pH conditions, which is favourable with respect to denaturation. Because the proteins are migrating in the upstream mode, *i.e.*,

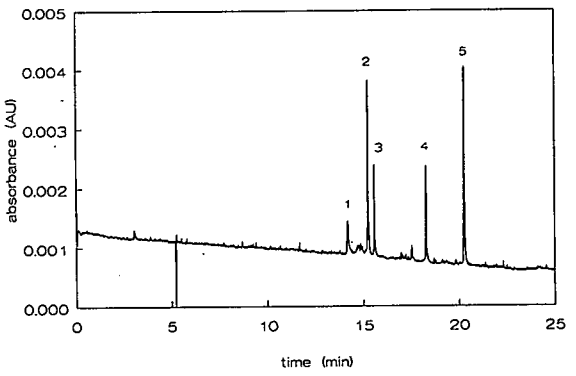

Fig. 4. Electropherogram for the separation of (1) mesityl oxide, (2) α-chymotrypsinogen, (3) ribonuclease A, (4) cytochrome *c* and (5) lysozyme. Capillary, l_c = 99.65 cm and l_d = 87.28 cm; injection, 5 s at 5 kV; separation voltage, 25 kV; buffer, 10 m*M* phosphate (pH 7.0) with 50 μg/ml of FC135 added.

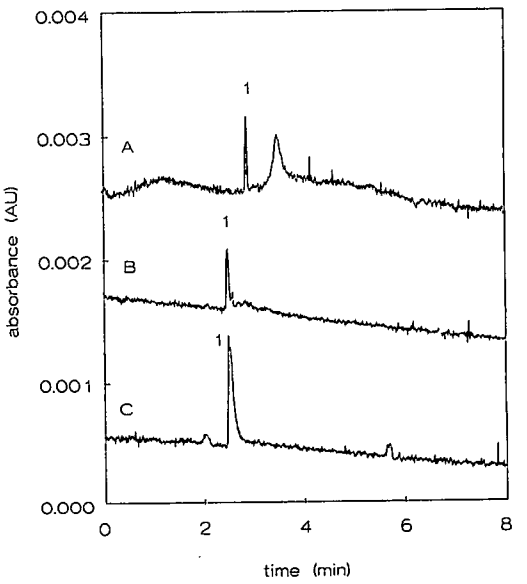

Fig. 5. Electropherograms obtained under conditions without a dynamic coating. Capillary, l_c = 42.15 cm and l_d = 34.60 cm. Anode at the inlet side and cathode at the outlet side, respectively. Injection, 5 s at 5 kV; separation voltage, 15 kV; buffer, 10 m*M* borate at (A) pH 11.0, (B) pH 9.0 and (C) pH 7.0. See Fig. 4 for the composition of the sample.

their electrophoretic mobility is opposite to the direction of the EOF, the EOF must be high enough to detect all components injected and to avoid long separation times. Further, the surfactant should not interact with the proteins, which occurs, for example, if cetyltrimetylammonium bromide (CTAB) is used [16].

Good results were obtained with the fluorinated cationic surfactant FC135 [14,17]. In Fig. 4 the electropherogram is shown of the separation of four basic proteins under neutral pH conditions. As can be seen from the results, listed in Table I, highly efficient separations ($N > 10^6$) can be achieved using this method.

To compare these results with separations under conditions without a dynamic coating, three experiments were carried out at different buffer pH values, without a surfactant added to the buffer. As can be seen from the electropherograms, shown in Fig. 5, at pH 11.0 only one peak for the proteins is observed, whereas at pH 9.0 and 7.0 no separation is obtained at all. The tailing of the peak at pH 7.0 is caused by one of the proteins co-eluting with mesityl oxide.

Influence of buffer pH

In order to study the influence of the buffer pH

TABLE I

ISOELECTRIC POINTS, p*I*, MOLECULAR WEIGHTS, MW, MEASURED MIGRATION TIMES, *t*, CALCULATED EFFECTIVE MOBILITIES, m_{eff}, AND THEORETICAL PLATE NUMBERS, *N*, FOR THE DIFFERENT SAMPLE COMPONENTS

Conditions as in Fig. 4.

No.	Component	p*I*	MW	*t* (min)	m_{eff} (10^{-5} cm/V · s)	$N \times 10^{-5}$
1	Mesityl oxyde			14.20	−40.83	1.94
2	α-Chymotrypsinogen	8.8	25 000	15.26	2.84	9.47
3	Ribonuclease A	8.7	13 500	15.59	3.64	12.43
4	Cytochrome *c*	10.8	12 200	18.30	9.15	11.13
5	Lysozyme	10.0	14 000	20.29	12.26	10.00

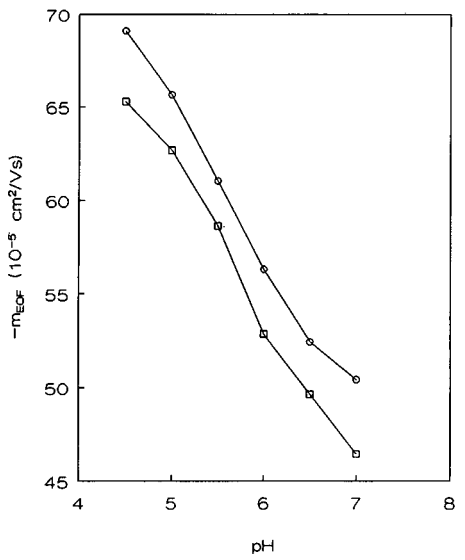

Fig. 6. Electroosmotic flow, m_{EOF}, *versus* buffer pH. Capillary, l_c = 66.32 cm and l_d = 53.45 cm. Injection, 5 s at 5 kV. Separation voltage, 25 kV. Buffer, 10 m*M* phosphate (pH 7.0) with (□) 25 μg/ml and (○) 50 μ/ml of FC135 added.

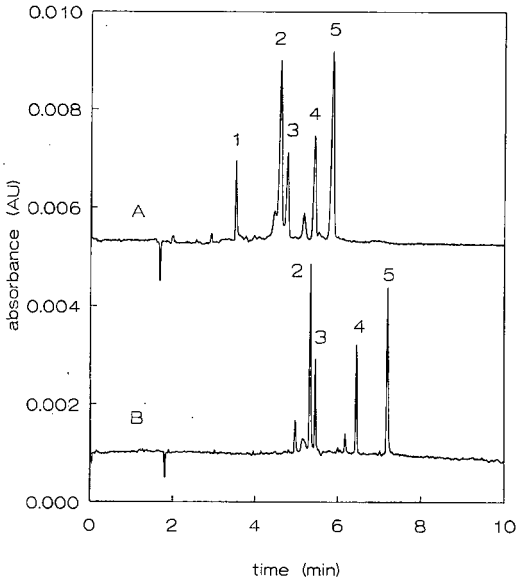

Fig. 7. Electropherograms for the separation of (1) mesityl oxide, (2) α-chymotrypsinogen, (3) ribonuclease A, (4) cytochrome *c* and (5) lysozyme. Capillary, l_c = 64.54 cm and l_d = 51.54 cm; injection, 5 s at 5 kV; separation voltage, 25 kV; buffer, 10 m*M* phosphate with 50 μg/ml of FC135 added at (A) pH 4.5 and (B) pH 7.0.

on the EOF, experiments were carried out at several pH values and two different surfactant concentrations. From the results, shown in Fig. 6, it can be seen that a higher EOF is obtained at a lower buffer pH and that an increase in the surfactant concentration leads to an increase in the EOF, suggesting that the capillary surface is not covered completely by the dynamic coating.

In Table II, the results are listed of separations at different buffer pH values. Owing to a higher net positive charge, the effective mobility increases with a decrease in buffer pH. At lower buffer pH values less efficient separations were obtained. Fig. 7 shows the electropherograms of separations at pH 4.5 and 7.0. This decrease in efficiency may be caused by adsorption on the uncovered ionized silanol groups at larger pH − p*I* differences and by denaturation. The most efficient and reproducible results were obtained at neutral pH.

TABLE II

AVERAGE EFFECTIVE MOBILITIES, m_{eff}, WITH STANDARD DEVIATIONS FOR THE DIFFERENT SAMPLE COMPONENTS AT DIFFERENT BUFFER pH VALUES (n = 5)

Conditions as in Fig. 7.

pH	m_{eff} ± S.D. (10^{-5} cm²/V · s)				
	Mesityl oxyde	α-Chymotrypsinogen	Ribonuclease A	Cytochrome *c*	Lysozyme
4.5	−64.67 ± 1.12	16.25 ± 1.01	17.94 ± 1.00	23.60 ± 1.10	15.86 ± 0.71
5.0	−56.43 ± 0.38	12.18 ± 0.13	13.91 ± 0.15	19.62 ± 0.34	23.37 ± 0.37
5.5	−53.62 ± 0.35	10.47 ± 0.13	12.12 ± 0.13	17.78 ± 0.16	21.51 ± 0.16
6.0	−49.19 ± 0.37	8.08 ± 0.12	9.54 ± 0.13	15.19 ± 0.17	18.85 ± 0.20
6.5	−44.78 ± 0.27	5.28 ± 0.07	6.40 ± 0.06	12.06 ± 0.13	15.55 ± 0.18
7.0	−44.18 ± 0.33	2.97 ± 0.04	3.90 ± 0.03	10.14 ± 0.07	13.69 ± 0.07

TABLE III

MEASURED MIGRATION TIMES, t, AND CALCULATED EFFECTIVE MOBILITIES, m_{eff}, FOR THE DIFFERENT SAMPLE COMPONENTS AT DIFFERENT PROGRAMME TIMES, t_p

Conditions as in Fig. 8.

t_p (s)	Mesityl oxide		α-Chymotrypsinogen		Ribonuclease A		Cytochrome *c*		Lysozyme	
	t (min)	m_{eff} (10^{-5} cm^2/V · s)	t (min)	m_{eff} (10^{-5} cm^2/V · s)	t (min)	m_{eff} (10^{-5} cm^2/V · s)	t (min)	m_{eff} (10^{-5} cm^2/V · s)	t (min)	m_{eff} (10^{-5} cm^2/V · s)
0	5.20	−42.65	5.59	2.98	5.71	3.81	6.72	9.65	7.47	12.96
10	5.21	−43.28	5.59	2.99	5.71	3.85	6.71	9.80	7.46	13.21
50	5.59	−42.84	5.96	2.86	6.09	3.77	7.10	9.67	7.85	13.02
100	6.04	−42.62	6.41	2.83	6.53	3.67	7.53	9.49	8.28	12.83
200	6.93	−42.11	7.31	2.83	7.43	3.65	8.45	9.43	9.19	12.64
300	7.79	−41.92	8.16	2.74	8.19	3.62	9.30	9.31	10.06	12.59
400	8.72	−41.19	9.09	2.65	9.22	3.50	10.22	8.98	10.98	12.18
500	9.61	−40.71	9.99	2.66	10.11	3.42	11.15	8.97	11.92	12.13
Average		−42.17		2.82		3.66		9.41		12.69
S.D.		0.81		0.12		0.14		0.29		0.36

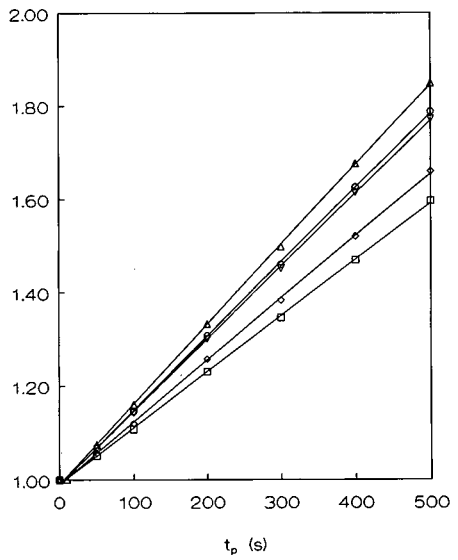

Fig. 8. Measured graphs of τ *versus* the program time, t_p, for (△) mesityl oxide, (○) α-chymotrypsinogen, (▽) ribonuclease A, (◇) cytochrome *c* and (□) lysozyme. Capillary, l_c = 64.54 cm and l_d = 51.54 cm; injection, 5 s at 5 kV; initial and final voltage, 0 and 25 kV, respectively; buffer, 10 m*M* phosphate (pH 7.0) with 50 μg/ml of FC135 added. For further explanation, see text.

Influence of a voltage gradient

To examine the influence of a programmed separation voltage, eight experiments were carried out with a linear voltage gradient and increasing programme times. The initial and final separation voltages were 0 kV (β = 0, eqn. 7) and 25 kV, respectively. As discussed in the theoretical section, the effective mobility of a component will be constant with a given electrolyte system and independent of the voltage gradient. In Table III, measured migration times, *t*, and effective mobilities, m_{eff}, calculated with eqn. 7 are listed. The slight decrease in the effective mobility with an increase in programme time can be explained by less Joule heating at longer programme times.

For the graphs of τ *versus* the programme time, t_p, almost linear plots were obtained, as shown in Fig. 8. From these graphs effective mobilities were calculated using eqn. 8, and are listed in Table IV. Using this calculation method, less Joule heating at longer programme times will lead to longer migration times and more positive slopes, which explains the higher values obtained for the effective mobilities.

The influence of the voltage gradient on the separation efficiency is illustrated in Fig. 9, where the peak variance, σ^2, is shown as a function of the programme time, t_p. A minimum in the peak variance is observed with an increase in programme time. This phenomenon was described by Bushey and Jorgenson [18], who used a stepped separation voltage to obtain a higher separation efficiency. If the Joule heating of the buffer causes an expansion of the buffer present in the capillary, a small part of the injection plug will be pushed back into the buffer vial. This results in a larger injection volume and broader peaks will be observed. If, however, a voltage gradient is applied at the beginning of the separation, the injected components have migrated further into the capillary when Joule heating becomes significant and smaller peaks are obtained. At longer separation times the peak variance due to diffusion increases, which explains the broader peaks obtained at longer programme times.

Huang *et al.* [19] pointed out that the peak variance in CZE is mainly affected by the injection length of the sample, longitudinal diffusion and

TABLE IV

CALCULATED EFFECTIVE MOBILITY, m_{eff}, SLOPE AND INTERCEPT (ARBITRARY UNITS) AND CORRELATION COEFFICIENT FOR THE GRAPHS SHOWN IN FIG. 8

No.	Component	Correlation coefficient	Slope	Intercept	m_{eff} (10^{-5} cm^2/V · s)
1	Mesityl oxide	0.99976	17.10	−0.009	−45.53
2	α-Chymotrypsinogen	0.99966	15.89	−0.011	3.23
3	Ribonuclease A	0.99970	15.57	−0.010	4.09
4	Cytochrome *c*	0.99957	13.29	−0.010	10.16
5	Lysozyme	0.99955	12.00	−0.009	13.58

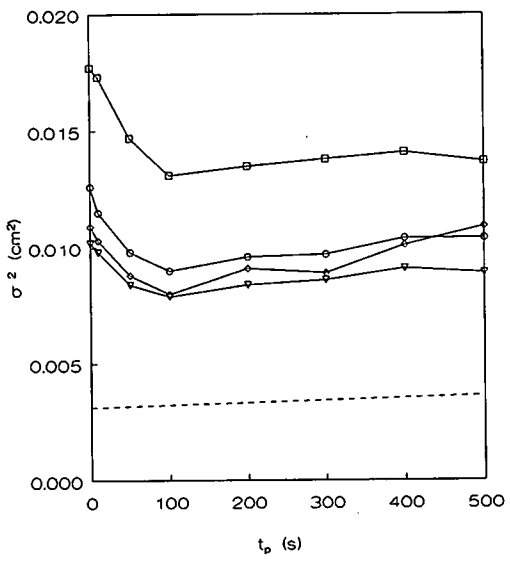

Fig. 9. Measured peak variances, σ^2, for (○) α-chymotrypsinogen, (▽) ribonuclease A, (◇) cytochrome *c* and (□) lysozyme, and calculated values (dashed line). Conditions as in Fig. 8. For further explanation, see text.

analyte–wall interactions. If the variance due to a finite detection path length is taken into account separately, the total peak variance, σ^2, can be written as

$$\sigma^2 = \sigma^2_{inj} + \sigma^2_{det} + \sigma^2{}_{diff} + \sigma^2_{ads} \quad (9)$$

where σ^2_{inj}, σ^2_{det}, σ^2_{diff} and σ^2_{ads} are the variances due to injection, detection, diffusion and adsorption, respectively. The first three terms in eqn. 9 are given by

$$\sigma^2_{inj} = l_{inj}/12 \quad (10)$$

$$\sigma^2_{det} = l_{det}/12 \quad (11)$$

and

$$\sigma^2_{diff} = 2Dt \quad (12)$$

where l_{inj} is the length of the injection plug (cm), l_{det} the length of the detection path (cm) and D the diffusion constant of the component (cm²/s). In Fig. 9 calculated peak variances are shown (dashed line), assuming an apparent mobility of $35 \cdot 10^{-5}$ cm²/V · s and a diffusion constant of $1 \cdot 10^{-6}$ cm²/s [20]. Analyte–wall interactions were not taken into account. From Fig. 9 it can be concluded that the theoretical values are lower than the experimentally obtained values, irrespective of whether a voltage gradient is applied or not, indicating that other zone broadening effects such as adsorption and temperature effects still play a significant role.

CONCLUSION

From the foregoing experiments, it can be concluded that highly efficient separations of basic proteins can be achieved at neutral pH with the cationic fluorinated surfactant FC135 as a dynamic surfactant coating. With this method untreated fused-silica capillaries can be used for the separation of proteins.

The separation efficiency can be improved by applying a voltage gradient at the beginning of the experiment and effective mobilities under these conditions can be calculated with the method presented. The measured peak variances pass through a minimum with increasing programme times. These variances are, however, larger than the theoretically calculated values.

ACKNOWLEDGEMENTS

The authors express their gratitude to the Organization for Biomedical and Health Technology (BMGT, Eindhoven University of Technology) for financial support of this investigation and to Mr. B. J. Wanders for his assistance with programming.

REFERENCES

1 J. W. Jorgenson and K. D. Lukacs, *Science (Washington, D.C.)*, 222 (1983) 266.
2 B. L. Karger, A. S. Cohen and A. Guttman, *J. Chromatogr.*, 492 (1989) 585.
3 H. H. Lauer and D. McManigill, *Anal. Chem.*, 58 (1986) 166.
4 M. Zhu, R. Rodriguez, D. Hansen and T. Wehr, *J. Chromatogr.*, 516 (1990) 123.
5 J. S. Green and J. W. Jorgenson, *J. Chromatogr.*, 478 (1989) 63.
6 M. M. Bushey and J. W. Jorgenson, *J. Chromatogr.*, 480 (1989) 301.
7 R. M. McCormick, *Anal. Chem.*, 60 (1988) 2322.
8 G. J. M. Bruin, J. P. Chang, R. H. Kuhlman, K. Zegers, J. C. Kraak and H. Poppe, *J. Chromatogr.*, 471 (1989) 429.
9 G. J. M. Bruin, R. Huisden, J. C. Kraak and H. Poppe, *J. Chromatogr.*, 480 (1989) 339.
10 K. A. Cobb, V. Dolnik and M. Novotny, *Anal. Chem.*, 62 (190) 2478.

11 J. K. Towns and F. E. Regnier, *J. Chromatogr.*, 516 (1990) 69.
12 J. K. Towns and F. E. Regnier, *Anal. Chem.*, 63 (1991) 1126.
13 W. Nashabeh and Z. El Rassi, *J. Chromatogr.*, 559 (1991) 367.
14 A. Emmer, M. Jansson and J. Roeraade, *J. Chromatogr.*, 547 (1991) 544.
15 J. L. Beckers, F. M. Everaerts and M. T. Ackermans, *J. Chromatogr.*, 537 (1991) 407.
16 J. C. Reijenga, G. V. A. Aben, Th. P. E. M. Verheggen and F. M. Everaerts, *J. Chromatogr.*, 260 (1983) 241.
17 G. J. M. Bruin, personal communication, 1991.
18 M. M. Bushey and J. W. Jorgenson, *J. Microcol. Sep.*, 1 (1989) 125.
19 X. Huang, W. F. Coleman and R. N. Zare, *J. Chromatogr.*, 480 (1989) 95.
20 Y. Walbroehl and J. W. Jorgenson, *J. Microcol. Sep.*, 1 (1989) 41.

Journal of Chromatography, 605 (1992) 124–128
Elsevier Science Publishers B.V., Amsterdam

CHROM. 24 247

Short Communication

Extraction and high-performance liquid chromatographic methods for the γ-lactones parthenolide (*Chrysanthemum parthenium* Bernh.), marrubiin (*Marrubium vulgare* L.) and artemisinin (*Artemisia annua* L.)

Jean-Pierre Rey, Joël Levesque and Jean Louis Pousset

Laboratoire de Pharmacognosie, Faculté de Médecine et de Pharmacie, 34 Rue du Jardin des Plantes, B.P. 199, 86005 Poitiers Cedex (France)

(First received January 31st, 1992; revised manuscript received April 7th, 1992)

ABSTRACT

A low-pressure liquid chromatographic method using silica gel 60 with hexane–chloroform–ethyl acetate proportions varying from 80:20:0 to 80:20:6 (v/v/v) as eluent is described as a simple and inexpensive process for the isolation of the γ-lactones parthenolide, marrubiin and artemisinin from the aerial parts of feverfew, white horehound and quinghao, respectively. A selective high-performance liquid chromatographic (HPLC) method using a Superspher Si 60 column with hexane–dioxane (85:15, v/v) for elution of parthenolide and marrubiin and (90:10, v/v) for artemisinin and UV detection at 210 nm for parthenolide and artemisinin and 225 nm for marrubiin is described that allows the determination of these γ-lactones in plants. Compared with the HPLC method, the extraction yield of the large-scale process was calculated to be 72.3, 78.4 and 74.1% of the total amount of parthenolide, marrubiin and artemisinin, respectively, contained in each plant.

INTRODUCTION

Further to our study of the application of high-performance liquid chromatography (HPLC) to the analysis of medicinal plants with anti-inflammatory, antispasmodic and antimalarial properties, we have examined the components of *Chrysanthemum parthenium* Bernh. (feverfew), *Marrubium vulgare* L. (white horehound) and *Artemisia annua* L. (quinghao). Feverfew contains almost 30 sesquiterpene lactones [1] and mainly parthenolide in the European species [2]. This compound is mainly responsible of the therapeutic efficiency of this drug against migraine [3]. White horehound contains many diterpenic lactones [4], the main one being marrubiin [5], whose sodium salt has a pronounced action on biliary secretion [6]. Quinghao, used for many centuries in chinese folk medicine, contains artemisinin [7,8], a sesquiterpenic endoperoxide lactone used in the treatment of chloroquine-resistant and cerebral malarias [9–11].

Numerous studies have been reported on the isolation of parthenolide [1,12,13], marrubiin [14,15] and artemisinin [16–19], but all of them involved expensive solvents (acetonitrile, diethyl ether and acetone) and time-consuming methods. Moreover,

Correspondence to: Dr. J.-P. Rey, Laboratoire de Pharmacognosie, Faculté de Médecine et de Pharmacie, 34 Rue du Jardin des Plantes, B.P. 199, 86005 Poitiers Cedex, France.

0021-9673/92/$05.00

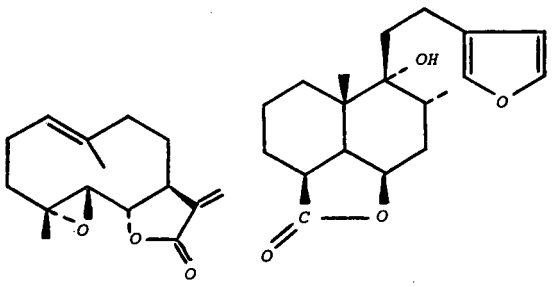

PARTHENOLIDE **MARRUBIIN**

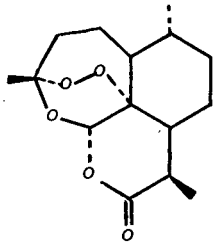

ARTEMISININ

whereas many determinations have been achieved by infrared spectroscopy [13], thin-layer chromatography (TLC) [20,21] and reversed-phase HPLC [22,23], there have been no reports of the determination of parthenolide, marrubiin and artemisinin by normal-phase HPLC. In this paper we describe a rapid and inexpensive process for the isolation of these pure lactones which can be extrapolated to an industrial scale. We also describe a normal-phase HPLC method for their determination in the aerial parts of plants.

EXPERIMENTAL

Chemicals

Hexane and 1,4-dioxane were of HPLC quality from Rathburn Chemicals (Walkerburn, UK). All other solvents were of analytical-reagent grade quality from Labosi (Paris, France).

Thin-layer chromatography

Silica gel Si 60 F_{254} plates were obtained from Merck (Darmstadt, Germany). The mobile phase was chloroform–acetone (90:10, v/v). All TLC separations were performed at room temperature (20°C). The mobile phase was allowed to remain in the closed glass tank for 1 h before chromatography. The inside of the tank was lined with filter-paper. A distance of 15 cm was used for the development of the chromatograms. Detection was effected with a 2% methanolic solution of resorcinol mixed with an equal volume of 2% sulphuric acid (reagent No. 1 [20]) and with a 1% ethanolic solution of vanillin mixed with 2% concentrated sulphuric acid (reagent No. 2 [21]). Dried chromatograms treated with reagent 1 or 2 were kept for 2–4 min at 110°C.

High-performance liquid chromatography

A Varian Model 5000 chromatograph was used, equipped with a Rheodyne Model 7125 injector and a Merck L 3000 photodiode-array detector under computer control (Merck HPLC Manager). Analyses were conducted at 20°C.

Analytical HPLC was carried out on a normal-phase Superspher Si 60 column (125 × 4 mm I.D., particle size 4 μm) (Merck) used with a LiChrospher Si 60 precolumn (4 × 4 mm I.D., particle size 5 μm) (Merck). The mobile phase was hexane–dioxane (85:15, v/v) at a flow-rate of 1 ml/min for parthenolide and marrubiin elution and hexane–dioxane (90:10, v/v) at a flow-rate of 2 ml/min for artemisinin elution. The injection volume was 10 μl and UV detection was at 210 nm for parthenolide and artemisinin and 225 nm for marrubiin.

Isolation of artemisinin

Extraction of the lactonic fraction. A 1.7-kg amount of flowered aerial parts of *Artemisia annua* L. (harvested in China and received dried), finely powdered, was subjected to a Soxhlet extraction with chloroform (4 l) for 4 h. The solvent was evaporated under reduced pressure at 40°C to give a residue of 105 g (R_1, 6.2% dry material).

Purification with liquid–liquid extraction. This residue was dissolved in warm methanol (1 l), then 200 ml of distilled water were added. The mixture was kept cool, filtered, and extracted with 4 × 500 ml of hexane. We monitored by TLC that artemisinin was present in the methanolic layer [purple spot at R_F = 0.72 (reagent No. 2)], but not in the hexane phases, which were discarded.

Low-pressure column chromatography. The meth-

anolic layer was evaporated under reduced pressure and the residue (R_2, 52 g) was diluted with chloroform (250 ml) and washed out on a column (700 × 40 mm I.D.) containing 150 g of silica gel 60 (Merck) (particle size 0.063–0.2 mm) for low-pressure column chromatography with chloroform (until eluate remained colourless) to remove polar compounds. The eluate was evaporated (R_3, 35 g) and chromatographed on an identical-sized column containing 350 g of silica gel 60. Fractions of 500 ml were recovered according to the following elution profile: hexane–chloroform (80:20, v/v) (solvent A, 1 l) for fractions I–II; hexane–chloroform–ethyl acetate (80:20:2, v/v/v) (solvent B, 2 l) for fractions III–VI; hexane–chloroform–ethyl acetate (80:20:4, v/v/v) (solvent C, 3 l) for fractions VII–XII; and hexane–chloroform–ethyl acetate (80:20:6, v/v/v) (solvent D, 2 l) for fractions XIII–XVI. The product was checked using TLC. Fractions VIII–XI, mixed, evaporated to dryness and crystallized from cyclohexane, afforded 2.74 g of pure compound (0.16% dry material). ^{13}C and ^{1}H NMR spectroscopy (Brucker AC 200 P), melting point determination, UV spectrophotometric analysis and TLC confirmed its identification as artemisinin: m.p. 154°C [7,17,18]; ^{13}C and ^{1}H NMR spectra identical with the literature [24]; UV λ_{max} [hexane–dioxane (90:10, v/v)], 210 nm; TLC, R_F = 0.72.

Isolation of parthenolide

The latter process was applied to 1.7 kg of flowered aerial of *Chrystanthenum parthenium* Bernh. [harvested in Maine et Loire (France) and dried at room temperature]. We obtained the following results: R_1 = 132 g (7.78% dry material); cherry-coloured spot in the methanolic layer at R_F = 0.60 (reagent No. 1); R_2 = 5.47 g; R_3 = 15.7 g; fractions X–XIII, mixed, evaporated to dryness and crystallized from cyclohexane, afforded 4.08 g of pure compound (0.24% dry material). ^{1}H NMR spectroscopy (Bruker AC 200 P), melting point determination, UV spectrophotometric analysis and TLC confirmed its identification as parthenolide: m.p. 115°C [25]; ^{1}H NMR spectra identical with the literature [25]; UV λ_{max} [hexane–dioxane (85:15, v/v)], 210 nm; TLC, R_F = 0.60 [20].

Isolation of marrubiin

The latter process was applied to 1.7 kg of flowered aerial parts of *Marrubium vulgare* L. [harvested in Maine et Loire (France) and dried at room temperature]. We obtained the following results: R_1 = 77 g (4.53% dry material); purple spot in the methanolic layer at R_F = 0.66 (reagent No. 2); R_2 = 3.17 g; R_3 = 11.8 g; fractions IX–XI, mixed, evaporated to dryness and crystallized from ethanol, afforded 2.13 g of pure compound. (0.12% dry material). ^{1}H NMR spectroscopoy (Brucker AC 200 P), melting point determination, UV spectrophotometric analysis and TLC confirmed its identification as marrubiin: m.p. 160°C [15,26,27]; ^{1}H NMR spectra identical with the literature [4,5,26,28]; UV λ_{max} [hexane–dioxane (85:15, v/v)], 225 nm; TLC, R_F = 0.66.

HPLC sample preparation method

Amounts of 10 g of flowered aerial parts of each plant from the same batch processed via the large-scale method were subjected to a Soxhlet extraction with chloroform (500 ml) for 4 h. The solvent was evaporated under reduced pressure at 40°C and sample washed out on a column (200 × 20 mm I.D.) containing 10 g of silica gel 60 (particle size 0.063–0.2 mm) for low-pressure column chromatography (Merck), with chloroform (400 ml) until the eluate remained colourless. The eluate was evaporated to dryness and then diluted with 5 ml of chloroform (quinghao and white horehound samples) or 20 ml of chloroform (feverfew sample) accurately before HPLC analysis.

RESULTS AND DISCUSSION

In comparison with the separation of sesquiterpene lactones [23] and particularly of parthenolide [22] by reversed-phase HPLC, we adopted normal-phase HPLC on silica gel 60, which resulted in good-quality chromatographic profiles. For quantitative analysis, the calibration graphs show a linear correlation from 0.2 to 5 mg/ml between the amounts of the three injected lactones and the intensity of the absorption at 210 nm [correlation coefficient (R^2) 0.9938 for artemisinin and 0.9975 for parthenolide] and at 225 nm (R^2 = 0.9956 for marrubiin). Five determinations were carried out on each sample of feverfew, white horehound and quinghao, in order to test the precision of the method. The determination of each lactone was attempt-

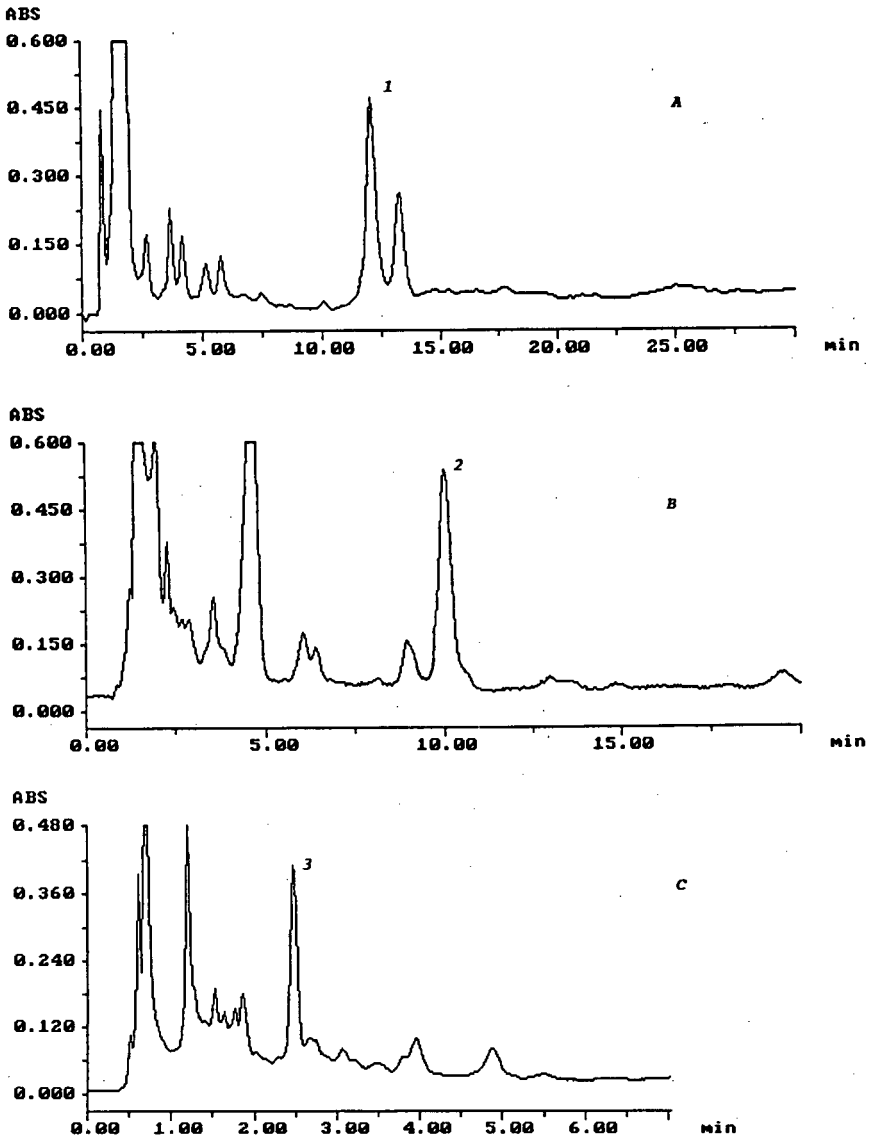

Fig. 1. HPLC of the total lactonic fraction of flowered aerial parts of (A) *Chrysanthemum parthenium* Bernh., (B) *Marrubium vulgare* L. and (C) *Artemisia annua* L. Peaks: 1 = parthenolide; 2 = marrubiin; 3 = artemisinin. Conditions: column, Superspher Si 60 (125 × 4 mm I.D.; particle size 4 μm); precolumn, LiChrospher Si 60 (4 × 4 mm I.D.; particle size 5 μm); mobile phase (A and B) hexane–dioxane (85:15, v/v) and (C) (90:10, v/v); flow-rate (A and B) 1 ml/min and (C) 2 ml/min; UV detection at (A and C) 210 nm and (B) 225 nm.

ed on the total lactonic fraction of flowered aerial parts of *Chrysanthemum parthenium* Bernh. (Fig. 1a), *Marrubium vulgare* L. (Fig. 1b) and *Artemisia annua* L. (Fig. 1c). The results indicated that with this new extraction process, we extracted 72.3, 78.4 and 74.1% of the total amount of parthenolide, marrubiin and artemisinin, respectively, contained in each plant.

In conclusion, the proposed process allows the use of inexpensive solvents (chloroform, hexane and ethyl acetate) and of a simple low-pressure liquid chromatographic method in general for the

isolation of γ-lactones, which can be extrapolated to an industrial scale. Moreover, the extraction yields with this process are better than those mentioned in the literature [13,14,17]. Finally, the proposed HPLC method allows the isocratic separation of parthenolide, marrubiin and artemisinin and can be used in their routine determination in drugs.

ACKNOWLEDGEMENT

The authors thank Dr. Etienne Legendre for assistance in obtaining *Artemisia annua* L.

REFERENCES

1 F. Bohlann and C. Zdero, *Phytochemistry*, 21 (1982) 2543.
2 D. V. C. Awang, *Can. J. Pharm.*, 122 (1989) 266.
3 J. J. Murphy, S. Hepstintall and J. R. Mitchell, *Lancet*, ii (1988) 189.
4 G. Laonigro, R. Lanzetta, M. Parrilli, M. Adinolfi and L. Mangoni, *Gazz. Chim. Ital.*, 109 (1979) 145.
5 R. A. Appleton, J. W. B. Fulke, M. S. Henderson and R. McCrindle, *J. Chem. Soc. C*, (1967) 1943.
6 F. Mercier and G. Rizzo, *C.R. Soc. Biol.*, 114 (1933) 263.
7 J. M. Liu, M. Y. Ni, J. F. Fan, Y. Y. Tu, Z. H. Wu, Y. L. Wu and W. S. Chou, *Acta Chim. Sin.*, 37 (1979) 129.
8 G. Schmid and W. Hofheim, *J. Am. Chem. Soc.*, 105 (1983) 624.
9 China Cooperative Research Group, *J. Trad. Chin. Med.*, 2 (1982) 3 and 45.
10 China Cooperative Research Group, *Chin. Med. J.*, 92 (1979) 811.
11 D. L. Klayman, *Science*, 228 (1985) 1049.
12 M. Soucek, V. Herout and F. Sorm, *Collect. Czech. Chem. Commun.*, 26 (1961) 803.
13 E. Bloszyk, B. Geppert and B. Drozdz, *Planta Med.*, 34 (1978) 79.
14 L. J. and F. Mercier, *C.R. Acad. Sci.*, 195 (1932) 1102.
15 H. J. Nicholas, *J. Pharm. Sci.*, 53 (1964) 895.
16 D. Klayman, A. J. Lin, N. Acton, J. P. Scouill, J. M. Hoch, W. K. Milhous and A. D. Theoharides, *J. Nat. Prod.*, 47 (1984) 715.
17 H. N. El-Sohly, E. M. Croom, F. S. El-Feraly and M. M. El-Sherei, *J. Nat. Prod.*, 53 (1990) 1560.
18 A. Singh, R. A. Vishawakarma and A. Husain, *Planta Med.*, 54 (1988) 475.
19 N. Acton, D. L. Klayman, I. J. Rollman and J. F. Novotny, *J. Chromatogr.*, 355 (1986) 448.
20 B. Drozdz and E. Bloszyk, *Planta Med.*, 33 (1978) 379.
21 A. K. Picman, R. L. Ranieri, G. H. N. Towers and J. Lam, *J. Chromatogr.*, 189 (1980) 187.
22 D. Fontanel, S. Bizot and P. Beaufils, *Plant. Med. Phytother.*, 24 (1990) 231.
23 B. Marchand, H. Mohan Behl and E. Rodriguez, *J. Chromatogr.*, 265 (1983) 97.
24 G. Blasko and G. A. Cordell, *J. Nat. Prod.*, 51 (1988) 1273.
25 T. R. Govindachari, B. S. Joshi and V. N. Kamat, *Tetrahedron*, 21 (1965) 1509.
26 J. W. B. Fulke, M. S. Henderson and R. McCrindle, *J. Chem. Soc. C.*, (1968) 807.
27 W. Cocker, B. E. Cross, S. R. Duff, J. T. Edward and T. F. Holley, *J. Chem. Soc.*, (1953) 2540.
28 M. S. Henderson and R. McCrindle, *J. Chem. Soc. C*, (1969) 2014.

Journal of Chromatography, 605 (1992) 129–133
Elsevier Science Publishers B.V., Amsterdam

CHROM. 24 267

Short Communication

Specific gas chromatography–mass spectrometry analytical method for the determination of cyhexatin in animal feed

E. Benfenati and M. Natangelo

Istituto di Ricerche Farmacologiche "Mario Negri", Via Eritrea 62, 20157 Milan (Italy)

E. Pallucca

Oxon Italia S.p.A., Via Sempione 195, 20016 Pero (Mi) (Italy)

R. Tridico, E. Borghetti and G. Lualdi

Istituto di Ricerche e Collaudi "M. Masini", Via Moscova 11, 20017 Rho (Mi) (Italy)

(First received November 13th, 1991; revised manuscript received April 21st, 1992)

ABSTRACT

The acaricide tricyclohexyltin hydroxide (cyhexatin) was determined in animal feed samples, using gas chromatographic–mass spectrometry in the electron impact mode. Sample extraction and derivatization (converting the analyte to an alkylated derivative) were performed using a tricyclopentyl analogue of this acaricide as internal standard to obtain a better analytical precision.

INTRODUCTION

Tricyclohexyltin hydroxide (cyhexatin; Fig. 1) is an acaricide effective against mites, used in a wide range of vegetables [1]. Methods of analysing this compound in commercial insecticide samples [2] and environmental samples [3,4] have been developed. Müller and co-workers [3,4] measured cyhexatin in water, sediments [3] and soil [4] samples, using ethyl magnesium bromide as a derivatizing reagent. Our goal was to develop a specific analytical method for cyhexatin to test animal feed samples for toxicological investigation. The method developed represents a modification of those described by Müller and co-workers. The resulting ethylated derivative was analysed by gas chromatography (GC)–mass-spectrometry (MS) operating in the selected ion recording mode. Tricyclopentyltin hy-

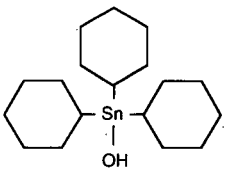

Fig. 1. The formula of cyhexatin.

Correspondence to: Dr. Emilio Benfenati, Istituto di Ricerche Farmacologiche "Mario Negri", Via Eritrea 62, 20157 Milan, Italy.

0021-9673/92/$05.00

droxide was added as internal standard before extraction of the samples.

MATERIALS AND METHODS

Reagents

Cyhexatin and tricyclopentyltin hydroxide were from Oxon Italia (Pero, Milan, Italy); *n*-hexane (pesticide grade), hydrochloric acid, anhydrous calcium chloride and sodium sulphate were from Merck (Darmstadt, Germany); diethyl ether and 2-hydroxy-2,4,6-cycloheptatrien-1-one (tropolone) were from Fluka (Buchs, Switzerland); 2 *M* ethyl magnesium bromide in tetrahydrofuran was from Aldrich (Milwaukee, USA); Supelclean LC-Si silica gel columns were from Supelco (Bellefonte, USA).

TABLE I

INSTRUMENTAL CONDITIONS

Gas chromatograph	Varian 3400
Mass spectrometer	Finnigan MAT Incos 50
GC column	J&W DB-5, 30 m × 0.25 mm, film thickness 0.25 μm
Carrier gas	Helium, 0.5 m/s
GC injector	270°C, splitless mode (valve closed for 1 min, then open, split flow 10 ml/min)
GC programme	80°C for 2 min, 20°C/min gradient up to 270°C, final temperature maintained for 10 min
Ions monitored	315 *m/z* for cyhexatin 287 *m/z* for the internal standard
Scan time	50 ms

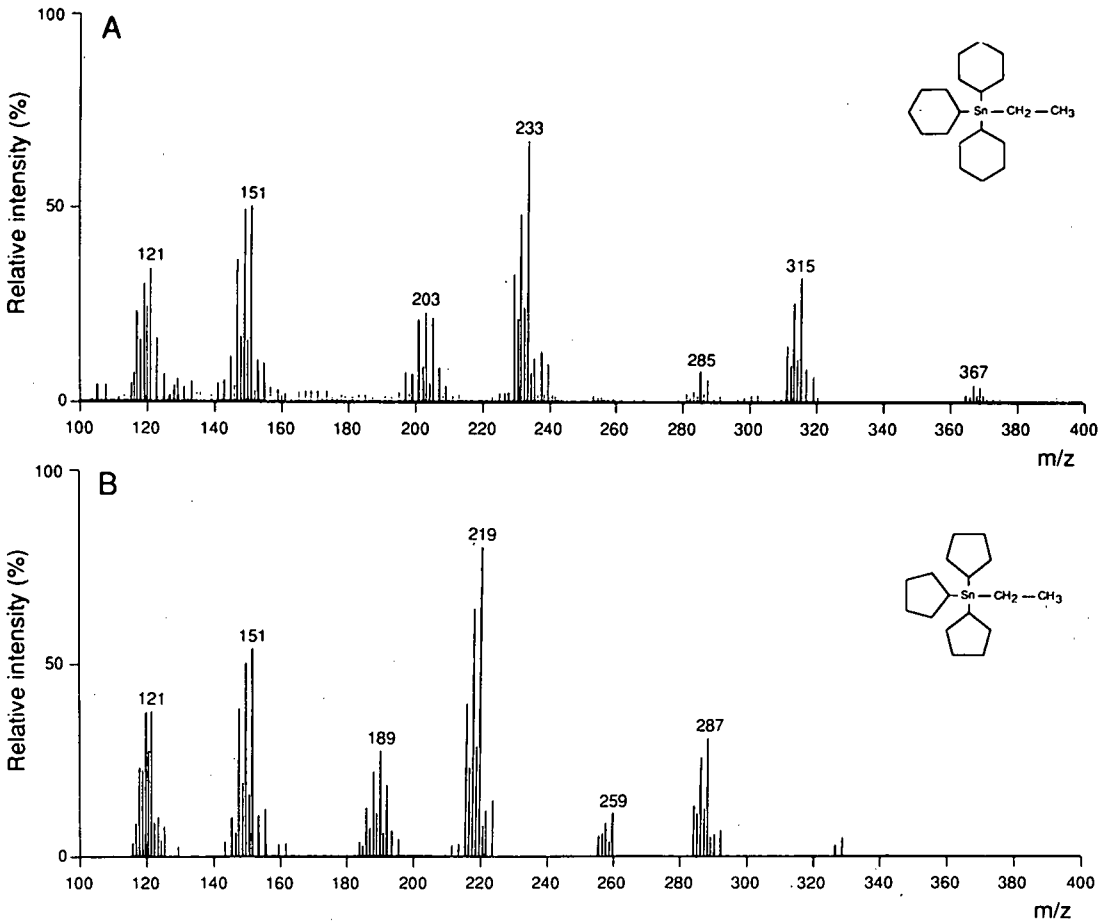

Fig. 2. (A) Mass spectrum of derivatized cyhexatin. (B) Mass spectrum of derivatized tricyclopentyltin hydroxide.

Standard solutions

Standard solutions of cyhexatin and tricyclopentyltin hydroxide were prepared in acetone.

Animal feed composition

The animal feed contained carbohydrates (56.3%, of which starch 38.6%), protein (17.7%), lipids (3.2%), cellulose (4.7%), water (12.9%) and ash (5.2%), including calcium (8400 mg/kg), sodium (2300 mg/kg), potassium (7300 mg/kg), phosphorus (5100 mg/kg) and magnesium (2130 mg/kg).

Sample extraction and derivatization

Analyses were done on standard animal feed with different amounts of cyhexatin added.

A 4-g aliquot of each sample was weighed. After addition of 80 μg of internal standard in acetone, the samples were acidified with 0.5 ml of 2 *M* hydrochloric acid then extracted twice with 10 ml of a 0.25% tropolone solution in diethyl ether. The organic phase was centrifuged and filtered on anhydrous calcium chloride. After concentration to 2 ml under a gentle stream of air, this extract was ready for derivatization according to Müller [3].

The derivatized extract was purified with a silica gel microcolumn (Supelclean LC-Si); the sample was first deposited on the column, then eluted with 10 ml of a diethyl ether–*n*-hexane (10:90) solution. A 1-μl aliquot of this solution was injected into the

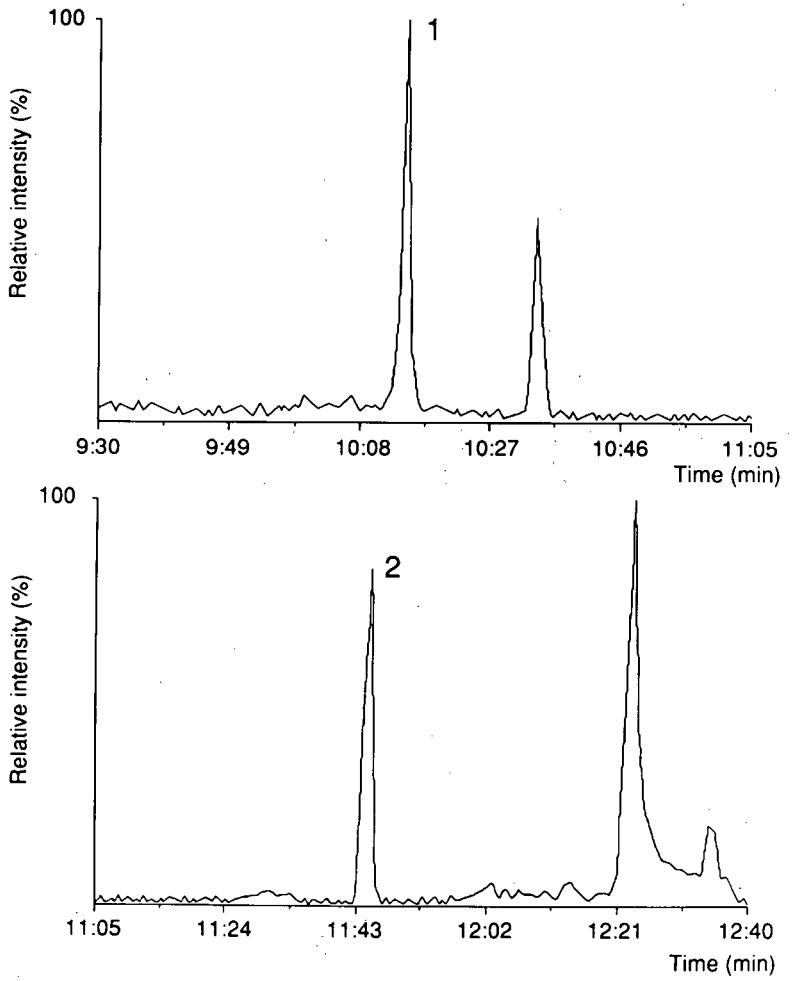

Fig. 3. Fragmentograms of *m/z* 315 (upper panel) and *m/z* 287 (lower panel), relative to a standard feed sample, showing the cyhexatin (1) and the internal standard (2) peaks.

GC–MS system for analysis. The GC–MS instrumental conditions are listed in Table I.

Calibration curve

Calculations were made on the basis of the analyte/internal standard peak area ratios in the samples with reference to a calibration curve obtained with standards of herbicide-free feed (4 g each), enriched with known amounts of cyhexatin (0, 10, 20 and 40 μg) and a constant amount of internal standard (80 μg).

RESULTS

Fig. 2 shows the mass spectra of cyhexatin (Fig. 2A) and of the internal standard (Fig. 2B) after derivatization.

The chromatogram of a calibration curve sample is shown in Fig. 3. The data of the calibration curves obtained on different days are reported in Table II as well as the standard deviation of these results. Average ratios and standard deviations of the 1-day replicates (four replicates for each concentration point) were: 0.22 ± 0.025 (for 2.5 μg/g), 0.493 ± 0.04 (for 5 μg/g) and 1.049 ± 0.133 (for 10 μg/g).

The calibration curve obtained using the internal standard in several cyhexatin-enriched feed samples at different concentrations is shown in Fig. 4. Linearity was good in the concentration range of interest. The blank feed samples and those spiked only with the internal standard made no detectable contribution and did not interfere with the cyhexatin peak.

Other organotin compounds similar to cyhexatin (triphenyl and tributyltin hydroxides) were tested as internal standards, together with the cyclopentyl analogue: this last gave the best results. Indeed, the other compounds gave a poor 1-day reproducibility in the fortified diet. Deuterium-labelled cyhexatin could be used as internal standard instead of the cyclopentyl analogue to achieve better accuracy.

The recoveries in feed samples varied from 46.1 to 77.4% with a mean of 56%; calculations were based on the internal standard peak areas in comparison with those found in pure samples of the ethylated compound. The relative standard deviation (R.S.D.) relative to eight replicates of a standard solution of cyhexatin plus the internal standard, derivatized as described, was 13.5%. The analysis of this same standard solution added to the diet (at a level of 5 μg/g) gave a R.S.D. of 15.0% for n (number of replicates) = 13. This suggests that the derivatization step is the major source of the variation found in the recoveries assay.

Considering the addition of cyhexatin in various amounts to samples of uncontaminated diet, the limit of detection of the method was about 20 ng/g. The limit of quantitation was about 45 ng/g.

TABLE II

RAW DATA OF EACH ASSAY CONCENTRATION DETERMINED ON DAY-TO-DAY REPLICATES

	Cyhexatin/internal standard response ratio		
	Concentration (μg/g)		
	2.5	5	10
	0.265	0.444	0.965
	0.172	0.380	1.055
	0.188	0.450	0.947
	0.240	0.442	1.040
	0.312	0.558	0.956
		0.494	1.035
		0.420	0.857
		0.466	1.035
		0.444	0.791
		0.365	0.714
		0.338	1.107
		0.555	0.999
		0.522	
Mean	0.235	0.452	0.958
S.D.	0.057	0.068	0.117

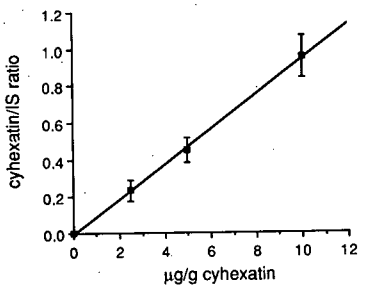

Fig. 4. Calibration curve of the method: each point is the mean ± S.D. of n samples: 0 μg/g (n = 1), 2.5 μg/g (n = 5), 5 μg/g (n = 13), 10 μg/g (n = 12). $y = -0.0072 + 0.0956x$. IS = Internal standard.

CONCLUSIONS

MS was used successfully to analyse an organotin compound, cyhexatin, and the method was more specific than using conventional GC detectors.

The use of an analogue of cyhexatin as internal standard for quantification ensures good precision in the desired concentration range.

REFERENCES

1 C. R. Worthing (Editor), *The Pesticide Manual. A World Compendium*, The British Crop Protection Council, Croydon, 7th ed., 1983, p. 147.
2 I. Camoni, E. Chiacchierini, R. Iachetta and A. L. Magri, *Ann. Chim.*, 65 (1975) 267.
3 M. D. Müller, *Anal. Chem.*, 59 (1987) 617.
4 M. D. Müller and H. P. Bosshardt, *Bull. Environ. Contam. Toxicol.*, 38 (1987) 627.

Journal of Chromatography, 605 (1992) 134–138
Elsevier Science Publishers B.V., Amsterdam

CHROM. 24 280

Short Communication

Determination of 3-chloropropanediol and related dioxolanes by gas chromatography☆

Erik Kissa

Jackson Laboratory, Chemicals Department, E.I. Du Pont de Nemours & Co., Deepwater, NJ 08023 (USA)

(First received January 31st, 1992; revised manuscript received April 14th, 1992)

ABSTRACT

3-Chloropropanediol has been derivatized with N,O-bis(trimethylsilyl)trifluoroacetamide and determined by capillary gas chromatography in extracts of resins and in solvents containing ketones and the corresponding ketals (dioxolanes). *n*-Tetradecane was used as the internal standard.

Underivatized 3-chloropropanediol reacts with ketones and forms the corresponding ketals (dioxolanes). Ketones interfere therefore with the determination of underivatized 3-chloropropanediol. The reaction between 3-chloropropanediol and acetone in excess obeys pseudo-first-order kinetics.

The precision of gas chromatography, expressed as the standard deviation, was found to be 0.43 μg/ml or (relative standard deviation) 0.42%.

INTRODUCTION

3-Chloropropanediol is a toxic compound [1–5] which has been shown to be an antifertility agent in male rats [1,2] and mutagen in bacterial assays [3,4]. Although there is no direct evidence for toxic effects in humans, the results of animal tests dictate that 3-chloropropanediol must be monitored. When used as an intermediate, unreacted 3-chloropropanediol in the product has to be determined and removed if present in amounts above the allowable limit. The determination of 3-chloropropanediol by gas chromatography (GC) is difficult [6]. 3-Chloropropanediol can react during GC with other components of the sample, to form hydrochloric acid in the presence of water, react with active sites on the column and non-volatile residues in the column inlet. As a result, the peak shape deteriorates with repeated injections and the precision is poor.

GC of 3-chloropropanediol derivatized with *n*-butaneboronic acid and phenylboronic acid has been reported [6–8]. We have been using in our laboratory N,O-bis(trimethylsilyl)trifluoroacetamide (BSTFA), a more powerful derivatization agent, along with an internal standard for the determination of 3-chloropropanediol in extracts of resins and in solvents containing ketones and the corresponding ketals (dioxolanes). Trimethylsilylation with BSTFA has been used for the characterization of aliphatic diols [9] and dihydroarenediols [10] by GC–mass spectrometry.

Correspondence to: Dr. E. Kissa, Jackson Laboratory Chemicals Department, E. I. du Pont de Nemours & Co., Deepwater, NJ 08023, USA.

☆ Research and Development Division Publication No. 148.

0021-9673/92/$05.00

EXPERIMENTAL

Chemicals

3-Chloropropanediol and n-tetradecane were purchased from Aldrich. BSTFA was purchased from Kodak Laboratory Chemicals. Acetonitrile, distilled in glass, was purchased from Burdick & Jackson Labs.

2-Isobutyl-2-methyl-4-(chloromethyl)-1,3-dioxolane, formed by reacting 3-chloropropanediol with methyl isobutyl ketone (MIBK), was prepared by E. Pechold (Jackson Lab., Du Pont) and purified by distillation (b.p. 79–80°C/7 mmHg).

Instrumentation

A Varian Model 6000 chromatograph was equipped with an autosampler and a flame ionization detector. A 30 m × 0.75 mm I.D. SPB-5 megabore borosilicate glass capillary column, or alternatively a SPB-5 0.25 mm I.D. capillary fused-silica column was used. The SPB-5 columns (purchased from Supelco, Bellefonte, PA, USA) have a bonded 1.0 μm thick film of 94% dimethyl–5% diphenyl–1% vinyl polysiloxane and correspond to DB-5 capillary columns obtainable from other suppliers.

Carrier gas (helium) flow was for the megabore column 5 ml/min and for the 0.25 mm capillary column 0.8 ml/min. The make up gas flow was 30 ml/min for both columns. The injector was held at 220°C, the detector at 300°C. The oven temperature program was a 3 min hold at 60°C, then a 6°C/min temperature rise to 265°C and no post-program hold.

Procedure

The SPB-5 column with a bonded 1.0 μm thick film of 94% dimethyl–5% diphenyl–1% vinyl polysiloxane exhibited less peak tailing than the moderately polar SPB-20 (20% diphenyl–80% dimethylpolysiloxane phase) column or the polar Supelcowax-10 (polyethylene glycol phase) column with similar dimensions.

n-Tetradecane, 1.0 mg/ml in acetonitrile, was used as the internal standard because its retention time was sufficiently long to exceed that of components found in extracts of the material analyzed. A 4-ml sample of the 3-chloropropanediol solution in acetonitrile (or another solvent) was transferred to a septum vial and 0.5 ml of BSTFA were added. (If an alcohol is used to extract 3-chloropropanediol from a sample, more BSTFA is needed). The closed septum vial was heated for 10 min at 80°C. After allowing the reaction mixture to cool, 0.5 μl of the reaction mixture was injected in a splitless mode (megabore column) or 1.0 μl in a 1:50 split mode (0.25 mm capillary column).

RESULTS AND DISCUSSION

A 1-mol amount of 3-chloropropanediol reacts with 2 mol of BSTFA in two steps. Presumably the primary hydroxyl group reacts at a faster rate than the secondary hydroxyl:

$$HOCH_2CH(OH)CH_2Cl \xrightarrow{BSTFA} (CH_3)_3SiOCH_2CH(OH)CH_2Cl$$

$$\downarrow \text{BSTFA, heat}$$

$$(CH_3)_3SiOCH_2CH(OSi(CH_3)_3)CH_2Cl$$

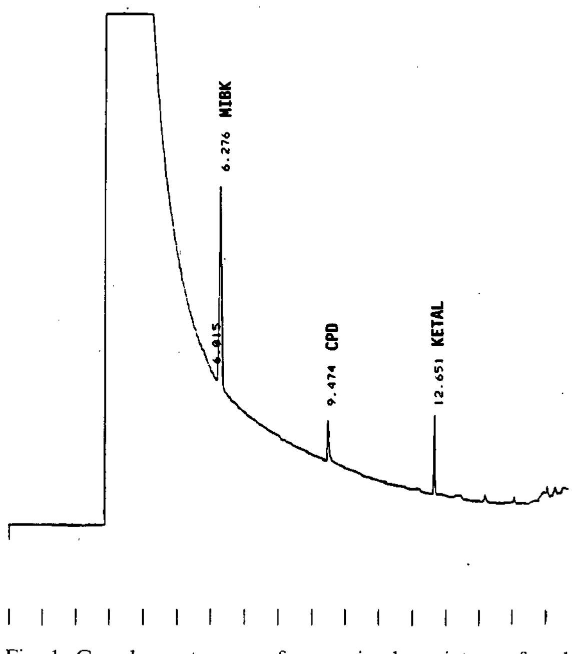

Fig. 1. Gas chromatogram of an equimolar mixture of underivatized 3-chloropropanediol (CPD) and methylisobutylketone (MIBK). Megabore 30 m × 0.75 mm I.D. SPB-5 capillary column. Splitless injection. Numbers at peaks indicate retention times in min.

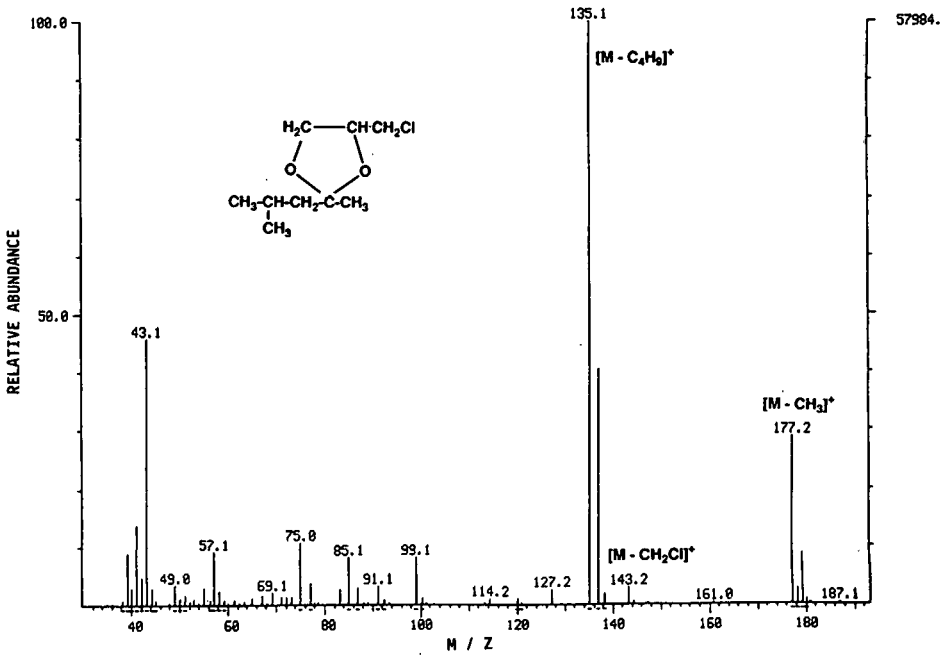

Fig. 2. Mass spectrum of 2-isobutyl-2-methyl-4-(chloromethyl)-1,3-dioxolane.

Although BSTFA reacts with 3-chloropropanediol at ambient temperature, heating for 10 min at 80°C assures complete silylation, especially when other less reactive species may be present in the sample. As an added benefit, trimethylsilylation increases the flame ionization detector response by adding three carbons to each hydroxyl group derivatized.

Underivatized 3-chloropropanediol reacts with ketones during GC, as shown in Fig. 1 with an equimolar mixture of MIBK and 3-chloropropanediol dissolved in acetonitrile. A peak corresponding to the reaction product was identified by mass spectrometry (Fig. 2) as the ketal of MIBK (2-isobutyl-2-methyl-4-(chloromethyl)-1,3-dioxolane):

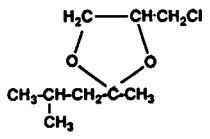

Consequently, ketones interfere with the determination of underivatized 3-chloropropanediol by GC. Derivatized 3-chloropropanediol, however, does not react with ketones. Kinetics of the reaction between 3-chloropropanediol and ketones can be determined therefore by using BSTFA to terminate the reaction. This is illustrated with a pseudo-first order plot (Fig. 3) of 3-chloropropanediol in acetone. The rate of the reaction is fairly rapid and the use of acetone as the solvent for preparing analytical standards of 3-chloropropanediol [8] is therefore not advisable.

Ketals of 3-chloropropanediol do not react with

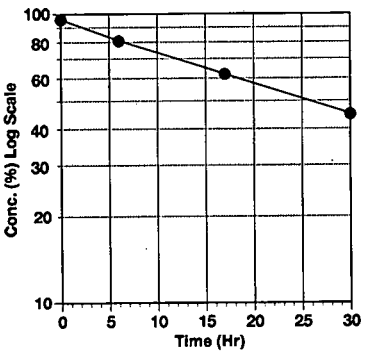

Fig. 3. A pseudo-first order plot of 3-chloropropanediol reacting with acetone at 25°C. Initial concentration of 3-chloropropanediol in acetone 3.11 g/l.

TABLE I

ANALYSIS OF MIXTURES OF 3-CHLOROPROPANEDIOL AND 2-METHYL-2-ISOBUTYL-4-(CHLOROMETHYL)-1,3-DIOXOLANE

3-Chloropropanediol			2-Methyl-2-isobutyl-4-(chloromethyl)-1,3-dioxolane		
Prepared concentration (mg/ml)	Found concentration (mg/ml)	Recovery (%)	Prepared concentration (mg/ml)	Found concentration (mg/ml)	Recovery (%)
0.412	0.405	98.3	0	0	
0.330	0.337	102.2	0.161	0.158	98.1
0.247	0.249	100.7	0.321	0.311	96.9
0.165	0.161	97.3	0.482	0.476	98.8
0	0		0.803	0.797	99.3

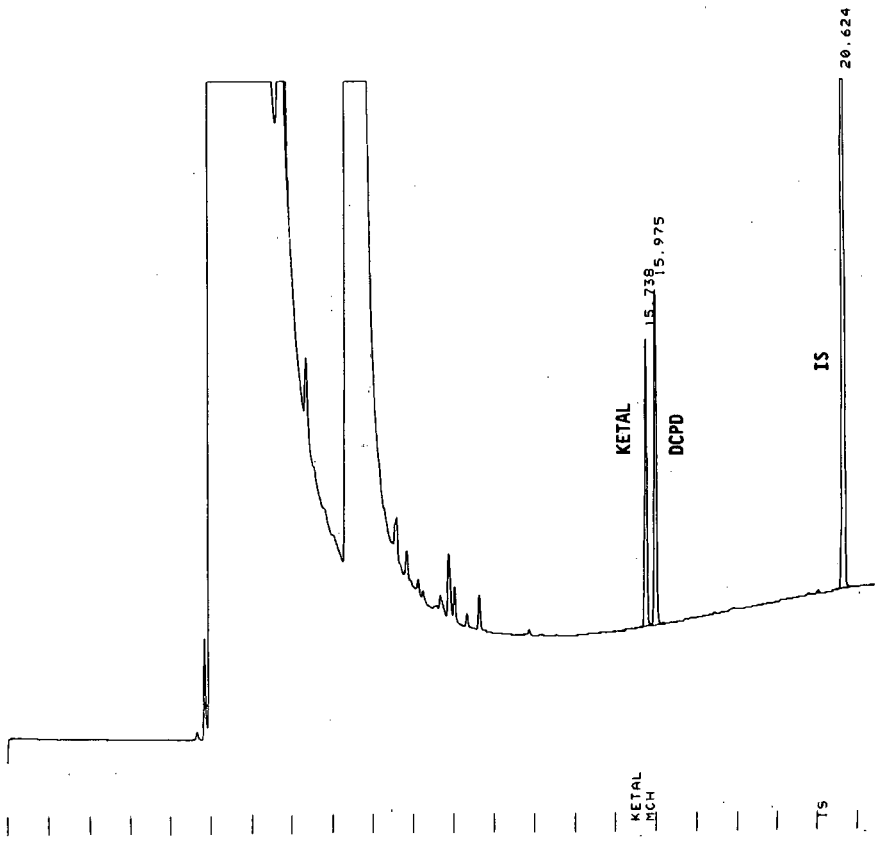

Fig. 4 Gas chromatogram of derivatized 3-chloropropanediol (DCPD) and 2-isobutyl-2-methyl-4-(chloromethyl)-1,3-dioxolane (KETAL) in acetonitrile. Internal standard: *n*-tetradecane (IS). Megabore 30 m × 0.75 mm I.D. SPB-5 capillary column.

BSTFA (Table I) and can be determined in the presence of 3-chloropropanediol by GC (Fig. 4).

The accuracy of the analyses is shown with data in Table I. The precision of gas chromatography was expressed as the standard deviation of five replicate analyses of the same solution containing 103.3 μg/ml 3-chloropropanediol in acetonitrile. The standard deviation was found to be 0.43 μg/ml or (relative standard deviation) 0.42%. The detection limit of 3-chloropropanediol is about 5 μg/ml.

ACKNOWLEDGEMENT

The author is indebted to James R. Valentine and Frank J. Van Lenten for mass spectrometry. Technical assistance was provided by Ward R. Gibson.

REFERENCES

1 K. T. Kirton, R. J. Ericsson, J. A. Ray and A. D. Forbes, *J. Reprod. Fert.*, 21 (1970) 275.
2 A. R. Jones, *Life Sci.*, 23 (1978) 1625.
3 E. K. Weisburger, B. M. Uliand, J. Nam, J. J. Gart and J. H. Weisburger, *J. Natl. Cancer Inst.*, 67 (1981) 75.
4 L. Silhankova, F. Smid, M. Cerna, J. Davidek and J. Velisek, *Mutat. Res.*, 103 (1982) 77.
5 J. K. Morris and L. M. Williams, *J. Pharm. Pharmacol.*, 32 (1980) 35.
6 L. E. Rodman and R. D. Ross, *J. Chromatogr.*, 369 (1986) 97.
7 V. Schurig and D. Wistuba, *Tetrahedron Lett.*, 25 (1984) 5633.
8 R. L. Pesselman and M. J. Feit, *J. Chromatogr.*, 439 (1988) 448.
9 A. I. Mikaya, A. V. Antonova, V. G. Zaikin, N. S. Prostakov, V. Yu. Rumyantsev, E. V. Slivinskii and S. M. Loktev, *Izv. Akad. Nauk. SSSR, Ser. Khim.*, 11 (1983) 2502.
10 C. J. W. Brooks, W. J. Cole, J. H. Borthwick and G. M. Brown, *J. Chromatogr.*, 239 (1982) 191.

Journal of Chromatography, 605 (1992) 139–142
Elsevier Science Publishers B.V., Amsterdam

CHROM. 24 320

Short Communication

Computer-controlled generation of pH gradients in capillary zone electrophoresis

V. Purghart* and D. E. Games

Mass Spectrometry Research Unit, University College of Swansea, Singleton Park, Swansea SA2 8PP (UK)

(First received August 9th, 1991; revised manuscript received May 4th, 1992)

ABSTRACT

A new capillary zone electrophoresis (CZE) apparatus was developed with the possibility of computer-controlled pH-gradient elution. The details of the apparatus are described together with an example showing the analysis of aspartame, benzoate and caffeine in diet Pepsi.

INTRODUCTION

Electrophoresis is a powerful technique for the separation of charged species in solution. Capillary zone electrophoresis (CZE) is a high-resolution separation method conducted in small-I.D. capillaries. Two effects are responsible for the migration of the charged solutes: electrophoretic and electroosmotic displacement. The strong electro-osmotic flow in CZE, which results from the substantial ζ-potential of the capillary surface, is sufficiently large under many conditions to result in the elution of ions with both positive and negative electrophoretic mobilities.

Typically CZE is performed with a uniform buffer [1]. Having complex samples, it is difficult to find the correct buffer to analyze different compounds in one run. To cope with this problem special conditions have to be generated. A temperature gradient [2] or pH gradient [3–6] are the most common approaches to get better separation. Here we report an approach which permits the generation of a smooth, computer-controlled pH gradient. Its effectiveness is illustrated with a simple sample (diet Pepsi).

EXPERIMENTAL

Apparatus

A schematic view of the apparatus used for the development of pH gradients is shown in Fig. 1. A high-voltage power supply (Brandenburg, Model alpha III type 3807) with reversible polarity was used. For acquisition of the UV–VIS spectra we used the Spectra-Physics Focus fast scanning detector with an IBM PS/2 computer. A laboratory-made box of Perspex with three buffer containers, a mixing system and a piece of capillary of 70 cm length (to the detector) are the main parts of the apparatus. Two of the containers (will be called

Correspondence to: Professor D. E. Games, Mass Spectrometry Research Unit, University College of Swansea, Singleton Park, Swansea SA2 8PP. UK.

* Present address: Spectronex AG, Rotterdam-Strasse 21, P.O. Box, 4002 Basle, Switzerland.

0021-9673/92/$05.00

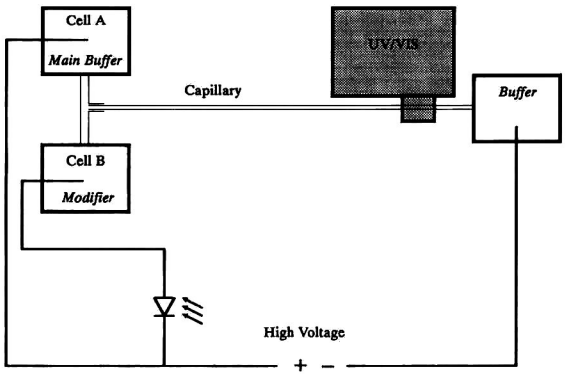

Fig. 1. Apparatus for the experiments with pH-gradient CZE.

cells A and B) are screwed into a Perspex block where the mixing chamber is situated. Cell A contains the main buffer (10 m*M* phosphate buffer of pH 2.5) the pH value of which is increased by the modifier out of cell B (100 m*M* phosphate buffer of pH 11.0). The mixing chamber (Fig. 2) is basically a T-piece channel of 350 μm diameter drilled in the Perspex block (2 mm length). To avoid a quick homogenization of the buffers due to the brownian migration, two short pieces of capillary (1 mm length and 10 μm I.D.) were fixed in a rubber seal to lower the flow of the buffer into the T-piece.

The mixing of the two buffers is controlled by a computer. The current is split continuously at a constant voltage over the two cells. A digital-to-analog converter output of the computer is interfaced by a "sweetspot" (light emitting transistor, RS 301-915) and a photodiode (RS 305-462) connected by a fibre optics cable to control the current splitting. The photodiode is installed in the direction of no conductivity. There is no current throught the photodiode unless light has been emitted from the "sweetspot". The current is (as far the photodiode allows) direct proportional to the emitted light intensity. Fig. 3 shows the programmed and measured currents during the separation. The programmed current is the calculated curve which the computer had to generate, the measured current was calculated from the measured voltage over a 100 kΩ resistor. The computer programme provided any linear, horizontal constant or exponential curve or combination of these, of up to ten different segments. The time per segment could be arbitrarily set to any time with a minimum dwell time of 1 s (gradients showing a non-linear, concave or convex current profile are not shown here).

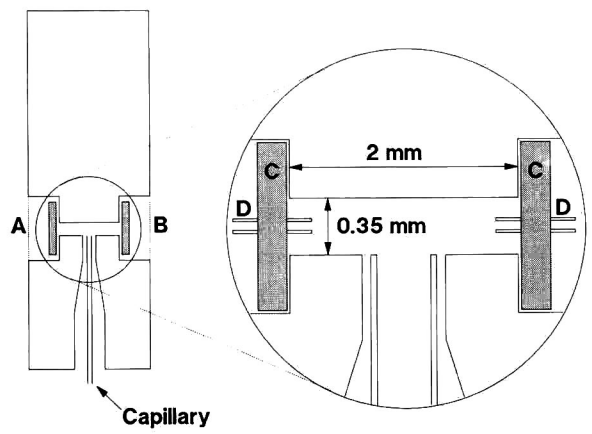

Fig. 2. Scheme of the mixing chamber. A = Connection to cell A; B = connection to cell B; C = rubber seak; D = capillary for flow reduction (1 mm length and 10 μm I.D.).

Procedure

In our example experiment, cell A contains 10 m*M* phosphate buffer of pH 2.5 which is modified by 100 m*M* phosphate buffer of pH 11.0 out of the cell B.

The T-piece was filled by pumping (by air pressure on the orifice where the buffer is filled into the cell) the buffer out of cell B into the T-piece while

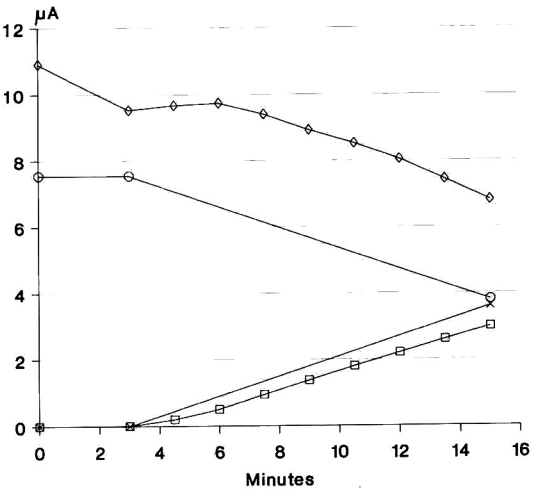

Fig. 3. Diagrammatic presentation of the currents through cell A and B during the pH-gradient CZE. ○ = Cell A calculated; ◇ = cell A measured; × = cell B calculated; □ = cell B measured.

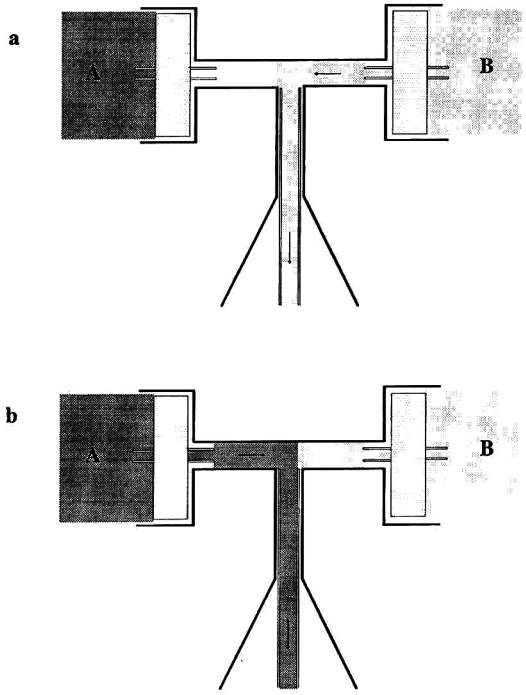

Fig. 4. Principle of filling the T-piece of the mixing chamber with (a) the modifier and (b) the main buffer.

cell A was plugged to avoid entrance of the modifier into cell A (Fig. 4a). Then cell B was plugged and the buffer of cell A was pumped to fill the T-piece to the junction (Fig. 4b).

In the beginning of the experiment the capillary was flushed (by vacuum using a small rotary pump which was connected by a plastic tubing with a reduction in the end to the capillary) with 1 *M* sodium hydroxide solution for 5 min and with the main buffer (10 m*M* phosphate buffer of pH 2.5) for an additional 10 min.

The sample was injected without further treatment after degassing for 5 min in a ultrasonic bath. It was injected by syphoning (lifting the sample tube with the capillary entrance to 30 cm above the other capillary end). The determined sample volume was approximately 60 nl. The capillary was introduced into the T-piece of the mixing chamber, fastened by a ferrule and a nut and the door of the perspec box was closed to switch on the power supply by a micro switch situated next to the edge of the box. The acquisition and the gradient programme were started.

RESULTS AND DISCUSSION

A simple sample, diet Pepsi which contains large quantities of aspartame, benzoate and caffeine, was chosen.

Fig. 5 shows three electropherograms of diet Pepsi at pH 2.5, 4.9 and 8.3 respectively. Aspartame (1) is the fastest compound at pH 2.5. If the pH value is increased, its direction of migration changes and the corresponding peak can be observed at reversed polarity. Peak 2 has not yet been identified. Compounds 2 and 2′ show identical UV spectra. Peaks 3 and 4 were found to be caffeine and benzoate respectively, by comparison of the retention time and UV spectra of the pure compounds.

The pH-gradient electropherogram is shown in Fig. 6. Compared to the data shown in Fig. 5 aspartame appears not to be affected, but the retention times of the other compounds change. The applied gradient considerably speeds up elution of caffeine. Furthermore, peak 2 (unknown compound) is retarded. This experiment proves the functionality of

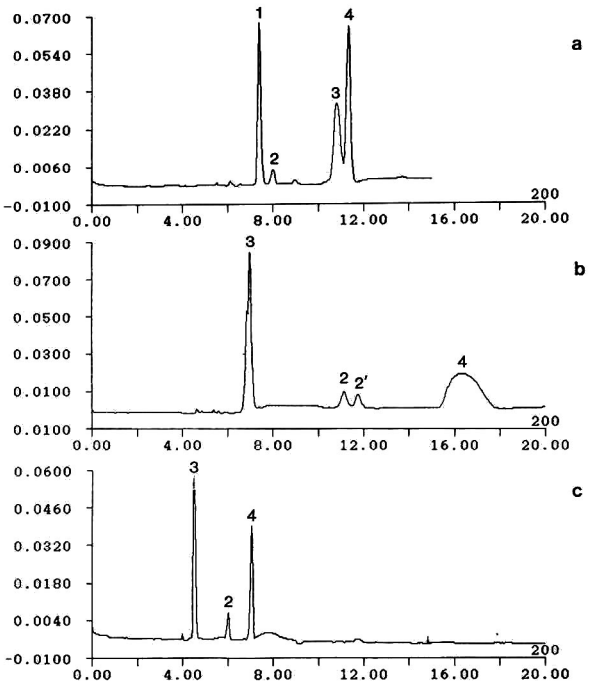

Fig. 5. Electropherograms of diet Pepsi at three different pH values with 100 m*M* phosphate buffer: (a) pH 2.5; (b) pH 4.9; (c) 8.3. Time scale in min. *y*-axes represent absorbance units. Peaks: 1 = aspartame; 2 and 2′ = unknown; 3 = caffeine; 4 = benzoate.

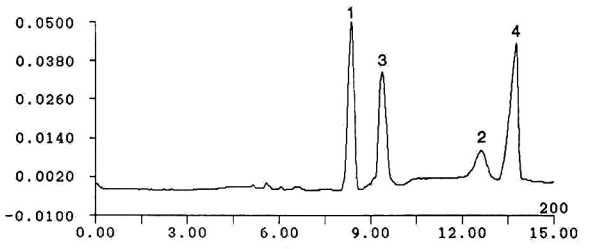

Fig. 6. Electropherogram of diet Pepsi with the use of pH-gradient CZE. Scales and peaks as in Fig. 5.

the new technique for pH-gradient generation. It is important to introduce the capillary carefully into the mixing chamber to get reasonable reproducibility. The retention time of the last peak may vary up to ± 1 min. We expect that changes in temperature and chemistry on the capillary surface (activation–desactivation) are rather responsible for that variation in retention time than the generation of the gradients, because the relative retention time between the peaks do not vary a lot.

CONCLUSION

In a simple experiment we have proved that the new technique of generating pH gradients is a powerful method. There is no doubt that it can be used in many separation problems. More work is required to produce a better reproducibility.

ACKNOWLEDGEMENTS

We would like to thank Dr. A. G. Brenton for writing the computer programme to control the unit and Mr. B. Cooper for his help in developing the computer–electrodes interface.

V. P. thanks the Swiss National Science Foundation for granting this research (grant No. 81BE-28089).

REFERENCES

1 W. G. Kuhr, *Anal. Chem.*, 62 (1990) 403R.
2 E. Grushka, R. M. McCormick and J. J. Kirkland, *Anal. Chem.*, 61 (1989) 241.
3 J. Pospíchal, M. Deml, P. Gebauer and P. Boček, *J. Chromatogr.*, 470 (1989) 43.
4 P. Boček, M. Deml, J. Pospíchal and J. Sudor, *J. Chromatogr.*, 470 (1989) 309.
5 V. Šustáček, F. Foret and P. Boček, *J. Chromatogr.*, 480 (1989) 271.
6 J. Pawliszyn, *J. Liq. Chromatogr.*, 13(8) (1990) 1529.

Journal of Chromatography, 605 (1992) 143–147
Elsevier Science Publishers B.V., Amsterdam

CHROM. 24 305

Short Communication

Determination of sodium vinyl sulphonate in water-soluble polymers using capillary zone electrophoresis

D. S. Ryder

Research Department, FMC Corporation (UK) Ltd., Process Additives Division, Trafford Park, Manchester (UK)

(First received December 31st, 1991; revised manuscript received April 22nd, 1992)

ABSTRACT

A robust capillary zone electrophoretic (CZE) method is developed for the quantitative determination of sodium vinyl sulphonate in water-soluble polymers. At the optimum concentration a precision of ± 0.26% relative standard deviation is obtained for standard solutions whereas "real samples" show a precision of ± 1.9% relative standard deviation with recoveries of 99%. The calibration is linear at least over two orders of magnitude and a detection limit of 1 mg/l is found. The CZE method is faster, more sensitive and less prone to interference than high-performance liquid chromatography and is consequently both more precise and accurate for this determination. In addition CZE is significantly more economical to perform than high-performance liquid chromatography for this analysis.

INTRODUCTION

Since the pioneering work of Jörgenson and Lukas [1] and particularly since the introduction of commercial instrumentation capillary electrophoresis (CE) has developed into a now widely accepted technique in the biomedical and related fields; however, despite the increasing number of publications few describe adequate quantitative determinations and even fewer papers concern the use of CE in industrial applications [2]. The advantages of CE such as high efficiency, small sample size and unique selectivities compared to high-performance liquid chromatography (HPLC) have frequently been discussed but the significant reduction in running costs and the avoidance of the use of large volumes of expensive and hazardous solvents also renders CE an attractive alternative to HPLC in solving problematic industrial applications.

CE has been applied by the author to the analysis of various water-soluble monomers and polymers and the present paper describes the method developed for one such product which presented difficulties for analysis by HPLC. Products based on vinyl sulphonate polymers and copolymers may be used as barium sulphate scale inhibitors, in electroplating, as powder dispersants, in photographic films and in membrane technology particularly for use in gas detectors. In researching into such polymers it is important to know the residual monomer content. Literature searches have revealed no analytical methods for the determination of sodium vinyl sulphonate in polymers.

The very polar nature of the analyte and its relatively poor UV absorbance above 205 nm together with the requirement to elute the polymer before the

Correspondence to: David S. Ryder, Research Department, FMC Corporation (UK) Ltd, Process Additives Division, Tenax Road, Trafford Park, Manchester M17 1WT, UK.

0021-9673/92/$05.00

next analysis renders this a difficult determination by reversed-phase HPLC. Consequently a method based on a previous [3] publication employing a single-column ion chromatography system with conductivity detection was attempted. However this has been found to be subject to interferences from polymer components and in addition employs expensive ion-exchange columns which exhibit a short life in this application due to polymer adsorption.

As a consequence capillary zone electrophoresis was investigated and found to yield a rapid robust method with a precision equal to that expected for many HPLC methods.

EXPERIMENTS

All experiments were carried out using an ABI Model 270A electrophoresis instrument (Applied Biosystems, Warrington, UK) fitted with a Polymicro 50 μm internal diameter fused-silica capillary (Composite Metal Services, Worcester, UK) cut to a length of 50 cm, with a distance of 27 cm between the injector and detector. The capillary was washed with molar sodium hydroxide for 30 min when first prepared. The system was configured in the positive mode, *i.e.* the anode at the injection end and the capillary compartment temperature set at 30°C. For the optimum conditions the running buffer was 20 m*M* disodium tetraborate decahydrate (BDH, Poole, UK) adjusted to a pH of 8.0 using orthophosphoric acid.

The capillary was washed with a 1-min vacuum flush of 0.1 *M* sodium hydroxide followed by a 2-min flush of the running buffer between each analysis. The samples were introduced as one per cent aqueous solutions using a 2-s vacuum injection, equivalent to approximately 12 nl. A voltage of +20 kV was applied, normally for 8 min, generating a current of approximately 50 μA. The analytes were detected by the UV detector at 190 nm and the data were collected and quantified using a Waters Millipore 860, VAX-based multitasking, multi-user data system.

RESULTS AND DISCUSSION

Sodium vinyl sulphonate was found to give a good peak shape with an adequate migration of less than 6 min employing borate buffer at pH 8.0 (see Fig. 1). The net migration of the vinyl sulphonate anion is towards the cathode due to the high electroosmotic flow at this pH. The analyte ion was separated from the polymer components most of which require considerably longer than 10 min to emerge (see Fig. 2); however, for quantitative determination of the vinyl sulphonate this is not necessary as after detection of the analyte during an 8-min run the polymer is removed from the capillary by a vacuum flush before the next run.

Changes in the pH of the buffer had only a marginal effect on the migration time but the peak showed marked fronting at pH 8.5, indicating an increased differential between the migration velocity of the analyte and the electrolyte. The efficiency was slightly better at pH 7.25 than pH 8.0 but a baseline rise seen in some polymer samples was greater at this pH, therefore pH 8.0 was considered optimum. Varying the ionic strength of the buffer at a constant pH of 8.0 had little effect on the peak shape or efficiency though the migration time increased from 4.9 to 6.4 min for a change of from 15 to 25 m*M* borate.

An exceptional increase in UV absorption was observed, from a barely detectable peak at 210 nm for a 0.05% vinyl sulphonate solution to a 70-fold increase in sensitivity at 190 nm.

The baseline noise is only marginally worse at 190 nm than at 210 nm. This is in contrast to HPLC where the noise increases considerably at the lower wavelengths and where organic solvents are required the very low wavelengths become unusable. This is important for the analysis of aliphatic materials and in part compensates for the generally poorer concentration sensitivity of electrophoresis as compared to HPLC, due to the inability to inject large sample volumes.

Linearity was tested by eight repeat injections of vinyl sulphonate solutions at six concentration levels. The precision obtained for this calibration is shown in Table I. The calibration has a linear regression coefficient of 1.0000 over a 200-fold concentration range at least from 0.001 to 0.2% of vinyl sulphonate in aqueous solution which is equivalent to 0.1 to 20% in the sample. Fronting became increasingly evident at higher concentrations but this does not adversely affect the precision of measurement.

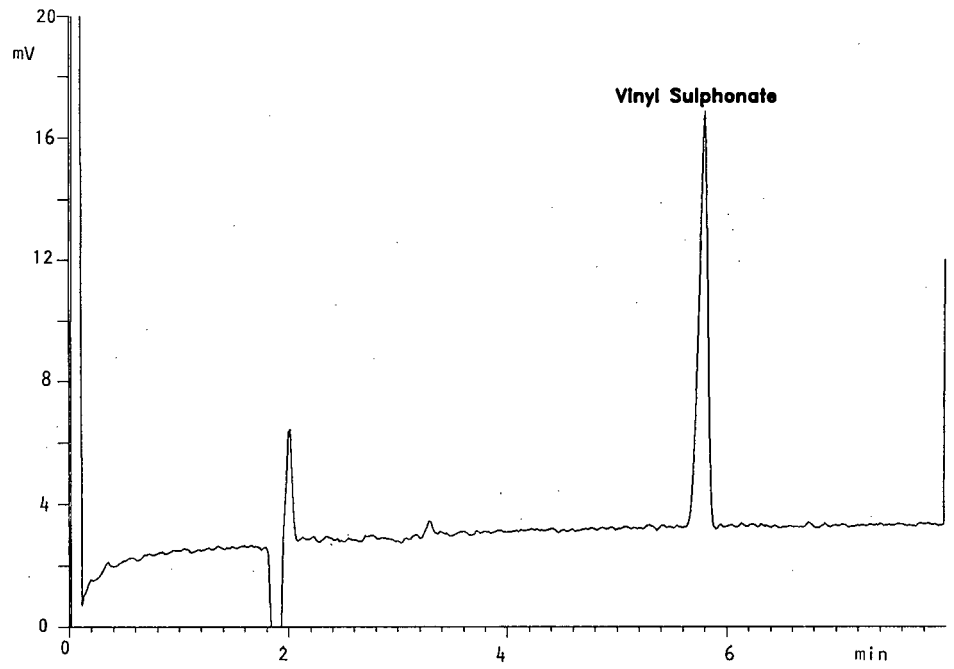

Fig. 1. Electropherogram of sodium vinyl sulphonate 0.01% aqueous solution, 2-s vacuum injection. Buffer, 20 m*M* sodium tetraborate adjusted to pH 8.0 using phosphoric acid. Applied voltage +20 kV and UV detection at 190 nm and 30°C.

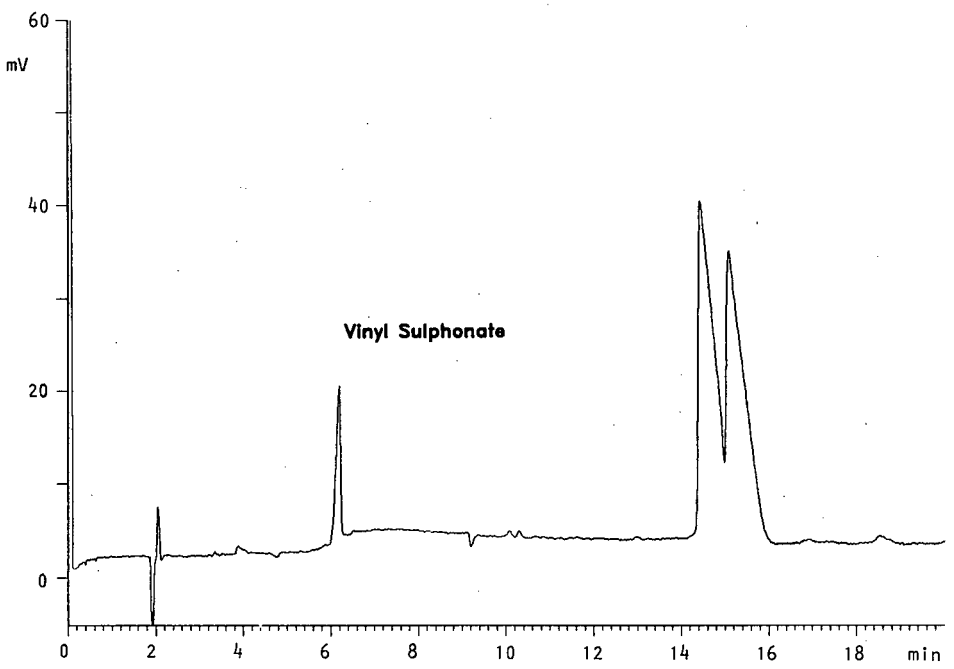

Fig. 2. Sodium vinyl sulphonate determination in a water-soluble polymer. The vinyl sulphonate level is 1.3%. Electrophoretic conditions as in Fig. 1.

TABLE I

VINYL SULPHONATE CALIBRATION, EIGHT INJECTIONS PER LEVEL

R.S.D. = Relative standard deviation.

Vinyl sulphonate standard (%)	R.S.D. (%), migration time	R.S.D. (%), peak height	Mean number of theoretical plates	Mean response area units $\times 10^{-3}$	R.S.D. (%), peak area
0.2	0.14	0.92%	1 490	1566.07	0.26
0.1	1.04[a]	1.20%	2 860	776.53	0.54
0.05	0.28	1.16%	4 450	378.31	0.64
0.01	0.28	1.15%	16 440	76.02	0.87
0.005	0.34	0.72%	23 850	37.45	1.35
0.001	0.23	2.92%	31 410	7.86	4.49

Linear regression = 1.000, slope = 7834, intercept = −4.139

[a] Contains an outlier.

Spiking tests were carried out where levels equivalent to 0.5 and 2.5% of vinyl sulphonate were spiked into a "real" polymer sample previously found to contain no vinyl sulphonate. The recoveries over eight determinations averaged 99% for four determinations at each level.

Using the standard 2-s injection of the method the concentration limit of detection is 3 mg/l of so-

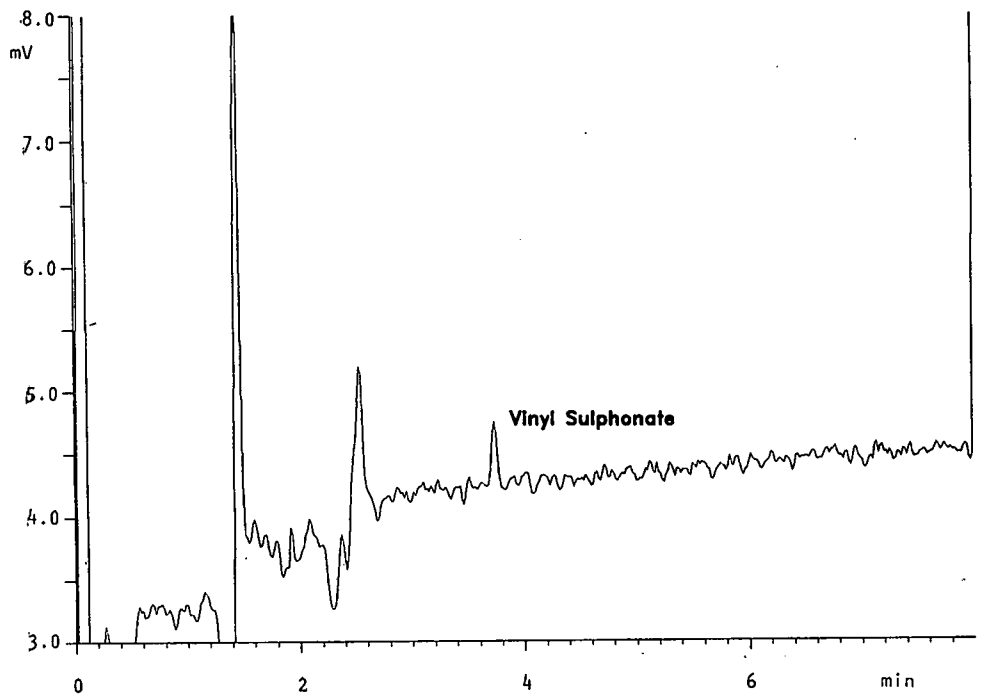

Fig. 3. Electropherogram showing limit of detection of 1 mg/l or approximately 100 fmol of sodium vinyl sulphonate in aqueous solution. Electrophoretic conditions as in Fig. 1 but 4-s vacuum injection.

dium vinyl sulphonate in aqueous solution. Using a 4-s injection the detection limit is 1 mg/l with a signal-to-noise ratio of 3:1, this is equivalent to approximately 100 fmol injected. A decrease in migration time is seen with this increased loading (see Fig. 3) and further increases in injection time are detrimental to the peak shape even for the standard alone and therefore show no gain in sensitivity. This is likely to be due to the relatively short capillary used; however, the system was optimised for speed of analysis rather than sensitivity of detection.

CONCLUSIONS

CE was found to provide a robust, precise method for the determination of residual vinyl sulphonate in water-soluble polymers which shows significant advantages over HPLC in particular yielding benefits in more accurate and economical analysis. It is likely that other ionic monomers will be equally amenable to capillary electrophoretic separation from their water-soluble polymers and that CE will become the preferred technique for their determination.

ACKNOWLEDGEMENT

The author thanks Mrs. V. Carr for her valued technical assistance.

REFERENCES

1 J. W. Jorgenson and K. D. Lukas, *Anal. Chem.*, 53 (1981) 1298.
2 T. Dulffer, R. Herb, H. Herrman and U. Kobold, *Chromatographia*, 30 (1990) 675.
3 D. S. Ryder, *J. Chromatogr.*, 354 (1986) 438.

Journal of Chromatography, 605 (1992) 148
Elsevier Science Publishers B.V., Amsterdam

CHROM. 24 303

Letter to the Editor

Sir,

Our paper "Separation of soy lecithin using gel permeation chromatography", *J. Chromatogr.*, 589 (1992) 165–170, referenced several prior reports on the aggregation of surfactant-like molecules during size-exclusion chromatography (refs. 12–18 therein). A paper entitled, "Gel filtration of lipid mixtures", *J. Chromatogr.*, 14 (1964) 486–489, by C. L. Tipton, J. W. Paulis and M. D. Pierson also described the observation of aggregation of phosphatides in a non-polar solvent during gel filtration chromatography and may, in fact, represent the earliest such report on this subject. We wish to apologize for our failure to reference this work. This was clearly an oversight on our part.

Richard E. Shansky

Boehringer Ingelheim Pharmaceutical, Inc., Research and Development Center, Analytical Sciences Department, 175 Briar Ridge Road, Ridgefield, CT 06877 (USA)

Journal of Chromatography, 605 (1992) 149
Elsevier Science Publishers B.V., Amsterdam

CHROM. 24 331

Book Review

Preparative and process-scale liquid chromatography, edited by G. Subramanian, Ellis Horwood, Chichester, 1991, 286 pp., price £ 55.00, US$ 94.00, ISBN 0-8412-2090-5.

This book provides a general overview of the basic issues which should be considered when using chromatography on a plant scale. It would primarily be helpful for chemists, engineers and managers who have no experience or background in the field, and who need to acquire general information regarding process chromatography. For this, the book would serve them well. However, the 14-chapter book does not tell how to develop a process-scale separation and is not a comprehensive source of information with which to begin the research, development or design stages of such a project.

Various chapters make the reader aware of the differences between analytical and process chromatography and the differences between normal- and reversed-phase chromatography. It also gives an introduction to the different ways of operating: recycle, overloaded elution or displacement mode. Basic design and control issues such as explosion proofing, achieving gradient accuracy, detection and fraction collection are discussed in general terms with cost implications. Different column technologies are reviewed in general terms discussing technical points as well as the choices one has to make in flexibility and in the amount of operator handling, which will determine how columns are packed and unpacked. The parameters involved in choosing a stationary phase such as particle size, pore volume, surface modifier and mechanical strength of the particle are presented from different points of view. Various chapters point out how the choice of stationary phase affects the solvent choice and has major consequences for plant design, solvent handling, safety requirements and waste disposal. Overall aspects of plant design are presented in various chapters pointing out the sources of the variables which contribute to cost.

A solid introduction to continuous chromatography in a low-pressure environment is presented with examples. A brief and elementary discussion of enantioseparations is given, including an explanation of chirality, a review of the stationary phases available and some applications.

The general overview introducing chromatography on the plant scale is good. The chapters are in general lacking in depth and substance. Many of the band profiles drawn in the figures are incorrect in their detail. It appears that the authors and the editors have rushed to put the book together. There are many spelling mistakes, one figure is not drawn and the affiliation of the author of one chapter is missing.

There is useful and important information in this book that is waiting to be applied. However, it is the challenge for the reader to find it amongst the dilute and vague generalities. The reader must also discriminate between the important issues of how to engineer a plant which involves chromatography as an economical unit operation and not just build a bigger analytical high-performance liquid chromatograph.

St. Louis, MO (USA) Anita M. Katti

PUBLICATION SCHEDULE FOR 1992

Journal of Chromatography and *Journal of Chromatography, Biomedical Applications*

MONTH	O 1991–F 1992	M	A	M	J	J	
Journal of Chromatography	Vols. 585–593	594/1 + 2 595/1 + 2	596/1 596/2 597/1 + 2	598/1 598/2 599/1 + 2 600/1 600/2	602/1 + 2 603/1 + 2 604/1	604/2 605/1 605/2 606/1	The publication schedule for further issues will be published later.
Cumulative Indexes, Vols. 551–600					[a]		
Bibliography Section		610/1			610/2		
Biomedical Applications	Vols. 573 and 574	575/1 575/2	576/1	576/2 577/1	577/2	578/1 578/2	

[a] Cumulative Indexes will be Vol. 601, to appear early 1993.

INFORMATION FOR AUTHORS

(Detailed *Instructions to Authors* were published in Vol. 558, pp. 469–472. A free reprint can be obtained by application to the publisher, Elsevier Science Publishers B.V., P.O. Box 330, 1000 AH Amsterdam, The Netherlands.)

Types of Contributions. The following types of papers are published in the *Journal of Chromatography* and the section on *Biomedical Applications:* Regular research papers (Full-length papers), Review articles and Short Communications. Short Communications are usually descriptions of short investigations, or they can report minor technical improvements of previously published procedures; they reflect the same quality of research as Full-length papers, but should preferably not exceed five printed pages. For Review articles, see inside front cover under Submission of Papers.

Submission. Every paper must be accompanied by a letter from the senior author, stating that he/she is submitting the paper for publication in the *Journal of Chromatography*.

Manuscripts. Manuscripts should be typed in double spacing on consecutively numbered pages of uniform size. The manuscript should be preceded by a sheet of manuscript paper carrying the title of the paper and the name and full postal address of the person to whom the proofs are to be sent. As a rule, papers should be divided into sections, headed by a caption (*e.g.*, Abstract, Introduction, Experimental, Results, Discussion, etc.). All illustrations, photographs, tables, etc., should be on separate sheets.

Introduction. Every paper must have a concise introduction mentioning what has been done before on the topic described, and stating clearly what is new in the paper now submitted.

Abstract. All articles should have an abstract of 50–100 words which clearly and briefly indicates what is new, different and significant.

Illustrations. The figures should be submitted in a form suitable for reproduction, drawn in Indian ink on drawing or tracing paper. Each illustration should have a legend, all the *legends* being typed (with double spacing) together on a *separate sheet.* If structures are given in the text, the original drawings should be supplied. Coloured illustrations are reproduced at the author's expense, the cost being determined by the number of pages and by the number of colours needed. The written permission of the author and publisher must be obtained for the use of any figure already published. Its source must be indicated in the legend.

References. References should be numbered in the order in which they are cited in the text, and listed in numerical sequence on a separate sheet at the end of the article. Please check a recent issue for the layout of the reference list. Abbreviations for the titles of journals should follow the system used by *Chemical Abstracts.* Articles not yet published should be given as "in press" (journal should be specified), "submitted for publication" (journal should be specified), "in preparation" or "personal communication".

Dispatch. Before sending the manuscript to the Editor please check that the envelope contains four copies of the paper complete with references, legends and figures. One of the sets of figures must be the originals suitable for direct reproduction. Please also ensure that permission to publish has been obtained from your institute.

Proofs. One set of proofs will be sent to the author to be carefully checked for printer's errors. Corrections must be restricted to instances in which the proof is at variance with the manuscript. "Extra corrections" will be inserted at the author's expense.

Reprints. Fifty reprints of Full-length papers and Short Communications will be supplied free of charge. Additional reprints can be ordered by the authors. An order form containing price quotations will be sent to the authors together with the proofs of their article.

Announcement from the Publisher

ELSEVIER SCIENCE PUBLISHERS

prefers the submission of electronic manuscripts

Electronic manuscripts have the advantage that there is no need for the rekeying of text, thereby avoiding the possibility of introducing errors and resulting in reliable and fast delivery of proofs.

The preferred storage medium is a $5\frac{1}{4}$ or $3\frac{1}{2}$ inch disk in MS-DOS format, although other systems are welcome, e.g. Macintosh.

Your disk and (**exactly matching**) printed version (printout, hardcopy) should be submitted together to the accepting editor. In case of revision, the same procedure should be followed such that, on acceptance of the article, the file on disk and the printout are **identical**. Both will then be forwarded by the editor to Elsevier.

Please follow the general instructions on style/arrangement and, in particular, the reference style of this journal as given in 'Instructions to Authors'.

Please label the disk with your name, the software & hardware used and the name of the file to be processed.

Further information can be found under 'Instructions to Authors - Electronic manuscripts'.

Contact the Publisher for further information.

ELSEVIER SCIENCE PUBLISHERS B.V.
P.O. Box 330, 1000 AH Amsterdam
Netherlands
Fax: (+31-20) 5862-304